Towards the quantification of alpha-synuclein fibrils by combining seed amplification assays and single particle counting

Master's assignment report

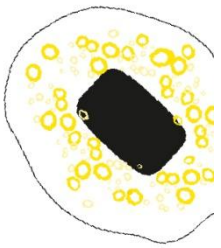

Student:	Paulien van den Berg
Date:	April 2025
Programme:	Biomedical Engineering
Track:	Bioengineering Technologies
Course name:	Master's Assignment
Course code:	193650999
University:	University of Twente (UT)
Faculty:	Science & Technology (S&T) (TNW)
Research group:	Nanobiophysics (NBP)
Committee:	prof. dr. Mireille Claessens dr. Christian Blum dr.ir. Jos Paulusse

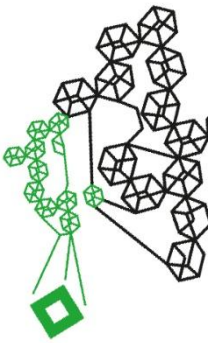

Abstract

Parkinson's disease is a neurological disorder without a cure and without adequate means of diagnosis. It is expected to affect 14 million people worldwide by 2040, which is more than a quadruplication since 1990. Diagnosis is currently based on symptoms, but biomarker detection might allow for earlier and more accurate diagnosis. This master's assignment has been a step in the development of a method to quantitatively detect αS fibrils – the protein aggregates that characterize Parkinson's disease. The novel method combines two existing techniques: the sensitive but non-quantitative method of seeded aggregation assay (SAA) and single particle counting (SPC). The SAA amplifies the number of αS fibrils, and SPC quantifies single fibrils. Measuring the αS fibril increase over time yields a doubling time, which can be used to find the αS fibril amount in original patient sample. This would not only allow for quantitative diagnosis, but also the monitoring of disease progression which supports treatment development. An SPC setup in which αS fibrils can be counted during an SAA was successfully constructed and tested. Various parameters were investigated for optimization, such as the αS fibril concentration, the mechanical sonication of αS fibrils, and type of fluorescent dye staining the αS fibrils. This project has not established a definitive functioning method, but has advanced its development.

Contents

1. Introduction

Parkinson's disease and alpha synuclein (αS)

Parkinson's disease is a neurological disorder characterized by motor symptoms such as tremor, bradykinesia, rigidity and postural instability, but also non-motor symptoms as autonomic dysfunction (e.g. constipation), and neuropsychiatric disorders (e.g. depression).[1,2] Between 1990 and 2015, the number of patients worldwide more than doubled to 6 million individuals[3] and is projected to more than double to 14 million by 2040[4]. Many symptoms can be treated through various therapies, but Parkinson's disease currently remains a neurodegenerative disease without a cure.[2,5]

Diagnosis is merely based on symptoms provided by patient history and physical examination, and sometimes by additional imaging techniques.[1,5] A diagnosis is however only conclusive after a post-mortem examination of the brain.[5] As such, Parkinson's disease is prone to misdiagnosis. Diagnostic accuracy was found to be only 81% (based on pooled data of 11 studies), without significant improvement over the 25 years between 1988 and 2014.[6] For early stage diagnosis, this is even less at 58% (based pooled data of 3 studies).[7]

In recent years, the protein alpha synuclein (αS) has been noted and studied as a potential biomarker for Parkinson's disease.[8,9] Aggregates of abnormally formed αS in the brain are a hallmark of Parkinson's disease[10], and they have also been found in both neural and non-neural peripheral tissues such as the spinal cord, peripheral nervous system, and the submandibular gland[11]. As a result, the detection of αS has been thoroughly investigated in biofluids such as cerebrospinal fluid (CSF), saliva, whole blood, plasma, and serum, and in biopsies of peripheral tissues such as skin, colonic submucosa, and submandibular gland.[8,12–14] Unfortunately, none of these efforts have resulted in an accurate premortem diagnostic method for Parkinson's disease.[2]

Seeded aggregation assay (SAA)

Most of these studies have utilized immunoassays to detect αS, but the more novel approach of seeding assays is emerging.[8] The so-called seed amplification assay (SAA) was developed from two techniques originating from prion research: protein misfolding cyclic amplification (PMCA)[15] and real-time quaking-induced conversion (RT-QuIC)[16,17].[18] Please note that the latter terms are still used in recent publications on αS detection.[18] SAA can be viewed as an umbrella term. For a comparison between PMCA and RT-QuIC in context of αS detection, please be referred to Kuang et al.[19]

An SAA exploits the self-aggregation ability of misfolded αS.[19] αS is an intrinsically disordered protein (IDP)[20], meaning it does not have a stable structure[21]. It can misfold into a so-called seed (or fibril); an ordered, fibrillar, insoluble, beta-sheet rich aggregate conformation.[20] αS can misfold spontaneously, also known as primary nucleation or de novo fibril formation[18]; or by encountering another αS seed, since αS seeds spread in a prion-like manner.[20] When a seed encounters another non-seed αS protein, this protein is misfolded into the same conformation as the seed and is incorporated into the growing aggregate.[18,20] αS seeds only

grow from their two ends into rod-like structures known as amyloid fibrils or fibrils.[22] The terms αS seed and αS fibril are often used interchangeably.

The increase of fibril mass during αS aggregation is typically modeled as having three phases that together follow a sigmoidal curve (Figure 1).[18] The process starts with the lag phase or nucleation phase where no aggregation is observable. Aggregation starts either through primary nucleation or seeding (i.e. preformed nuclei are present). Nucleation is thermodynamically unfavorable, whereas the addition of monomers to an already formed nucleus is thermodynamically favorable.[23] Seeding increases the initial aggregation rate as compared to not seeding.[24,25] After enough aggregates have formed to be observable, the second phase begins. During the growth or elongation phase, the amount of aggregates increases sharply at the expense of reactant αS monomers. Eventually an equilibrium is reached which marks the onset of the third phase: the stationary phase.

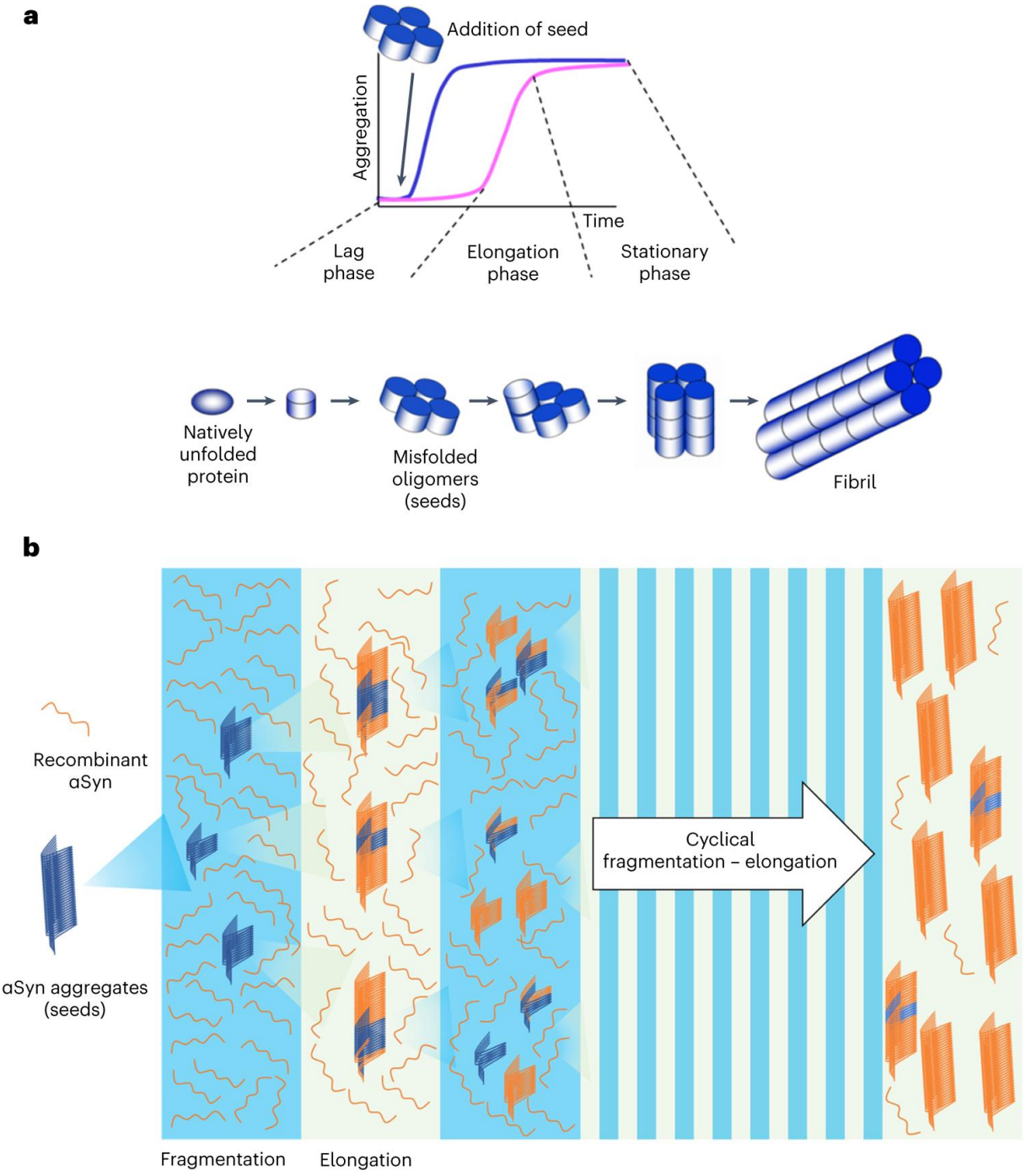

Figure 1. (a) The sigmoidal curve of typical αS aggregation. (b) The cyclical fragmentation-elongation process of the SAA. Adapted from Concha-Marambio et al.[18]

An SAA tests whether a sample contains αS seeds by adding recombinant monomeric αS substrate.[18] If so, aggregation starts and will be accelerated by means of agitation. The fibrils elongate and after some time, the reaction mixture is agitated so that the aggregates break into smaller fragments. Since fibrils only grow from their ends, the rate of fibril elongation is largely dependent on the concentration of fibril ends.[25] Breaking the fibrils into smaller pieces increases the number of fibril ends and thus accelerates the aggregation. They again

are left to elongate before they are fragmented. These cycles of elongation and fragmentation amplify the fibril mass exponentially during the elongation phase.

The amount of αS fibrils in an SAA is monitored by means of a fluorescent dye, most notably thioflavin T (THT) which has been used to stain amyloid fibrils since 1959.[26] When THT binds to amyloid fibrils, it sustains a shift in excitation and emission wavelength and an increase in its emitted fluorescence, making it a sensitive marker of amyloid fibrils specifically.

Currently, a single sample in an SAA only gives a binary outcome, i.e. the sample contains αS fibrils or it does not, based on a fluorescence threshold.[27,28] Often multiple replicates are used to determine the final verdict of positive or negative (or sometimes inconclusive). The threshold determination and result interpretation differ per publication.[27,28]

SAA performance

An SAA precursor (PMCA) using the same cyclic elongation-fragmentation approach could after seven cycles detect 1.3 ag of misfolded prion derived from scrapie hamster brain.[29] This corresponds to about 26 monomers, which is within the size range of a single prion aggregate. The one single prion aggregate had then been amplified multimillion-fold.

An advantage of SAA over other methods that rely on immunoblotting is that the readout can be both automated and high-throughput.[16] If a well plate with e.g. 96 wells is used, many samples can be measured simultaneously and automatically by a fluorescence plate reader. Furthermore, earlier methods used sonication to agitate the fibrils during amplification, which mostly requires manual fluorescent readout.[18] Replacing sonicating with shaking allowed it be automatically done by the fluorescence detector itself.[18]

The reproducibility of SAAs remains difficult despite numerous strategies to increase it.[30,31] Nonetheless, multiple publications report the results of the SAA to be reproducible for different sites, practitioners, experimental protocols, and analyses.[27,28] Russo et al. sent blinded CSF samples from a pre-existing cohort to three different laboratories with each their own established SAA protocol.[27] The results of the three groups shared similar impressive diagnostic performances: Parkinson's disease could be diagnosed with a sensitivity of 86–96% and a specificity of 97–100%.

SAAs are a promising diagnostic tool for Parkinson's disease.[19,31] In addition to detecting advanced Parkinson's disease, SAAs have also been reported to detect Parkinson's disease in recently diagnosed patients[32]. Fernandes Gomes et al. found that SAAs are able to distinguish between synucleinopathies and tauopathies.[33]

SAAs have been performed on many different sample types such as brain tissue, skin and CSF with various sensitivity and specificity with regard to detecting αS.[19] For an overview, please be referred to Kuang et al..[19] For a detailed minireview specifically focused on the use of SAAs as a diagnostic tool for synucleinopathies, please be referred Paciotti et al..[31]

SAAs are not yet quantitative

A major limitation of the SAA is that it is not quantitative.[18,34] The number of αS fibrils cannot be directly counted or derived by means of fluorescence for two reasons. First, the total amount of fluorescence only loosely correlates with the amount of fibrils. Fibrils exist in various morphological forms, for which THT binding and observed fluorescence intensities differ.[35] This means that measuring the fluorescence of an unidentified sample is no precise indicator of αS fibril amount. Second, the sample composition varies between patients and over time for a single patient. Matrix components influence the SAA results, for example by interfering with the aggregation.[19] Certain matrix components are suggested to directly interact with αS fibrils or monomers.[36,37]

The lack of quantitation impedes the monitoring of disease progression and treatment efficacy.[38] This hinders the diagnosis, prognosis and treatment of patients, and researchers' ability to develop new medicines.

A plethora of articles have been published that claim to have created or used some form of quantitative SAA. The quantitation in these articles however is relative, and the actual seed concentration is only estimated.

The previously mentioned study by Saá et al. estimated the number of prions in scrapie hamster brain before the amplification.[29] They used the signal intensity of western blots of 'normal' recombinant prion proteins with known concentration to establish a calibration curve of signal intensity versus concentration. The misfolded prion's concentration was then extrapolated from this. The number of molecules of the misfolded prion were calculated using the concentration (the authors omitted these calculations from the publication).

Chen et al. developed the so-called quantitative PMCA (qPMCA) based on the supposed linear relationship between misfolded prion quantity in a sample and the minimum number elongation-fragmentation cycles required for it to be detected.[39] First, the concentration of misfolded prion in a stock solution is estimated by comparing its western blot and ELISA assay results to those of recombinant prions. The details and data were omitted from the publication, but I expect it to be similar to by Saá et al.. Second, PMCA was performed for samples with various dilutions of the misfolded prions. For each dilution the minimum number of elongation-fragmentation cycles required for detection of misfolded prions was determined. Plotting the misfolded prion quantity against the required number of cycles for detection establishes a (linear) calibration curve. Then for unknown samples, measuring the minimum number of cycles required for detection and using the calibration curve yields an estimate for the amount of misfolded prion in the original sample.

Multiple studies used end-point dilution analysis for relative seed quantitation.[16,27,40] An SAA (or SAA precursor) is performed on a range of sample dilutions; the dilution for which 50% of the replicates is positive is known as the end-point dilution. Statistical analysis (e.g. Spearman-Käber) estimates the corresponding seeding dose (SD50), i.e. the amount of seed resulting in 50% positive replicates. This is expressed as for example SD50/g or SD50/µL. The amount of SD50 in the original sample can be calculated and is expected to linearly relate to the seed concentration. Please note that is method is analogous to an animal bioassay

titration to establish a 50% lethal dose (LD50), i.e. the amount of virus particles resulting in 50% animal death. This was a measure for lethality, and not a direct measure of concentration, although it does correspond to concentration.

Other groups have used the relation between lag time and amount of misfolded prion to create a calibration curve.[41,42] The different amounts of prion were obtained through dilution. Shi et al. estimated the concentration of a misfolded prion stock solution used for the dilutions based on "semi-quantitative" immunoblotting and comparison of its signal intensity to a reference of recombinant prions (data were not shown).[41] This method is probably similar to Saá et al.. Henderson et al. first expressed the relative amount of prion only as dilutions, and then related it to the LD50 dose of a previously completed end-point dilution bioassay.[42] This allowed to estimate misfolded prion mass, concentration and infectivity.

Pfammatter et al. introduced the microfluidics-based method named digital amyloid quantitative assay (d-AQuA).[43] Insulin is the model protein because It also forms amyloid fibrils, and the term propagon is used for what would be an αS seed. Amplification reactions are performed in parallel in thousands of uniform pL-sizes droplets and are monitored by THT. The fragmentation step is omitted. Each droplet is labeled as positive or negative by means of thresholding the fluorescent signal. The amount of propagons in a sample is determined by measuring a dilution series of this original sample. All dilutions can be measured at once in the same microfluidic device because the droplets containing different dilutions are separated into different capillaries. A Poisson distribution model is fitted to the fraction of positive droplets to find the amount of propagons in the original sample.

The results of the d-AQuA were then compared to AFM measurements.[43] The average length and height of insulin fibril were measured using AFM. These together with a calculation based on mass conversation convert the fibril concentration (monomer equivalent) to number of fibrils per volume (the equation is explicitly stated in the methods section of the paper). The number of fibrils per volume as found by AFM results is greater than as found by d-AQuA, with the difference being less than one order of magnitude. The authors speculate that perhaps not all fibrils have successfully functioned as propagons in the d-AQuA. The results of the d-AQuA were also compared to SAA results of insulin in a 384-well microplate, which finds two orders of magnitude fewer propagons per volume than d-AQuA. Proposed possible explanations are a loss of fibrils to solid surfaces in the microplate experiment and more effective amplification without solid surfaces with in the d-AQuA.

A digital SAA for αS was developed by Gilboa et al.. [34] They tested SAAs in three compartmentalizations – microwells, droplets, or hydrogel microcapsules – and created calibration curves of percentage of positive wells versus seed concentration. This is more quantitative than just a bulk SAA, but is still not truly quantitative.[38]

Towards a quantitative SAA

The Nanobiophysics research group (the group that hosted this project) has published a proof of principle study on quantitative SAA in 2023, with Vaneyck as the first author.[44]

Vaneyck et al. ran SAA experiments in three different model solutions. Each sample contained a known initial concentration of αS seeds (or fibrils). Vaneyck et al. estimated the number of αS fibrils per volume unit by converting αS fibril concentration (in equivalent reactant αS monomer concentration) to number of αS fibrils. The fibril concentration was determined by centrifuging αS fibrils, so that fibrils and residual monomers would be separated. The residual monomer concentration in the supernatant was determined by measuring the absorbance, which was used to infer the fibril concentration. The conversion itself requires the number of monomers per median fibril, which is established based on the median αS fibril length as found using AFM and an assumed αS fibril structure. The conversion is described in more detail on page 16 in the materials and methods section.

Because this conversion requires the αS fibril concentration to be known, it is not directly useful for unknown samples such as patient material. Vaneyck et al. also provided a theoretical framework for determining the amount of fibrils in an unknown sample. This involves a doubling time (t_D) – the time in which the amount of fibrils doubles. First, it must be assumed that t_D is constant. Therefore the de novo fibril formation should be negligible as compared to seed amplification, and fragmentation and elongation rates should be constant. $N(t)$ – the number of fibrils at timepoint t – can then be expressed as follows:

$$N(t) = N_{seed} 2^{\frac{t}{t_D}}$$

This formula indicates exponential growth, with N_{seed} being the initial number of seeds. Then, at time $t_{threshold}$ – the time it takes to reach a fluorescence threshold – the expression can be rewritten as:

$$N_{threshold} = N_{seed} 2^{\frac{t_{threshold}}{t_D}}$$

It must be noted that $N_{threshold}$ – the number of fibrils at time $t_{threshold}$ – is a fixed number. Rearranging this formula shows how N_{seed} scales with regard to $t_{threshold}$:

$$\log\left(\frac{1}{N_{seed}}\right) \propto \frac{\log(2)}{t_D} t_{threshold}$$

If t_D is constant, the relation between $\log\left(\frac{1}{N_{seed}}\right)$ and $t_{threshold}$ is linear. Vaneyck et al. had run SAA experiments in three different model solutions. They found in each model solution the values of N_{seed} that lead to shorter lag times than the control without seeds, which indicates that seed amplification dominates over de novo fibril formation. For these N_{seed} values a linear relation between $\log\left(\frac{1}{N_{seed}}\right)$ and $t_{threshold}$ can be observed in each model solution. This confirms that – for these values of N_{seed} – t_D was constant, meaning that t_D does not depend on N_{seed}, and that de novo fibril formation had indeed been negligible.

The linear relations in the three model solutions are not the same; there is an offset between them, with unknown causes. As such, it is needed to establish separate reference curves for different biomatrices in order to convert the observed $t_{threshold}$ to N_{seed}.

This project

The goal of this project is to develop a quantitative SAA in which the number of αS seeds (fibrils) will be determined at multiple time points by means of single particle counting (SPC). This project builds further on the work of Vaneyck et al..[44] The SPC allows to verify whether the number of fibrils increases over time, and to directly find the doubling time. This can then be used to quantitatively determine the amount of αS fibrils in the original sample. First, the SPC setup will be established using a model system. Second, various SAA variables will be optimized such as αS strain, fluorescent dye, and αS seed concentration. Third, SAA and SPC will be combined, and further optimized.

2. Materials and methods

1. Seeded aggregation assay (SAA)

1.1. SAA: Experimental methods

All seeded aggregation assays (SAA) were performed in the following buffer: 10 mM NaCl, 10 mM TRIS, 0.02 wt% NaN_3, pH 7.4. The expression and purification of alpha-synculein (αS), and production of αS fibril seeds are described elsewhere.[44] The αS fibril seeds were produced in 10 mM Tris, 10 mM NaCl and 0.1 mM EDTA at pH 7.4. The reactant αS monomer concentration is 50 µM unless specified otherwise. The used concentrations of αS fibril seeds are specified in the main text. The SAA was monitored by either thioflavin T (THT) (10 µM) or Amytracker 630 (concentration is specified in main text), as specified in the main text.

Low-binding pipet tips and Eppendorf tubes (Protein LoBind Tube, Eppendorf) were used for all instances that αS was handled. The used well plates are low-binding as well (Corning® 96-well Half Area Black/Clear Flat Bottom Polystyrene NBS Microplate). Wells were filled with 50 µL of sample, and each condition was measured in triplo (requiring three wells). The well plates were sealed with VIEWseal plate sealer (Greiner, product number 676070). The sealed well plates were then covered with a lid, which was taped shut to avoid evaporation.

Fluorescence was bottom read in a plate reader (Infinite M200 fluorescence plate reader, Tecan) at 37 °C in cycles of 600 s of shaking with an orbital amplitude of 1.5 mm and rpm of 335.8. The number of flashed was set to 5, the integration time to 20 µs, the lag time to 0 µs, and gain to 80. THT fluorescence was measured with 445 ± 4.5 nm excitation and 485 ± 10 nm emission wavelengths; Amytracker 630 with 520 ± 4.5 nm excitation and 630 ± 10 nm emission wavelengths. All measurements were done using the associated i-control software.

1.2. SAA: Data analysis

The lag time determination and evaluation is achieved through self-written MATLAB code.

Determining lag time
The fluorescence data is first smoothed using a Gaussian-weighted moving average filter with a five element sliding window. Then a baseline fluorescence is determined separately for each sample by taking the mean fluorescence of the first five hours. If a sample starts aggregating within this time, a shorter period is chosen. The fluorescence threshold is determined per sample as the baseline fluorescence plus 20 times the standard deviation of the baseline. The lag time is defined here as the time when the fluorescence has permanently crossed this threshold. That is the time after which the fluorescence never drops below the threshold again, i.e. the time of the last fluorescence datapoint under the threshold.

Evaluating found lag times

The outcomes of the lag time determination are first split into two categories: samples that failed to reach the threshold ('non-aggregated samples') and samples that succeeded ('aggregated samples'). The latter are further evaluated by comparing two methods of determining lag times. One method determines the lag time as the time when the threshold is exceeded for the first time ('first point over'), and the other as the time after which the fluorescence never drops below the threshold again ('last point under'). The difference between these two gives information about the quality of the aggregation curve. If 'first point over' minus 'last point under' equals the time between two measurements, then the 'last point under' is immediately followed by 'first point over', which is considered an ideal case. If the absolute difference exceeds that, it means that after crossing the threshold for the first time, the fluorescence falls below it again later, which is not ideal. If the difference in lag time is at most 5 h, it is considered sufficient. If the difference is more than 5 h, the results are inspected and if needed manually processed, such as noting the sample did not aggregate properly at all or setting a different baseline.

2. αS fibril concentration determination

The NanoDrop ND-1000 Spectrophotometer was used to measure the absorbance of residual αS monomers in solution, which is then used to calculate the αS fibril concentration.

The total αS concentration is assumed to consist of the fibril concentration and the residual monomer concentration. It is assumed that centrifuging 50 µL of sample at 18,000 g for 1 hour at room temperature completely separates these two components; that the residual monomer concentration fully resides within the supernatant and the fibril concentration within the pellet. The residual monomer concentration can then be determined by measuring the absorbance using the Nanodrop and plugging this value into the Beer-Lambert law. The fibril concentration can then be calculated by subtracting the residual monomer concentration from the total αS concentration.

Absorbance can be converted to concentration via the Beer-Lambert law, which is as follows[45]:

$$A = \varepsilon l c$$

A is the absorbance, ε is the molar extinction coefficient, l is the optical path length, and c is the concentration.

A buffer solution of TRIS, NaCl, NaN_3, and MilliQ with the concentrations as described for the SAA was used as the blank measurement. About 2 µL of sample is required for each measurement with the Nanodrop. The absorbance was measured at 280 nm and an extinction coefficient of 5600 M^{-1} cm^{-1} was used for αS.[44] The optical path length depends on the chosen setting of the Nanodrop. The absorbance was measured with two different settings on the Nanodrop, Protein A280 and UV-VIS. The optical path length differs for these two settings, it is 1 cm for Protein A280 and 0.1 cm for UV-VIS. The setting Protein A280 is

meant for purified protein populations and UV-VIS for any sample; both measure the absorbance at 280 nm.[46]

3. Conversion of αS fibril concentration to number of αS fibrils

Vaneyck et al. describes a procedure to convert αS fibril concentration (in equivalent reactant αS monomer concentration) to number of αS fibrils.[44]

The αS fibril concentration expressed as equivalent reactant αS monomer concentration specifies the total concentration (M) of reactant αS monomers that are part of fibrils. Each fibril is an aggregate consisting of multiple monomers, but this number is different per fibril. The number of monomers per median fibril is a suitable approximation. Vaneyck et al. assume a fibril structure described in Guerrero-Ferreira et al.: double-stranded with a β-strand distance of 0.5 nm.[44,47] This translates into the following determination of the number of monomers per median fibril:

$$\#\,monomers/median\ fibril = \frac{median\ fibril\ length}{\beta - strand\ distance} \cdot 2$$
$$= median\ fibril\ length \cdot 4 \cdot 10^{9}$$

The median fibril length was determined by means of AFM.

The αS fibril concentration is expressed in M (=mol/L), so it must be multiplied by Avogadro's number to convert it to the number of monomers per L:

$$\#\,monomers\ located\ in\ fibrils \cdot L^{-1}$$
$$= monomer\ equivalent\ fibril\ concentration \cdot\ Avogadro's\ number$$

Finally, the conversion is finalized by combining these two steps:

$$N_{seed} = {}^{\#fibrils}/_{L} = \frac{\#\,monomers\ located\ in\ fibrils \cdot L^{-1}}{(\#\,monomers/median\ fibril)}$$

4. Fluorescence microscopy

An inverted fluorescence microscope (Eclipse TE 2000-U, Nikon) was used to image particles (beads or αS fibrils). αS fibrils were imaged in a 96 well plate unless specified otherwise.

The Amytracker dye was excited with a green 520 nm laser, and the emission was filtered with a 560 nm long-pass filter. The dichroic mirror separates the emission wavelengths from

the excitation wavelengths by reflecting wavelengths shorter than 538 nm and letting through wavelengths longer than 538 nm. THT was excited with a blue-violet 450 nm laser.

Images were acquired through a tailor-made program in LabVIEW. A sequence of images was taken automatically by means of a systematic area scan.

The objective magnification and tube magnification per experiment is listed in Table 1.

Table 1. The objective magnification and tube magnification per experiment.

Experiment and page number	Objective Magnification	Tube Magnification
R1 (page 20)	60	0.52
R3 (page 26)	60	0.52
R7 (page 41)	48.5	1
R8 (page 43)	48.5	1
R9 (page 48)	60	1
R10 (page 50)	60	1
R15 (page 73)	60	1

5. Single particle counting (SPC)

Single particle counting (SPC) was performed using an altered version of TrackPy v0.4.2.[48] TrackPy is a soft matter particle tracking software package for tracking and analyzing moving blob-like particles in Python. The altered version's main purpose is to count particles.

A plethora of particle search parameters can be set to optimize results. It can also produce review images; images that indicate the detected particles, which can be used for visual evaluation. This was used extensively to determine the optimal particle search parameters for each dataset. Images with artefacts were manually removed.

Image sizes are not consistent through all experiments, so all SPC results are corrected to represent the results for images of 100 x 100 µm. The image depth is assumed to be 6 µm.

6. Atomic force microscopy (AFM)

The atomic force microscope (AFM) sample preparation, image acquisition, and image analysis are based on Vaneyck et al..[44]

Sample preparation
Tape was used to cleave a mica disk (muscovite mica, V-1 quality EMS), then 5 µL of sample was pipetted onto it and left to incubate for 15 min, covered by a plastic lid to protect it against dust. The mica disc was washed three times with MilliQ, dried with nitrogen, and left to dry overnight, covered by a plastic lid.

AFM image acquisition
The fibrils on the mica were imaged using the atomic force microscope BioScope Catalyst (Bruker, Santa Barbara, CA, USA) equipped with the probe HQ:NSC36/Cr-Au BS (MikroMasch, Tallinn, Estonia), using cantilever B (force constant is 2 N/m, resonance frequency 130 kHz). The mode was set to soft tapping in air. The scan size was set to 5 µm by 5 µm, the scan rate to 1.0 Hz, the samples/line to 256, and the number of lines to 256.

Image analysis
The obtained AFM images were first flattened in NanoScope Analysis Version 1.50 (Bruker). Fibrils were then manually traced in FiberApp, which automatically measures the length of these tracings.[49]

The fibril lengths were described as a histogram, which was then fitted to an exponential model because the lengths of the fibrils is expected to follow an exponential distribution. The bins in the histogram act as a second variable. The exponential fit is used to find and subsequently remove outlier data that do not fit it. A median fibril length was then obtained, which is necessary for the conversion of fibril concentration to number of fibrils.

7. Sonication and vortexing

Samples were sonicated using a tip sonicator (Branson). Samples of either 500 µL or 200 µL (specified in main text) were placed in 0.5 mL Eppendorf cups and put on ice before and after sonication. Samples were sonicated one at a time by immersing the probe into the sample. During sonication the cup is held in place by a clamp such that the tip sonicator does not touch the walls of the cup. The sonication intensity was set to the lowest. Each sample was sonicated for a duration specified in the main text.

Samples were vortexed in Eppendorf cups using a Vortex-Genie (Scientific Industries).

8. Beads dilution series

Microbeads (Fluoresbrite plain Yellow Green 0.2 micron microspheres; Polysciences, Inc. Warrington, PA) were serially diluted in distilled water into six dilutions: 5,000, 10,000, 15,000, 20,000, 30,000, and 40,000 times diluted. The beads were fluorescently dyed using NileRed. Each dilution was sampled by pipetting 70 µL onto a coverslip cleaned with acetone, and imaged using the fluorescence microscope. The number of particles per image was then counted using the TrackPy software. Bootstrapping was used to construct 95% confidence intervals, by means of 300 bootstrapped samples with each 10 values.

9. Double staining αS fibrils with THT and Amytracker

1 µM of αS fibrils in buffer (as described for SAA) was stained with 1.7 µM Amytracker for about an hour, then 10 µM THT was added. This mixture was left to stand for about two hours. 70 µL of sample was placed in a microscope chamber and analyzed using a confocal microscope (Zeiss LSM 880) with its associated software (ZEN 2.3 SP1 (black edition)). THT fluorescence and Amytracker fluorescence were measured simultaneously. The emission was filtered using a grating monochromator. For THT the excitation wavelength is 458 nm, and the emission filter was set to detect wavelengths between 463 and 554 nm. For Amytracker the excitation wavelength is 561 nm, and the emission filter was set to detect wavelengths between 573 and 710 nm.

The confocal microscope produces images by scanning in horizontal lines. Because fast-moving fibrils in solution lead to distortions in the images, it was decided to opt for images with small horizontal width (64x1024 pixels).

10. SAA and SPC combination experiments

When SPC is combined with an SAA, the SAA monitoring is temporarily halted to be able to perform the SPC. The timings of the SPC measurements were selected as the experiment proceeded. It was intended to perform SPC at least once during each of the three phases of seeded aggregation: lag phase, elongation phase (in which exponential growth occurs), and stationary phase (Figure 1 on page 8).[18] The samples remained in the well plate during SPC measurements.

3. Results

1. Establishing a calibration curve for single particle counting (SPC) within a microbead model system

Introduction
The first step is to establish that the experimental set-up can be used to properly count single particles. For this end a calibration curve within a model system should be obtained.

Materials and methods
The model system consists of fluorescently labeled microbeads that were serially diluted in distilled water. The dilution series consists of six dilutions: 5,000, 10,000, 15,000, 20,000, 30,000, and 40,000 times diluted. Each sample was imaged using the fluorescence microscope. 200 images per sample were obtained. SPC was performed on these images.

These measurements were then compared to the expected number of particles per dilution. Since the concentration of the beads stock solution is unreliable due to imperfect mixing of the beads in the solution, the expected number of particles is not based on the concentration of beads stock solution. The expected number of particles was calculated by taking the measured number of particles of the first dilution (5,000 times) as the base value, and dividing it by the dilution factor of each dilution.

Results and discussion
Figure 2 plots the observed and expected mean number of particles per image. The observed number of particles of the first four dilutions (5,000, 10,000, 15,000, and 20,000) equal the expected number very closely (Figure 2, and Table 7 in appendix). There is a drop between the fourth and fifth dilution (20,000 and 30,000 respectively), the observed ratio between these is 0.28 instead of the expected 0.67. The ratio between the fifth and sixth dilution (30,000 and 40,000 respectively) is again nearly exactly as expected (observed: 0.74, expected: 0.75). Since only one observed ratio is off compared to the expected ratio, it is likely one pipetting error.

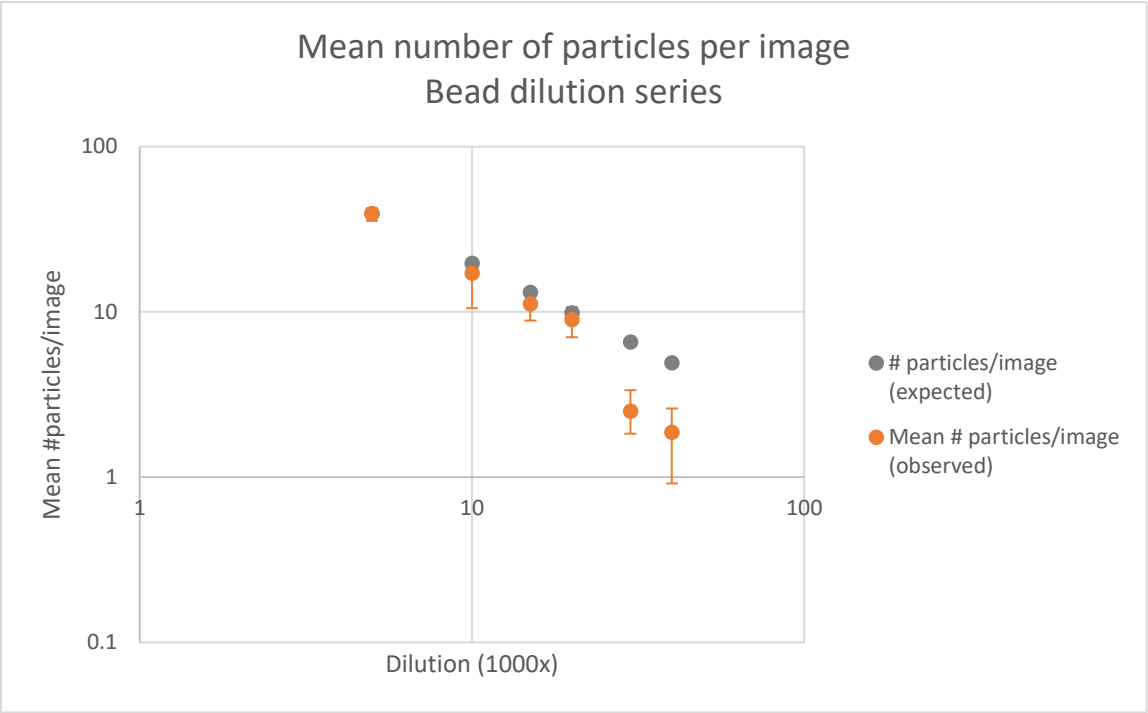

Figure 2. The mean number of particles per image as observed, and expected based on the first measurement.

Conclusion

A sufficient calibration curve of the beads model system was obtained, supporting that this experimental set-up can be used to count single particles.

The only observation inconsistent with the expectation is probably an one-off experimental error.

2. The αS K23Q mutant does not suppress de novo fibril formation in an SAA

Introduction

The potential use of the αS mutant K23Q as reactant monomers is investigated because the K23Q αS mutant has been reported to suppress de novo fibril formation.[40,50] It was found that the K23Q αS mutant fibrillizes similarly to αS WT in presence of αS seeds, but slower in absence of αS seeds (when only de novo fibrillization occurs).[40,50] It would be ideal for the de novo fibril formation to be kept to a minimum. An SAA tests for the presence of αS seeds, so de novo fibril formation gives a false positive result.[18] Also, if the fibril doubling time is to be calculated, the de novo fibril formation is ought to be negligible compared to seeding. Here, it is tested whether K23Q does suppress de novo fibril formation.

Materials and methods

Ten conditions were prepared; they contained 100 µM of either WT αS or K23Q αS mutant monomers, with one of the following five (monomer equivalent) concentrations of αS fibrils: 0 µM (negative control), 0.25 µM, 0.5 µM, 1 µM, and 2 µM. Each sample was measured in triplo. The aggregation was monitored by means of THT fluorescence, for 200 h.

Results and discussion

The aggregation curves are displayed in Figure 51 (appendix).

None of the 0 µM αS fibril control samples aggregated, indicating no de novo fibril formation in either αS type within 200 h (Figure 3, Figure 4). This contradicts the notion that the K23Q αS mutant in absence of αS seeds spontaneously fibrillizes slower than WT αS.[40,50] Koo et al. found that the lag time in absence of seeds is 1.75 ± 0.3 days (= 42 ± 7.2 h) for WT αS and 5.5 ± 0.6 days (= 132 ± 14.4 h) for the K23Q αS mutant.[50]

Multiple explanations can be given for this discrepancy. First and foremost, nucleation is in itself a stochastic process.[51] This hinders the reproducibility.[30] Second, the aforementioned papers had different experimental conditions, such as buffer compositions and methods to measure THT fluorescence intensity. αS aggregation is known to be influenced significantly by a host of environmental factors, such as salt concentration, ionic strength conditions, and pH.[51,52] Also, in this experiment a low binding well plate was used, which suppresses de novo fibril formation.[53]

All seeded WT αS samples reached threshold, except one measurement of 2 µM fibril concentration. Figure 3 displays the lag time for WT αS per αS fibril concentration. The fibril concentrations of 0.5 µM, 1 µM, and 2 µM have similar lag times, but 0.25 µM clearly has a larger lag time.

For the K23Q samples, all samples of the 0, 0.25, and 1 µM fibril concentration failed to start aggregating within 200 h (Figure 4). Only two of the non-control K23Q αS samples reached threshold: 0.5 and 2 µM. Their lag times do no differ significantly.

Compiling all lag times per reactant αS monomer type (while omitting non-aggregated samples) shows that the lag times for WT αS are significantly shorter than for K23Q αS (Figure 5). The mean lag time for WT αS is 26 ± 21 h and for K23Q αS 151 ± 13 h. In total, 11 out of 12 seeded WT αS samples reached threshold and only 5 out of 12 K23Q αS samples. This failed elongation of K23Q contradicts previous reports, which found the K23Q αS mutant to fibrillize similarly to WT αS in presence of fibrils[40,50]; Koo et al. found a lag time of 0.75 ± 0.2 days (= 18 ± 4.8 h) for both.

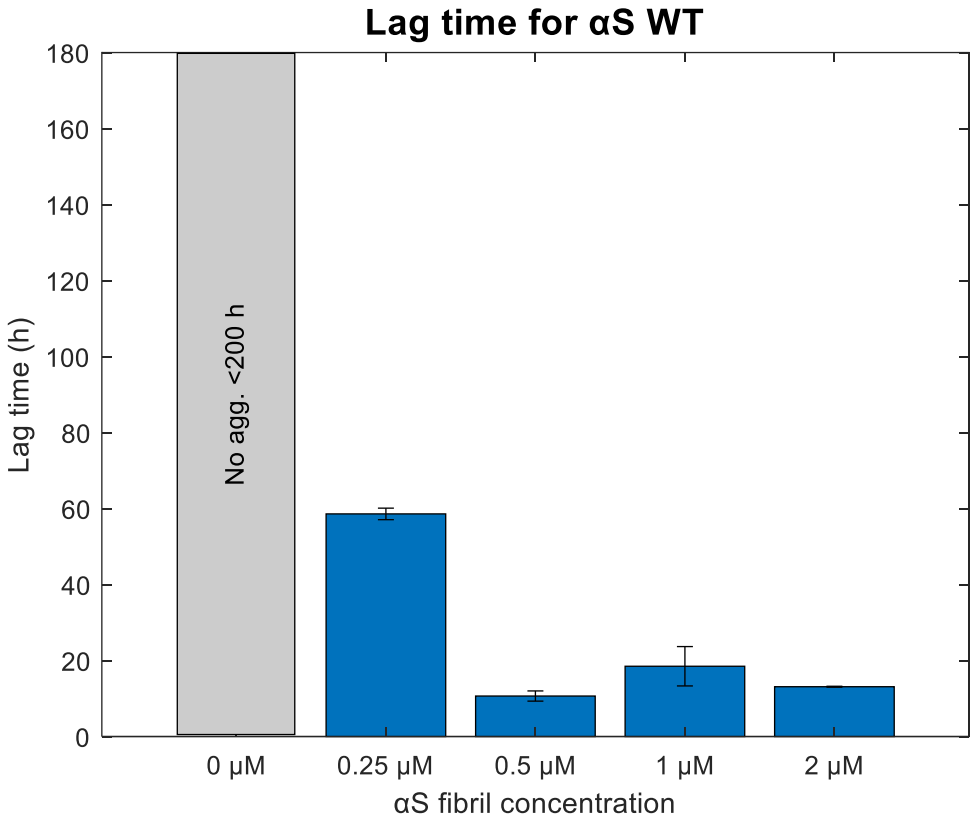

Figure 3. The lag time for WT reactant αS monomers per αS fibril concentration (0 µM, 0.25 µM, 0.5 µM, 1 µM, and 2 µM monomer equivalent). One of the three samples of 2 µM did not aggregate.

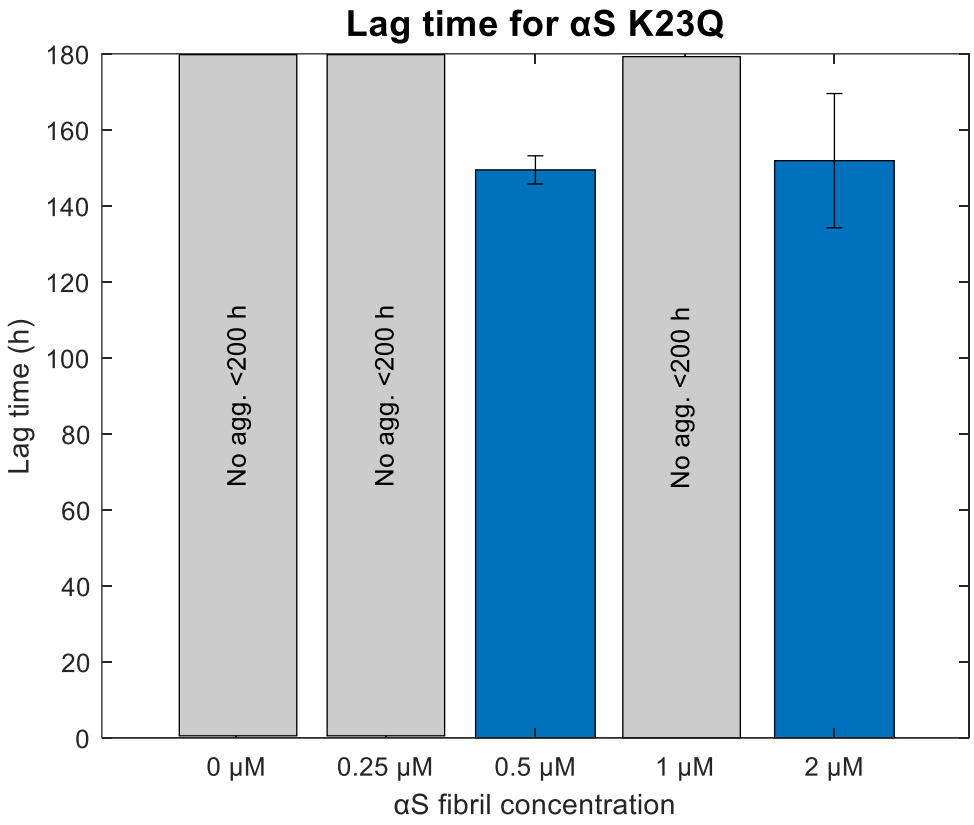

Figure 4. The lag time for K23Q reactant αS monomers per αS fibril concentration (0 μM, 0.25 μM, 0.5 μM, 1 μM, and 2 μM monomer equivalent). One of the three samples of 0.5 μM did not aggregate.

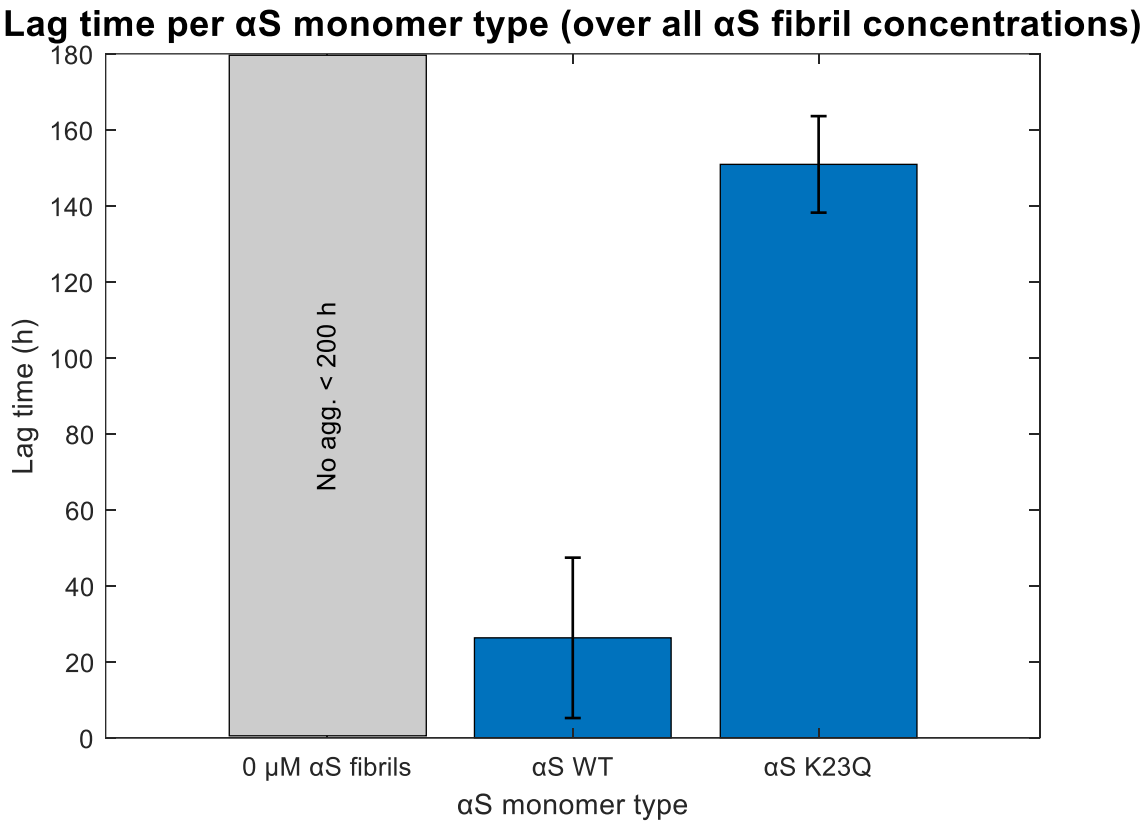

Figure 5. Lag times compiled per reactant αS monomer type. None of the samples of 0 μM aggregated withing the 200 h timeframe of the experiment, so no lag times were obtained.

Conclusion

This experiment found no difference in the de novo fibril formation with either WT αS or K23Q αS mutant within 200 h timescale of the experiment; both failed to aggregate. The K23Q αS mutant more often fails to elongate and elongates slower in presence of αS seeds than the WT αS. Taking these two findings into account, it was decided to use the αS WT as monomeric reactant in all subsequent experiments of this project.

3. Validating the use of Amytracker in SPC of αS fibrils

Introduction
Amyloid fibrils can be stained with THT, but also with other molecules such as Amytracker 630 (referred to as Amytracker for brevity). Its use in SPC of αS fibrils is investigated in this chapter.

Amytracker operates within a different spectrum than THT; Amytracker's emission peak is located at 630 nm (red)[54] whereas THT's emission peak – after binding to an amyloid fibril – is located at 482 nm (blue)[26]. Biological autofluorescence is more common in the green-blue part of the visible light spectrum[55,56], so the fluorescent signal of Amytracker might be more easily distinguished from biological autofluorescence. This is relevant for the goal of diagnosing disease because that involves analyzing samples containing biological fluid or tissue.

In order for Amytracker to perform correctly, it must be diluted into the right concentration range. The suitable range of Amytracker concentration is determined in relation with the αS fibril concentration. Because aggregated samples of WT αS from the previous SAA were used, some additional experiments are needed; for the concentration of αS fibrils is unknown and the fibrils have already been stained with THT. Therefore, this section is split in three parts. First, the αS fibril concentration is determined. These fibrils have been subjected to an aggregation experiment, so the fibril concentration changed and must be redetermined. The fibril concentration cannot be deduced from the initial monomer concentration because generally there are remaining monomers that have not been converted into fibrils.[51] Second, SPC was performed on a dilution series of Amytracker with a constant concentration of αS fibrils, to determine a suitable Amytracker-fibril ratio. Third, it is tested whether Amytracker and THT can simultaneously stain fibrils. This is done last because this is only relevant to evaluate at the Amytracker concentration established by the Amytracker-fibril ratio since this is the Amytracker concentration that will be used in further experiments.

3.1. Determining the αS fibril concentration

Materials and methods
One 0.25 µM αS seed sample that successfully aggregated in a previous SAA experiment (R2 'The αS K23Q mutant does not suppress de novo fibril formation in an SAA' on page 22) was used to determine the αS fibril concentration.

The procedure on the determination of the αS fibril concentration is described in the general materials and methods section. For each of the settings Protein A280 and UV-VIS, four measurements were taken. The total αS concentration is assumed to be the initial reactant αS monomer concentration of 100 µM, because the added seed of at most 2 µM is negligible.

Results
If all measurements are combined, the resulting concentration of αS fibrils is 62.3 ± 13.0 µM (range: [49.3, 75.3] µM).

Discussion
An obvious improvement of the experimental set-up would be to pool all aggregated samples, mix them well, and take a small volume to determine the αS fibril concentration. This would have been more accurate than analyzing one separate sample. Nonetheless, since all samples were fully aggregated, the result of analyzing one sample is probably accurate enough. Also, a more precise spectrophotometer than the Nanodrop could be used.

Conclusion
Taking all measurements together results in a concentration of αS fibrils of 62.3 ± 13.0 µM, that is a range of [49.3, 75.3] µM.

3.2. Determining a suitable Amytracker-fibril ratio by means of a dilution series

The Amytracker-dilution series experiment was performed twice. Only the second is included in the main text. The first, along with more details on experimental choices of the second, can be found in the appendix.

Materials and methods
Five samples were prepared with varying Amytracker concentrations (0.5, 0.6, 0.75, 1, and 1.5 nM) and a constant αS fibril concentration (31.1 ± 6.5 nM, i.e. [24.7, 37.6] nM) in MilliQ. The Amytracker and αS fibrils were diluted separately with MilliQ to the proper concentrations before mixing them to create the final samples.

The used αS fibrils are pooled aggregated samples from a previous SAA experiment (R2 'The αS K23Q mutant does not suppress de novo fibril formation in an SAA' on page 22). It consists of the 0.25 µM, 0.5 µM, 1 µM αS seed samples, with exception of the one sample of 0.25 µM that was used up to determine the αS fibril concentration (R3.1 'Determining the αS fibril concentration' on page 26). All three 2 µM samples were excluded because one failed to aggregate.

Each sample was pipetted onto a coverslip cleaned with acetone, and imaged using the fluorescence microscope. 100 images were taken per sample. SPC was performed on these images.

Results
In total three images with artefacts were removed, i.e. 0.6% of the total number of images across all samples.

Figure 6 displays the mean number of particles per image for each Amytracker concentration, for the original image size instead of the standardized 100 x 100 µm. The aim is to determine an Amytracker range for which fibrils are observable and countable within the volume that the microscope captures. In this case, the original image size is 202 x 81 µm. The number of particles per 100 x 100 µm image is included in the appendix to allow comparison of SPC

results of different experiments. The Amytracker concentrations of 0.75, 1 and 1.5 nM each visualize a similar number of particles per image, of on average 10.6 particles. The Amytracker concentrations of 0.5 and 0.6 nM on the other hand visualize fewer particles, each fewer than 5 particles.

Discussion

Based on these results, the Amytracker concentrations of 0.5 and 0.6 nM seem to underestimate the amount of particles. The fibril concentration is the same for all samples. Therefore, 0.75 –1.5 nM is probably an acceptable Amytracker concentration range. The ratio Amytracker to fibrils would then be between 1:21 and 1:42 (assuming a concentration of 31.1 µM of αS fibrils. See the appendix for the ratio when other values of αS fibrils concentration are considered).

It is important to note that this experiment has established a lower limit on the Amytracker concentration, but not an upper limit. An upper limit does exist, please be referred to the appendix ('Amytracker-fibril dilution series I').

The Amytracker concentrations in this experiment are listed as molar concentrations instead of dilutions (see the appendix for corresponding dilution factors for each concentration). This is necessary to determine an Amytracker-fibril ratio. The stock concentration on the vial of Amytracker 630 was listed as 1 mg/mL. The conversion to molar concentration is complicated by the fact that the molecular weight of Amytracker 630 is not readily available information. I found a product datasheet of Amytracker 680 listing its molecular weight (668.7 g/mol), and I assumed it to be the same for Amytracker 630.[57] Both Amytracker 630 and 680 are recommended for fibrillation assays by the manufacturer.[54] The listed molar concentrations might thus deviate from the true values, but it cannot be confirmed whether this is the case or how much they would deviate. Therefore it is assumed they are correct.

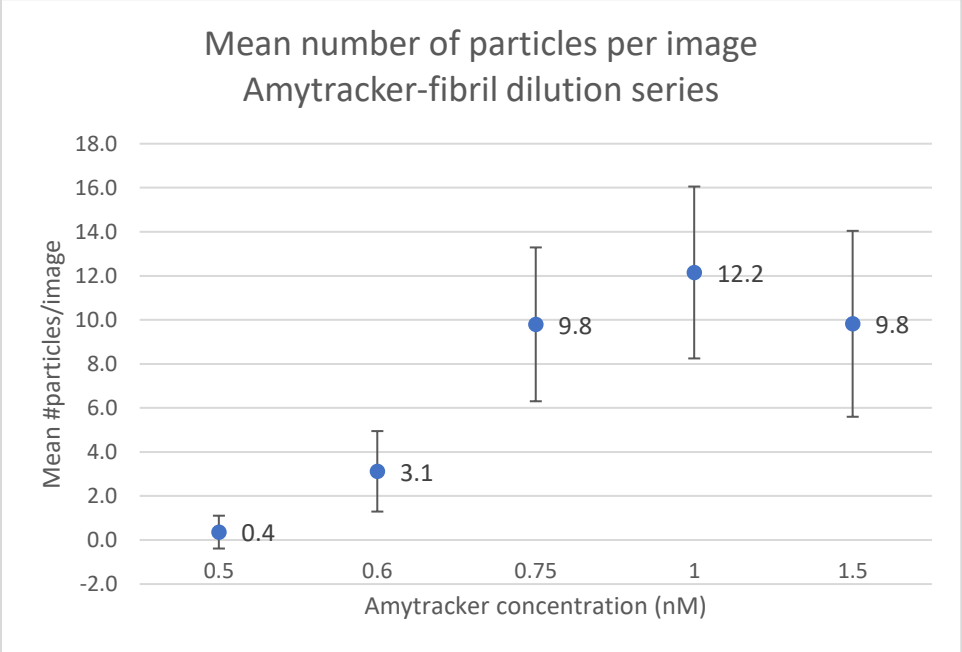

Figure 6. The mean number of particles per image for each Amytracker concentration, for the original image size of 202 x 81 µm.

Conclusion
Staining αS fibrils (31.1 ± 6.5 nM) with 0.75, 1.0 or 1.5 nM Amytracker leads to images with a similar number of fibrils. Therefore, it is concluded that 0.75 –1.5 nM is a suitable Amytracker concentration range to be used in future experiments. The corresponding ratio of Amytracker to fibrils is then between 1:21 and 1:42 (assuming a concentration of 31.1 nM of αS fibrils). It must be noted that this range's 0.75 nM lower limit is actually the smallest concentration that can be used, but that the 1.5 nM is not a true upper limit.

3.3. Amytracker and THT can simultaneously stain αS fibrils

Materials and methods
αS fibrils in buffer were first stained with Amytracker for about an hour and then with THT for an additional two hours. They were subsequently imaged using a confocal microscope where THT fluorescence and Amytracker fluorescence were measured simultaneously.

Results and discussion
90 useable images were obtained. All datapoints from all images were compiled and analyzed. Figure 7 plots the THT intensity against the Amytracker intensity of any given pixel, with a threshold of 5. This means each datapoint represents the THT fluorescence and Amytracker fluorescence for one pixel. Multiple pixels can have the same value for a datapoint. The opacity of a data point very roughly indicates its occurrence (face transparency is set at 0.2 on a [0,1] scale), see the appendix for a more detailed representation. The data is thresholded to remove irrelevant data, see the appendix for details.

Fitting a linear model to the thresholded data shows a linear correlation between THT and Amytracker fluorescence intensity (Figure 7). The fit is good enough to conclude that fluorescence correlates per pixel, and thus that Amytracker and THT can simultaneously stain fibrils.

There is a group of datapoints for which the Amytracker intensity is lower than the THT intensity, which is more pronounced in the non-thresholded data (see appendix). This indicates that THT stains certain areas more than Amytracker.

Please note that the intended Amytracker-fibril ratio for this experiment was 1:30, but due to a simple error the produced Amytracker-fibril ratio is 1:0.6. This is a 50 times difference because the complementary Amytracker concentration was calculated based on an erroneous 50 µM of fibrils instead of 1 µM. This nonetheless led to useable results for this particular experiment using the confocal microscope. Whether an Amytracker concentration of 1.7 µM and an Amytracker-fibril ratio of 1:0.6 will also produce useful results using the fluorescence microscope cannot be confirmed.

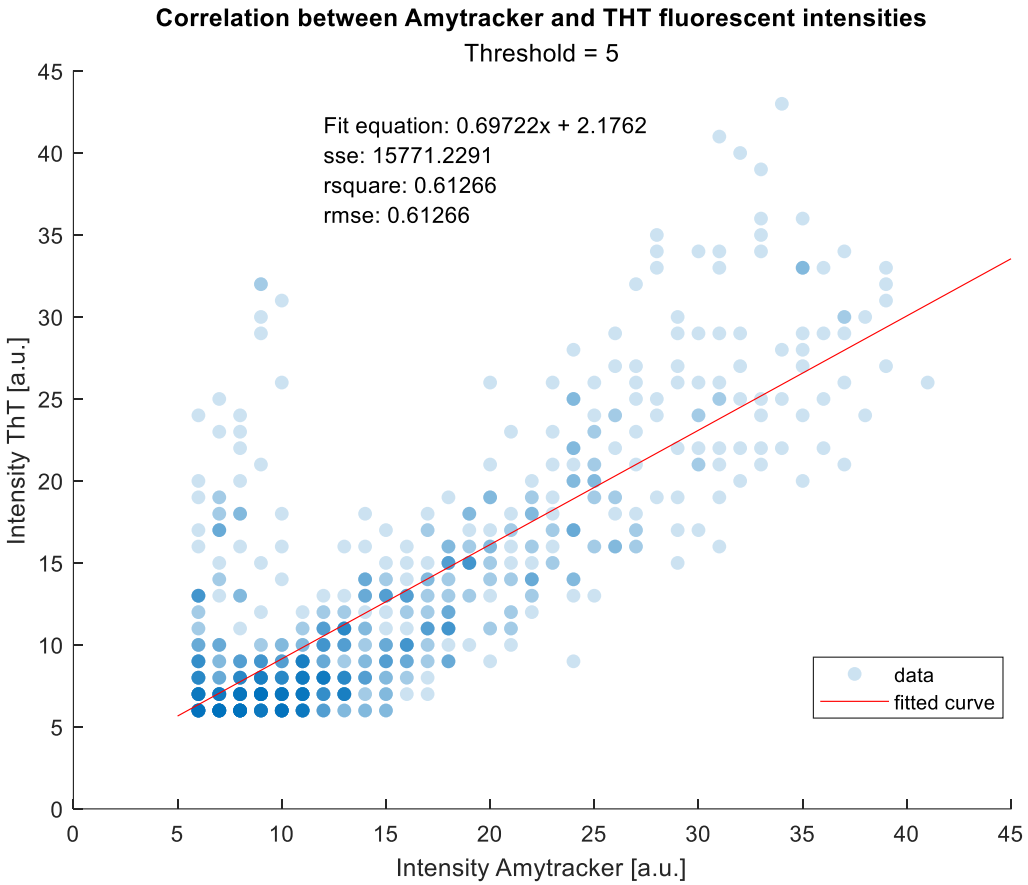

Figure 7. Correlation between THT and Amytracker intensities and a linear fit, with a threshold of 5. Face transparency of data points is set at 0.2 on a [0,1] scale.

Conclusion

Amytracker and THT can simultaneously stain fibrils. This validates the use of THT-stained fibrils in the Amytracker dilution series, and thus supports its conclusion.

4. The effect of sonication on αS fibril concentration

Introduction
Sonicating αS fibrils is known to accelerate αS aggregation[25,58] and improve reproducibility[24]. In this experiment, αS fibrils are sonicated for various time durations and their resultant αS fibril concentrations are determined. These sonicated αS fibrils will be used in forthcoming SAA experiments.

Materials and methods
A stock solution of 50 µM αS fibrils was split into 4 samples of 500 µL each, which were sonicated for 0 s, 1 s , 3 s or 5 s using a tip sonicator.

The procedure on the determination of the αS fibril concentration is described in the general materials and methods section. For each of the settings Protein A280 and UV-VIS, three measurements were taken. The total αS concentration is assumed to be the initial αS concentration of 50 µM.

Results and discussion
Figure 8 displays the average αS fibril concentration per sonication time, as a percentage of the total αS concentration (the results obtained by Nanodrop settings ProteinA280 and UV-VIS are combined, see the appendix for more details). The averages of all samples and the sonicated samples are also shown.

Applying two-sided two-sample t-tests (assuming equal variances) for each pair of samples reveals only significant differences between 0 s and 1 s ($p = 0.015$), and 0 s and 5 s ($p = 0.045$). This indicates that sonication significantly impacts the αS fibril concentration. Also, the unsonicated sample has the largest estimated error of all samples (12.7) (see appendix for all numerical values).

There are no significant differences between the different sonication times with regard to αS fibril concentration. For these sonicated samples, the average αS fibril concentration as a percentage of total αS concentration is 78 ± 4.1%. That corresponds to a αS fibril concentration of 39 ± 2.1 µM.

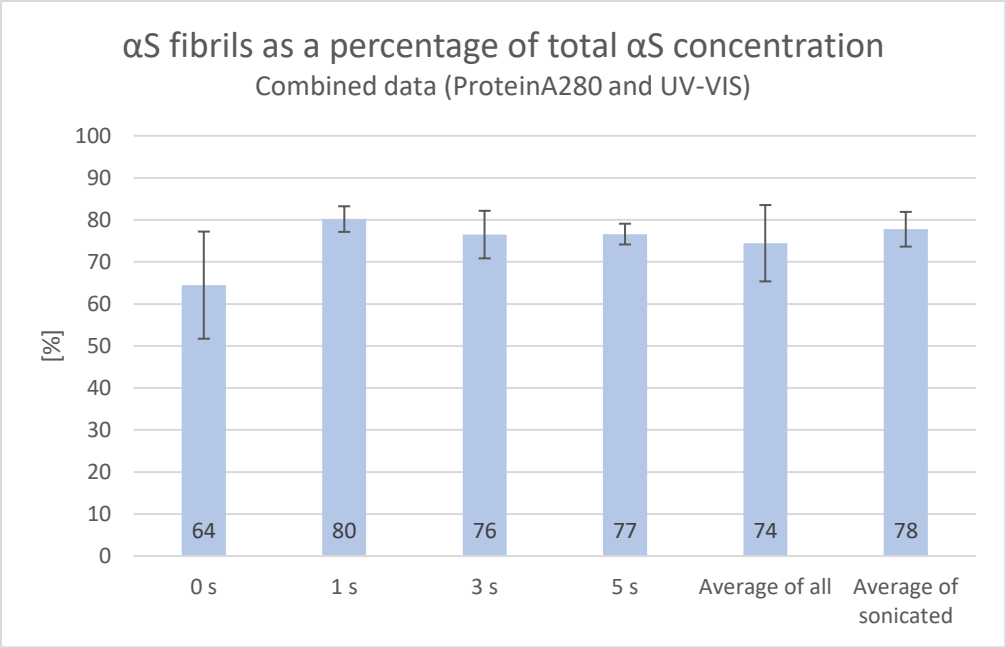

Figure 8. αS fibril concentration per sonication time, as a percentage of the total αS concentration.

Conclusion

Two out of three sonicated samples (1 s and 5 s) had a significantly higher αS fibril concentration than the unsonicated sample, and all had smaller estimated errors. There are no significant differences between the three different sonication times (1 s, 3 s , and 5 s) with regard to αS fibril concentration. Taking all sonicated samples together results in an average αS fibril concentration of 39 ± 2.1 µM, which is 78 ± 4.1% of the total αS concentration.

5. The effect of αS fibril concentration and αS fibril sonication on αS aggregation

Introduction

The ideal aggregation would occur quickly and consistently, for both practical reasons and reproducibility, for both research and diagnostic purposes. Shorter lag times are correlated with higher reproducibility, but lag times can vary from hours, days, and weeks to even months depending on experimental conditions.[51] αS fibril concentration and αS fibril sonication have been reported to influence αS aggregation. A higher αS seed concentration leads to earlier onset of exponential growth[44] and a higher initial aggregation rate[24,25]. Sonicating αS fibrils fragments them and – because fibrils grow from their ends and breakage increases the number of fibril ends[25] – leads to faster aggregation than not sonicating seeds.[25,58] Sonication also improves aggregation reproducibility.[24] Therefore the effect of these two parameters – αS fibril concentration and αS fibril sonication – on αS aggregation is investigated here.

Materials and methods

A total of 32 conditions were prepared. Samples contained αS fibrils at one of 8 concentrations (0, 10^{-6}, 10^{-8}, 10^{-10}, 10^{-12}, 10^{-14}, 10^{-16}, 10^{-17} M equivalent reactant αS monomer concentration) which were sonicated for one of 4 sonication times (0, 1, 3, and 5 s). The aggregation was monitored by means of THT fluorescence, for 1445 h (60.2 days). The chosen concentrations are based on Vaneyck et al..[44]

Results and discussion

The aggregation curves are displayed in Figure 63 (appendix).

Only one sample out of a total of 96 failed to aggregate, one with the lowest αS fibril concentration (10^{-17} M) and an 0 s sonication time.

The highest αS fibril concentration of 10^{-6} M clearly has the lowest compiled mean lag time (10 ± 17 h) (Figure 9). None of other αS fibril concentrations differ so drastically from the negative control with 0 M αS fibrils (508 ± 265 h).

Increasing the sonication time shows a downward trend in lag times (Figure 10 and Figure 11). It also seems to decrease the variance among the triplos (Figure 11). This supports the notion that decreased lag times are correlated with increased reproducibility[51] and that increased sonication time accelerates aggregation[58].

In the 10^{-6} M sample, the lag time of unsonicated sample is notably larger than of the sonicated sample: 32 ± 25 h vs. 2.8 ± 0.1 (1 s sonicated), 2.7 ± 0.1 (3 s sonicated), and 2.5 ± 0.1 h (5 s sonicated). Here too the does the largest sonication time lead to the lowest lag time, albeit with a small difference.

αS aggregation is known to follow a sigmoidal curve.[18] Here it was observed that the fluorescence hits its highest point right after the exponential increase, after which the

fluorescence decreases. The decrease can be slight and then remain roughly constant, or keep decreasing for a longer period of time (Figure 63 in appendix). One interesting finding is that this fluorescence maximum decreases exponentially as the lag time increases (Figure 12). In other words, the later a sample aggregates, the lower its maximum fluorescence. This is probably not the result of photobleaching because then the fluorescence would reduce to zero over time. Perhaps the fluorescent dye is somehow corroded during the course of the SAA. Fibril polymorphs can affect aggregation; certain polymorphs for example are reported to have shorter lag times than others.[59,60] If different αS fibril polymorphs were the cause of the observation in Figure 12, then a more stepwise, grouped relation would be expected.

This experiment had an excessive amount of negative controls. Four conditions contained no αS fibrils at all, one for each of the sonication times. However, since there were no fibrils that could have been sonicated, these four conditions are identical.

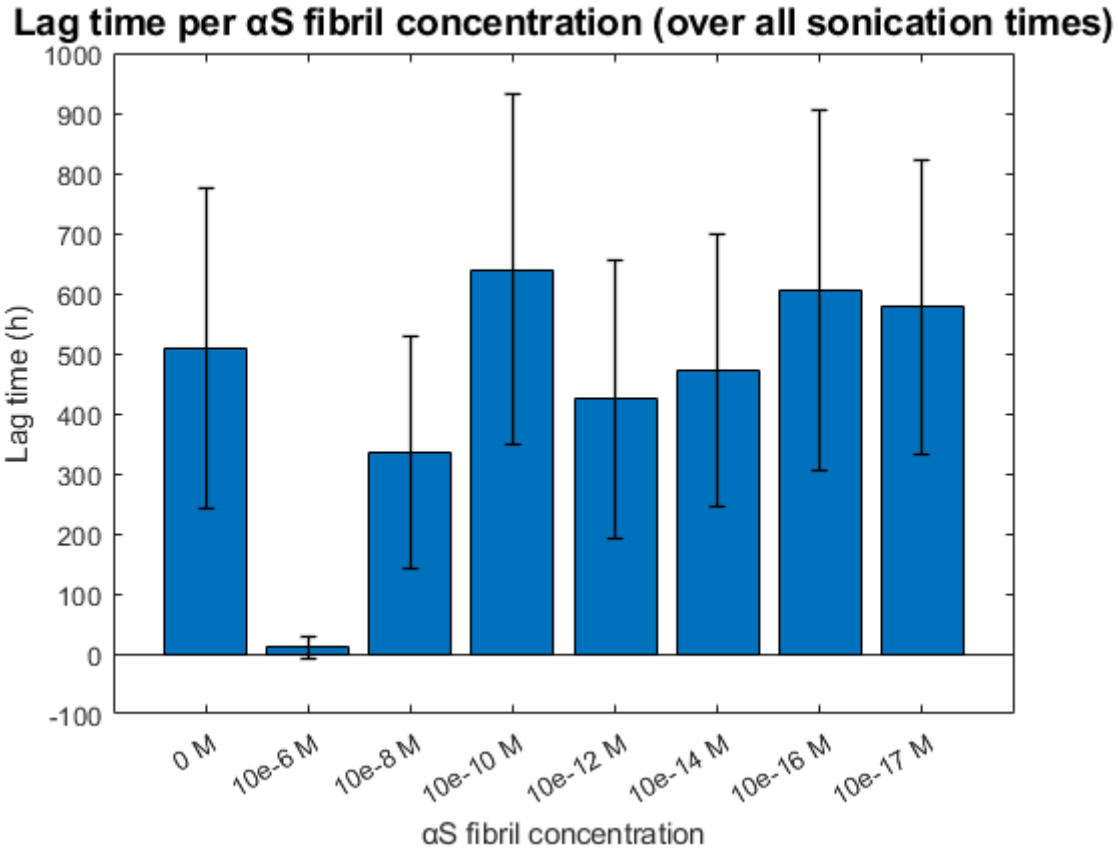

Figure 9. Mean lag time per αS fibril concentration, when all sonication times are compiled per αS fibril concentration.

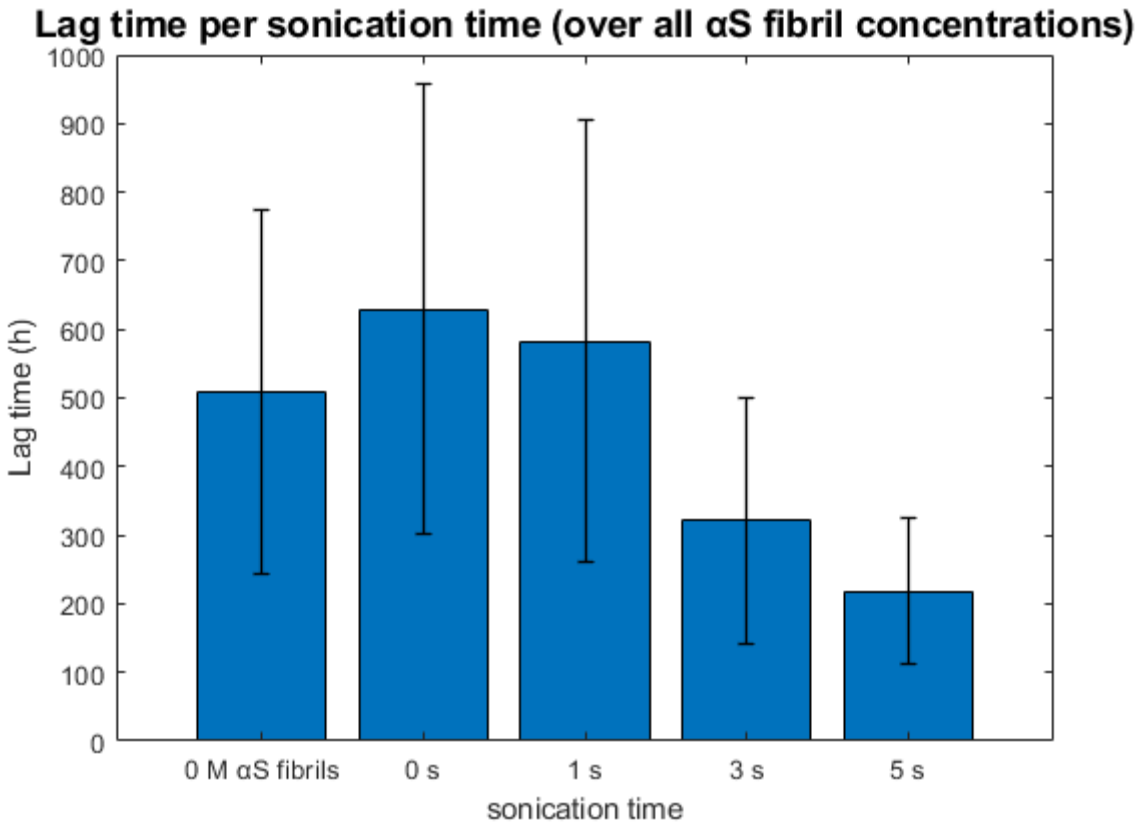

Figure 10. Mean lag time per sonication time, when all αS fibril concentrations are compiled per sonication time.

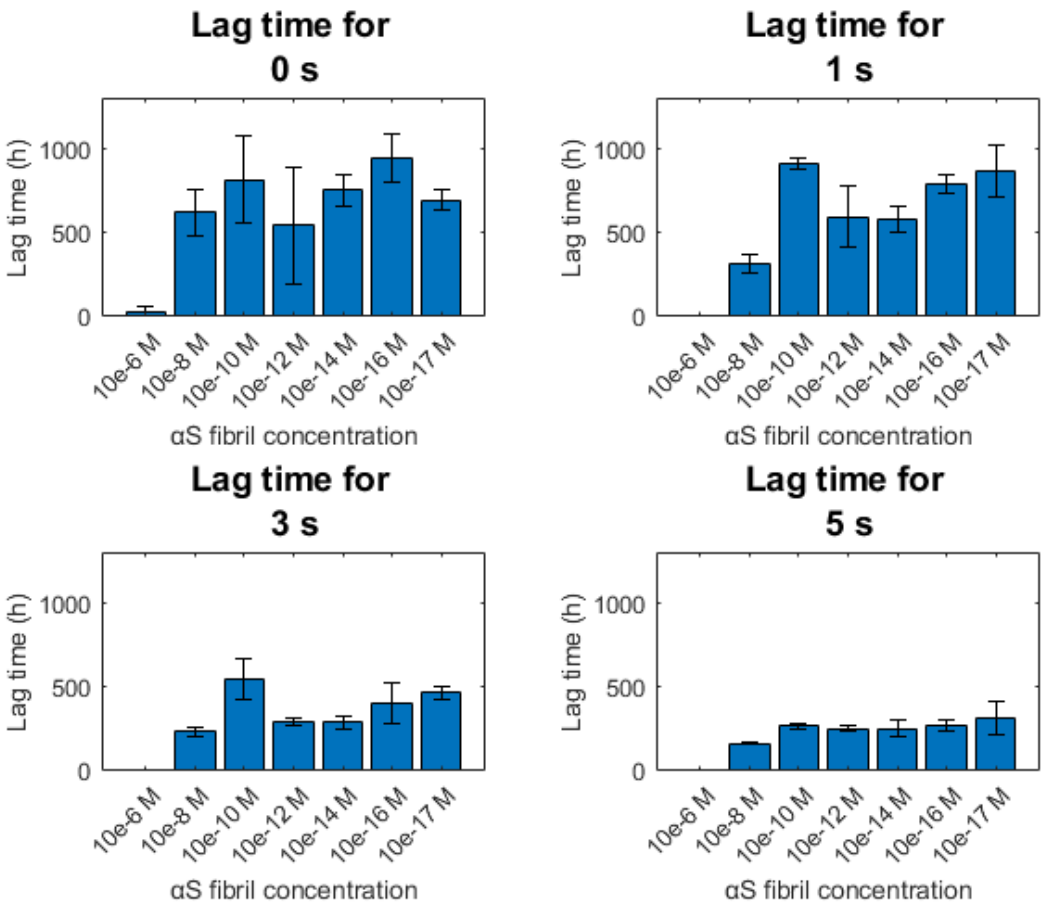

Figure 11. Lag times per sonication time, plotted separately. Please note that the lag times of 10^{-6} M αS fibril concentration are not zero.

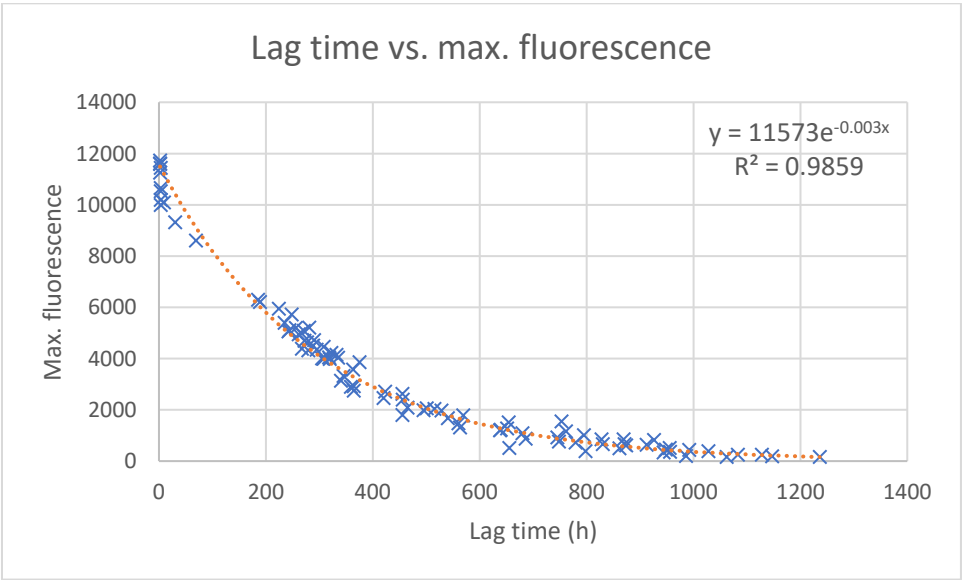

Figure 12. Relation between lag time and maximum fluorescence.

Conclusion

The largest tested concentration of αS fibrils (10^{-6} M) has the lowest lag times. Sonicating the αS fibrils prior to the SAA seems to decrease lag time and variance, with the highest tested time of 5 s leading to the greatest effect.

The fastest aggregating sample tested in this experiment is indeed the one with an αS fibril concentration of 10^{-6} M and a sonication time of 5 s. Its lag time is and 2.5 ± 0.1 h. The difference between the non-zero sonication times for the 10^{-6} M αS fibril concentration is marginal however.

6. Finding the median αS fibril length by means of AFM

Introduction

A core component of this project is quantitatively determining the number of αS fibrils by means of SPC. There also exist methods to estimate the number of αS fibrils based on concentration, such as the one used by Vaneyck et al..[44] Vaneyck et al. describe a method for converting αS fibril concentration (in equivalent reactant αS monomer concentration) to number of αS fibrils based on an assumed αS fibril structure. The only input of this conversion that needs to be experimentally measured is the median αS fibril length.
In this experiment, the median length of sonicated αS fibrils is determined by means of atomic force microscopy (AFM). In other experiments the results of the SPC and Vaneyck's estimation will be compared.

Materials and methods

The αS fibrils that were sonicated for 5 s from a previous experiment (R4 'The effect of sonication on αS fibril concentration' on page 31) are imaged by means of AFM in order to find the median fibril length. This parameter is then used in the conversion from αS fibril concentration to number of fibrils as described by Vaneyck et al..[44]

Results and discussion

22 AFM images with in total 2213 fibrils were obtained. A typical image is shown in Figure 13. Fibrils smaller than 60 nm and larger than 700 nm were removed from the dataset (the appendix describes the specific motivation for removing data). This resulted in a total count of 1581 fibrils (71% of total number of measured fibrils) ranging in length from 78 to 686 nm.

The fibrils lengths are plotted in a histogram with 30 bins in Figure 14. An exponential model was fitted to this data (Figure 15). With an R^2 of 0.9760 and adjusted R^2 of 0.9751 (see appendix), the model was deemed a good fit, supporting the notion that the fibril lengths follow an exponential distribution.

The median seed length was derived from this model and compared to the results of Vaneyck et al..[44] (Table 2. Comparing this experiment's outcome of measuring median fibril length by means of AFM and the literature. Table 2). The median fibril length and thus also the number of monomers per median fibril is about five times smaller than of Vaneyck et al.. The number of seeds per µL is a factor 10 larger. The median fibril length in this experiment might be smaller because the fibrils were sonicated using a tip sonicator instead of a bath sonicator. A tip sonicator is inserted into the sample itself and transfers more energy to the system, possibly resulting in more fibril breakage and thus shorter fibrils.

The used method for fibril measuring introduces some limitations. First, tracing the fibrils is a manual process, so it is subject to human error and subjectivity. Second, the FiberApp program limits the range of fibril lengths that can be measured. Lengths can only be measured in step sizes of 19.6 nm. It also introduces a minimal length that can be measured, so fibrils shorter than that cannot be correctly measured.

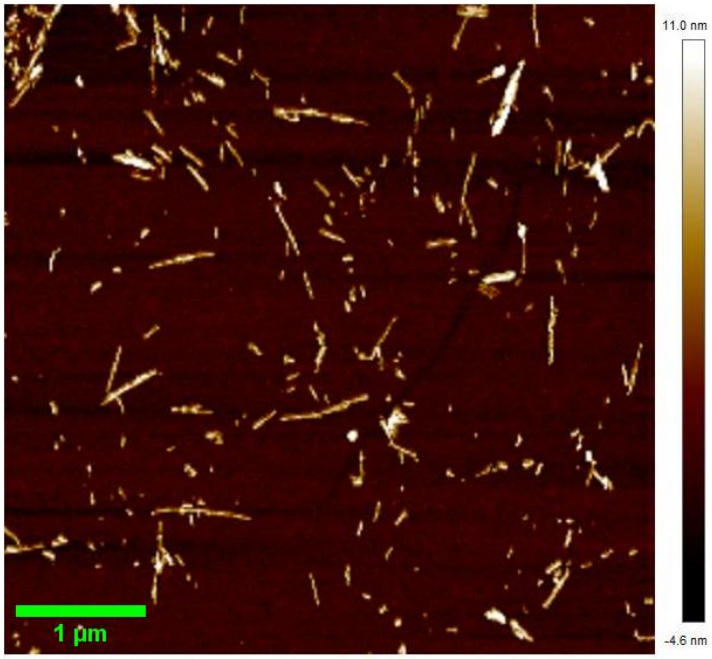

Figure 13. Typical AFM image of αS fibrils (after flattening). The vertical color scale bar indicates height. The image size is 5 µm by 5 µm.

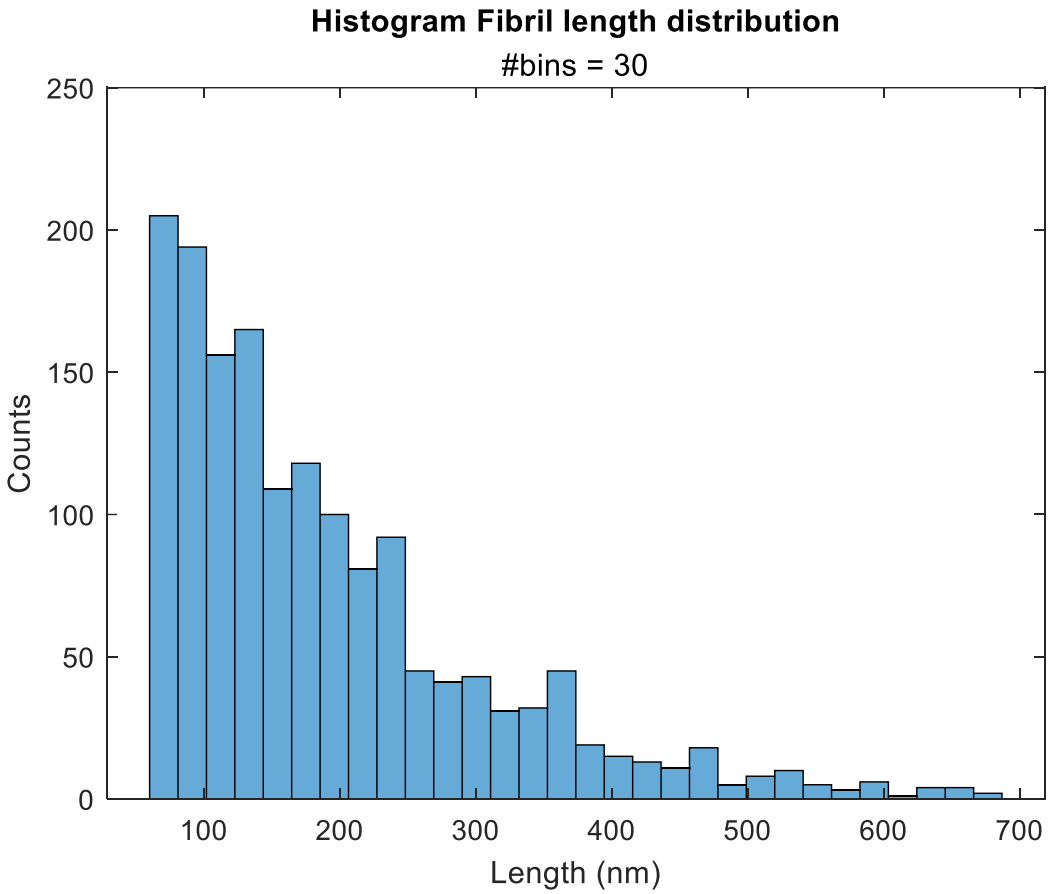

Figure 14. Histogram of measured fibril lengths, with fibrils smaller than 60 nm and larger than 700 nm removed.

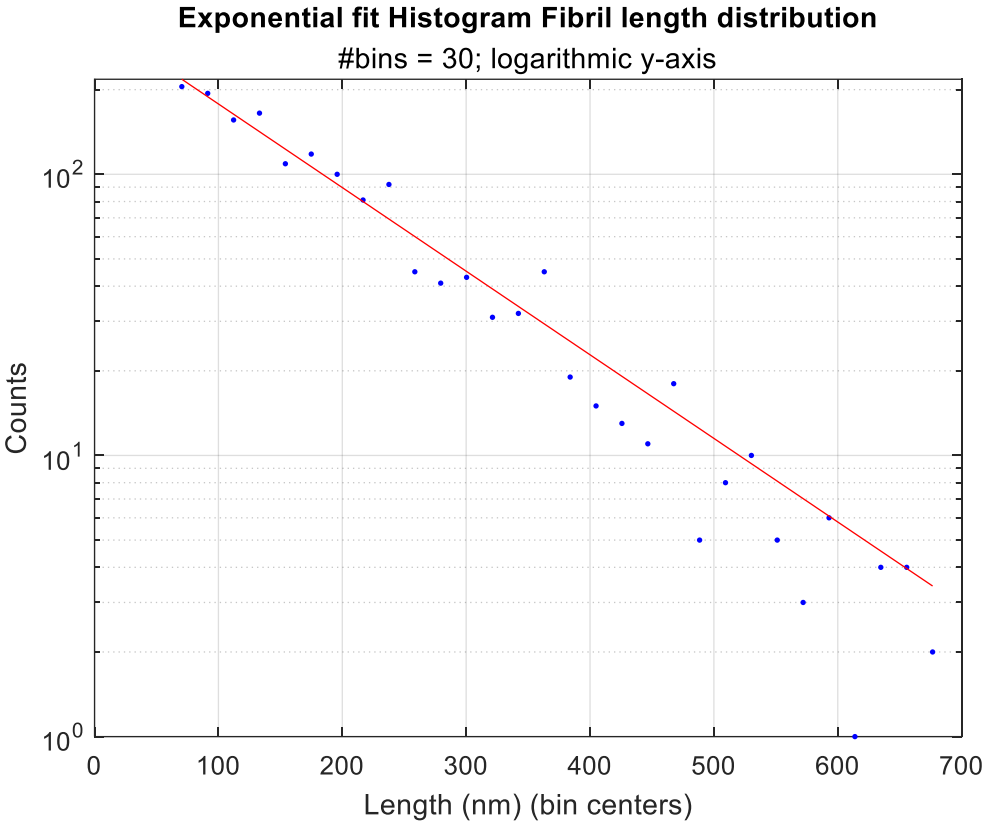

Figure 15. Exponential fit of histogram of measured fibril lengths, with fibrils smaller than 60 nm and larger than 700 nm removed.

Table 2. Comparing this experiment's outcome of measuring median fibril length by means of AFM and the literature.

Source	**Median fibril length (nm)**	**# monomers per median fibril**	**# seeds / µL ([seed] = 1 nM)**
Vaneyck et al.[44]	570	2280	2.64E+05
This experiment	101	404	1.49E+06

Conclusion

The median fibril length of αS fibrils that were sonicated for 5 s in a previous experiment ('The effect of sonication on αS fibril concentration' on page 31) was determined to be 101 nm and the number of monomers per median fibril 404. This information can be used to convert αS fibril concentration (expressed as monomer equivalent monomer concentration) to number of fibrils. (this was applied in R7 'SPC can be performed on Amytracker-stained αS fibrils in a 96 well plate' on page 41, and R9 'SPC can be performed on THT-stained αS fibrils in a 96 well plate' on page 48.)

7. SPC can be performed on Amytracker-stained αS fibrils in a 96 well plate

Introduction

The major step of this project is to construct an experimental set-up in which an SAA can be run while intermittently performing SPC without removing the sample from the 96 well plate. A 96 well plate is not a common container to use for single molecule fluorescence microscopy. Therefore, it is tested whether the fluorescence microscope can image countable αS fibrils stained with Amytracker in a 96 well plate.

Additionally, the number of counted αS fibrils and the expected number of αS fibrils are compared. The number of counted αS fibrils is found in this experiment through SPC using the fluorescence microscope. The expected number of αS fibrils is calculated based on the αS fibril concentration as described by Vaneyck et al., along with the required inputs found in previous experiments as detailed below.[44]

Materials and methods

The αS fibrils that were sonicated for 5 s from a previous experiment (R4 'The effect of sonication on αS fibril concentration' on page 31) were used in this experiment. A 50 µL sample consisting of 35 nM αS fibrils and 1.2 nM of Amytracker (Amytracker-fibril ratio is 30) (no monomers were added) in MilliQ was pipetted into a well of a 96 well plate, and imaged using a fluorescence microscope. Four times 100 images were obtained. SPC was performed on these images. The number of particles per volume could then be calculated using the image depth of 6 µm.

The expected number of αS fibrils is calculated as described by Vaneyck et al.[44], i.e. the αS fibril concentration (in equivalent reactant αS monomer concentration) is converted to number of αS fibrils. For the calculating this expected number of fibrils, the following two assumptions are made:

- The median fibril length is 101 nm, and thus there are 404 monomers per median seed (based on the experiment R6 'Finding the median αS fibril length by means of AFM' on page 38).
- 78% of the αS fibrils is in fibril form after sonication (based on the experiment R4 'The effect of sonication on αS fibril concentration' on page 31).

Results and discussion

Figure 16 displays representative images of αS fibrils stained with Amytracker in a 96 well plate. The contrast of the images is lesser than of the beads dilution series; the background is noticeably darker (compare to Table 8 in appendix). The fibrils are not as spherical as the beads, but are still mostly blob-like.

The mean number of counted fibrils per image is 4.6 ± 1.5. That corresponds to 7.7E+10 fibrils/L.

The expected number of fibrils based on the αS fibril concentration of 35 nM is 4.0E+13 fibrils/L. The corresponding number of fibrils per image would be 2.4E+03.

The expected number of fibrils is three orders of magnitude higher than the observed number of fibrils. An explanation for this discrepancy could be that the fibrils are arranged into clusters, or that the small fibrils are not detected due to the microscope's diffraction limit.

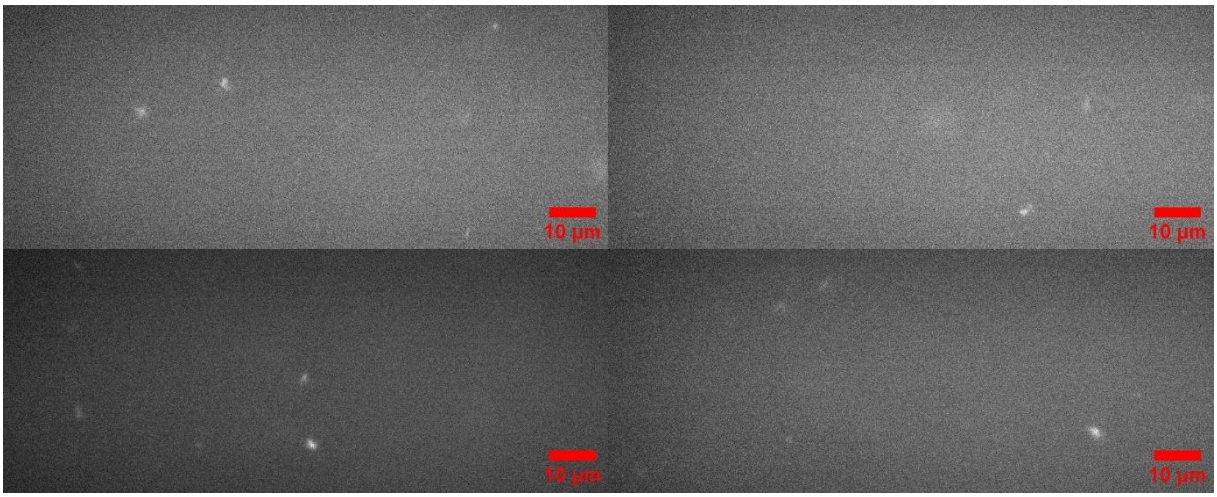

Figure 16. Representative images of αS fibrils stained with Amytracker in a 96 well plate (gain=20 dB). The image size is 130 x 52 µm; the scalebar is 10 µm.

Conclusion

The microscope set-up can obtain images of countable αS fibrils stained with Amytracker in a 96 well plate.

The expected number of αS fibrils based on the concentration (as described by Vaneyck et al. [44], and with the necessary information determined in previous experiments) does not accurately correspond with the observed number of αS fibrils based on SPC; the expected number is three orders of magnitude higher than the observed number.

8. Combining SAA and SPC: attempt 1 and 2 (Amytracker)

Introduction
After confirming that images with countable Amytracker-stained αS fibrils can be obtained in a 96 well plate (R7 'SPC can be performed on Amytracker-stained αS fibrils in a 96 well plate' on page 41), an experiment combining the SAA and SPC is executed. An SAA is run while SPC is intermittently performed without removing the sample from the 96 well plate.

Materials and methods
Four conditions with one of four different αS fibril concentrations were prepared (0, 10^{-6}, 10^{-8}, 10^{-10} M equivalent reactant αS monomer concentration). The aggregation was monitored by means of Amytracker fluorescence. 40 images per sample were obtained each measurement by fluorescence microscopy. SPC was performed on these images.

Results
SAA
This experiment was conducted twice. Neither attempt showed proper aggregation through the fluorescent signal.

In the first attempt, the emission and excitation wavelengths were initially set incorrectly on the Tecan – it was set to THT's spectra instead of Amytracker's – for the entire duration of the experiment (about 245 h ≈ 10 days). The fluorescent signal stayed constant and near zero (Figure 17), so the fluctuations in signal can be interpreted as noise. When this mistake was noted, the aggregation was measured for an additional 20 h using the correct settings, but this did not significantly affect the results (Figure 18).

In the second attempt, the settings were correct from the start, but no proper aggregation occurred within the measured time (290 h ≈ 12 days) (Figure 19). Direct after t = 0 h, there was only a very small increase in fluorescence, but the signal stayed close to zero (Figure 70 in the appendix). The SAA ran for 8 hours until it was stopped abruptly due to an error caused by the Tecan software, leading to a pause of 12 hours. There was a similarly small increase right after the restart. After this, the signal remained roughly constant, or even seemed to decrease to below zero. This also could be interpreted as merely noise.

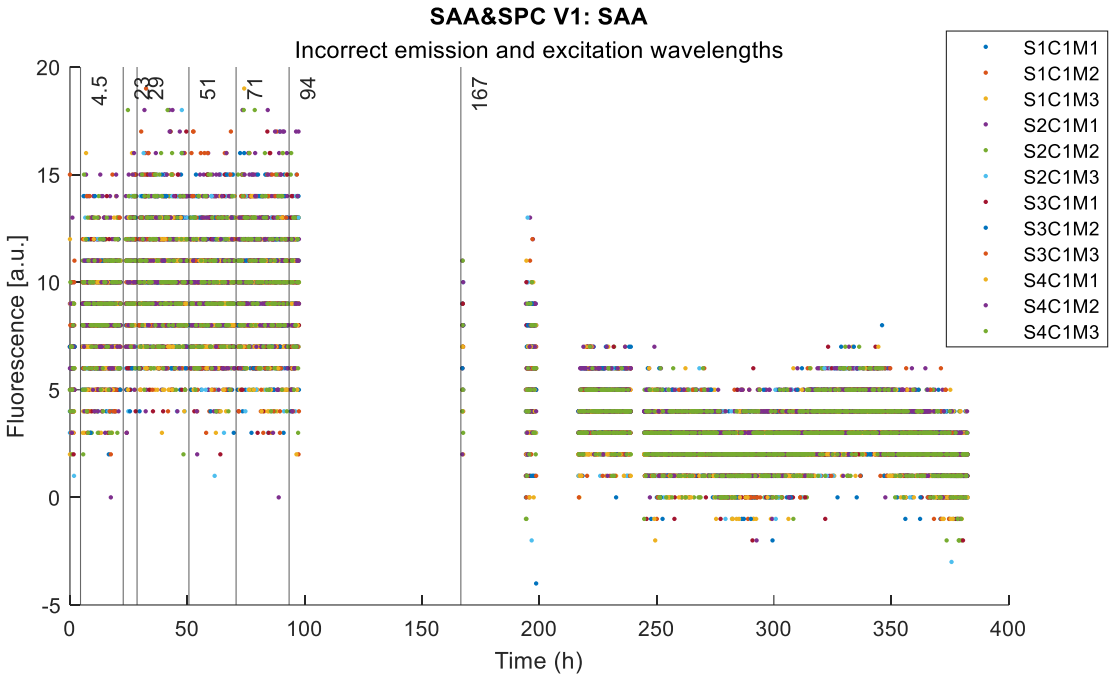

Figure 17. Fluorescent signal of the Amytracker-stained αS fibrils of the first attempt of combining SAA and SPC. The excitation and emission wavelengths were set incorrectly to 445 ± 4.5 nm and 485 ± 10 nm respectively, which match the spectra of THT and not those of Amytracker. The vertical lines indicate measurement times for the SPC measurements. The gaps starting from t = 98 h, 168 h, 199 h, and 239 h are the result of the software aborting the measurement for unknown reasons.

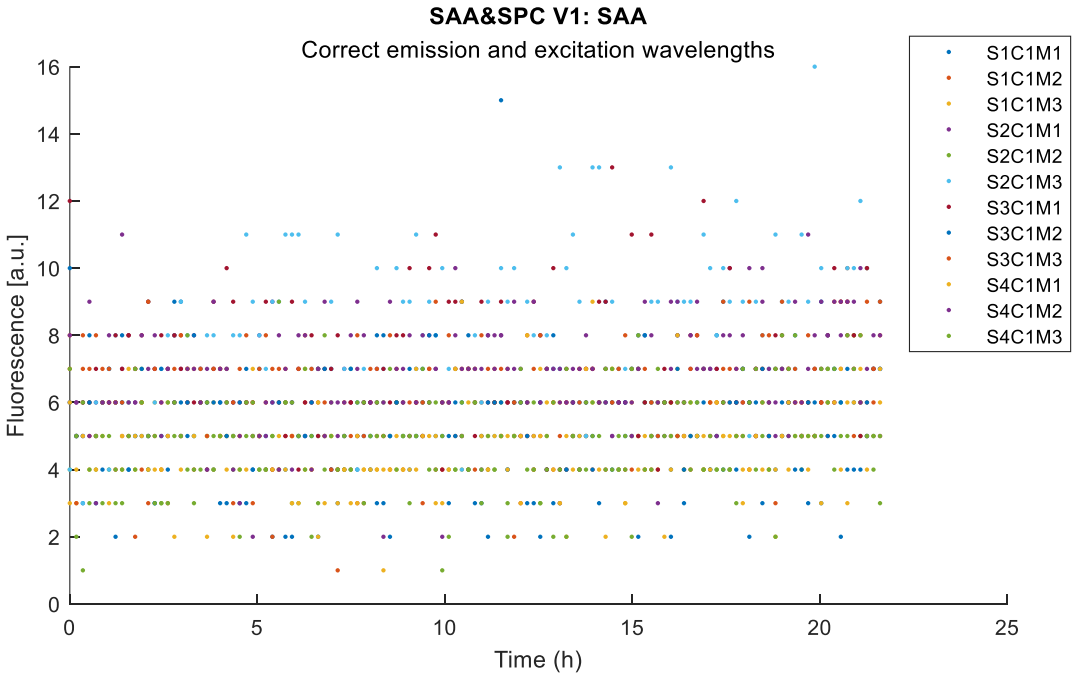

Figure 18. Fluorescent signal of the Amytracker-stained αS fibrils of the first attempt of combining SAA and SPC. The excitation and emission wavelengths were set correctly to 520 ± 4.5 nm and 630 ± 10 nm respectively.

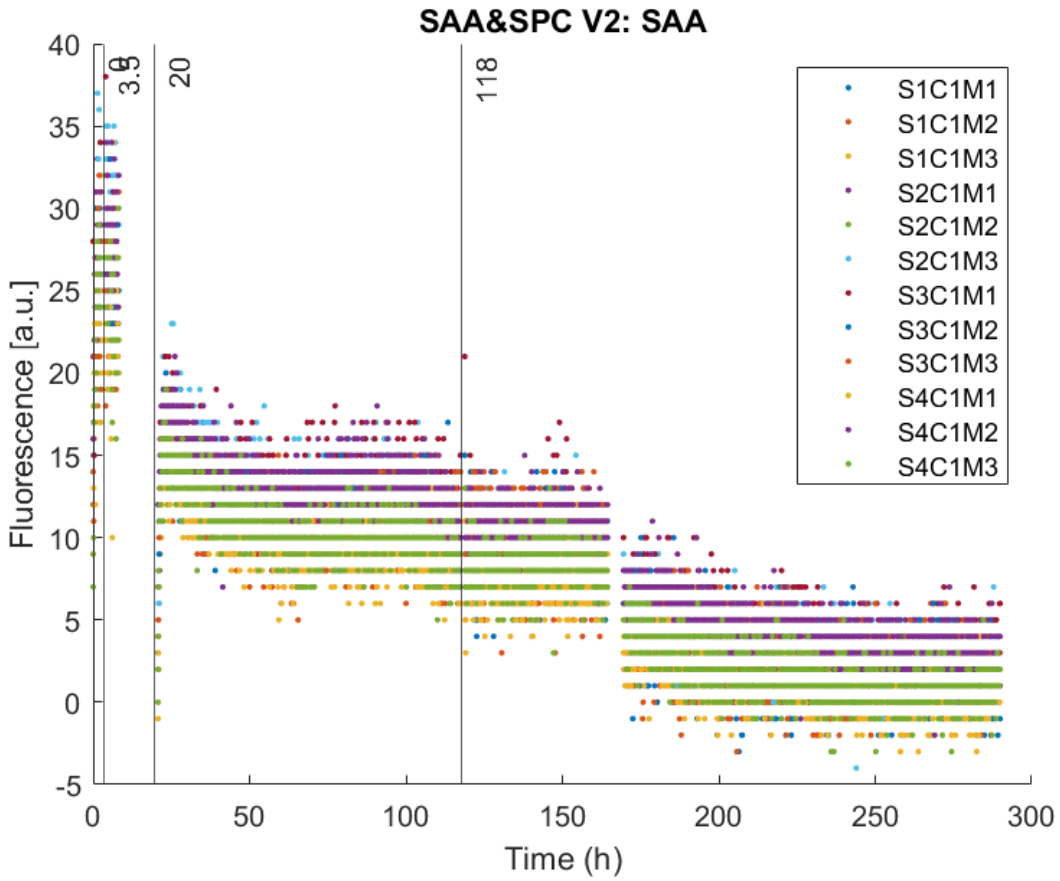

Figure 19. Fluorescent signal of the Amytracker-stained αS fibrils of the second attempt of combining SAA and SPC. The excitation and emission wavelengths were set correctly to 520 ± 4.5 nm and 630 ± 10 nm respectively. The vertical lines indicate measurement times for the SPC measurements. The gaps starting from t = 8 h and 164 h are the result of the software aborting the measurement for unknown reasons.

SPC

For the first attempt, the samples were imaged seven times in the timespan of seven days at timepoints 4.5 h (≈ 0.18 days), 22.7 h (≈ 0.95 days), 28.6 h (≈ 1.2 days), 50.7 h (≈ 2.1 days), 70.8 h (≈ 3.0 days), 93.4 h (≈ 3.9 days), and 166.6 h (≈ 6.9 days).

One of the three samples of 10^{-6} M αS seed condition was removed because particles could not be counted (Table 23 in the appendix). The number of counted particles of all conditions stays roughly constant; no clear increase was found (Figure 20). Nonetheless, images taken at 93.4 h of conditions with 10^{-8} M and 10^{-10} M αS seeds show very long fibrils, indicating that aggregation has occurred (Figure 21, and Table 24 in the appendix).

The concentration of initial fibrils does positively correlate with the number of fibrils per image, as the 10^{-6} M αS seed condition has the highest number of fibrils per frame, then 10^{-8} M, and 10^{-10} M and the negative control without αS seeds have the lowest. For the latter two, the mean number of fibrils per image is almost exclusively below one.

For the second attempt, the samples were imaged four times in the timespan of five days at timepoints 0 h (= 0 days), 3.5 h (≈ 0.15 days), 19.8 h (≈ 0.83 days), and 117.7 h (≈ 4.9 days).

The 10^{-6} M αS seed condition had to be removed because none of the triplicate could be counted (Table 25 in the appendix). Again, the number of counted particles of all conditions stays consistent without a significant increase (Figure 22). Like in first attempt, the 10^{-8} M αS seed condition has a higher number of fibrils per frame than the 10^{-10} M condition and the negative control.

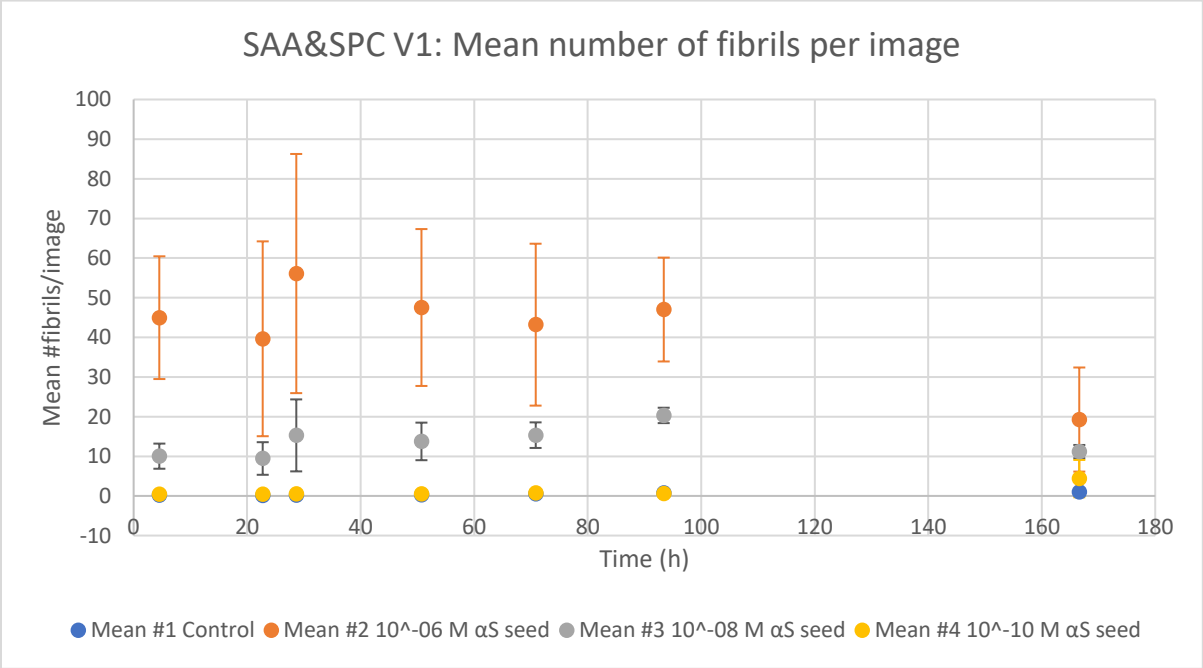

Figure 20. The mean number of fibrils per image as found by SPC for the first attempt of combining SAA and SPC.

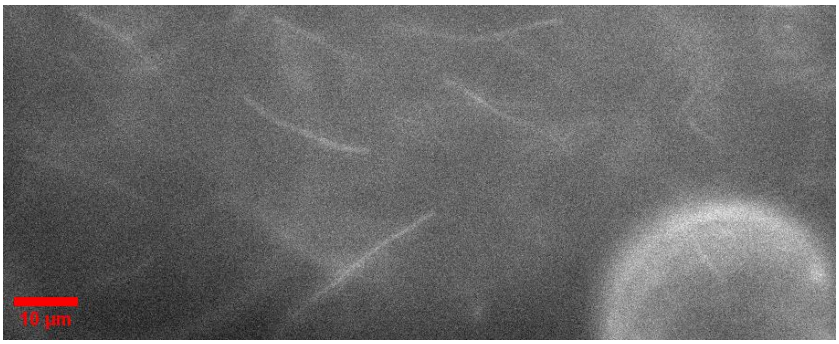

Figure 21. Fluorescence microscopy image of 10^{-8} M αS fibril sample #2 measured at t = 93 h, for the first attempt of combining SAA and SPC.

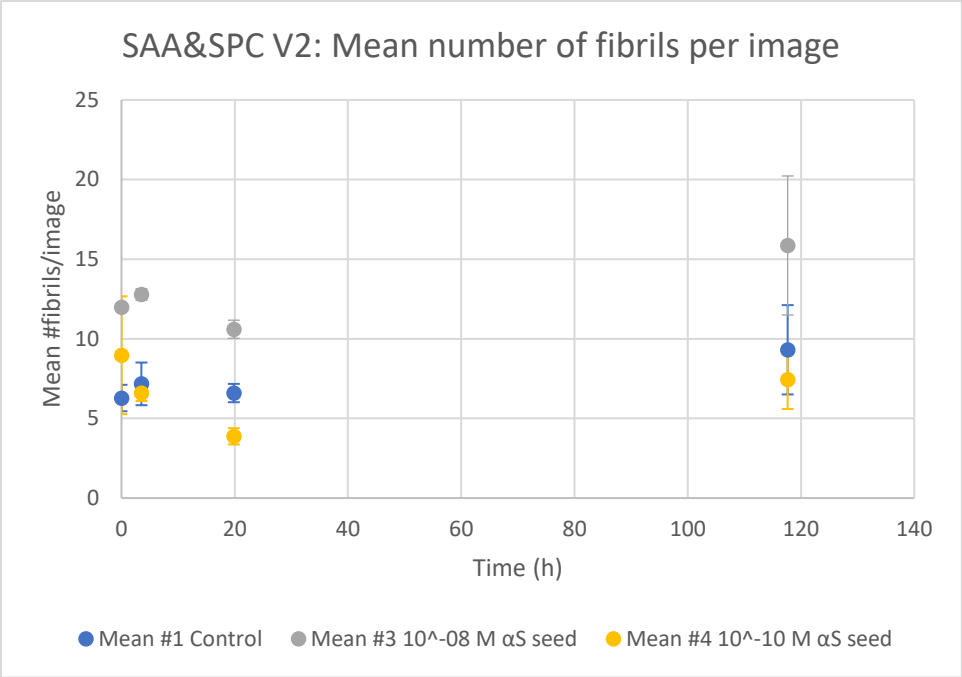

Figure 22. The mean number of particles per image as found by SPC for the second attempt of combining SAA and SPC.

Discussion

The experiment was conducted twice, and both times it was unsuccessful. This is most likely due to a small input error in calculating the pipetting scheme, which led to an erroneous Amytracker-fibril ratio of 1:300 instead of the intended 1:30. This probably stains some αS fibrils, but is too little to stain all αS fibrils. This would explain both the SAA and SPC results. The number of counted fibrils does not increase, while the images do show very long fibrils which indicates aggregation. The SAA of the second attempt showed a small increase in fluorescence only at the beginning, possibly because that is all the present Amytracker could stain. The fluorescent signals of both attempts further stayed constant over time. This mistake was unfortunately only discovered after completing the second attempt.

In total, SPC data of four of the six samples of the 10^{-6} M αS seed condition had to be removed because particles could not be counted properly. The images were too bright and lacked sufficient contrast. The total αS fibril concentration during or after aggregation might have been so high that the emitted fluorescence of the dye saturated the images. This then might be solved by lowering the amount of reactant αS monomers in the reaction mixture.

Conclusion

Neither the SAA nor the SPC shows significant aggregation in either attempt of the experiment. This most likely caused by mistakenly adding a deficit amount of Amytracker.

9. SPC can be performed on THT-stained αS fibrils in a 96 well plate

Introduction
The first two attempts combining SAA and SPC were unsuccessful. At the time being, the experimental mistakes had gone unnoticed, so it was decided to repeat the experiment with THT instead of Amytracker. Therefore, the test whether the fluorescence microscope can image countable αS fibrils in a 96 well plate must also be repeated, but now with THT-stained αS fibrils.

Materials and methods
The methods from 'SPC can be performed on Amytracker-stained αS fibrils in a 96 well plate' (page 41) were repeated, except the fibrils were dyed with THT instead of Amytracker, and the fibril concentration is 1 µM. 72 images were obtained though fluorescence microscopy.

Results and discussion
Figure 23 displays representative images of αS fibrils stained with THT in a 96 well plate. The obtained images with THT are higher in brightness and lesser in contrast than those obtained with Amytracker (compare with Figure 16). Particle counting might thus be less accurate and more subjective. Whether this is due to the higher fibril concentration or the dye cannot be determined from this experiment.

The mean number of counted αS fibrils per image is 161 ± 22. That corresponds to 2.7E+12 fibrils/L.

The expected number of αS fibrils based on the αS fibrils concentration of 1 µM as described by Vaneyck et al.[44] is 1.2E+15 fibrils/L. The corresponding number of fibrils per image would be 6.98E+04.

The expected number of αS fibrils is three orders of magnitude higher than the observed number of αS fibrils, which is the same as the Amytracker-stained αS fibrils ('SPC can be performed on Amytracker-stained αS fibrils in a 96 well plate' on page 41). The number of THT-stained fibrils per image or liter cannot be compared directly to the Amytracker-stained αS fibrils because the fibril concentrations differ (1 µM for THT-stained fibrils and 35 nM for the Amytracker-stained fibrils). Table 3 shows the results of both experiments, and the results of the Amytracker-stained fibrils linearly converted to 1 µM to enable comparison. The observed numbers of fibrils for THT-stained and Amytracker-stained fibrils at 1 µM are within the same order of magnitude.

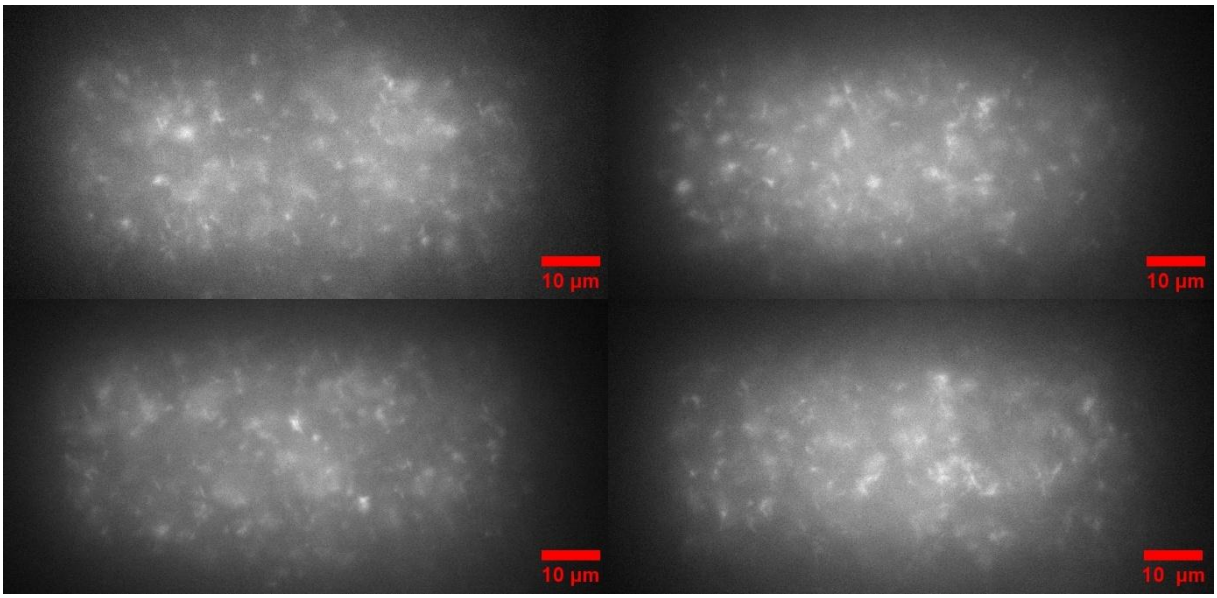

Figure 23. Representative images of αS fibrils stained with THT in a 96 well plate (gain=20 dB). The image size is 104 x 50 µm; the scalebar is 10 µm.

Table 3. The expected and observed amount of αS fibrils in a 96 well plate, stained by either Amytracker or THT. The results for Amytracker and THT were obtained in two separate experiments: 'SPC can be performed on Amytracker-stained αS fibrils in a 96 well plate' on page 41, and 'SPC can be performed on THT-stained αS fibrils in a 96 well plate ' on page 48. The Amytracker-stained fibrils had a concentration of 35 nM and the THT-stained fibrils of 1 µM. For comparison, the results of the Amytracker-stained fibrils are linearly converted to 1 µM.

	Expected number of αS fibrils based on concentration		**Observed number of αS fibrils through SPC**	
	Fibrils/image	Fibrils/L	Fibrils/image	Fibrils/L
Amytracker [fibril] = 35 nM	2.4E+03	4.0E+13	4.6E+00 ± 1.5E+00	7.7E+10 ± 2.5E+10
Amytracker [fibril] = 1 µM (calculated)	7.0E+04	1.2E+15	1.3E+02 ± 4.3E+01	2.2E+12 ± 7.2E+11
THT [fibril] = 1 µM	7.0E+04	1.2E+15	1.6E+02 ± 2.2E+01	2.7E+12 ± 3.7E+11

Conclusion

The microscope set-up can obtain images of visible αS fibrils stained with THT in a 96 well plate.

The expected number of αS fibrils based on the concentration (as described by Vaneyck et al. [44], and with the necessary information determined in previous experiments) does not accurately correspond with the observed number of αS fibrils based on SPC; the expected number is three orders of magnitude higher than the observed number.

10. Combining SAA and SPC: attempt 3 (THT)

Introduction
The first two attempts combining SAA and SPC did not produce successful results, so the experiment was repeated using THT instead of Amytracker. Please note that the most likely cause for the previous experiments' outcome – mistakenly adding not enough Amytracker – had not yet been discovered when to was decided to perform this experiment.

Materials and methods
The methods from R8 'Combining SAA and SPC: attempt 1 and 2 (Amytracker)' (page 43) were repeated, except that aggregation was monitored by means of THT fluorescence, for 145 h (≈6 days).

Results and discussion
SAA
The fluorescent signal of all conditions started increasing immediately before leveling off in a low plateau (Figure 24). The fluorescence level of the plateau is less than what has been observed in previous experiments for a completed aggregation (compared to Figure 51 on page 93 of R2 'The αS K23Q mutant does not suppress de novo fibril formation in an SAA', and Figure 63 on page 110 of R5 'The effect of αS fibril concentration and αS fibril sonication on αS aggregation').

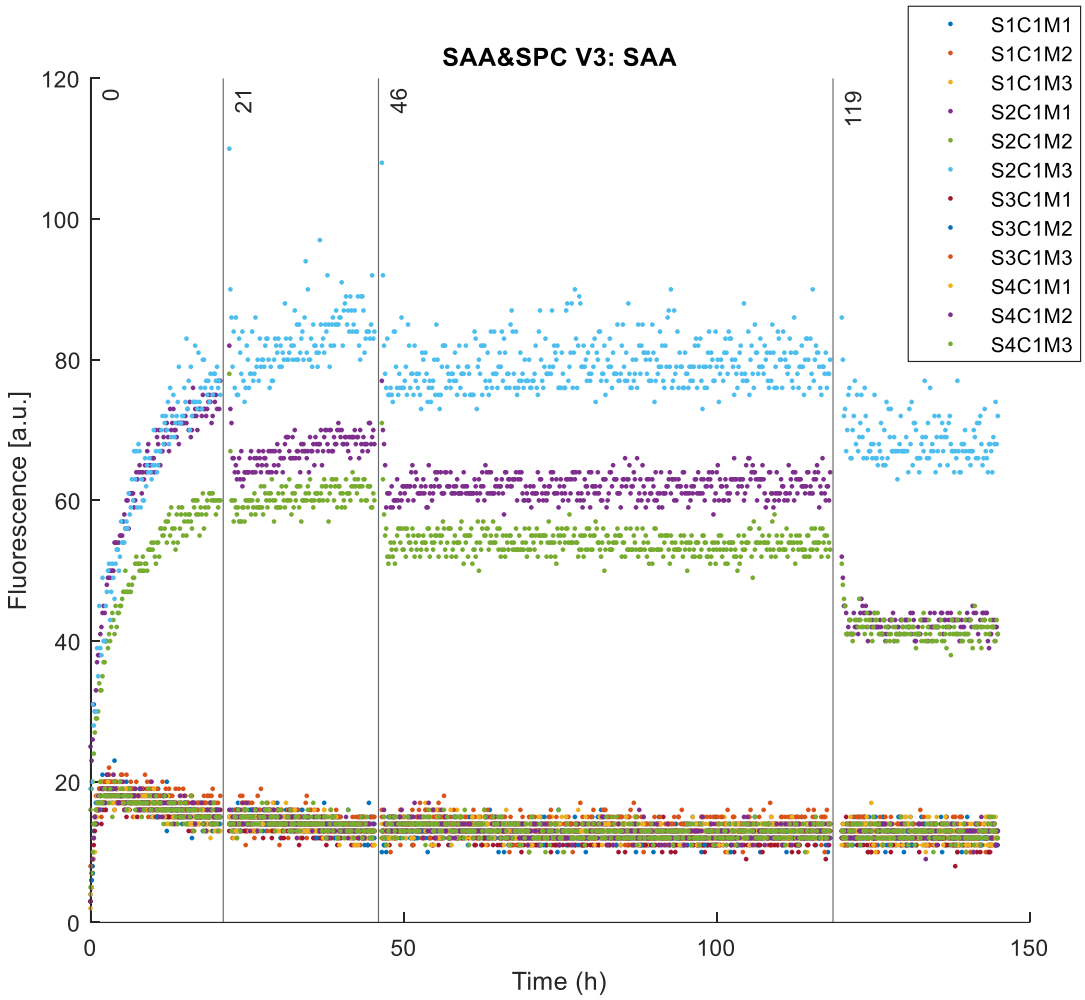

Figure 24. SAA curves for all samples. The vertical lines indicate measurement times for the SPC. The samples are described by their coded labels: S indicates αS fibril concentration (in monomer equivalent concentration), C indicates nothing here and M the samples of a triplo. S1 = 0 M αS fibrils (negative control); S2 = 10^{-6} M; S3 = 10^{-8} M; S4 = 10^{-10} M; M1 = sample 1 of triplo; M2 = sample 2 of triplo; M3 = sample 3 of triplo.

SPC

SPC was performed four times, at timepoints 0 h (= 0 days), 21.2 h (≈ 0.9 days), 46.0 h (≈ 1.9 days), and 118.6 h (≈ 4.9 days).

Already at t = 0 h, before the start of the SAA, some very long fibrils were observed in two out of three non-control conditions: 10^{-6} M and 10^{-10} M αS fibrils (Figure 25). Therefore it was decided to not finish the SPC analysis. First, the long fibrils indicate that they have been aggregating before the start of the experiment. Second, TrackPy cannot count long fibrils, meaning the counting should be done manually. Third, the SAA results already suggest that there will be no significant increase in number of counted particles per frame. The two previous experiments also did not show proper aggregation, and the number of particles remained mostly constant.

The fibrils might be so long because they were stored at room temperature for months. Storage temperature and duration affect fibril morphology.[58,59,61,62] Although none of these papers have experimented with the exact current situation, they still provide related information. Tarutani et al. found that leaving reactant αS monomers standing for seven days at room temperature (20~25°C) or 37°C both result in oligomer-like structures, but not at 4°C (for comparison: shaking at 37°C resulted in fibrous structures).[58] If monomers already undergo such changes at room temperature within days, it is not unlikely that fibrils do too within months. Sidhu et al. report that the morphology of wildtype αS fibril changes after being stored at 4°C for three and six months; no further change was observed at the 12 month measurement.[59] The measured changes are related to periodicity, and no SAA was run with the stored αS fibrils, but the changed morphologies might influence aggregation.

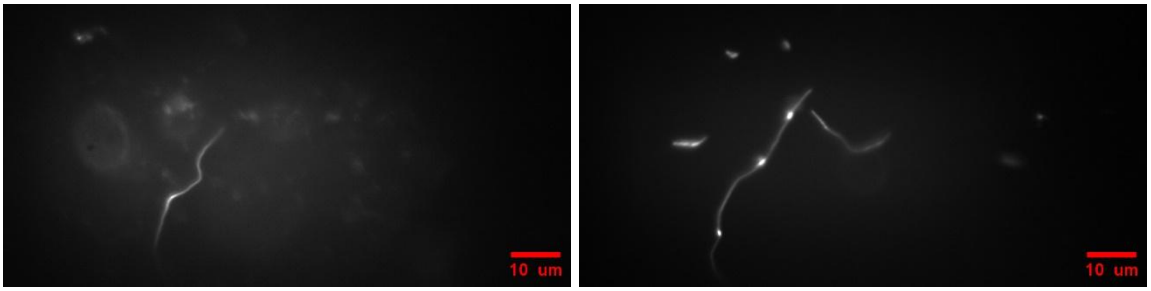

Figure 25. Fluorescence microscopy images of the sample with 10^{-6} M αS fibrils (left) and 10^{-10} M αS fibrils (right) measured on t = 0 h.

Conclusion

The SAA did not show significant aggregation, and the SPC analysis was aborted due to the presence of long fibrils before the SAA had even started.

11. Testing the αS aggregation of an alternative batch of αS fibrils and two monomer batches stored at different temperatures

Introduction
In the previous attempt to combine SAA and SPC no proper aggregation occurred. Also, unexpectedly long fibrils were found during SPC before the SAA had even started. Therefore it was decided to start using a different batch of αS fibrils, which has been stored at 4°C instead of at room temperature. Before using this alternative batch in another SAA and SPC combination experiment, it was first subjected to a test SAA to find whether these αS fibrils will aggregate.

Also the effect of two different batches of reactant αS monomers on the lag time was tested; one batch was being stored in the –80°C freezer and the other in the 4°C fridge. Polinski et al. recommend to store reactant αS monomers at –80°C "to prevent spontaneous aggregation that can occur at room temperature", but mentions nothing about storing reactant αS monomers at 4°C.[61] Tarutani et al. found that leaving reactant αS monomers standing for seven days at room temperature (20~25°C) or 37°C both result in oligomer-like structures, but not at 4°C (for comparison: shaking at 37°C resulted in fibrous structures).[58] Therefore, it is investigated here whether there is a difference between using reactant αS monomers stored at 4°C and –80°C with regard to the lag time.

Materials and methods
Two conditions were prepared; either with 50 µM reactant αS monomers that had been stored in the –80°C freezer or in the 4°C fridge. Both conditions were spiked with 1 µM αS fibrils from an alternative batch stored in the 4°C fridge. Each sample was measured in triplo. The aggregation was monitored by means of THT fluorescence, for at least 120 h (= 5 days).

Results
The aggregation curves are displayed in Figure 75 (appendix). The SAA with reactant αS monomers from the –80°C freezer was stopped after 122 h, because all had aggregated and plateaued. The other with monomers from the 4°C fridge was continued for an additional 45 h.

The samples with reactant αS monomers from the –80°C freezer have a shorter mean lag time than the samples with reactant αS monomers from the 4°C fridge; 19 ± 3 h versus 105 ± 42 h, respectively (Figure 26). The variance is also smaller.

Possibly it is the higher temperature that makes the reactant αS monomers stored at 4°C more prone to unintended aggregation or oligomer formation than at -80°C. Alternatively (or complementary), storing the reactant αS monomers in the 4°C fridge increases the chances of being contaminated with proteases as compared to the – 80°C freezer, which leads to monomer degradation, which could explain the longer lag times.

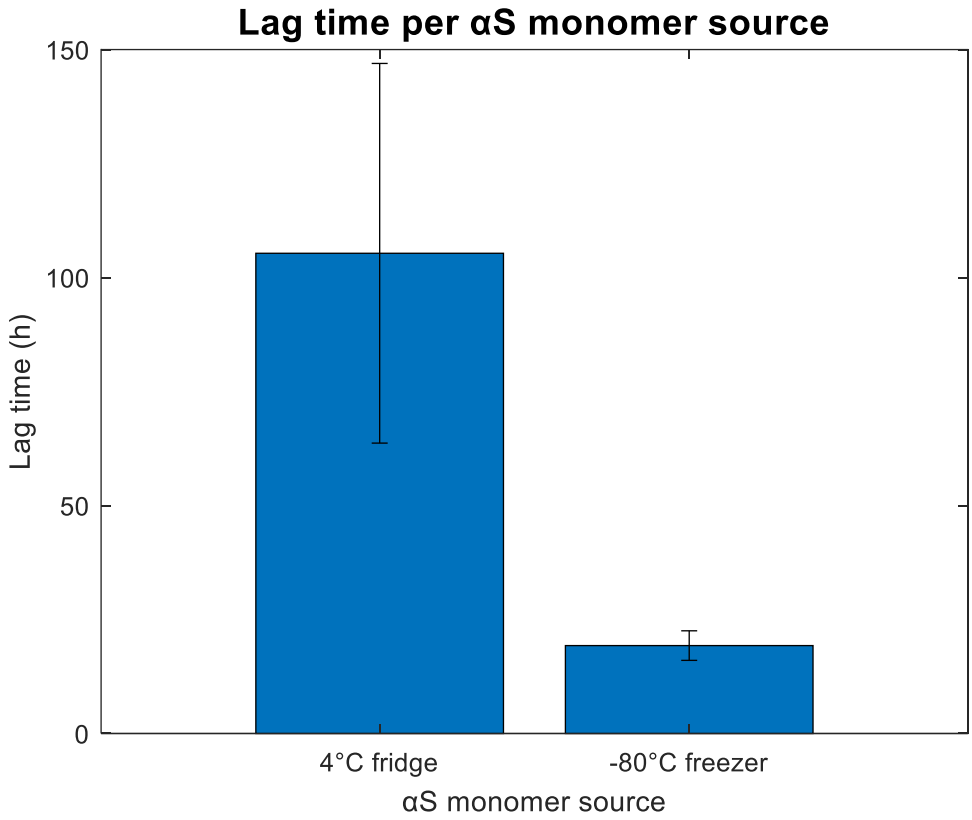

Figure 26. Mean lag time per reactant αS monomer storage temperature, using the alternative batch of αS fibrils.

Conclusion

The alternative batch αS fibrils is capable of aggregation. Using reactant αS monomers stored in the –80°C freezer led to shorter lag times and lower variance (19 ± 3 h) than the reactant αS monomers stored in the 4°C fridge (105 ± 42 h).

12. The effect of αS fibril sonication on αS aggregation of an alternative batch of αS fibrils

Introduction
The previous experiment showed that the alternative batch αS fibrils is capable of aggregation (R11 'Testing the αS aggregation of an alternative batch of αS fibrils and two monomer batches stored at different temperatures' on page 53). Here the effect of sonication by a tip sonicator on lag time is investigated. The tested sonication times are higher than previously tested because previous results showed that larger sonication times led to shorter lag times, as described in results section 5. 'The effect of αS fibril concentration and αS fibril sonication on αS aggregation' on page 33. This experiment will be referred to as R5 in this section.

Materials and methods
The alternative batch of αS fibrils was split into 4 samples of 200 µL each, which were sonicated for 0 s, 5 s , 7 s or 10 s using a tip sonicator. These samples were stored in the 4°C fridge before running the SAA. An SAA was run with 4 conditions, each with 1 µM αS fibrils of one of the different sonication times, and 50 µM reactant αS monomers that had been stored in the –80°C freezer. Each sample was measured in triplo. The aggregation was monitored by means of THT fluorescence for 176 h (= 7 days).

The left-over αS fibrils were divided and stored in either the 4°C fridge or –80°C freezer, to be used in coming experiments.

Results
The aggregation curves are displayed in Figure 76 (appendix).

The control samples without αS fibrils failed to aggregate within the 176 h duration of the experiment.

Increasing the sonication time does not lead to progressively smaller lag times (Figure 27). The 10 s sonicated samples have a larger mean lag time (69 ± 1.1 h) than the 5 s and 7 s sonicated samples (61 ± 8.5 h and 57 ± 1.3 h respectively). This contradicts the previous SAA experiment with sonicated αS fibrils (R5) where increasing the sonication did decrease the lag time. This could indicate that sonicating αS fibrils beyond 5 s no longer influences lag time, or the alternative batch of αS fibrils responds differently to sonication.

Two sonication times are tested in both experiments, but this experiment found much larger lag times for both (Figure 28). The mean lag time of the 0 s sonicated 1 µM αS fibrils is 84 ± 23 h in this experiment and 32 ± 25 h in R5; for the 5 s sonicated 1 µM αS fibrils this is 61 ± 8.5 h and 2.5 ± 0.10 h respectively. Sonication does seem to decrease variance in lag time among triplos, like in R5 (Figure 27).

This major difference indicates that the two batches of αS fibrils cannot be compared directly. There are myriads of reasons how the two batches could be different (e.g. fibril polymorphs

or contamination) and why, but the most obvious difference is their storage temperature. Polinski et al. recommend to store αS fibrils at room temperature or –80°C in their review paper on best practices for using αS fibrils to model Parkinson's disease.[61] They actually dissuade storing αS fibrils at 4°C [61] because fibrils can cold-denature to monomers at 0-20°C [62]. The αS fibrils used in this experiment have been stored at 4°C and the αS fibrils from R5 at room temperature, which thus might explain why the lag times in this experiment are so much longer. On the other hand, Sidhu et al. found that fibrils did not dissociate at 4°C in their specific experimental conditions.[59]

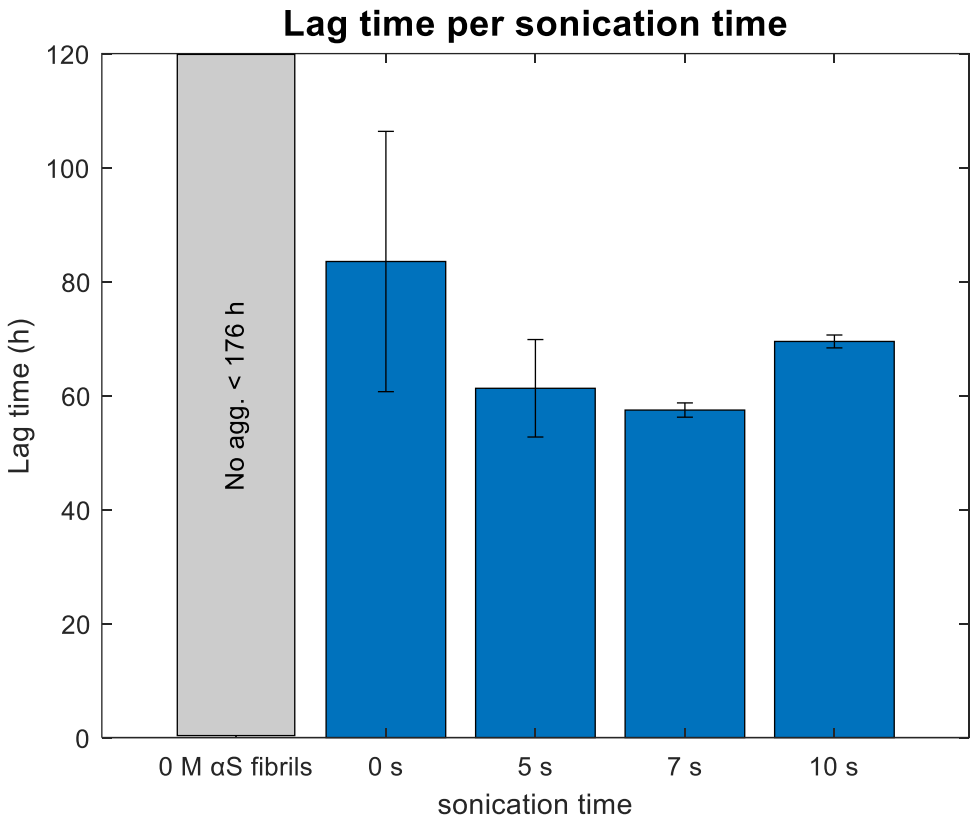

Figure 27. Mean lag time per sonication time.

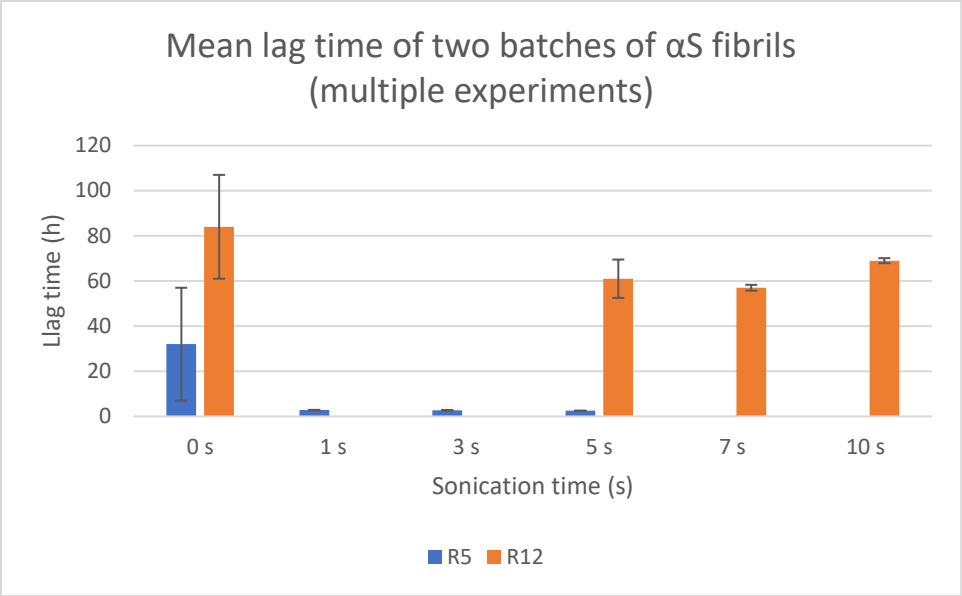

Figure 28. Comparing the lag times of this experiment's (R12) alternative batch of αS fibrils with the original batch of αS fibrils of R5. R12 also used a different batch of reactant αS monomers, which had been stored in the –80°C freezer. R5 refers to 'The effect of αS fibril concentration and αS fibril sonication on αS aggregation' (page 12); R12 refers to 'The effect of αS fibril sonication on αS aggregation of an alternative batch of αS fibrils' (page 33). R5 used a batch of reactant αS monomers that had been stored at room temperature, and R12 used another batch stored in the –80°C freezer.

Conclusion

Increasing sonication time from 5 s to 7 s and 10 s was not found to lead to consistently decrease lag times for the alternative batch of αS fibrils, which had been stored at 4°C. This contradicts the previous experiment R5 where increasing the sonication time from 1 s to 3 s and 5 s did consistently decrease lag times for the original batch of αS fibrils, which had been stored at room temperature. It does seem to decrease the variance in lag times, which is in line with R5. In general the alternative batch of αS fibrils seems to generate much longer lag times than the original batch, raising doubts on whether the found results would also apply to the original batch.

13. The effect of αS fibril sonication, storage temperature, and vortexing on αS aggregation of an alternative batch of αS fibrils

Introduction

Since the previous SAA did not show a linear relationship between sonication time and lag time, two more variables that might influence lag time are investigated: vortexing the αS fibrils and storage temperature of the αS fibrils.

Agitation is known to induce αS aggregation.[51] Here, an additional form of agitation prior to the SAA is tested: vortexing the αS fibrils.

As mentioned in the previous section, Polinski et al. recommend to store αS fibrils at room temperature or –80°C and dissuade to store them at 4°C[61] because αS fibril can then dissociate. Comparing the results of two previous experiments seems to support Polinski et al.'s notion. The experiment described in results section 5. 'The effect of αS fibril concentration and αS fibril sonication on αS aggregation' on page 33 will be referred to as R5, and 12. 'The effect of αS fibril sonication on αS aggregation of an alternative batch of αS fibrils' on page 55 as R12. In R5, the original batch of αS fibrils stored the room temperature was used in an SAA and the lag time determined. In R12 this happened for an alternative batch of fibrils stored at 4°C. By comparing these two, storage at 4°C indeed resulted in longer lag times than storage at room temperature. These however are two separate experiments performed months apart using two different batches of fibrils.

In the current experiment, the previously untested storage condition of –80°C is tested to determine whether –80°C is indeed a better storage option than 4°C. αS fibrils of the same (alternative) batch stored at either –80°C or 4°C are directly compared with regard to lag time.

The storage recommendation of Polinski et al. only applies to unsonicated fibrils.[61] They recommend to never store sonicated αS fibrils below room temperature. Since the aliquots of sonicated fibrils already had been placed in the -80°C freezer before this experiment, I decided to test them still.

Materials and methods

The same sonicated αS fibrils produced in previous experiment (R12) were used ('The effect of αS fibril sonication on αS aggregation of an alternative batch of αS fibrils' on page 55). Sixteen conditions and a negative control without αS fibrils were prepared. αS fibrils had been stored either at 4°C in the fridge or at –80°C in the freezer. αS fibrils had been sonicated for 0 s, 5 s, 7 s or 10 s. αS fibrils were either vortexed for 5 s or not vortexed. The fibril-containing samples each have a concentration of 1 µM αS fibrils. reactant αS monomers that had been stored in the –80 °C freezer were used. The aggregation during SAA was monitored by means of THT fluorescence for 165 h (=6.9 days).

Results and discussion
Only one out of twelve control samples started aggregating after 149 h, so no error bar could be established.

Vortexing
Vortexing does not seem to influence the lag times, not in general (Figure 31), nor for specific conditions (Figure 32, Figure 34).

Sonication time
Sonication time does not seem to strongly influence lag time. In general, no sonication seems to lead to larger lag times with a larger variance, but there is only a marginal difference in lag times or variance between the different sonication times (Figure 29).

This contradicts the results of R5, in which increased sonication time led to smaller lag times. It is however similar to R12, in which sonication was also not found to consistently decrease lag times (Figure 35).

Storage temperature
The storage temperature does seem to influence lag time in general, albeit not by much (Figure 30). αS fibrils stored at -80°C lead to smaller lag times, possibly validating Polinski et al.'s notion that protein dissociate at 4°C and thus have lower seeding capacity.[61] It might also be the result of freezing and thawing, which is known to affect, damage or even denature protein structure.[63] This perhaps fractures the αS fibrils stored at -80°C. Fragmented fibrils leads to faster aggregation.[58] On the other hand, the process of freezing and thawing can create variety among the αS fibrils, which might reduce reproducibility.[61]

Looking into more detail, it seem like the difference between storage temperature mainly is derived from the unsonicated samples; the unsonicated samples have a much larger lag time for 4°C than for -80°C (Figure 33). The sonicated samples differ little from each other. This seems to corroborate the notion of Polinski et al. that sonicated αS fibrils should not be stored below room temperature because of dissociation.[61] These results could support that the effects of sonication are lost due to the cold storage, especially considering that sonication of the αS fibrils stored at room temperature did have an effect on the lag times in R5.

Polinski et al. reference two papers for their recommendation for αS fibril storage: Bousset et al. and Ikenoue et al..[61] The authors do however not mention that both these papers note that cold denaturation is affected by experimental conditions. Ikenoue et al. found that that αS cold-denatures at 0–20°C, but that the dissociation is affected by fibril properties (length, concentration) and solvent conditions (sodium chloride concentration, presence of Gdn-HCl).[62] More strikingly, Bousset et al. saw that αS fibrils depolymerized at 4°C in buffer with physiological salt concentrations (50 mM Tris–HCl, pH 7.5, 150 mM KCl), but not in a lower salt buffer (5 mM Tris-HCl, pH 7.5).[60] This was further confirmed by Sidhu et al., who found that fibrils stored at 4°C did not dissociate at all under their specific experimental conditions.[59]

The buffer conditions of αS aggregation in this experiment (10 mM TRIS, 10 mM NaCl, 0.02 wt% NaN_3, pH 7.4) are more similar to those of Sidhu et al. (10 mM Tris-HCl, 10 mM NaCl, 0.1 mM EDTA, pH 7.4), in which no dissociation occurred, than Ikenoue et al. (20 mM sodium phosphate buffer, 100 mM NaCl, pH 7.4), in which dissociation occurred.[59,62] Although it cannot be concluded from this experiment that the fibrils have (partially) dissociated or that the buffer would be the direct cause, it is good to note that a change in buffer conditions might change the fibril behavior.

Identical conditions in previous experiments
The conditions using the αS fibrils stored at 4°C (non-vortexed) are identical to those of R12, and they give similar results (Figure 35). The lag times for each sonication time fall within a 30 h range of each other while the minimum lag time is 40 h. This suggests that the alternative batch of αS fibrils stored at –80°C or 4°C indeed behaves consistently differently that the original batch stored at room temperature.

General discussion
This experiment had an excessive amount of negative controls. There were four, one for each of the conditions. However, since there were no fibrils that could have been sonicated, vortexed or stored, these four negative controls are identical.

The αS fibril storage recommendations are relative; according to Polinski et al. it is preferable to make fresh αS fibrils and to use them within two weeks (stored at room temperature).[61]

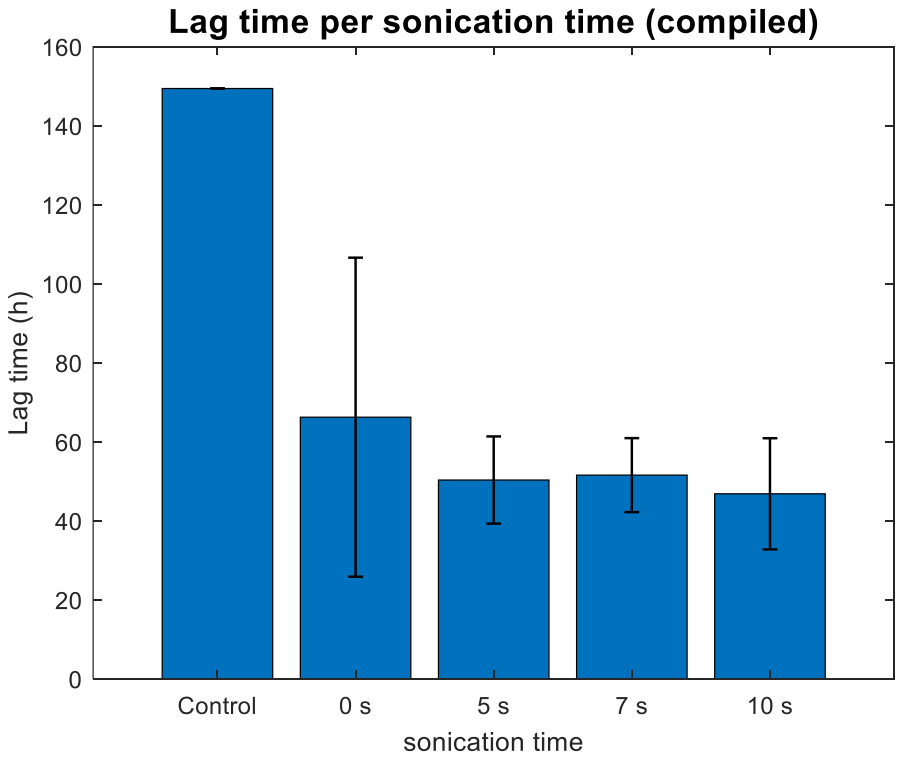

Figure 29. Mean lag time per sonication time, when all other conditions are compiled. Only one out of twelve control samples started aggregating within the timeframe of the experiment, so no error bar could be established.

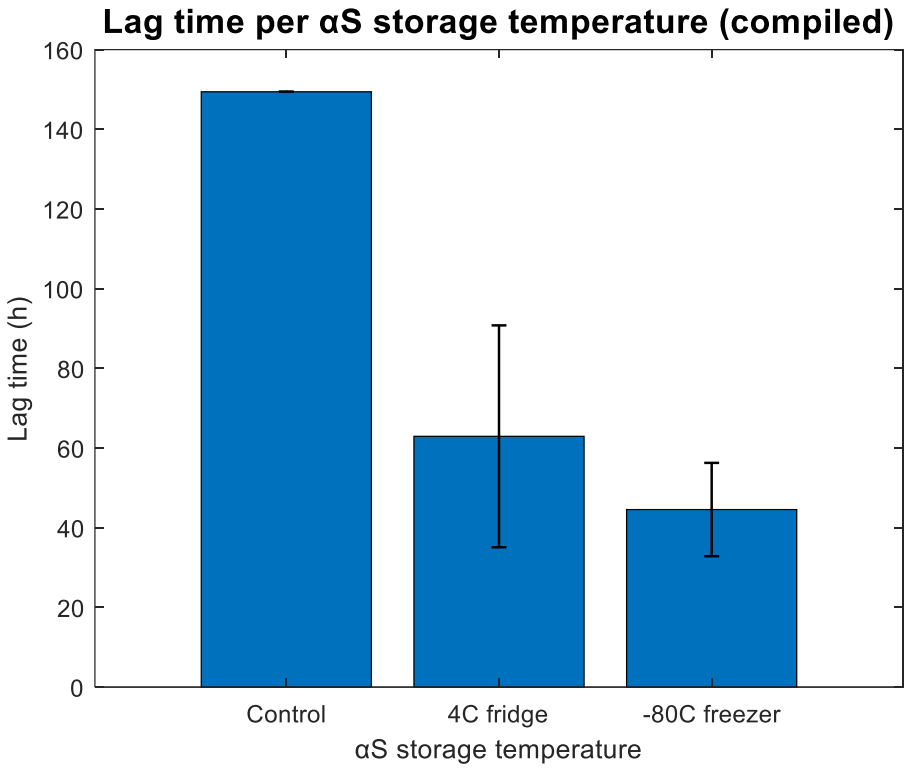

Figure 30. Mean lag time per αS fibril storage temperature, when all other conditions are compiled. Only one out of twelve control samples started aggregating within the timeframe of the experiment, so no error bar could be established.

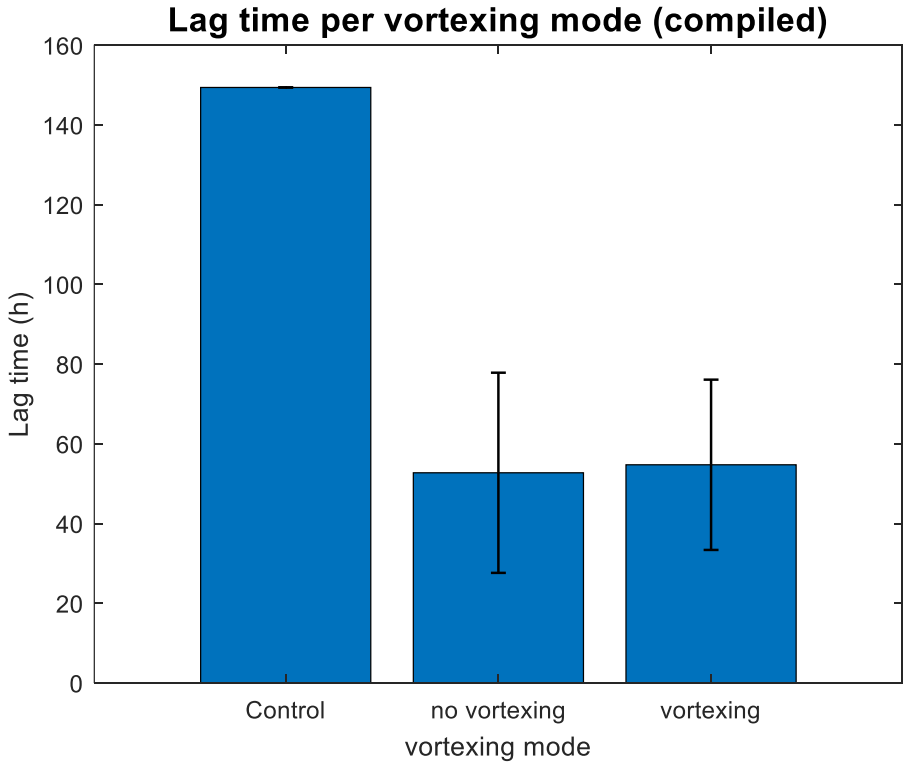

Figure 31. Mean lag time per vortexing mode, when all other conditions are compiled. Only one out of twelve control samples started aggregating within the timeframe of the experiment, so no error bar could be established.

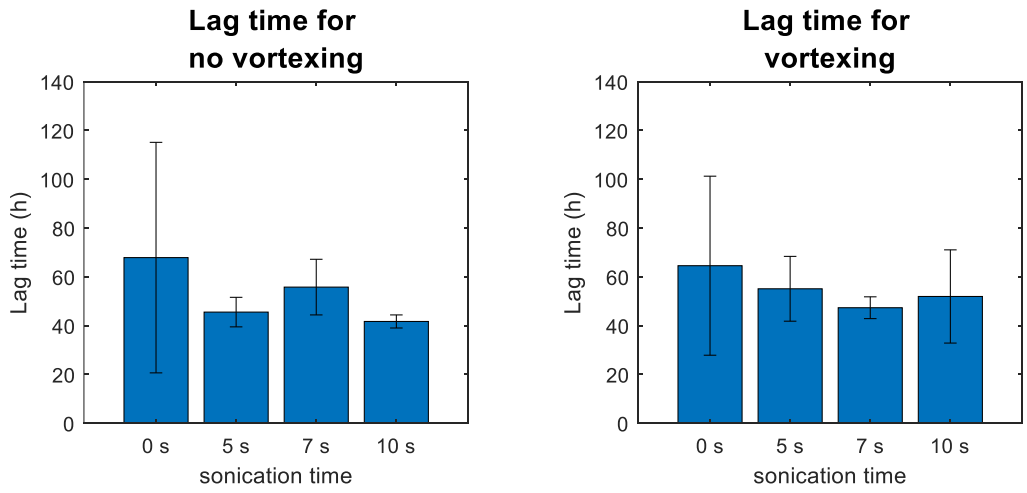

Figure 32. Mean lag time per sonication time, separated by vortexing mode, compiled over αS fibril storage temperature.

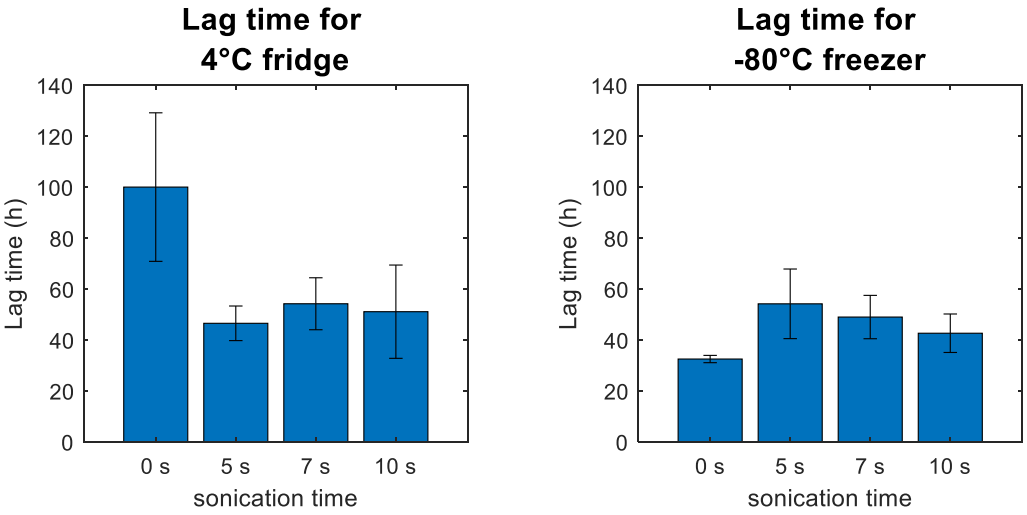

Figure 33. Mean lag time per sonication time, separated by αS fibril storage temperature, compiled over vortexing modes.

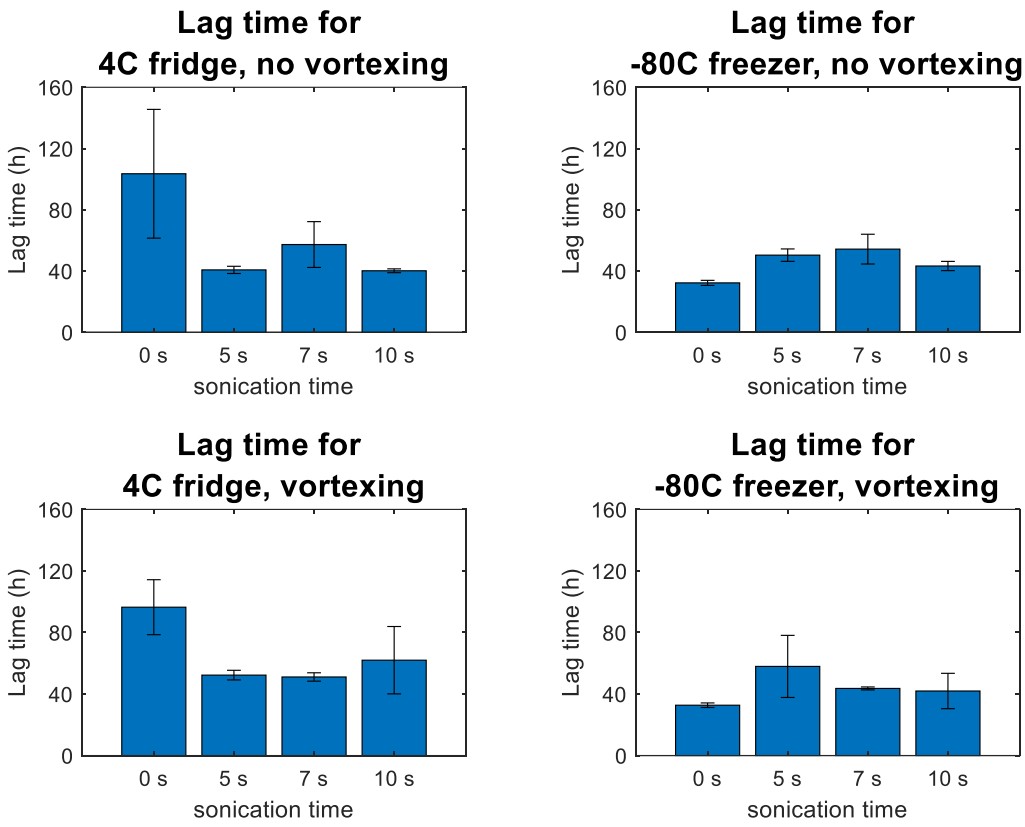

Figure 34. Mean lag time per sonication time, separated by the other conditions of αS fibril storage temperature and vortexing mode.

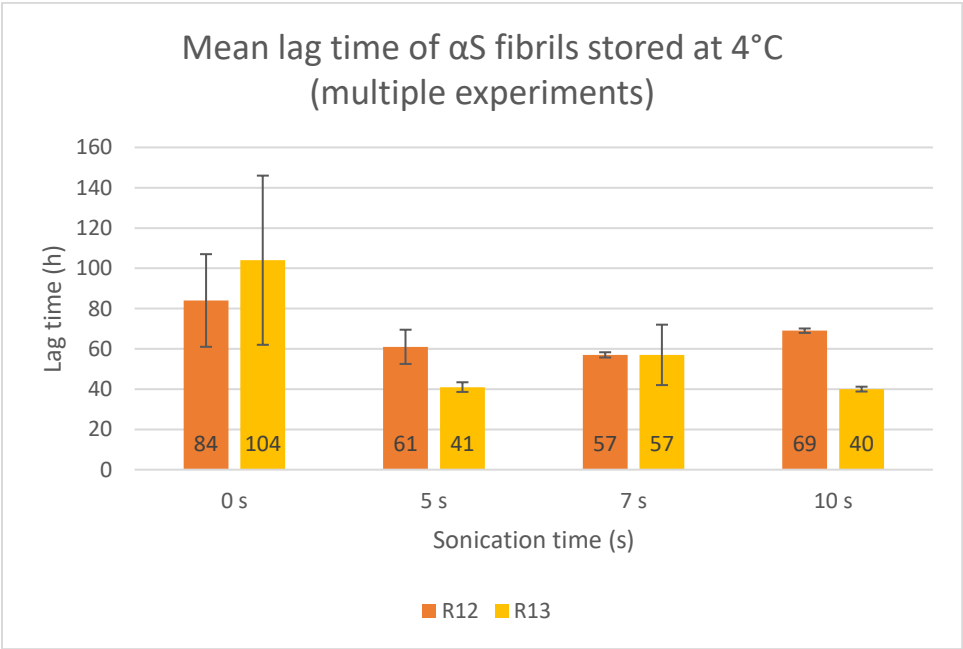

Figure 35. Comparing the lag times of this experiment's (R13) αS fibrils stored in the 4°C fridge (no vortexing) with the identical condition of R12. R12 refers to 'The effect of αS fibril sonication on αS aggregation of an alternative batch of αS fibrils' (page 33); R13 refers to 'The effect of αS fibril sonication, storage temperature, and vortexing on αS aggregation of an alternative batch of αS fibrils' (page 58).

Conclusion

No clear relationship between lag time and sonication time or vortexing could be established. Only the αS fibril storage location showed some effect, with the αS fibril stored in the -80°C freezer resulted in slightly smaller lag times than those stored in the 4°C fridge.

14. (Re)testing the effect of various αS fibril parameters on αS aggregation

Introduction

Since previous two SAAs showed no clear relationship between lag time and various parameters on the alternative batch of αS fibrils, here αS fibrils from both the original and alternative batch are tested. Some conditions are repeats from previous experiments to see whether the results are replicable. Based on these results, αS fibrils will be selected for the next SAA and SPC combination experiment.

Previous experiments will be referred to as follows: R5 refers to 'The effect of αS fibril concentration and αS fibril sonication on αS aggregation' (page 12); R12 refers to 'The effect of αS fibril sonication on αS aggregation of an alternative batch of αS fibrils' (page 33); R13 refers to 'The effect of αS fibril sonication, storage temperature, and vortexing on αS aggregation of an alternative batch of αS fibrils' (page 58).

Materials and methods

In total 20 unique conditions are prepared, making a total of 60 samples. An overview can be found in Table 4. The αS fibrils had been handled in one of four ways (different storage temperatures or freshly sonicated), and are sonicated for one of the listed times. The control contains no αS fibrils. The original batch of αS fibrils is the batch that has been used up to 10. 'Combining SAA and SPC: attempt 3 (THT)' (page 50), and the alternative batch has been used starting from 11. 'Testing the αS aggregation of an alternative batch of αS fibrils and two monomer batches stored at different temperatures' (page 53). For the freshly sonicated αS fibrils, the aggregated samples from R13 were pooled and then sonicated to create new αS fibrils, so they originated from the alternative batch. The fibril-containing samples each have a concentration of 1 µM αS fibrils, except the freshly sonicated αS fibrils with 0.83 µM. reactant αS monomers that had been stored in the –80 °C freezer were used. The aggregation was monitored by means of THT fluorescence for 72 h (= 3 days).

Table 4. Conditions prepared for the SAA. R5 refers to 'The effect of αS fibril concentration and αS fibril sonication on αS aggregation' (page 12); R12 refers to 'The effect of αS fibril sonication on αS aggregation of an alternative batch of αS fibrils' (page 33); R13 refers to 'The effect of αS fibril sonication, storage temperature, and vortexing on αS aggregation of an alternative batch of αS fibrils' (page 58).

#	αS fibril handling	αS fibril batch	Sonication times (s)	Shares identical conditions
1	Control sample with 0 M αS fibrils	-	-	-
2	αS fibrils stored at RT at the bench	Original batch	0, 1, 3, 5	R5
3	αS fibrils stored in the 4°C fridge	Alternative batch	0, 5, 7, 10	R12 R13
4	αS fibrils stored in the -80°C freezer	Alternative batch	0, 5, 7, 10	R13
5	Freshly sonicated αS fibrils	Alternative batch: aggregated samples of R13	1, 3, 5, 7, 10, 30, 60	-

Results
The control samples failed to aggregate within the 72 h of the experiment (Figure 78 in appendix).

Aggregation of αS was not induced by the freshly sonicated αS fibrils; the fluorescence remained constant at a level comparable to the plateau value after completed aggregation of other conditions (Figure 82 in appendix). This indicates that sonicating in order to create new seeds was unsuccessful. As such, no lag times for the 30 s or 60 s sonication times could be established. Also, now the only αS fibril handling that can be further investigated in this experiment is the storage temperature.

All samples of the αS fibrils stored at bench, in the 4°C fridge or in the -80°C freezer aggregated, except for four unsonicated samples (two samples with unsonicated αS fibrils stored at the bench, and two samples with unsonicated αS fibrils stored in the 4°C fridge). That means that only 56% of the unsonicated αS fibrils aggregated within 72 h, compared to the 100% of the stored sonicated samples.

Sonication time does not show a clear trend, in neither separate nor compiled results (Figure 37 and Figure 39). It must be noted that the compiled results cannot be directly compared, since not all αS fibrils were sonicated for all the different sonication times. For example, the 1 s and 3 s sonication were only performed on the αS stored at the bench, while the 5 s was performed for all four fibril-containing conditions. This significantly influences both the mean and the variance of the compiled results. Most eminently, the variance increases when a sonication time is tested with multiple different αS fibrils handlings.

The αS fibrils stored at the bench at room temperature clearly had the shortest lag times with a mean of 5.1 ± 1.5 h (Figure 36). Whether this is due to the storage temperature or the fibril batch cannot be concluded from this experimental setup; this particular storage temperature and the original fibril batch are both only tested in this one condition. This would have been solved if this experiment had at least two additional conditions: the alternative batch stored at room temperature and the original batch stored at a colder temperature. The former would have been practically feasible, but not the latter since the entire original batch of αS fibrils had been stored at room temperature for year at this point.

The 4°C and -80°C conditions are suitable to compare directly because they share the same sonication times and αS fibril batch. The mean lag times of αS fibrils stored in the 4°C fridge and in the -80°C freezer are more similar, with the -80°C having shorter lag times, albeit not by a lot (Figure 36). The obtained results are similar to R13 (Figure 41, Figure 42). Here however the difference between 4°C and -80°C conditions are not mainly derived from the unsonicated samples, but from both the unsonicated and sonicated samples (Figure 39).

The αS fibril handling (that is only storage temperature here) seems to be more impactful than sonication time, which is most clearly exemplified by comparing the sonicated conditions (5 s, 7 s and 10 s) of the αS fibrils stored in 4°C fridge or in the -80°C freezer (Figure 38).

Comparing identical conditions to previous experiments
The αS fibrils stored at the bench are from the same batch as used in R5. The conditions from this experiment are identical to the 10^{-6} M sample from R5, aside from the experiments being one year apart (Figure 40). As compared to the other samples, the found lag times are similar (Figure 36 versus Figure 40): all sonicated samples start aggregating quickly; within 10 h. The unsonicated samples cannot be compared directly because the two experiment's duration differ greatly (72 h for this experiment versus 1445 h for R5) and not all unsonicated samples from this experiment managed to aggregate within this experiment's timeframe.

The αS fibrils stored in the 4°C fridge's conditions in this experiment are identical to those in R12 and R13 (Figure 41). These experiments were performed within the timespan of a month. The outcomes of the three experiments for the sonicated samples fall roughly within the same range. Each lag time is at least 40 h, and the largest difference between lag times for one sonication time is 30 h. For the same reason as before, the unsonicated samples cannot be directly compared. Only one unsonicated sample from this experiment aggregated versus all in the other two. This experiment lasted 72 h while R12 lasted 176 h and R13 165 h.

The αS fibrils stored in the -80°C freezer in this experiment and R13 share identical conditions (Figure 42). Though the lag times from R13 are consistently higher, their mean lag times are similar. Each lag time is at least 29 h and the lag times per sonication time are within 20 h of each other.

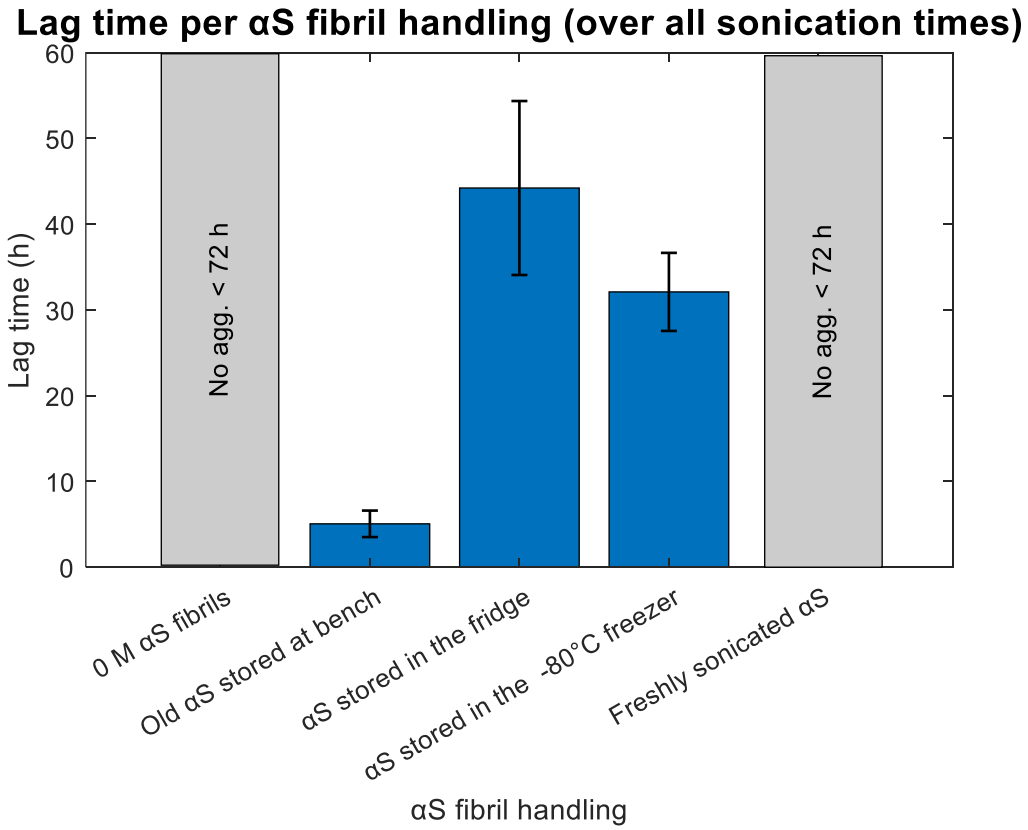

Figure 36. Mean lag time per αS fibril handling, when all sonication times are compiled per αS fibril handling.

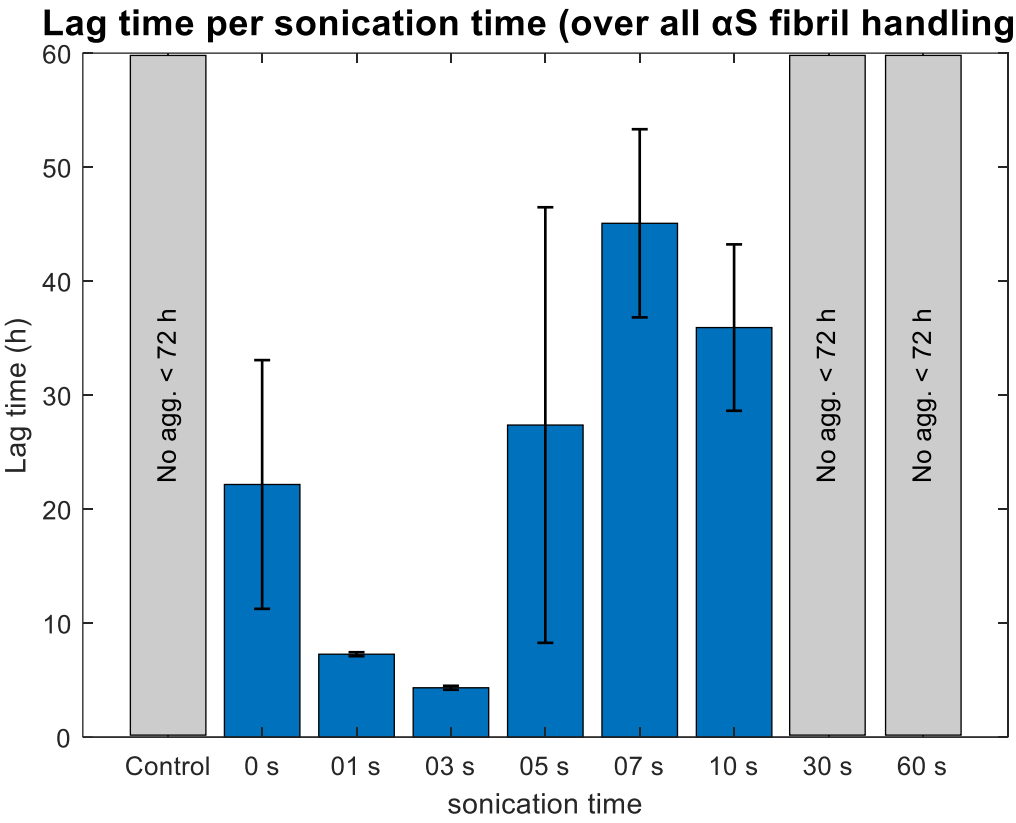

Figure 37. Mean lag time per sonication time, when all αS fibril handlings are compiled per sonication time.

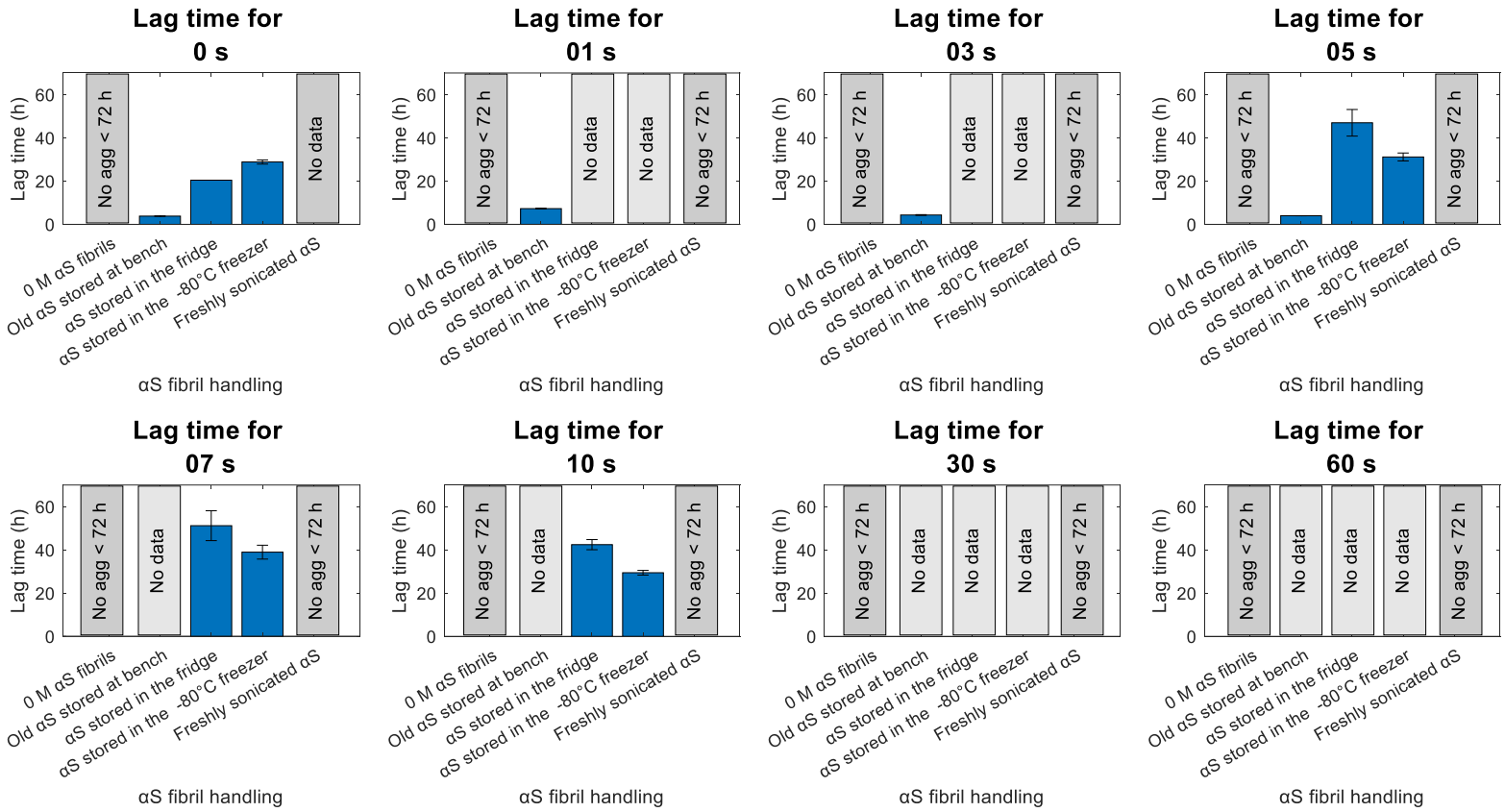

Figure 38. Mean lag time per sonication time, separated by αS fibril handling. Two of the three samples with unsonicated αS fibrils stored at the bench, and two of the three samples with unsonicated αS fibrils stored in the 4°C fridge failed to aggregate.

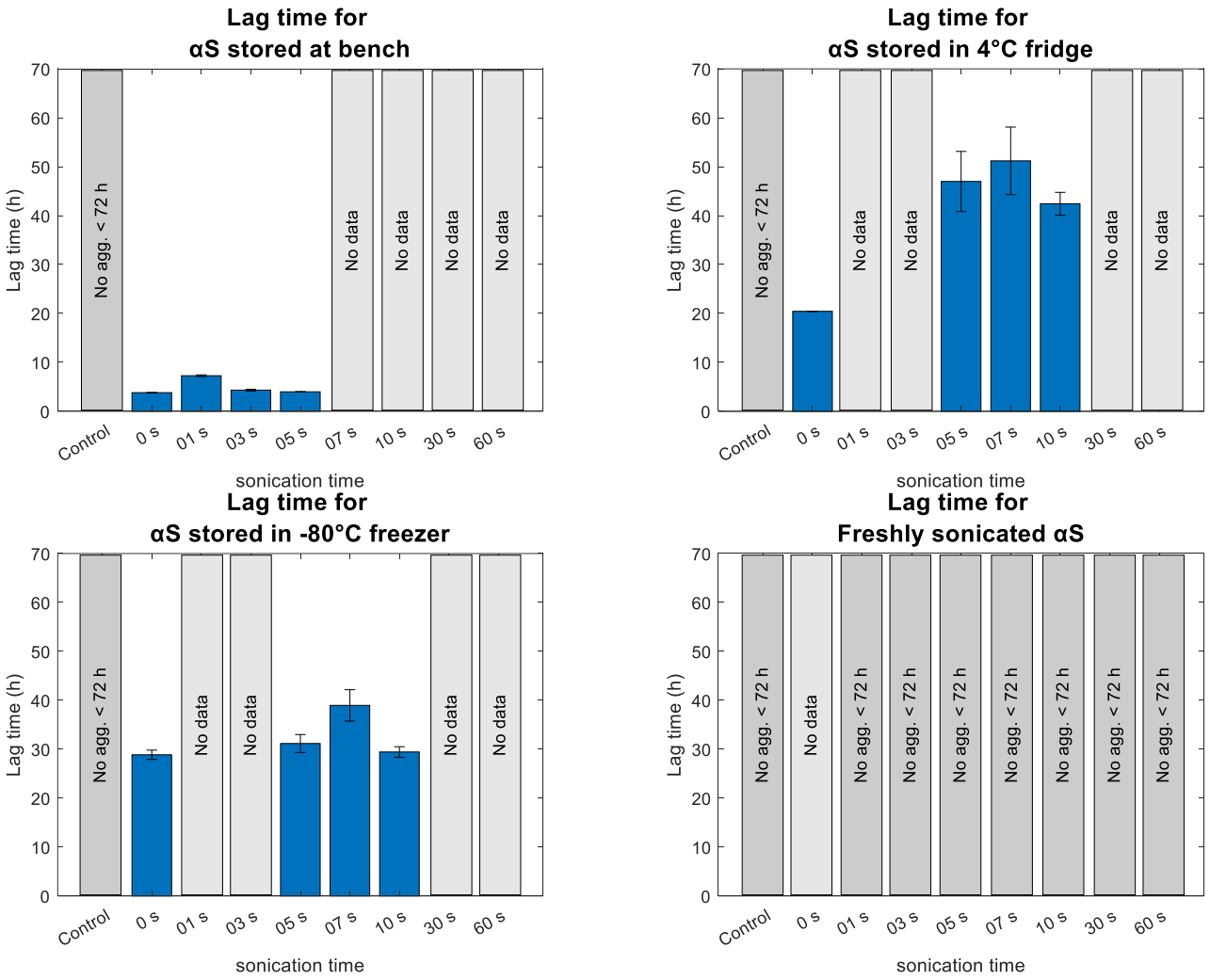

Figure 39. Mean lag time per sonication time, separated by αS fibril handling. Two of the three samples with unsonicated αS fibrils stored at the bench, and two of the three samples with unsonicated αS fibrils stored in the 4°C fridge failed to aggregate.

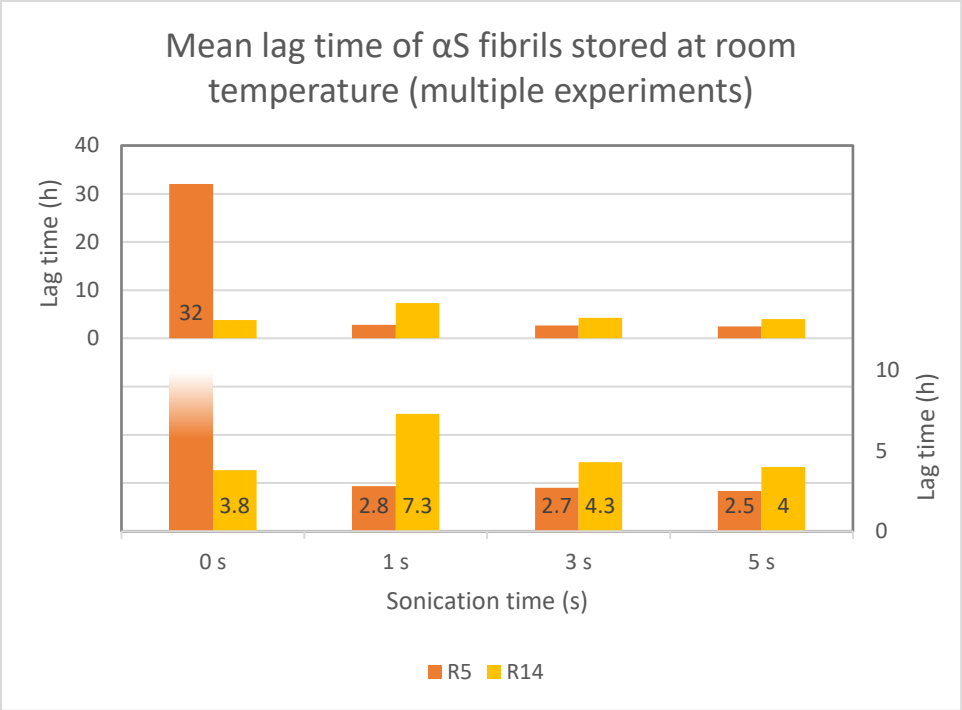

Figure 40. Comparing the lag times of this experiment's (R14) αS fibrils stored at the bench at room temperature with the almost identical conditions of R5. R14 used a different batch of reactant αS monomers, which had been stored in the –80°C freezer. Only one of the triplo with the 0 s sonicated αS fibrils of R14 aggregated, so no error bars could be established. R5 refers to 'The effect of αS fibril concentration and αS fibril sonication on αS aggregation' (page 12); R14 refers to '(Re)testing the effect of various αS fibril parameters on αS aggregation' (page 65).

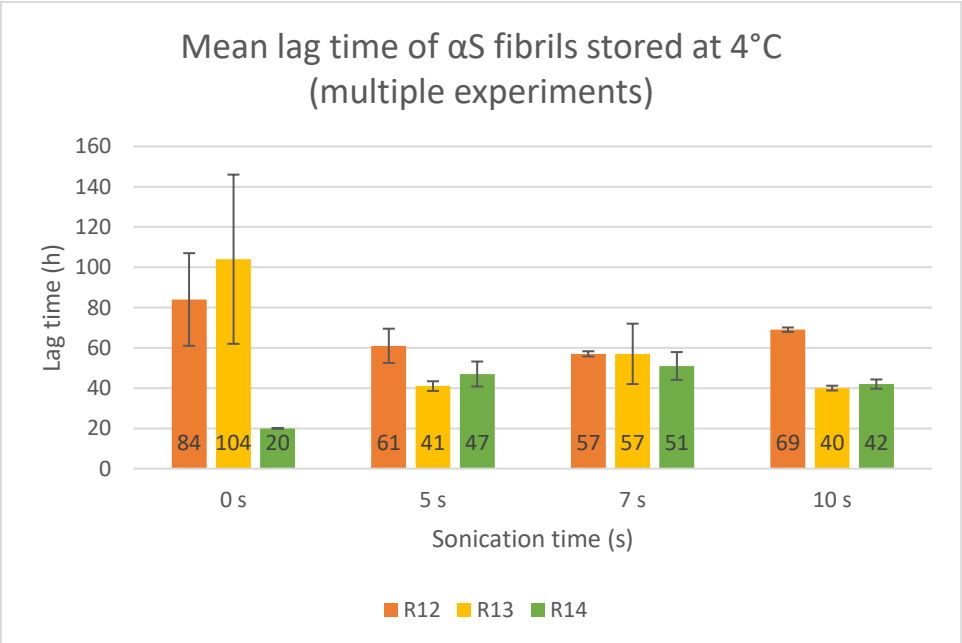

Figure 41. Comparing the lag times of this experiment's (R14) αS fibrils stored in the 4°C fridge with the identical condition of R12 and R13 (for the latter: no vortexing). Only one of the triplo with the 0 s sonicated αS fibrils of R14 aggregated, so no error bars could be established. R12 refers to 'The effect of αS fibril sonication on αS aggregation of an alternative batch of αS fibrils' (page 33); R13 refers to 'The effect of αS fibril sonication, storage temperature, and vortexing on αS aggregation of an alternative batch of αS fibrils' (page 58); R14 refers to '(Re)testing the effect of various αS fibril parameters on αS aggregation' (page 65).

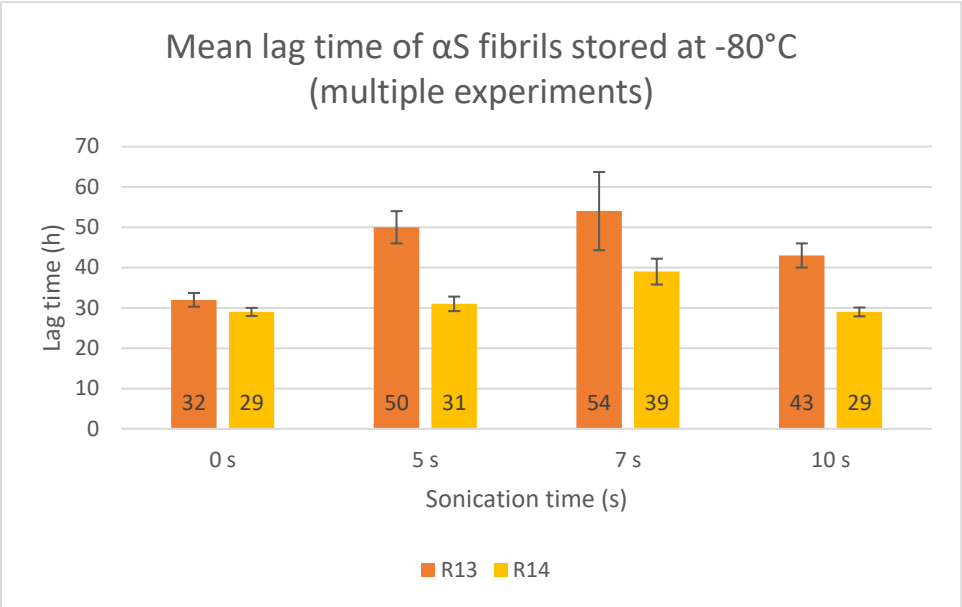

Figure 42. Comparing the lag times of this experiment's (R14) αS fibrils stored in the 4°C fridge with the identical condition of R13 (no vortexing). R13 refers to 'The effect of αS fibril sonication, storage temperature, and vortexing on αS aggregation of an alternative batch of αS fibrils' (page 58); R14 refers to '(Re)testing the effect of various αS fibril parameters on αS aggregation' (page 65).

Conclusion

The αS fibrils stored at the bench at room temperature had the shortest lag times, but it cannot be concluded from this experiment whether this is the result of the storage temperature or the use of the original αS fibril batch. The freshly sonicated αS fibrils did not act as functional αS seeds, so storage temperature is the only αS fibril handling that could be drawn conclusions for. The αS fibril handling seems to be more impactful on the lag time than sonication time. Sonication seems to lead to shorter lag times as compared to not sonicating, with more than half of unsonicated αS fibrils failed to aggregate within the duration of this experiment. No definite conclusion on the overall effect of sonication time can be made due to the experimental setup: not all sonication times are tested for all αS fibril handlings. Within each separate αS fibril handling, the different sonication times do not lead to a patterned effect on lag times. Conditions that were identical to conditions in previous experiments had similar lag times as these previous experiments, and the unsonicated samples remain inconsistent.

15. Combining SAA and SPC: attempt 4 (THT)

Introduction
This is the final attempt to combine SAA and SPC. The conditions are chosen based on previous experiments.

Previous experiments will be referred to as follows: R5 refers to 'The effect of αS fibril concentration and αS fibril sonication on αS aggregation' (page 12); R12 refers to 'The effect of αS fibril sonication on αS aggregation of an alternative batch of αS fibrils' (page 33); R13 refers to 'The effect of αS fibril sonication, storage temperature, and vortexing on αS aggregation of an alternative batch of αS fibrils' (page 58); R14 refers to '(Re)testing the effect of various αS fibril parameters on αS aggregation' (page 65).

Four conditions including a control have been selected for this experiment.
- A negative control with αS fibrils.
- The αS fibrils stored at the bench (original batch) that are 5 s sonicated have the most consistent and shortest lag time (< 10 h) in R5 and R14, despite their failure to properly aggregate in the previous SAA and SPC combination experiment using THT (R10 'Combining SAA and SPC: attempt 3 (THT)' on page 50).
- The αS fibrils stored in fridge (alternative batch) that are 5 s or 10 s sonicated both have a mean lag time of about 50 h in of R12, R13, and R14. This allows to test whether lag time influences SPC results.

Certain conditions are unavailable for this experiment. The αS fibrils stored in the –80 °C freezer have been fully used up. The freshly sonicated αS fibrils from R14 seemed to not have been transformed into functional seeds.

Materials and methods
Four conditions were prepared:
1. Control (0 M αS fibrils)
2. αS fibrils stored at bench (original batch); 5 s sonicated.
3. αS fibrils stored in fridge (alternative batch); 5 s sonicated.
4. αS fibrils stored in fridge (alternative batch); 10 s sonicated.

The fibril-containing samples each have a concentration of 1 µM αS fibrils. Reactant αS monomers that had been stored in the –80 °C freezer were used. The aggregation was monitored by means of THT fluorescence, for 139 h (≈ 5.8 days). 40 images per sample were obtained per measurement by fluorescence microscopy, or fewer if the images during measuring were deemed uncountable. SPC was performed on these images.

Results
SAA
The control samples failed to aggregate within the 139 h of the experiment (Figure 43).

The 5 s sonicated αS fibrils stored at the bench at room temperature clearly had the shortest lag time (2.7 ± 0.4 h) (Figure 47) and had a typical SAA curve (Figure 44). This follows the

results of previous experiments with the same condition, a short (<10 h) lag time and small variance (Figure 48).

The SAA curves of SAA for the 5 s sonicated αS fibrils stored in the 4°C fridge were very atypical (Figure 45). Only one was detected of having reached threshold, so no error bar could be established (Figure 47). This sample (S3C1M3) had three bouts of increasing fluorescence and subsequent falling down (Figure 45). This contrasts with previous experiments with this condition; the resulting SAA curves then were typical.

The SAA curves of SAA for the 10 s sonicated αS fibrils stored in the 4°C fridge on the other hand were typical (Figure 46), with a mean lag time of 73 ± 26 h (Figure 47). Compared to previous experiments with the same condition, the variance is large (Figure 49). The results for both the 5 s and 10 s sonicated αS fibrils stored in fridge lie within a 33 h range, with each the lag time being at least 40 h.

SAA discussion
The frequent pausing of the SAA in order to perform the SPC does seem to influence the SAA. For example, the 5 s sonicated αS fibrils stored at the bench at room temperature reached plateau as a proper S-curve, but when SPC was performed, the level of the plateau often shifted (Figure 44). The interruptions thus might be a factor why the 5 s sonicated αS fibrils stored in the fridge failed to properly aggregate, and especially why S3C1M3 has such a strange trajectory (Figure 45). On the other hand, the SAA curves for the 10 s sonicated αS fibrils stored in the fridge seem largely unaffected, even when SPC is performed during the exponential phase (Figure 46).

In several aggregation curves there is a small decrease in fluorescence immediately after an SPC session, especially notable in the 5 s sonicated αS fibrils stored at the bench. Due to its similarity across multiple curves of different conditions, it is most likely an instrumental artefact.

SPC
SPC was performed six times, at timepoints 0 h (= 0 days), 18.7 h (≈ 0.8 days), 48.2 h (≈ 2.0 days), 64.2 h (≈ 2.7 days), 71.3 h (≈ 3.0 days), and 91.9 h (≈ 3.8 days).

For the first three days, the control samples showed fewer than one particle per frame (Table 46 in appendix). This was is to be expected because no αS fibrils were added to the control samples, and the SAA did not take off. After the third measurement, the resulting images were completely black.

The 5 s sonicated αS fibrils stored at the bench at room temperature had a mean of 37 ± 9 particles per frame for the first SPC measurement (t = 0 h). The contrast was less than optimal, with a relatively bright background as compared to the particles (Table 47 in appendix). After this first measurement, the images were too bright for any particles to be counted, with some images being nearly completely white. This measurement was taken after the SAA reached plateau, so the concentration of αS might have risen too high for SPC in this setup (Figure 44). This could be the result of an excessive initial concentration of αS

fibrils or of reactant αS monomers, or both. The brightness decreased over time, but no countable particles were observed.

The number of fibrils for the samples with 5 s sonicated αS fibrils stored in the 4°C fridge could be determined for the first two SPC measurements: a mean number of particles per frame of 21 ± 8 for t = 0 h and 33 ± 2 for t = 19 h. After that, the contrast decreased; at the third measurement (t = 48 h) it is an edge case on whether the particles could be properly counted (Table 48 in appendix). Being an edge case is not sufficient for making strong conclusions, so the particle counting for this measurement was omitted. The fourth (t = 64 h) and fifth (t = 71 h) measurements showed bright clumps in which individual particles could not be counted, or merely a black screen. These images were notably less bright than those of the 5 s sonicated αS fibrils stored at the bench. The sixth measurement (t = 92 h) only led to almost or completely black images. Although all three aggregation curves increased between the first and third measurement, none properly started an exponential phase nor reached a plateau. Perhaps the αS fibrils that were formed clustered like the 5 s sonicated αS fibrils stored at the bench, but the total mass was so low that it resulted in empty black images.

Similarly, the number of fibrils for the 10 s sonicated αS fibrils stored in the 4°C fridge could be determined for the first two SPC measurements: a mean number of particles per frame of 5 ± 0.8 for t = 0 h and 25 ± 8 for t = 19 h. Also the contrast decreases afterwards, leading to again an edge case at the third measurement (t = 48 h) and uncountable images with bright clumps similar to those of the 5 s sonicated αS fibrils stored in 4°C fridge at the fourth (t = 64 h) and fifth (t = 71 h) measurements (Table 49 in appendix). At the sixth measurement (t = 92 h), there is a notable difference between the samples of the triplo. Two samples show clumped up bright clouds like previous images, and one shows just a black screen. At the sixth measurement, the two samples have reached plateau, but the one is still at baseline.

SPC discussion

Particles could often not be counted because the images were too bright and lacked sufficient contrast. The total αS fibril concentration during or after aggregation might have been so high that the emitted fluorescence of the dye saturated the images. The monomer concentration is 50 µM. If one assumes that at the end of aggregation all monomers are converted to fibrils, the expected number of fibrils would be 5.8E+16 fibrils/L (using the conversion as described by Vaneyck et al.[44], with assumptions as described in R7 'SPC can be performed on Amytracker-stained αS fibrils in a 96 well plate' (page 41). This corresponds to 3.5E+06 fibrils per image, which would probably indeed be so many fibrils as to saturate the image with fluorescence. Even if only a fraction of monomers would be converted into fibrils, the image probably still would be saturated. This then might be solved by lowering the amount of reactant αS monomers in the reaction mixture.

As time progressed, the brightness of SPC images decreased, leaving completely black images or bright clouds. This could indicate precipitation or other clustering of the fluorescent αS fibril mass. Herva et al. hypothesized that THT might not easily access large αS aggregates, when they found a decreasing THT signal in their PMCA reaction and no detectable monomers in their sample.[64] This might explain especially the trajectory of the 5 s

sonicated αS fibrils stored at room temperature (Table 47 in appendix). The SPC images quickly became so bright that no particles could be counted, and then the brightness decreased but particles could still not be distinguished in the bright clouds. It might be that as the reaction progressed, aggregates were formed that were too large to be properly stained by THT. A decrease in brightness was also observed in the SAA signal after plateau was reached (Figure 44), just like Herva et al..

Well plate

Figure 50 displays the bottom of the well plate at the sixth measurement (t = 92 h). Only certain wells look fluorescent by eye. The three wells belonging to the control samples (S1) do not look fluorescent, which is in line with the obtained black images at later SPC measurements and failed aggregation curves. The same holds for the 5 s sonicated αS fibrils stored in the 4°C fridge (S3). Similarly, the 5 s sonicated αS fibrils stored at the bench at room temperature (S2) has wells that look fluorescent by eye, and had typical aggregation curves and no black images. The wells of the 10 s sonicated αS fibrils stored in the 4°C fridge (S4) differ, the wells S4M2 and S4M3 look fluorescent and S4M1 does not. Well S4M1 contains the sample that indeed led to black microscope images, and whose SAA was still in its lag phase. Wells S4M2 and S4M3 did show fluorescence in the images, and proper SAA curves. So the visible fluorescence in the wells corresponds to microscopic images and aggregation curves.

A dried stain is visible under well S3M2 (Figure 50), which contains a sample of the 5 s sonicated αS fibrils stored in the 4°C fridge (S3C1M2 in Figure 45). One explanation is that prolonged exposure to the microscope's laser has burned a hole in the well plate and the contents of the well spilled out. Therefore, the volume of sample in each well was checked by pipetting it up with a pipet set to 50 µL (50 µL of sample was put in per well). C4 was indeed empty; all other wells contained about 50 µL. This well was then filled with red watercolor to test whether it would leak, which it did immediately. A broken well would explain the sudden drop-off in fluorescence (S3C1M2 in Figure 45).

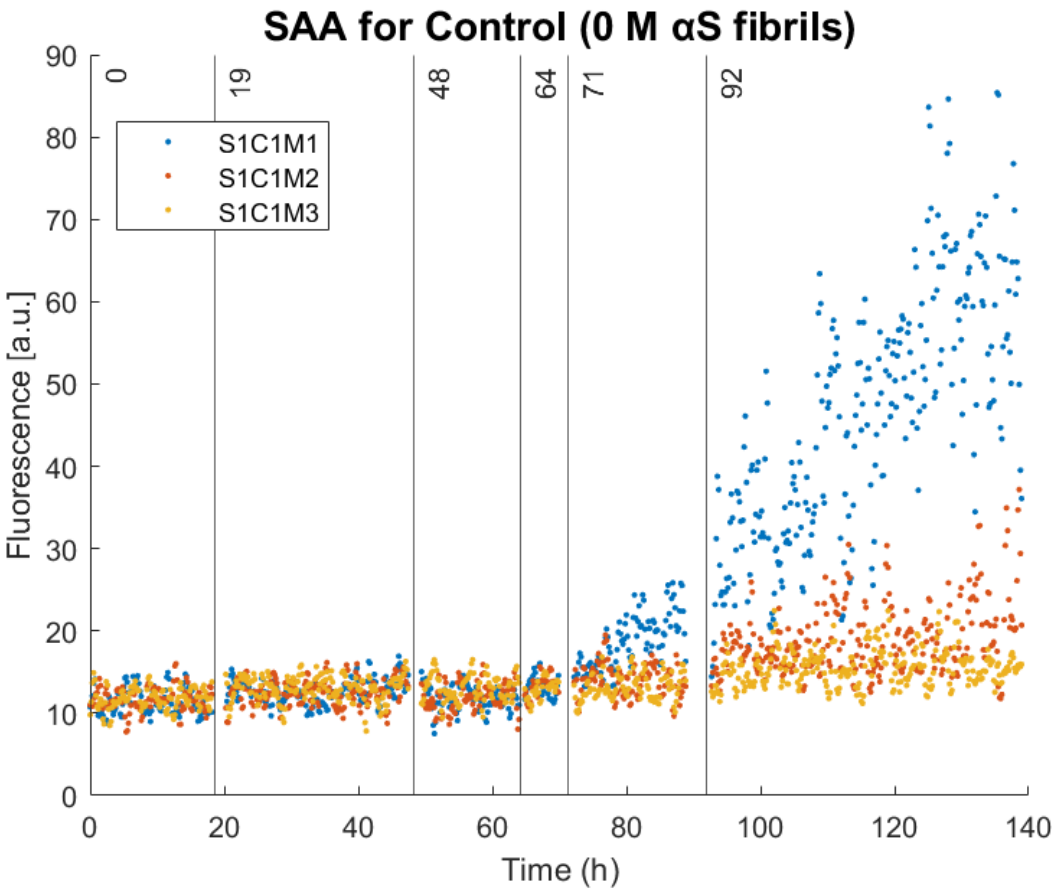

Figure 43. SAA curves for the negative control with 0 M αS fibrils (S1). The vertical lines indicate measurement times for the SPC.

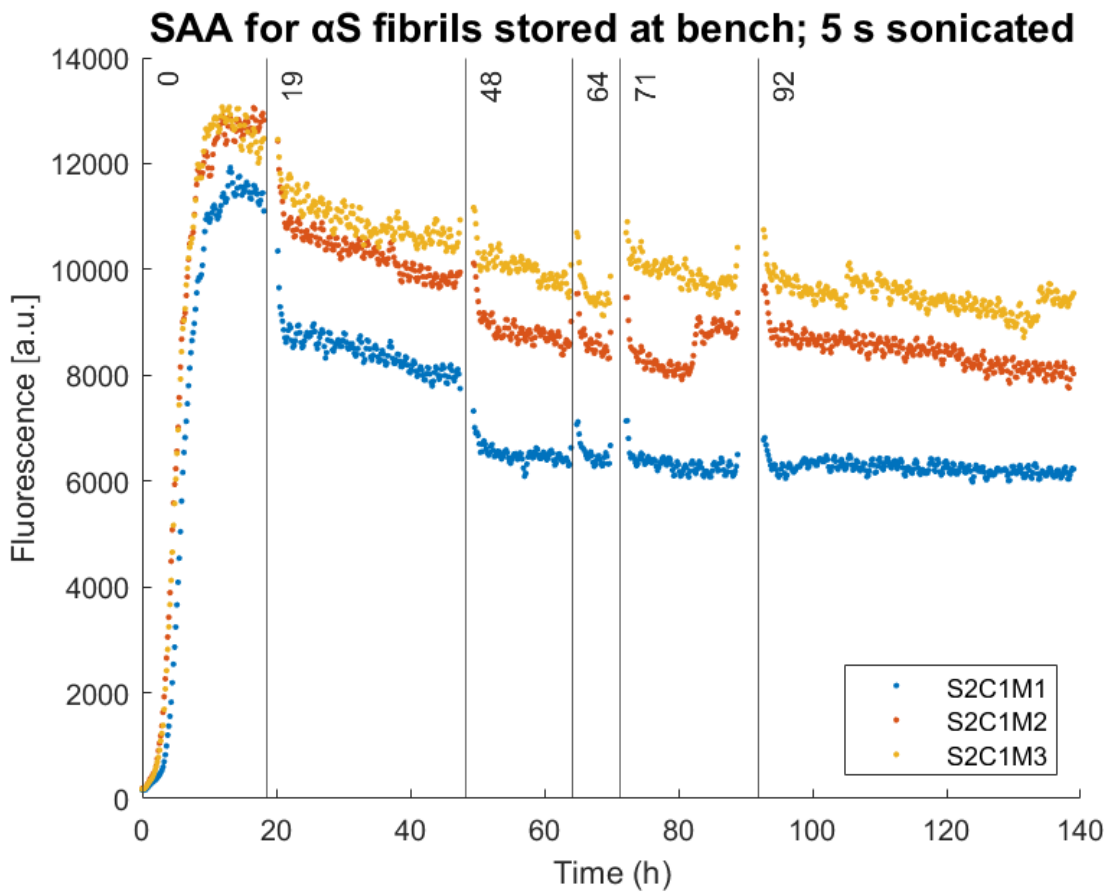

Figure 44. SAA curves for the 5 s sonicated αS fibrils stored at the bench at room temperature (S2). The vertical lines indicate measurement times for the SPC.

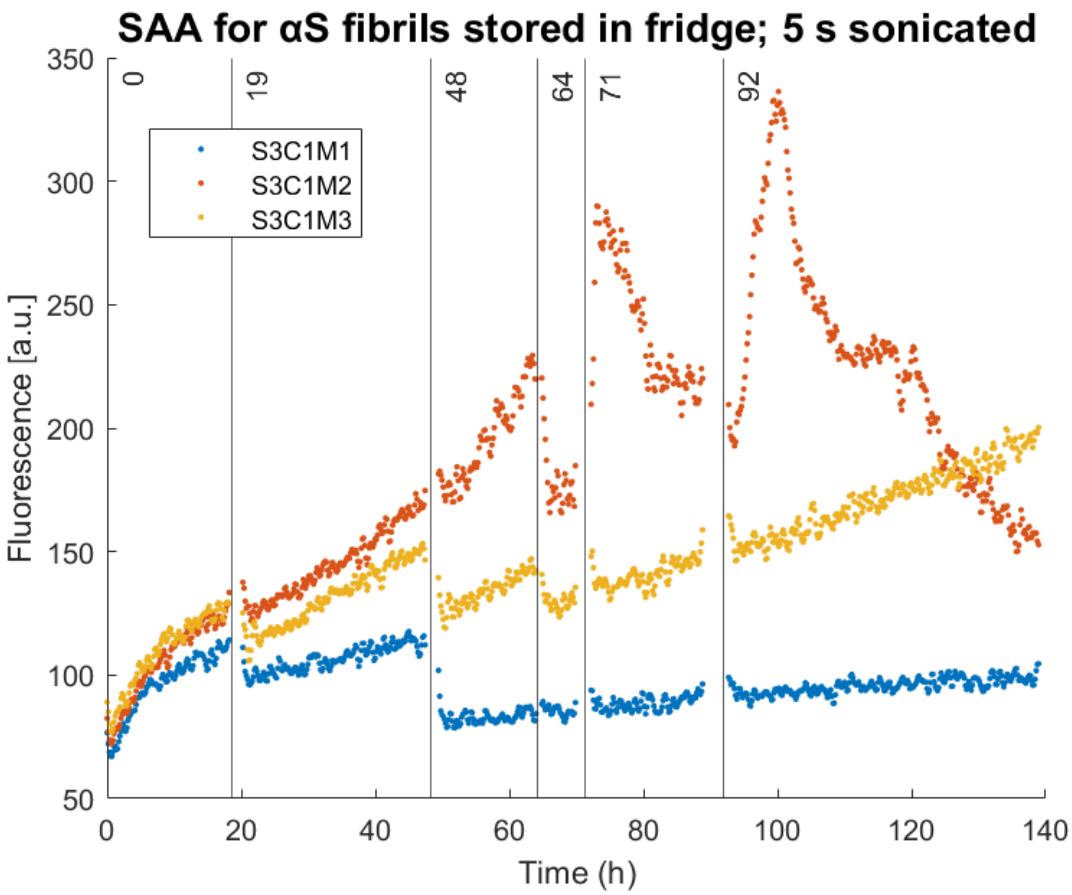

Figure 45. SAA curves for the 5 s sonicated αS fibrils stored in the 4°C fridge (S3). The vertical lines indicate measurement times for the SPC.

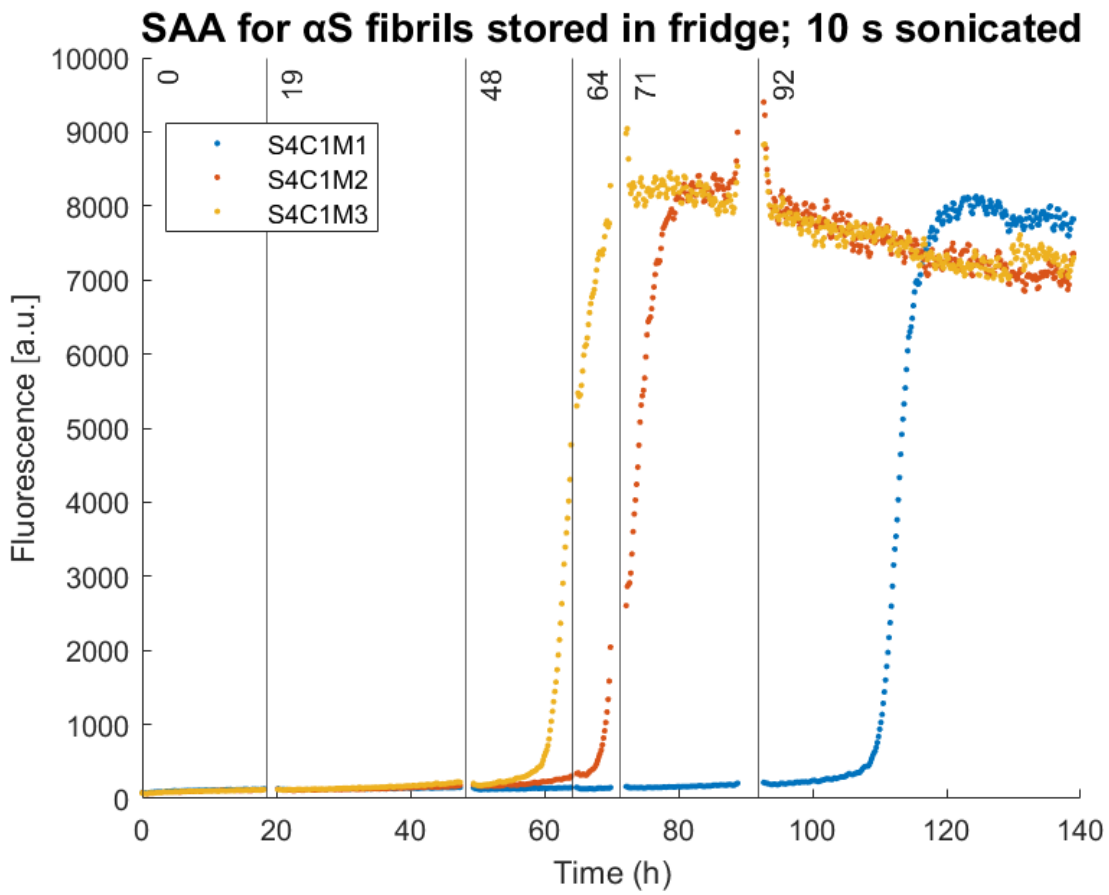

Figure 46. SAA curves for the 10 s sonicated αS fibrils stored in the 4°C fridge (S4). The vertical lines indicate measurement times for the SPC.

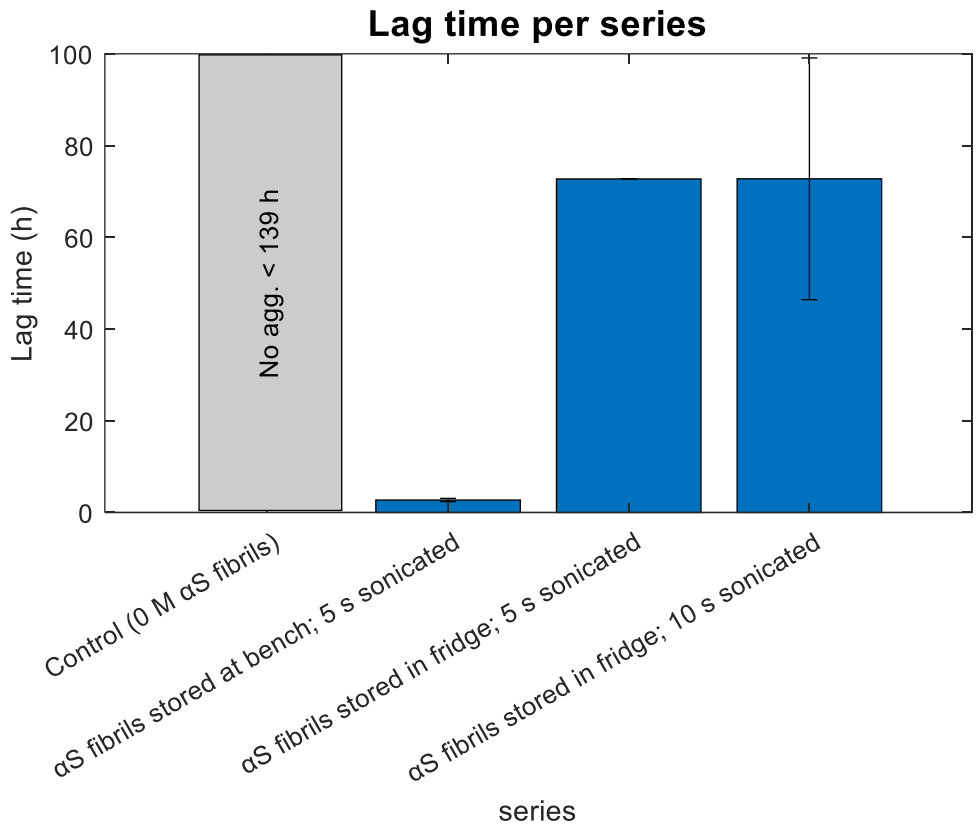

Figure 47. Lag times per series. Two of the three samples with the 5 s sonicated αS fibrils stored in the 4°C fridge failed to aggregate, so no error bar could be established.

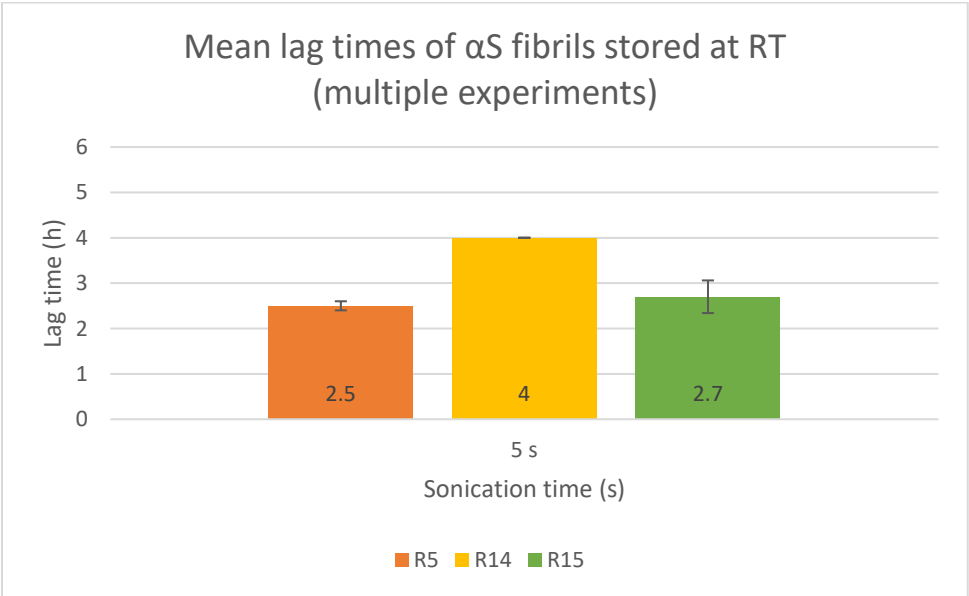

Figure 48. Comparing the lag times of this experiment's (R15) αS fibrils stored at the bench with the identical conditions of R14, and almost identical conditions of R5. R14 and R15 used a different batch of reactant αS monomers, which had been stored in the –80°C freezer.

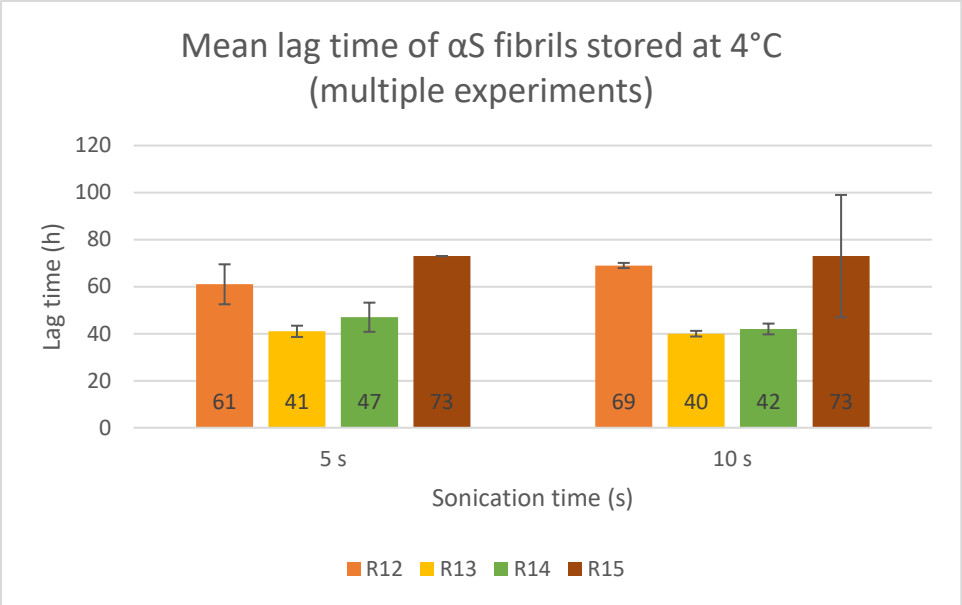

Figure 49. Comparing the lag times of this experiment's (R15) αS fibrils stored in the 4°C fridge with the identical condition of R12, R13, and R14. Two of the three samples of the 5 s condition of R15, so no error bar could be established.

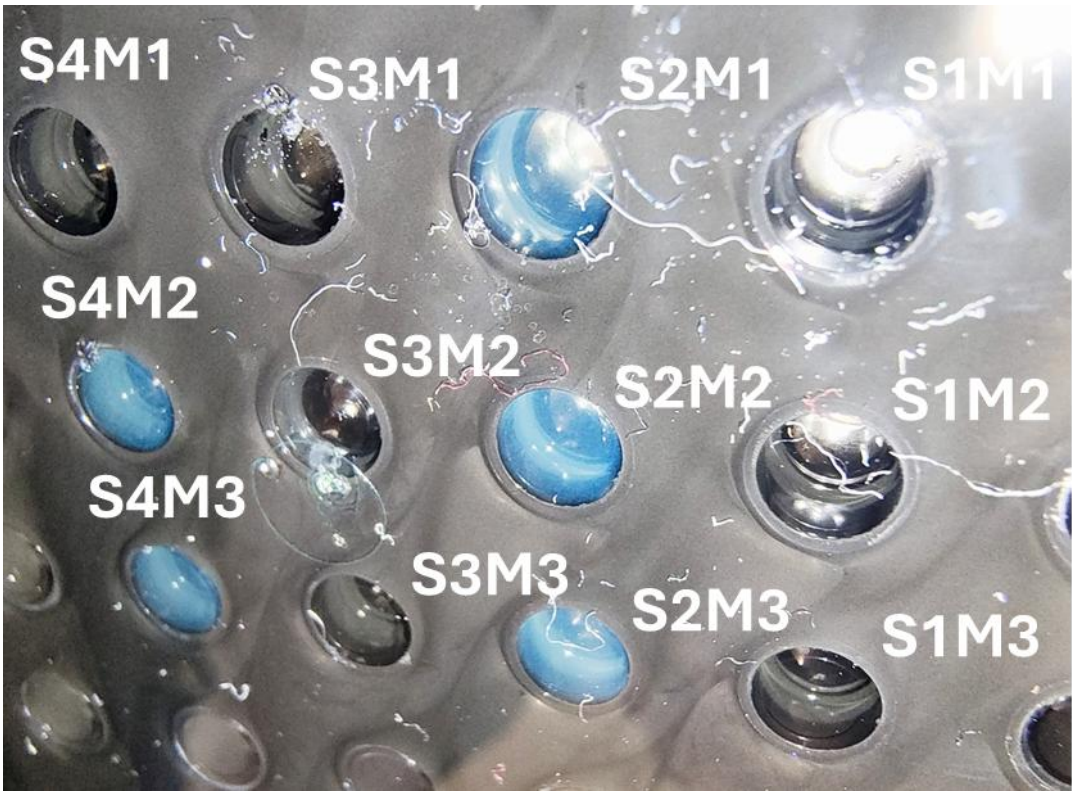

Figure 50. Bottom of the well plate. S1 = Control (0 M αS fibrils); S2 = αS fibrils stored at bench (original batch), 5 s sonicated; S3 = αS fibrils stored in 4°C fridge (alternative batch), 5 s sonicated; S4 = αS fibrils stored in 4°C fridge (alternative batch), 10 s sonicated. M1 = sample 1 of triplo; M2 = sample 2 of triplo; M3 = sample 3 of triplo.

Conclusion

Most aggregation curves are similar to previous experiments, but the multiple interruptions of the SAA might influence the SAA. This experiment confirms that the 5 s sonicated αS fibrils stored at the bench have the shortest lag time (< 10 h).

The current experimental conditions do not lead to satisfactory SPC results. No particles could be counted for images taken after 18 h.

4. Discussion

Improving SAA

There are many more parameters that can be tested that influence the SAA, such as iconic strength conditions (salt concentration)[44,51,52,65], pH[24,51,65,66], temperature[65,66], addition of beads (material, size, number)[24,30], detergents (e.g. sodium dodecyl sulfate (SDS))[24,51,65], glycosaminoglycans (e.g. heparin)[51,67], polyamines[66,67], polycations[51,65], negatively charged surfaces (e.g. glass or supported lipid bilayers)[68], the use of other mutant αS forms[19], reactant αS monomer concentration[24,25,51,65], and molecular crowding[51,65,66].

Articles reviewing parameters influencing SAAs include Giehm et al.[51], Ghosh et al.[67], Candelise et al.[66], and Narkiewicz et al.[65]. For practical advice on producing and using αS fibrils, please be referred to Polinski et al..[61]

Please note that altering a parameter can have positive effects, but also (simultaneous) negative effects. For example, the addition of beads can increase aggregation efficiency, but also increases the chances of non-specific aggregation.[19] Therefore all effects of altering a parameter must be taken into account in order to achieve proper optimization.

A promising development is the digital SAA, in which hundreds or thousands of SAAs are run simultaneously in tiny separate compartments.[34,38] If this could be combined with SPC, it would greatly increase the throughput.

Improving SPC

Although the capturing of SPC image sequences per well was automated, the well plate needed to be moved by hand over the microscope stage to switch between wells. Automating this process by programming stage movements would reduce manual labor and increases the measurement consistency.

Unfortunately, many images have not been suitable for SPC mostly due to either being too bright or lacking sufficient contrast. The first attempt to resolve this should be to lower the amount of monomeric αS in the reaction mixture, as mentioned in R15 ‘Combining SAA and SPC: attempt 4 (THT)’. This will decrease the amount of fluorescent fibrils during and after aggregation as to not saturate the image.

Using TrackPy for counting single fibrils has its drawbacks. First, TrackPy has been developed for analyzing blob-like particles.[48] If a fibril surpass a certain length, TrackPy becomes completely unsuitable for counting; it consistently detects it as multiple particles. There is most often no combination of parameter settings for which all fibrils are counted correctly. Setting the parameters as to avoid fibrils being missed often leads to other fibrils being counted as multiple or noise being detected as a fibril. The best result is mostly an imperfect compromise. Second, using TrackPy is inherently subjective. The program outputs images indicating found particles, which are evaluated by visual inspection. The result is either accepted, or parameters are altered manually as to obtain a better result. This is prone to

human subjectivity, inconsistency, and computer screen characteristics. Third, this whole process is rather time-consuming.

Shortcomings
The Amytracker dye was never validated in an SAA. The only experiments in which Amytracker was used to monitor aggregation are R8 'Combining SAA and SPC: attempt 1 and 2 (Amytracker)'. Unfortunately, the aggregation failed – most likely due to incorrect amount of dye – and a proper SAA curve was never obtained with Amytracker. If this project is continued, I would advise to validate whether Amytracker is a proper dye to monitor αS aggregation.

The found lag time depends on the used method of lag time determination, and the means by which it is implemented. I wrote MATLAB code myself to achieve this. The code does not perform well with non-ideal curves, such as curves that do not follow an S-curve or have a very long lag time, or if no aggregation occurs. I solved this mostly manually, e.g. by removing samples that failed to aggregate. So this automated MATLAB script requires a significant amount of manual dataset-specific changes. The code is not optimized; and since I do not have a strong formal training in programming, there probably are improvements possible that I am not even aware of.

An alternative to creating in-house code to analyze aggregation curves could be to use existing software such as AmyloFit.[69]

The lag times were not compared by means of statistical testing because each condition was measured in triplo, which is not enough to make strong statistical claims. The aforementioned digital SAAs might solve this.

Future: The path from simple compound to complex
If it is decided for the project to continue, these are the steps to reach to goal of quantitatively diagnosing Parkinson's disease. The setup to combine SAA with SPC should first be optimized until it performs sufficiently with a model fluid. Then, it can progress to artificial CSF. The next step is then human CSF, initially pooled CSF from multiple people, then CSF from a single healthy individual. Lastly, the setup should be tested on CSF from a patient with Parkinson's disease.

5. Conclusion

An SPC setup in which αS fibrils can be counted during an SAA was successfully constructed and tested. Various parameters influencing the SAA were tested; the reasonings for testing and the outcomes summarized in Table 5. The tested parameters influencing the SPC during an SAA are summarized in Table 6. Unfortunately, no experiment combining the SAA and SPC was completely successful, i.e. there was no experiment which simultaneously captured an adequate aggregation with SAA and images of countable particles with SPC for the full duration of the experiment. In conclusion, this project has not established a functioning quantitative SAA method, but has made steps towards it.

Table 5. Tested parameters influencing the SAA, the reasoning for testing, and the outcomes. The original batch of αS fibrils was stored at room temperature and the alternative batch at –80°C or 4°C.

Parameter	**Conditions**	**Reason to test**	**Outcome**	**αS fibril batch**	**Experiment**
Reactant αS monomer type	WT, K23Q	The K23Q αS mutant has been reported to suppress de novo fibril formation, while aggregating similarly to αS WT in presence of αS seeds.[40,50]	K23Q provided no benefit over WT: - There was no difference in the de novo fibril formation. - The K23Q failed to aggregate more often and aggregated slower in presence of αS seeds than the WT.	Original	R2 (page 22)
αS fibril concentration	0, 10^{-6}, 10^{-8}, 10^{-10}, 10^{-12}, 10^{-14}, 10^{-16}, 10^{-17} M equivalent reactant αS monomer concentration	A higher αS seed concentration leads to earlier onset of exponential growth[44] and a higher initial aggregation rate[24,25]. This limits the time expenditure of an SAA; and shorter lag times are correlated with higher reproducibility.[51]	An αS fibril concentration of 10^{-6} M resulted in the shortest lag time.	Original	R5 (page 33)
αS fibril sonication time	0 s, 1 s, 3 s, 5 s.	Sonicating αS fibrils fragments them and leads to faster aggregation than not sonicating seeds.[25,58]	Sonicating decreases lag time and variance. 5 s has the most effect.	Original	R5 (page 33) R14 (page 65)
	0 s, 5 s, 7 s, 10 s		Sonicating beyond 5 s does not decreases lag time, but decreases variance. No significant differences between sonication times. Please note that these larger sonication times were only tested for the alternative batch of αS fibrils.	Alternative	R12 (page 33) R13 (page 58) R14 (page 65)

Reactant αS monomer storage	–80°C freezer, 4°C fridge	Polinski et al. recommend to store reactant αS monomers at –80°C "to prevent spontaneous aggregation that can occur at room temperature", but mentions nothing about storing reactant αS monomers at 4°C.[61] Tarutani et al. found that leaving reactant αS monomers standing for seven days at room temperature (20~25°C) or 37°C both result in oligomer-like structures, but not at 4°C (for comparison: shaking at 37°C resulted in fibrous structures).[58]	Reactant αS monomers stored in the –80°C freezer resulted in shorter lag times and lower variance than those stored in the 4°C fridge.	Alternative	R11 (page 53)
αS fibril storage	–80°C freezer, 4°C fridge	Polinski et al. recommend to store αS fibrils at room temperature or –80°C and dissuade to store them at 4°C[61] because of αS fibril cold-denaturation into monomers at 0-20°C[62]. On the other hand, Sidhu et al. found that fibrils did not dissociate at 4°C in their specific experimental conditions.[59]	Only a small effect was observed: the αS fibril stored in the -80°C freezer resulted in smaller lag times than the 4°C fridge.	Alternative	R13 (page 58)
Vortexing αS fibrils	0 s, 5 s	Agitation is known to induce αS aggregation.[51]	Vortexing the αS fibrils prior to SAA does not seem to influence the lag times.	Alternative	R13 (page 58)

Table 6. Tested parameters influencing the SPC during an SAA, the reasoning for testing, and the outcomes. The original batch of αS fibrils was stored at room temperature and the alternative batch at –80°C or 4°C.

Parameter	**Conditions**	**Reason to test**	**Outcome**	**αS fibril batch**	**Experiment**
Fluorescent dye	Thioflavin T (THT), Amytracker	THT is an established dye for αS.[51] Amytracker is not, but contrary to THT its spectrum does not overlap with the most common biological autofluorescence.[55,56]	Amytracker can stain αS fibrils so that they can be counted in the SPC set-up, on both a coverslip and in a 96 well plate.	Original	R3 (page 26) R7 (page 41) (confirmed in R8 (page 43))
αS fibril concentration	0, 10^{-6}, 10^{-8}, 10^{-10} M equivalent reactant αS monomer concentration	The 10^{-6} M had the shortest lag time in the SAA. The two highest concentrations after that were added to see if it made a difference at the SPC.	No tested concentration result in countable images for the full duration of the experiment. Particles could often not be counted because the images were too bright and lacked sufficient contrast, possibly due to an excessive amount of fibrils. As time progressed, brightness decreased, possibly due to large fibril aggregates and/or precipitation.	Original	R15 (page 73)

Acknowledgements

First I would like to thank Mireille Claessens and Christian Blum for giving me the opportunity to complete my master's assignment at the Nanobiophysics research group. I am grateful for the received flexibility and patience in the face of nebulous medical issues, and for the continued support in the reorganizational mayhem.

Slav Semerdzhiev, thank you for being my daily supervisor for a major part of this project.

Jos Paulusse, thank you for being part of the master committee, in spite of the reorganization.

Then I would to thank the lab technicians Robert Molenaar and Kirsten van Leijenhorst-Groener for their support in the optical lab and chemical lab respectively. Your efforts have been indispensable in this project (and probably all other projects in this research group).

I would also like to thank our secretary Sylvia Winters, *die de zaken in goede banen leidt* (there is no proper direct English translation for this expression).

Lastly, I would like to thank Tim Nachtergaele for proofreading this entire report – without any background in the biomedical or biophysical field – and his unwavering support.

To those affected by the faculty reorganization: As you may be already aware, I find the proceedings of the faculty reorganization highly regrettable, especially the lack of communication and the seeming absence of a predetermined plan – or any meaningful forethought – for staff or students. I might have been disappointed by how the reorganization has been conducted, but I certainly was not in the staff who chose to continue without official obligation to do so. I recognize this choice was not a given, yet it has allowed me to graduate with (relatively) minimal complications. It is something I cannot be grateful enough for. I sincerely wish better prospects will arrive shortly and that the future brings better circumstances.

Appendix

1. Establishing a calibration curve for single particle counting (SPC) within a microbead model system

Table 7. The observed and expected mean number of particles per image, and the observed and expected ratio of the mean number of particles per image between each dilution step.

Dilution (x1000)	Mean # particles/image (observed)	Mean # particles/image (expected)	Ratio per step (observed)	Ratio per step (expected)
5	39	39	-	-
10	17	20	0.44	0.50
15	11	13	0.65	0.67
20	9.0	9.9	0.80	0.75
30	2.5	6.6	0.28	0.67
40	1.9	4.9	0.74	0.75

Table 8. Representative image of each dilution of the beads dilution series. The image size is 202 x 81 µm.

Dilution (x1000)	Representative image
5	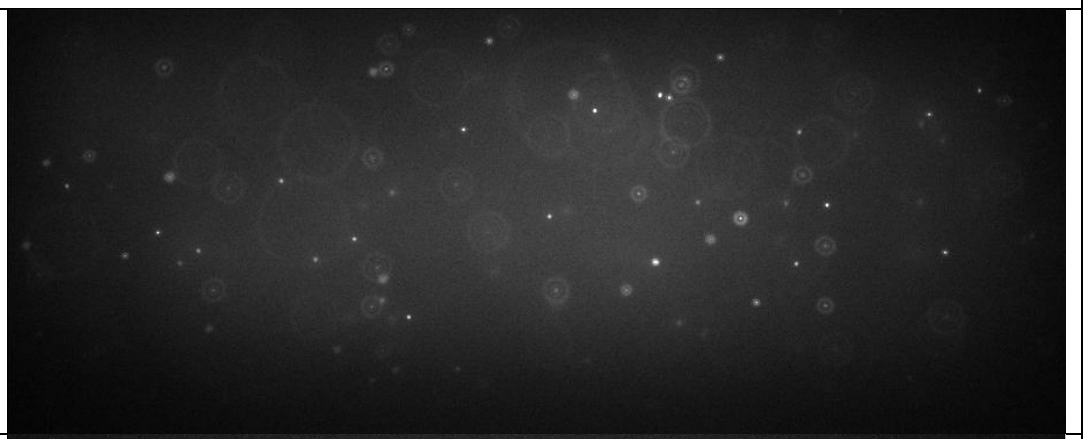
10	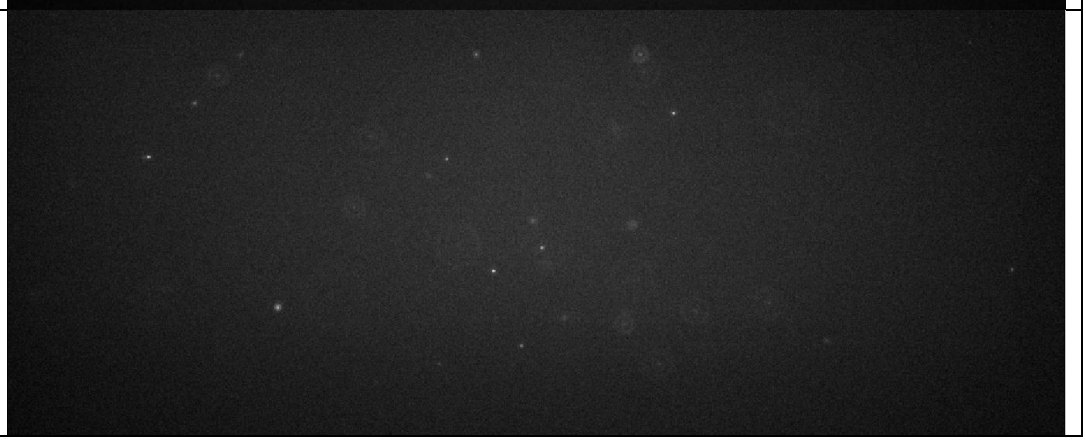

15	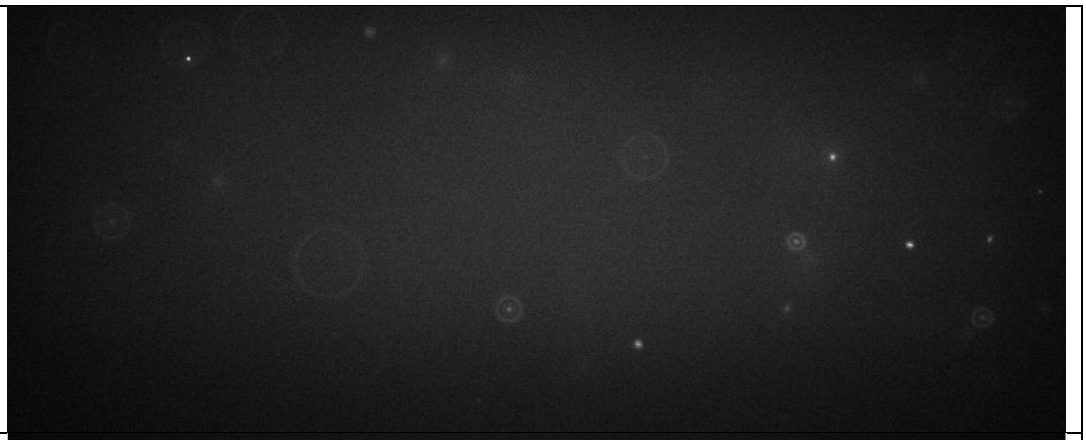
20	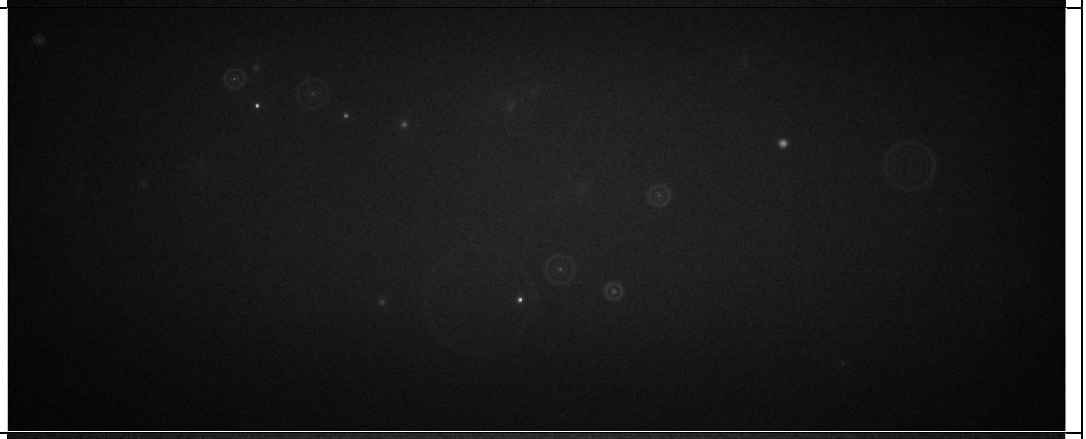
30	
40	

2. The αS K23Q mutant does not suppress de novo fibril formation in an SAA

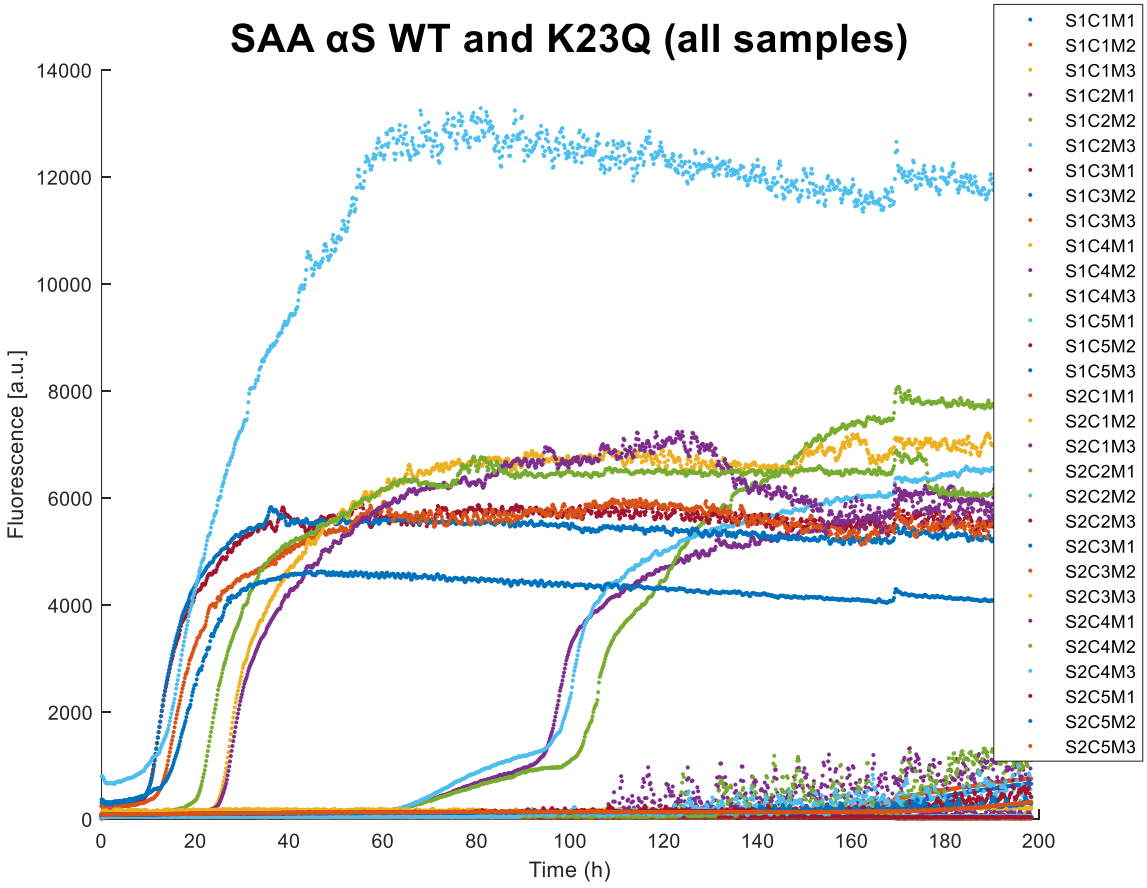

Figure 51. The SAA curves of all samples. The samples are described by their coded labels: S indicates αS fibril type, C indicates αS fibril concentration (in monomer equivalent concentration) and M the samples of a triplo. S1 = αS WT; S2 = αS K23Q. C1 = 0 M (negative control); C2 = 0.25 µM; C3 = 0.5 µM; C4 = 1 µM; C5 = 2 µM. M1 = sample 1 of triplo; M2 = sample 2 of triplo; M3 = sample 3 of triplo.

Table 9. Mean lag time, standard deviation and number of used measurements per condition.

aS monomer type →	**αS WT**			**αS K23Q**		
aS fibril concentration ↓	Mean	STD	#M	Mean	STD	#M
0.25 uM	59	2	3	NaN	NaN	0
0.5 uM	11	1	3	149	4	2
1 uM	18	5	3	NaN	NaN	0
2 uM	13	0	2	152	18	3

Table 10. The count and percentage of aggregation categories.

Category	Count	Percentage
# samples	30	100
# non-aggregated samples	14	47
# aggregated samples	16	53
# ideal cases	12	40
# diff lag time =< 5 h	1	3
# diff lag time > 5 h	3	10

3. Validating the use of Amytracker in SPC of αS fibrils

3.1. Determining the αS fibril concentration

Table 11 displays the absorbances as measured using the Nanodrop for the two settings Protein 280 and UV-VIS. The sample was measured four times per setting.

Table 12 displays the αS fibril concentration per Nanodrop setting, and the average αS fibril concentration when combining results from both settings. Figure 52 displays this information as a graph.

It was determined whether these two settings produced significantly different results by means of a two-sided two-sample t-test with independent samples (assuming normal distribution and equal variances) at a significance level of 5%. The associated p-value of the t-test is 0.11, which indicates that the means of measurements made with Protein A280 or UV-VIS setting are not significantly different (at a 5% significance level).

Table 11. Absorbances at 280 nm as measured using the Nanodrop, using the Protein A280 and UV-VIS settings.

Method	**Absorbance at 280 nm**
ProteinA280	0.143 0.164 0.133 0.227
UV-VIS	0.016 0.031 0.021 0.034

Table 12. Average αS fibril concentrations, per Nanodrop setting and combined.

Method	**αS fibril concentration (µM)**	**Standard deviation**
ProteinA280	70.2	6.53
UV-VIS	54.5	13.0
Combined	62.3	13.0

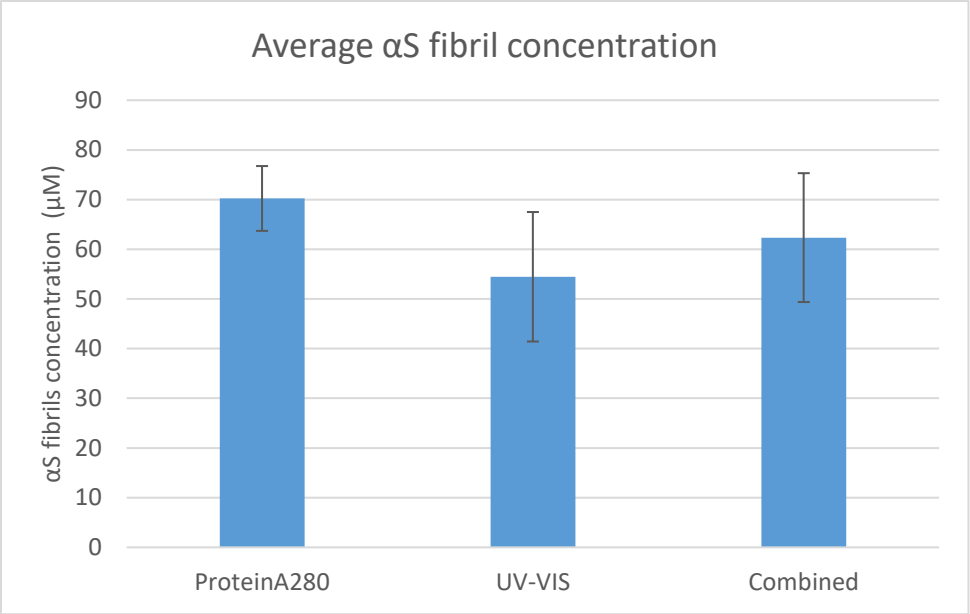

Figure 52. Average αS fibril concentrations, per Nanodrop setting, and combined.

3.2. Amytracker-fibril dilution series

3.2.1. Amytracker-fibril dilution series I

The Amytracker-fibril dilution series was performed twice. The outcomes of the second (dilution series II) can be found in the main text. The first (dilution series I) is discussed here in the appendix. Some experimental choices of the second were based on the results of the first.

Dilution series I comprised ten samples with ten different Amytracker concentrations and a constant αS fibril concentration. The dilution factor and concentration of Amytracker for each sample is listed in Table 13. The pooled WT αS fibrils from a previous experiment were used (R2 'The αS K23Q mutant does not suppress de novo fibril formation in an SAA' on page 22), as described in the main text. The αS fibrils were not diluted prior to mixing it with the Amytracker to create the final samples, so its concentration in the final sample was 31.1 ± 6.5 µM, i.e.[24.7, 37.6] µM.

This αS fibril concentration was found to be too high; images were so crowded with fibrils that they could not be counted. These existing samples were then incrementally diluted and imaged until it was found that diluting 1000x led to countable results. Table 14 displays the new dilution factor and concentration of Amytracker per sample. These 1000x diluted samples were then fully imaged and analyzed.

100 images were taken for each sample. Images with artefacts were removed, in total 55 images were removed among all samples, i.e. 5%. Then fibrils were counted using TrackPy. The TrackPy settings were the same for all samples: MinmassVal = 500, cluster radius = 15, diameter = 9, search radius = 11.

Figure 53 shows the mean number of particles per image per sample. Sample #1 (3.0 nM Amytracker) is missing due to improper measurements. The four samples with Amytracker concentrations ranging from 0.03 to 0.3 nM do not show a properly measurable amount of particles. The five samples with Amytracker concentrations of 0.5 to 1.5 nM do elucidate the fibrils so that they can be counted. That is why these five concentrations were chosen to be tested again in the Amytracker-fibril dilution series II.

The experiment was repeated due to the necessary extra 1000x dilution step. In the dilution series I, the already prepared samples (i.e. containing both Amytracker and fibrils) were diluted 1000x. Ideally, one would first dilute the separate components to the desired concentration and then mix them to avoid an extra unnecessary pipetting step. That is what was done in the dilution series II.

Table 13. The dilution factor and concentration of Amytracker for each sample of Amytracker-fibril dilution series I, as originally intended.

Sample #	#1	#2	#3	#4	#5	#6	#7	#8	#9	#10
Amytracker dilution (x)	500	1,000	1,500	2,000	2,500	3,000	5,000	10,000	20,000	50,000
Amytracker concentration (µM)	3.0	1.5	1.0	0.75	0.60	0.50	0.30	0.15	0.075	0.030

Table 14. The dilution factor and concentration of Amytracker for each sample of Amytracker-fibril dilution series I, after an additional 1000x dilution.

Sample #	#1	#2	#3	#4	#5	#6	#7	#8	#9	#10
Amytracker dilution ($x10^6$)	0.5	1.0	1.5	2.0	2.5	3.0	5.0	10	20	50
Amytracker concentration (nM)	3.0	1.5	1.0	0.75	0.60	0.50	0.30	0.15	0.075	0.030

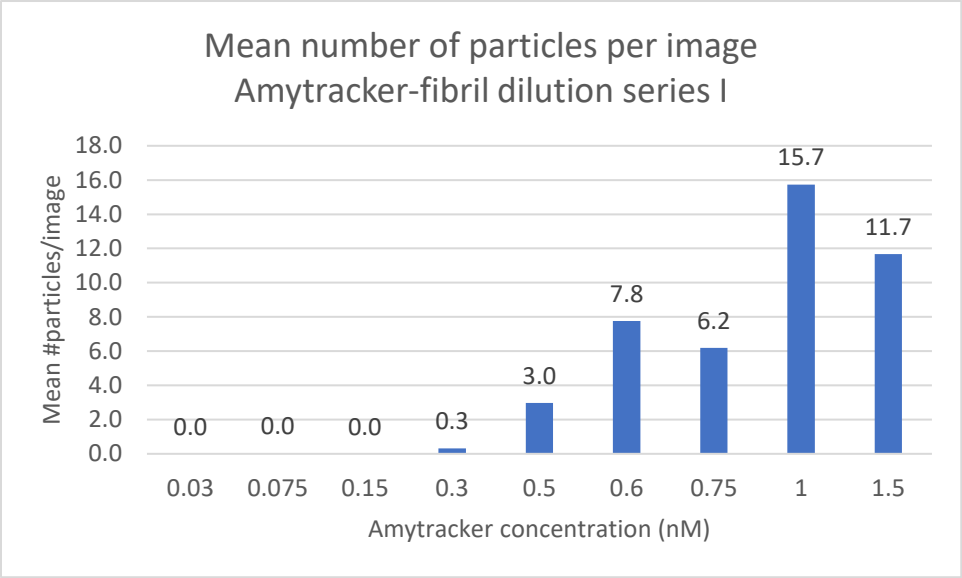

Figure 53. The mean number of particles per image for each sample of Amytracker-fibril dilution series I, after an additional 1000x dilution.

3.2.2. Amytracker-fibril dilution series II

In the main text it was established that an Amytracker range of 0.75 – 1.5 nM is suitable for producing images with a countable number of fibrils. A constant concentration of αS fibrils was used, but this concentration was determined as a range (31.1 ± 6.5 nM, i.e.[24.7, 37.6] nM). The Amytracker-fibril ratio depends on which part of this αS fibril range was used for calculation. Table 15 lists the Amytracker-fibril ratio not only based on the mean of the αS fibrils, but also the upper and lower bounds.

Table 16 contains representative images of each sample of the Amytracker-fibril dilution series II.

Figure 54 displays the mean number of particles per image for each Amytracker concentration, for the standardized image size of 100 x 100 µm.

Table 15. Amytracker-fibril ratios based on the mean, upper bounds and lower bounds of αS fibril concentration.

	31 nM fibrils (mean)	**25 nM fibrils (lower bound)**	**38 nM fibrils (upper bound)**
1.5 nM Amytracker	1:21	1:16	1:25
0.75 nM Amytracker	1:42	1:33	1:50

Table 16. Representative image of each dilution of the Amytracker-fibril dilution series II. The image size is 202 x 81 µm.

Amytracker concentration (nM)	**Representative image**
0.50	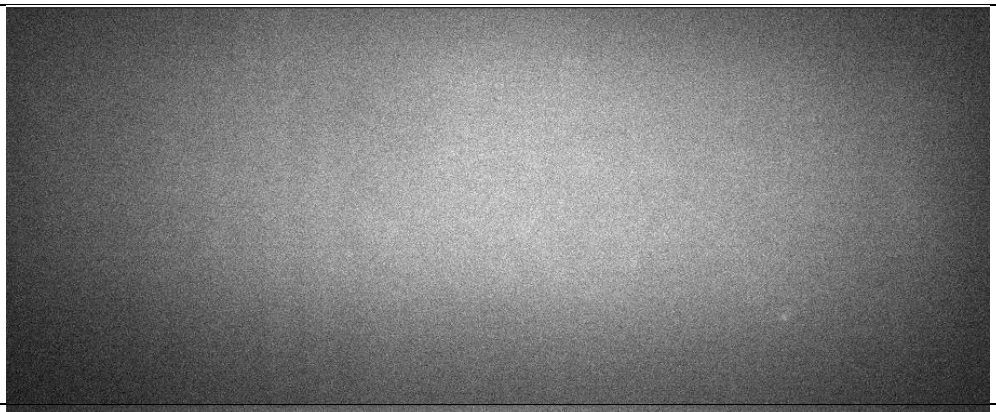
0.60	
0.75	
1.0	

1.5	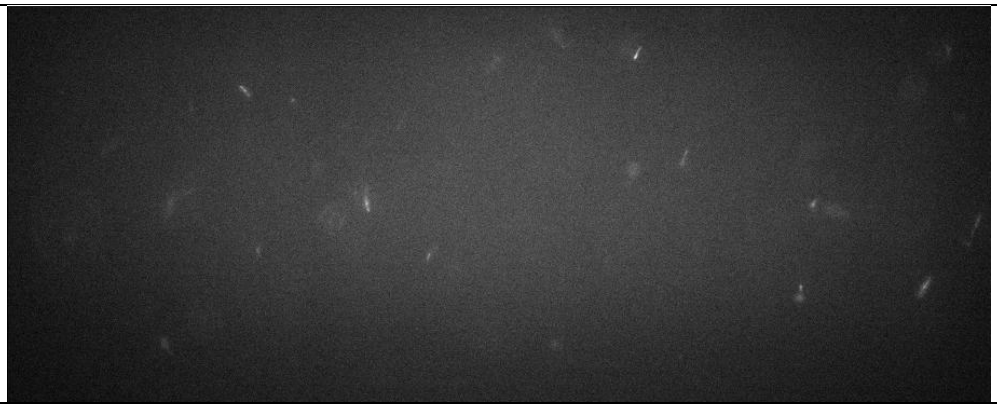

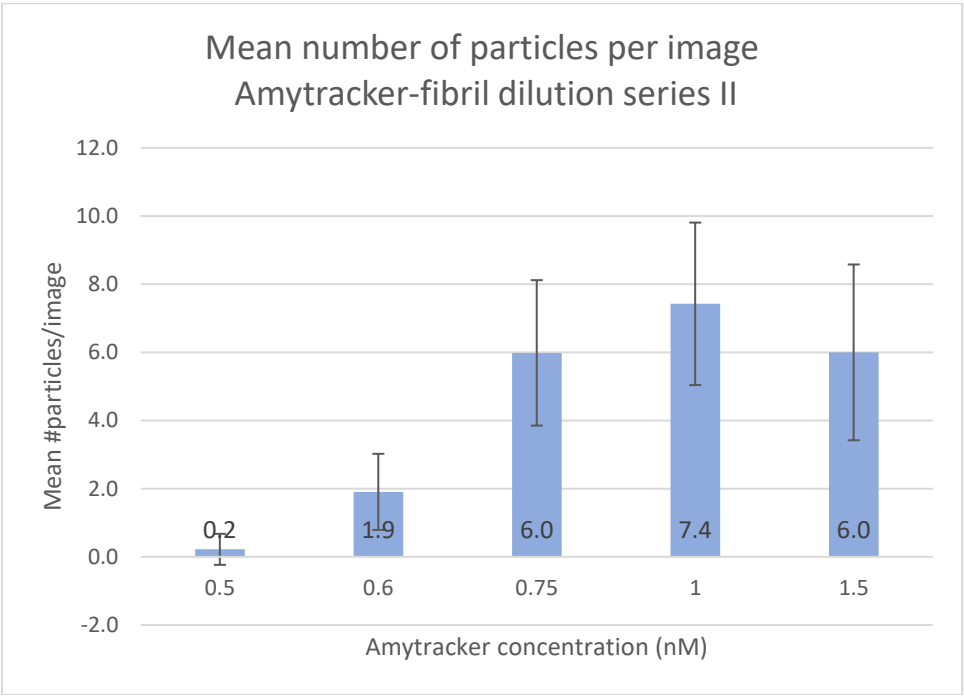

Figure 54. The mean number of particles per image for each Amytracker concentration, for the standardized image size of 100 x 100 µm.

3.2.3. Background signal

Aside from the goal stated in the main text, another intended goal of the Amytracker dilution series was to investigate the effect of Amytracker concentration on background signal when measuring αS fibrils. It was hypothesized that a higher concentration of Amytracker might decrease the signal-to-noise ratio in the following ways:

- Unbound Amytracker can still give fluorescent signal.
- Out-of-focus fibrils labeled with Amytracker can still give fluorescent signal that reaches the plane of focus.

To reach meaningful conclusions of Amytracker's effect on background signal, the background signal should be quantified. For this end, a clear threshold between background and fibrils should be able to be established. The obtained data are grey scale images, meaning each pixel has one value reflecting its brightness. Fibrils are lighter than the dark background. If these grey values are plotted in a histogram, there would ideally be two

separate peaks: one peak at the lower grey values for the background and one peak at the higher grey values for the fibrils.

For each Amytracker concentration, all grey values of all images were compiled and made into a histogram. Not all had the same number of images because images with artefacts were removed. This was corrected by dividing the histogram counts by the number of images for that Amytracker concentration, leading a 'normalized' result. Figure 55 and Figure 56 display the results for Amytracker dilution series I and II, respectively.

The ideal of two separate peaks do not occur in either series. A clear threshold between background and fibrils can thus not be easily established. There are various techniques to still set a threshold, but advanced image analysis is beyond the scope of this project. Therefore, the question how the Amytracker concentration affects the background signal remains unanswered.

The histograms do support the findings of the single particle counting. All have a peak at the lower grey value region indicating the background. Some have a 'shoulder' sloping downwards to the right (towards the higher grey values), indicating the presence of fibrils.

For dilution series I, Amytracker concentrations 0.5 to 1.5 nM have this shoulder, which corresponds to the single particle counting finding a countable number of particles for these concentrations. The 0.5 nM Amytracker has a smaller shoulder, corresponding to the smaller number of particles as found through single particle counting. Amytracker concentrations 0.03 to 0.3 nM lack this shoulder, indicating the absence of fibrils, again supporting the findings of the single particle counting.

For dilution series II, Amytracker concentrations 0.75, 1.0 and 1.5 nM do show this shoulder, and 0.5 and 0.6 nM lack this shoulder. This data thus also confirms what was found by single particle counting.

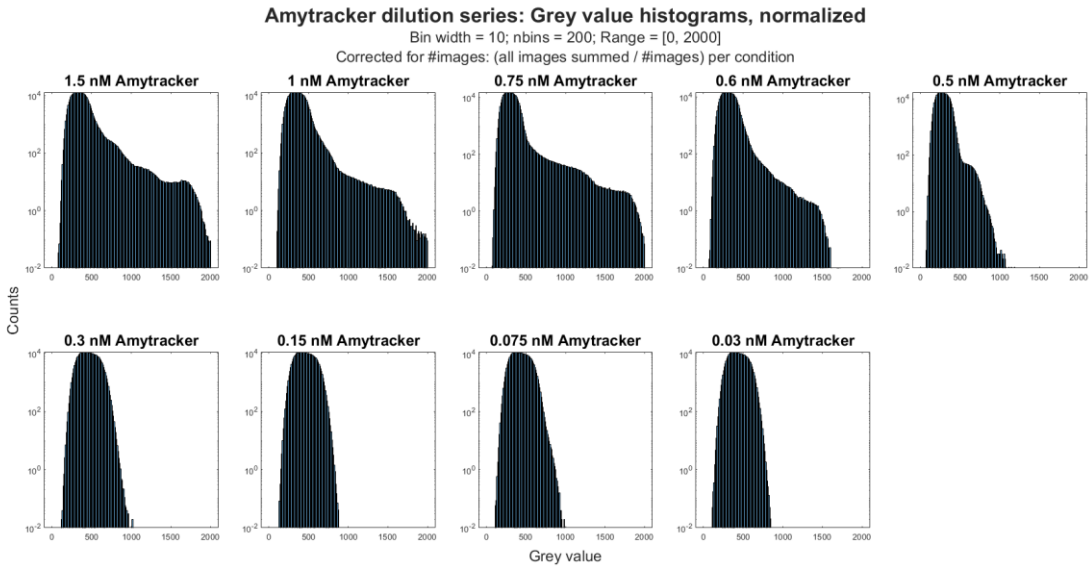

Figure 55. Histograms of grey values, per Amytracker concentration, for Amytracker dilution series I. The histograms are 'normalized' in the sense that the counts of each histogram were divided by the number of images for that particular Amytracker concentration. Please note the logarithmic y-axis.

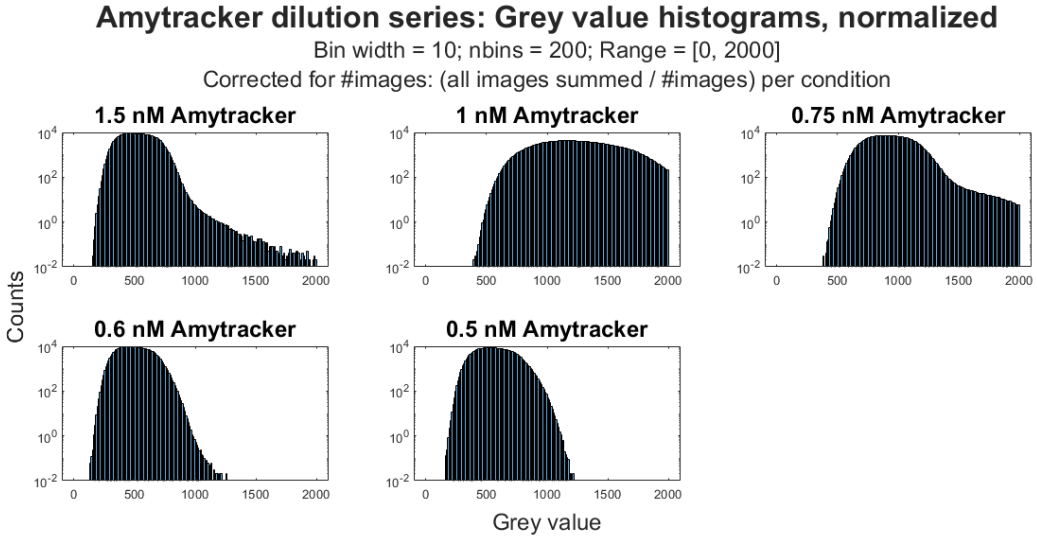

Figure 56. Histograms of grey values, per Amytracker concentration, for Amytracker dilution series II. The histograms are 'normalized' in the sense that the counts of each histogram were divided by the number of images for that particular Amytracker concentration. Please note the logarithmic y-axis.

3.3. Double-staining fibrils with THT and Amytracker

Figure 57 displays a compilation of all 90 image strips that were analyzed in the main text.

Figure 58 plots the THT intensity against the Amytracker intensity of any given pixel, without a threshold. There is a diagonal line indicating a linear relation between THT and Amytracker intensity and a vertical line indicating some parts are stained by THT, but not Amytracker.

The opacity of a data point very roughly indicates its occurrence (face transparency is set at 0.2 on a [0,1] scale). The majority of the points is located at lower values. A bivariate histogram of the same data gives more specific information on occurrence and it clearly confirms that the vast majority of points is near [0,0] (Figure 59). Because this part of the data does not answer the research question (very low fluorescence could be noise) and comes in a large quantity (which requires more computing power), a threshold was set to remove it.

For a threshold of 5, the amount of data points per dye goes from 5898240 to 772.
This is a decrease of 0.99987%. Figure 60 displays the bivariate histogram with a threshold of 5. An even more detailed representation can be found in Figure 61, which displays the THT intensity against the Amytracker intensity as a density plot with normalized fluorescence.

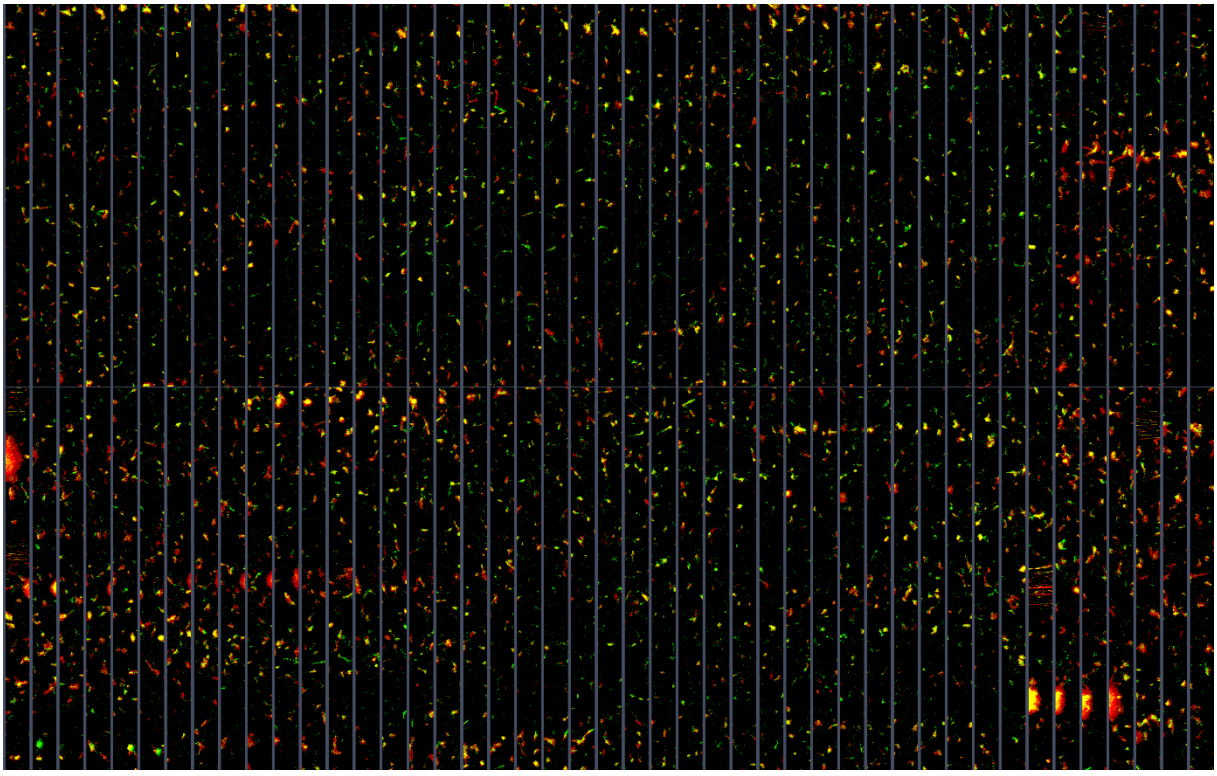

Figure 57. A compilation of all 90 image strips that were analyzed in the main text. THT is displayed in green, Amytracker in red and the overlap in yellow.

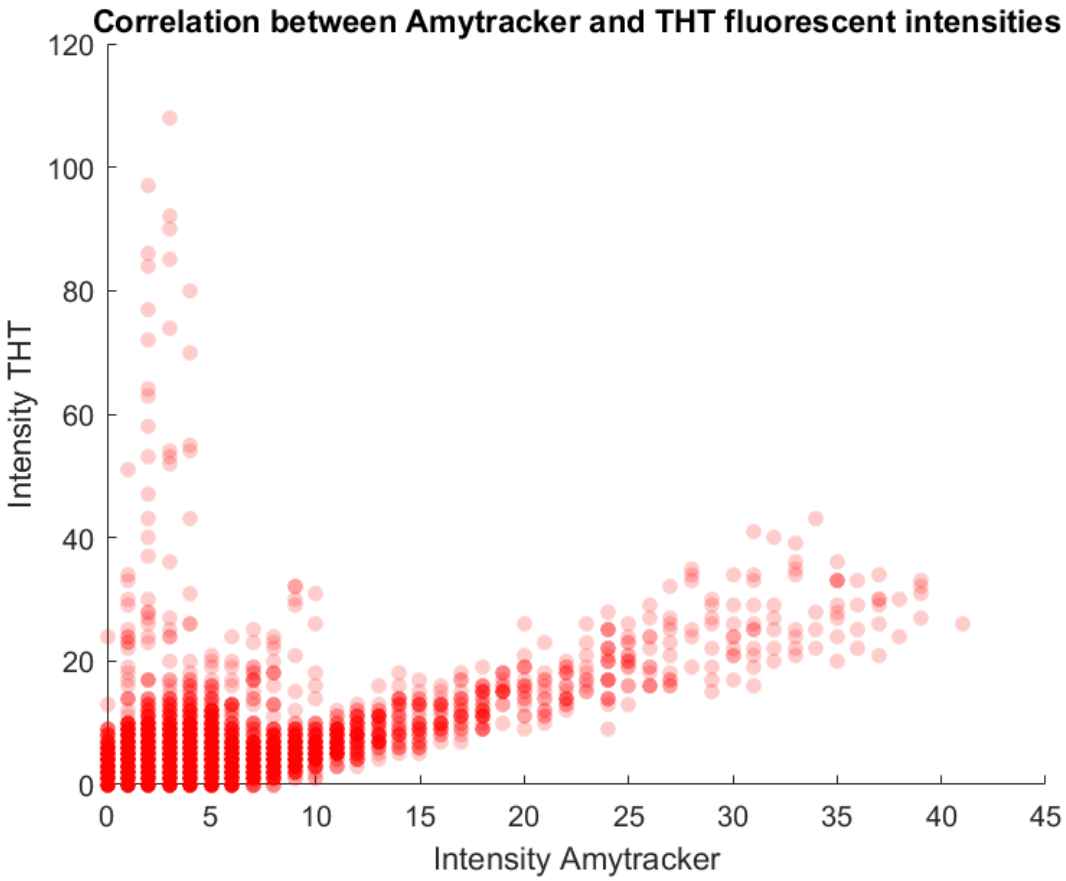

Figure 58. Correlation between THT and Amytracker intensities, without a threshold.

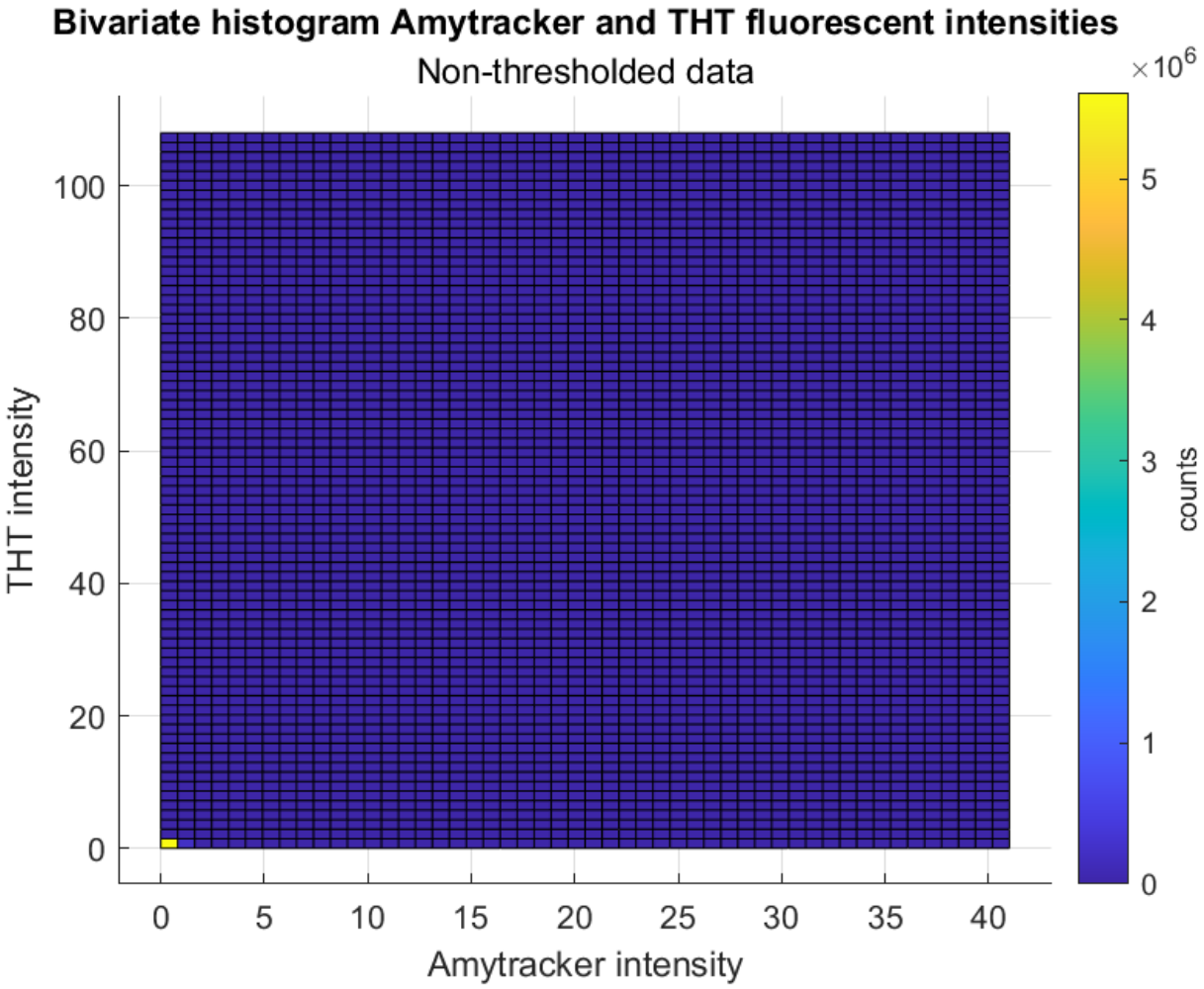

Figure 59. Bivariate histogram of THT and Amytracker intensities, without a threshold.

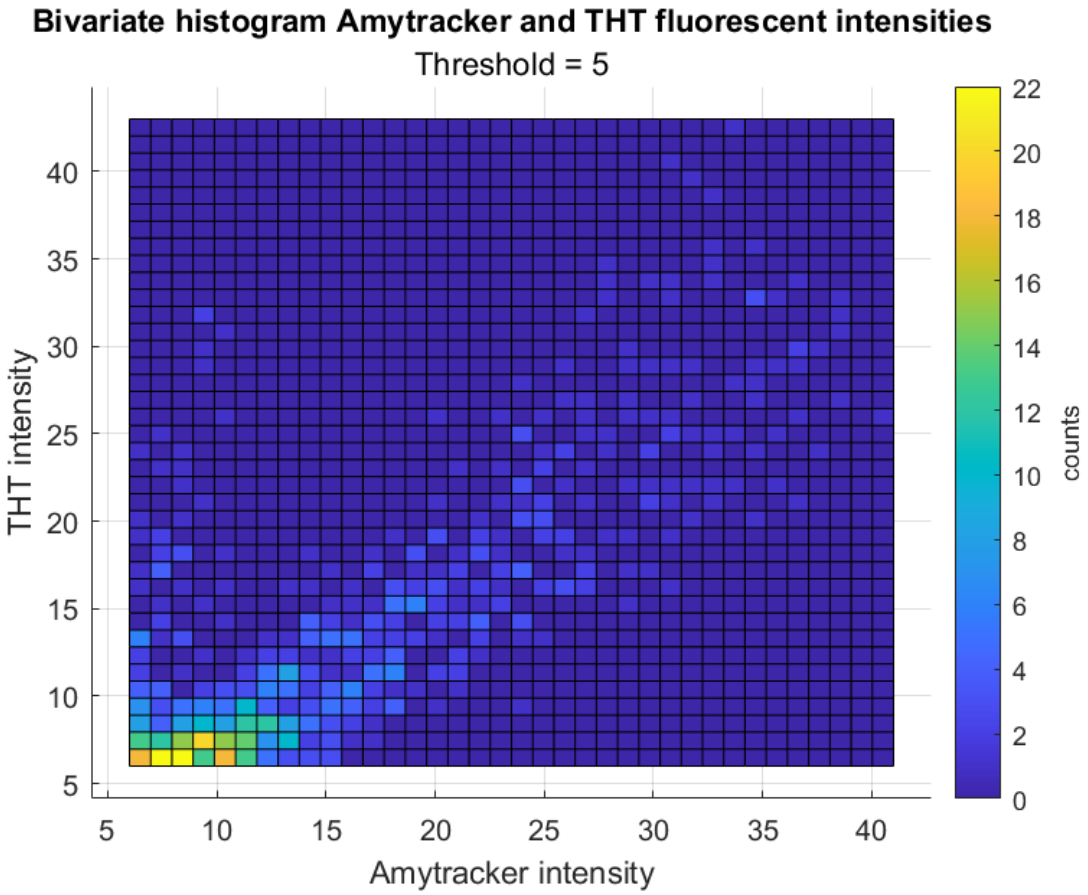

Figure 60. Bivariate histogram of THT and Amytracker intensities, with a threshold of 5.

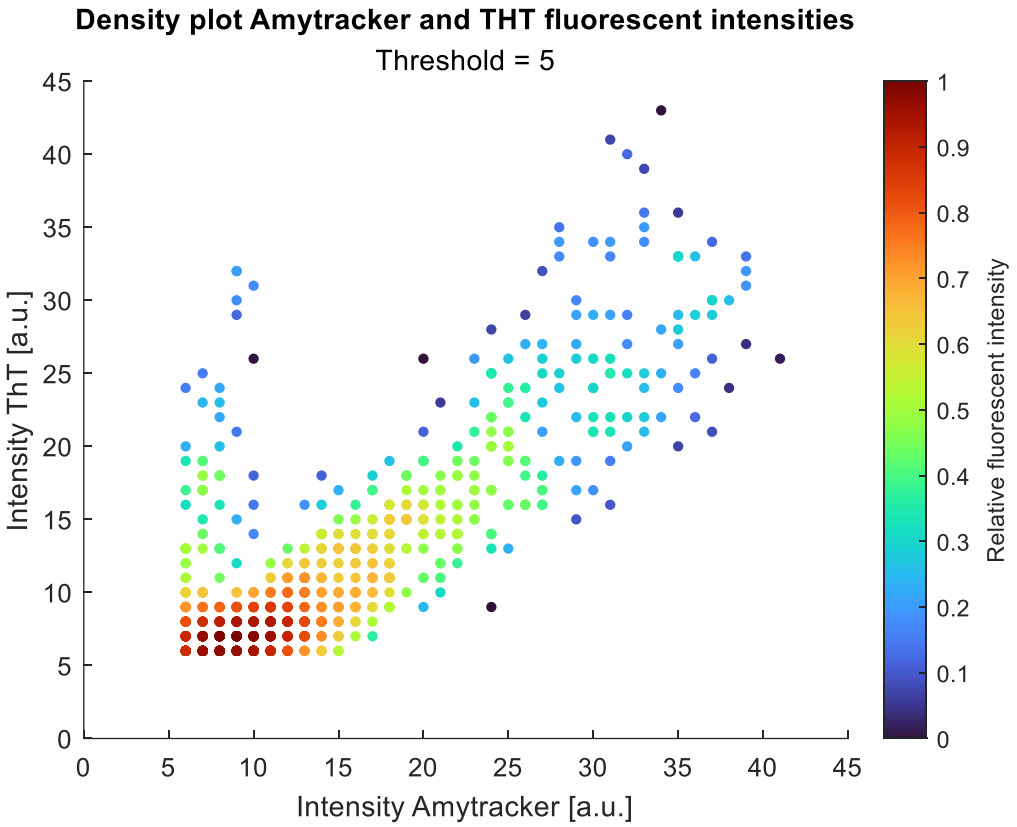

Figure 61. Density plot of the THT intensity against the Amytracker intensity with normalized fluorescence.

4. The effect of sonication on αS fibril concentration

Table 17 displays the absorbances per sample as measured using the Nanodrop, and the derived αS fibril concentrations. Two different settings on the Nanodrop were used: Protein 280 and UV-VIS. Each sample was measured three times per setting. The p-value of a two-sided two-sample t-test (assuming equal variances) comparing the αS fibril concentrations per sample as obtained by the two settings is also listed.

At a significance level of 5%, the two settings lead to significantly different results only for the 3 s sample (p=0.03). Figure 62 displays the average fibril concentration as a percentage of the total αS concentration, per Nanodrop setting. Although the difference between the two settings for the 3 s sample is statistically significant, it differs less than 10 percentage points. Together with the notion that the 3 s sample is the only sample with a significant difference, it was decided to combine the data obtained through the two settings for each sample.

Table 18 displays the average αS fibril concentration, as calculated from the combined measured absorbances and a total αS concentration of 50 µM. It also displays the conversion of the concentration to percentage of the total αS concentration.

Table 17. Absorbances at 280 nm per sample as measured using the Nanodrop, using the Protein A280 and UV-VIS settings. Also the derived αS fibril concentrations and the results of a two-sided two-sample t-test (assuming equal variances).

Sample	Measure-ment#	Absorbance at 280 nm		αS fibril concentration (µM)		p-value
		ProteinA280	UV-VIS	ProteinA280	UV-VIS	
0 s	1	0.137	0.008	25.5	35.7	0.12
	2	0.150	0.006	23.2	39.3	
	3	0.080	0.009	35.7	33.9	
1 s	1	0.050	0.007	41.1	37.5	0.23
	2	0.047	0.005	41.6	41.1	
	3	0.056	0.006	40.0	39.3	
3 s	1	0.081	0.005	35.5	41.1	0.03
	2	0.066	0.006	38.2	39.3	
	3	0.088	0.005	34.3	41.1	
5 s	1	0.074	0.006	36.8	39.3	0.73
	2	0.063	0.007	38.8	37.5	
	3	0.056	0.007	40.0	37.5	

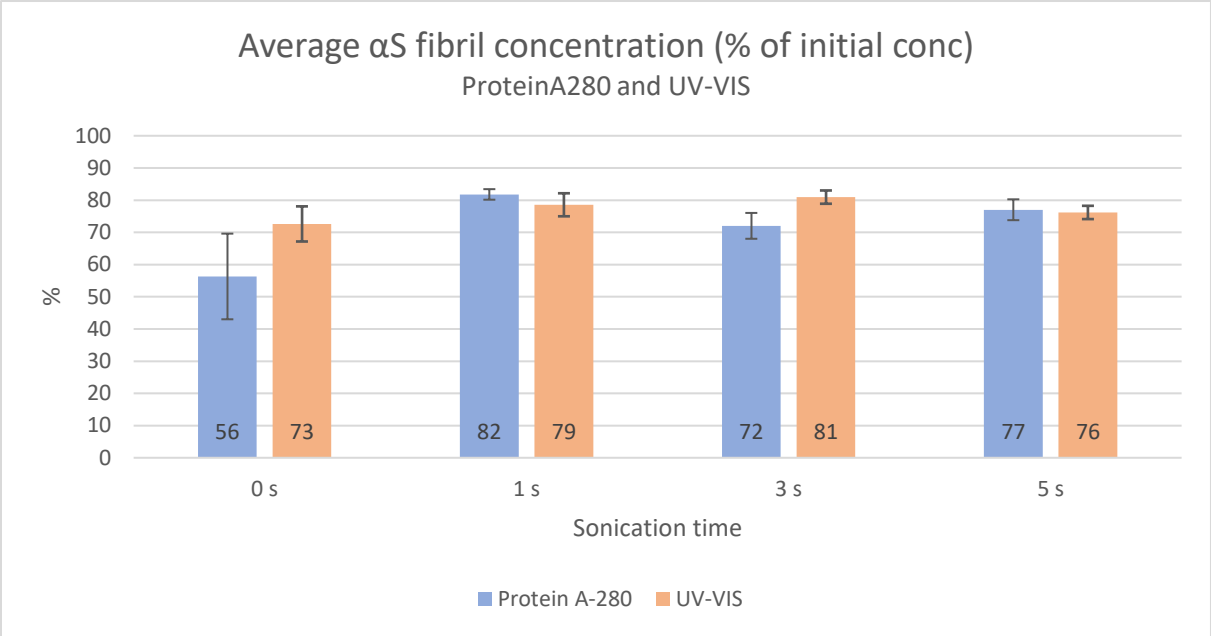

Figure 62. Average αS fibrils concentrations as a percentage of the total αS concentration, per Nanodrop setting.

Table 18. Average αS fibrils concentrations, in [M] and as a percentage of the total αS concentration of 50 µM.

Sample	αS fibril concentration (M)	Standard deviation (M)	αS fibril concentration (%)	Standard deviation (%)
0 s	3.22E-05	6.37E-06	64	12.7
1 s	4.01E-05	1.52E-06	80	3.0
3 s	3.82E-05	2.83E-06	76	5.7
5 s	3.83E-05	1.24E-06	77	2.5
Average of all	3.72E-05	4.54E-06	74	9.1
Average of sonicated	3.89E-05	2.07E-06	78	4.1

5. The effect of αS fibril concentration and αS fibril sonication on αS aggregation

Figure 63 displays the SAA curves of some illustrative samples, including the quickest to aggregate. There is a small gap between 688 and 727 h in which measuring was accidentally halted.

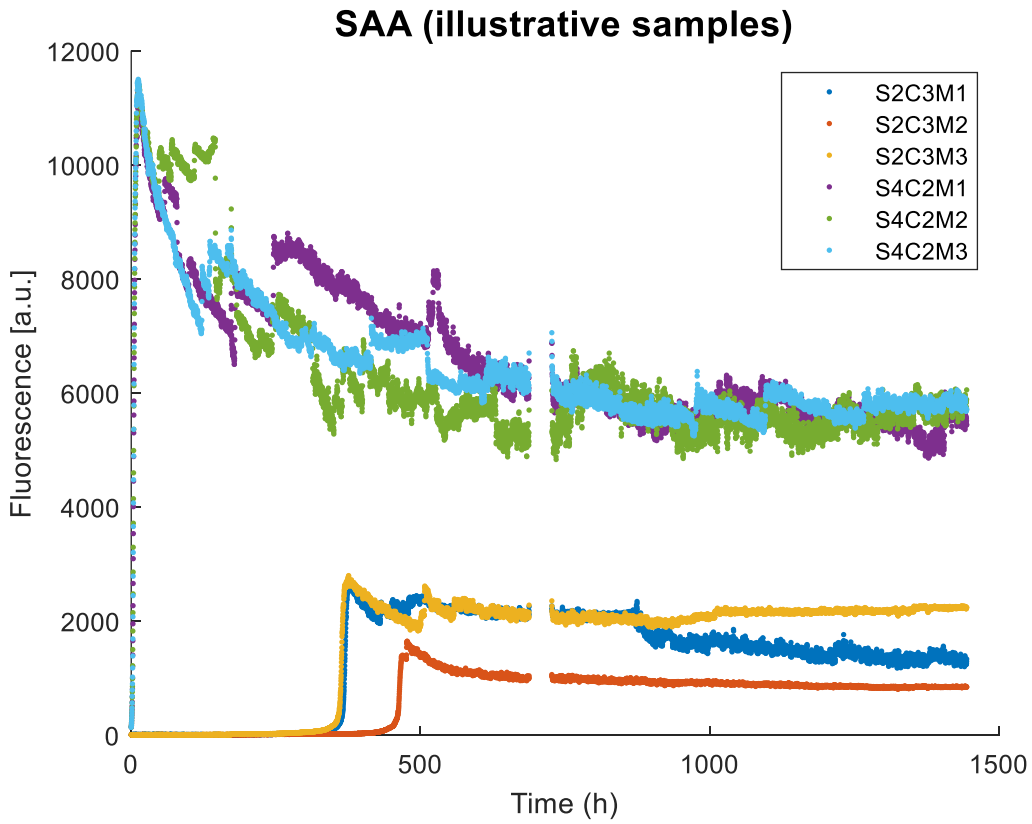

Figure 63. The SAA curves of some illustrative samples. The samples are described by their coded labels: S indicates sonication time of αS fibrils, C indicates αS fibril concentration (in monomer equivalent concentration) and M the samples of a triplo. S1 = 0 s sonicated; S2 = 1 s sonicated; S3 = 3 s sonicated; S4 = 5 s sonicated. C1 = 0 M (negative control); C2 = 10^{-6} M; C3 = 10^{-8} M; C4 = 10^{-10} M; C5 = 10^{-12} M; C6 = 10^{-14} M; C7 = 10^{-16} M; C8 = 10^{-17} M; M1 = sample 1 of triplo; M2 = sample 2 of triplo; M3 = sample 3 of triplo.

Table 19. Mean lag time, standard deviation and number of used measurements per condition.

Sonication time →	**0 s**			**1 s**			**3 s**			**5 s**		
αS fibril concentration ↓	Mean	STD	#M	Mean	STD	#M	Mean	STD	#M	Mean	STD	#M
10e-6 M	32	25	3	3	0	3	3	0	3	3	0	3
10e-8 M	622	134	3	315	58	3	235	26	3	164	7	3
10e-10 M	821	260	3	916	29	3	550	124	3	271	16	3
10e-12 M	546	351	3	599	185	3	297	21	3	252	15	3
10e-14 M	756	95	3	585	81	3	290	38	3	255	49	3
10e-16 M	949	142	3	794	54	3	406	120	3	270	32	3
10e-17 M	697	60	2	869	153	3	468	42	3	315	100	3

Table 20. The count and percentage of aggregation categories.

Category	**Count**	**Percentage**
# samples	96	100
# non-aggregated samples	1	1
# aggregated samples	95	99
# ideal cases	27	28
# diff lag time =< 5 h	29	30
# diff lag time > 5 h	39	41

6. Finding the median αS fibril length by means of AFM

22 AFM images with in total 2213 fibrils were obtained. The fibril lengths range from 59 to 2900 nm. Figure 64 displays the histogram of the fibril lengths.

The most common length is the smallest one: 58.8235 nm, with 601 occurrences. During the manual tracking, it seemed like there was minimum the program could measure. Fibrils that were actually shorter were then also measured as this minimum value. This makes the count of 58.8235 nm probably artificially bloated and thus incorrect. This value was removed from the dataset by setting a lower bound of 60; the second smallest value is 78.4 nm, so only the datapoints with value 58.8235 nm were removed.

Fitting an exponential model (Figure X3) shows that the higher lengths do not fit the model properly, so these were removed as well by setting an upper bound of 700 nm.

The details and goodness of fit statistics of the exponential model as described in the main text can be found in Table 21 and Table 22.

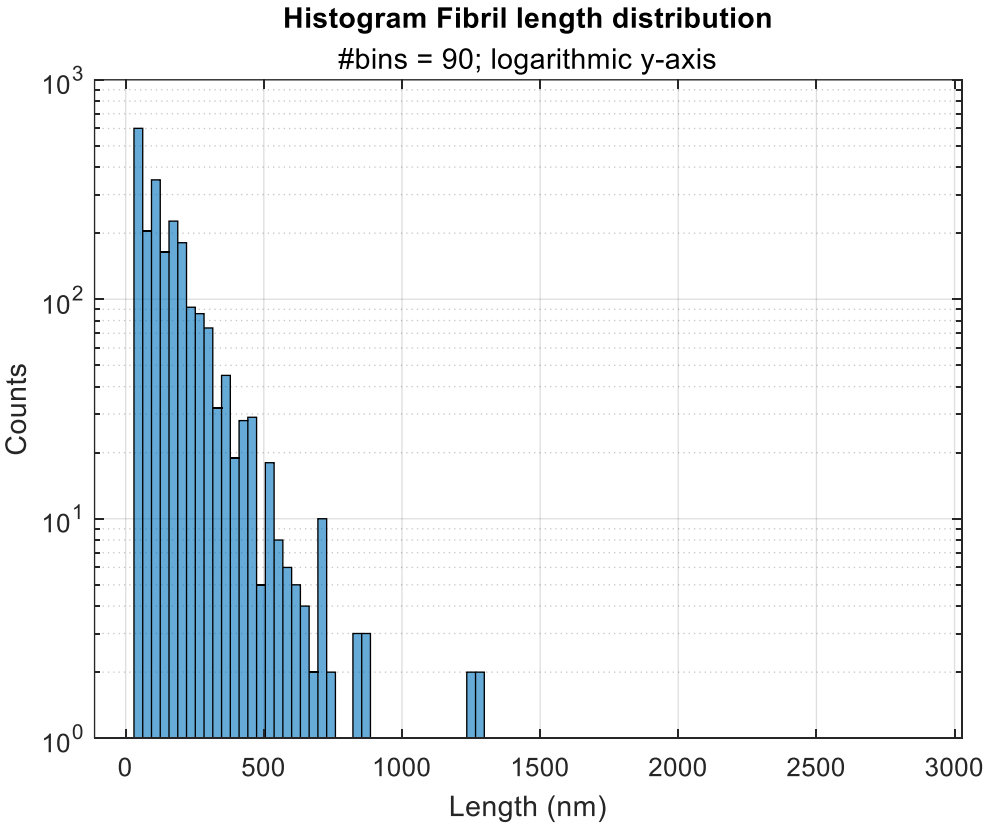

Figure 64. Histogram of measured fibril lengths.

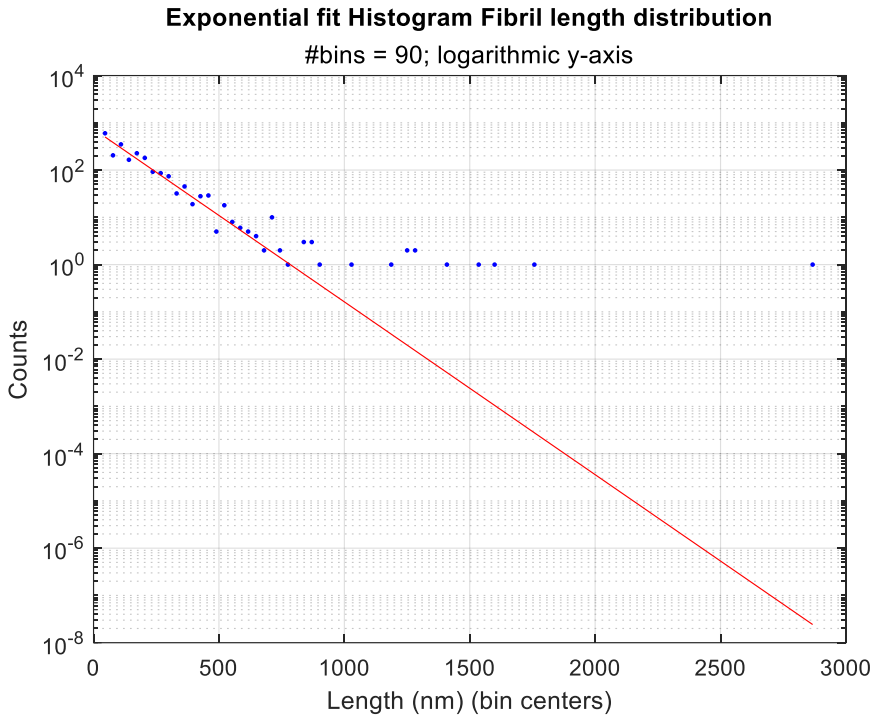

Figure 65. Exponential fit of histogram of measured fibril lengths.

Table 21. Details of exponential model fitted to the histogram of measured fibril lengths, with fibrils smaller than 60 nm and larger than 700 nm removed.

General model	Coefficient	Value	95% confidence bounds
f(x) = a*exp(b*x)	a	352.7	(319, 386.5)
	b	-0.006847	(-0.007477, -0.006216)

Table 22. Goodness of fit statistics of exponential model fitted to the histogram of measured fibril lengths, with fibrils smaller than 60 nm and larger than 700 nm removed.

Goodness of fit statistic	Value
SSE	2.6392e+03
R-square	0.9760
DFE	28
Adjusted R-square	0.9751
RMSE	9.7086

7. SPC can be performed on Amytracker-stained αS fibrils in a 96 well plate

A small test was performed to see whether the camera gain settings affected the number of counted particles. Four times 100 images were obtained though fluorescence microscopy, for each series the camera gain was set to a different value. The gain does not seem to significantly influence the mean number of counted particles per image (Figure 66). The gain should thus be chosen to optimize visibility of the fibrils. Representative images are displayed below (Figure 67, Figure 68, Figure 16, Figure 69).

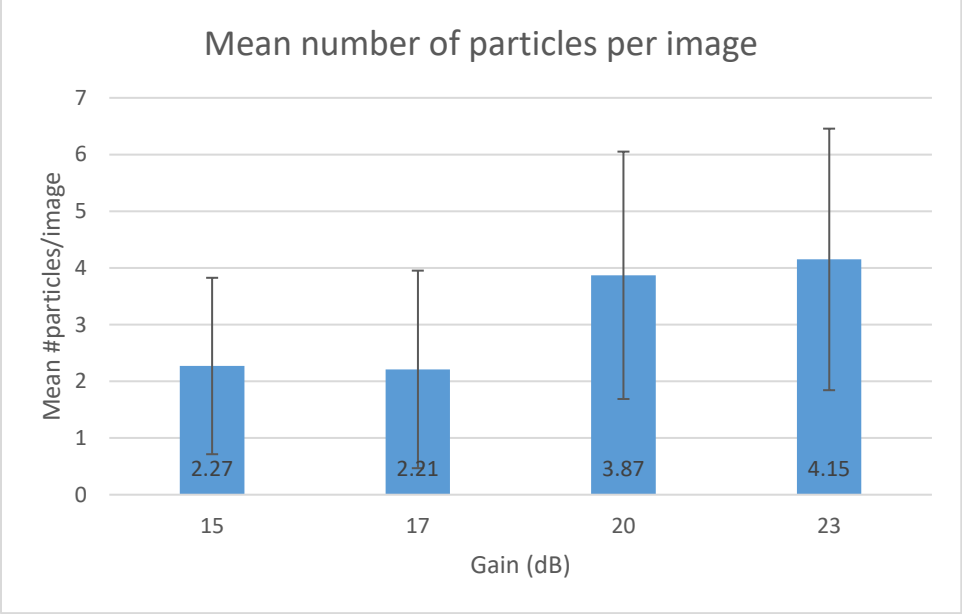

Figure 66. The mean number of counted particles per image, for different camera gain settings.

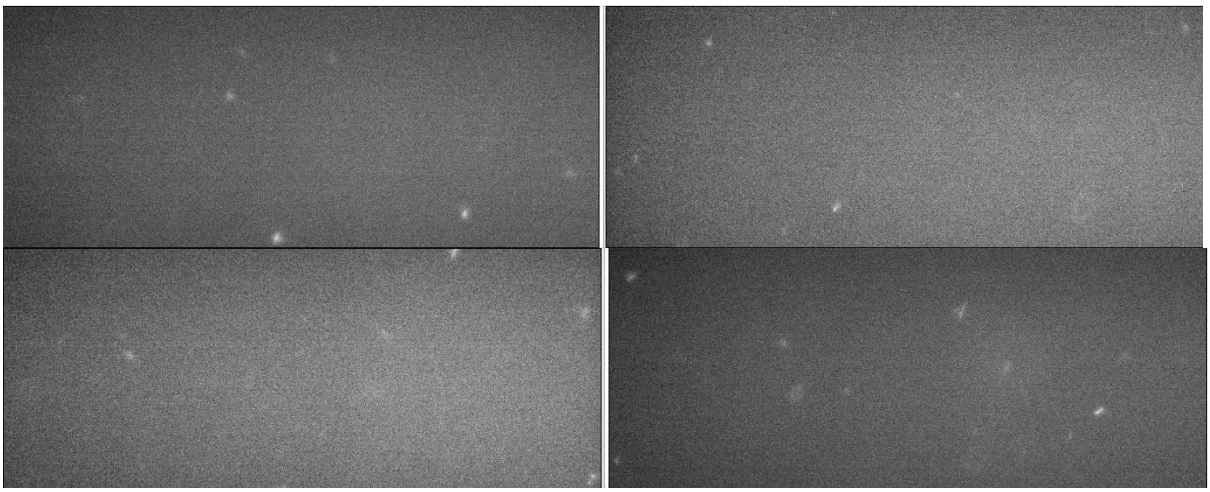

Figure 67. Representative images of αS fibrils stained with Amytracker in a 96 well plate (gain=15 dB). The image size is 130 x 52 µm.

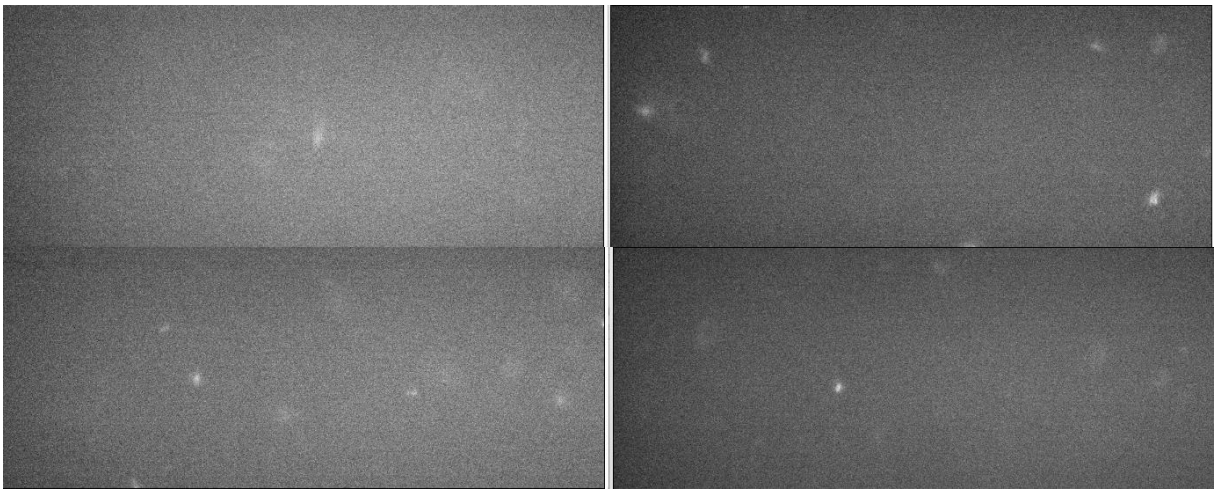

Figure 68. Representative images of αS fibrils stained with Amytracker in a 96 well plate (gain=17 dB). The image size is 130 x 52 µm.

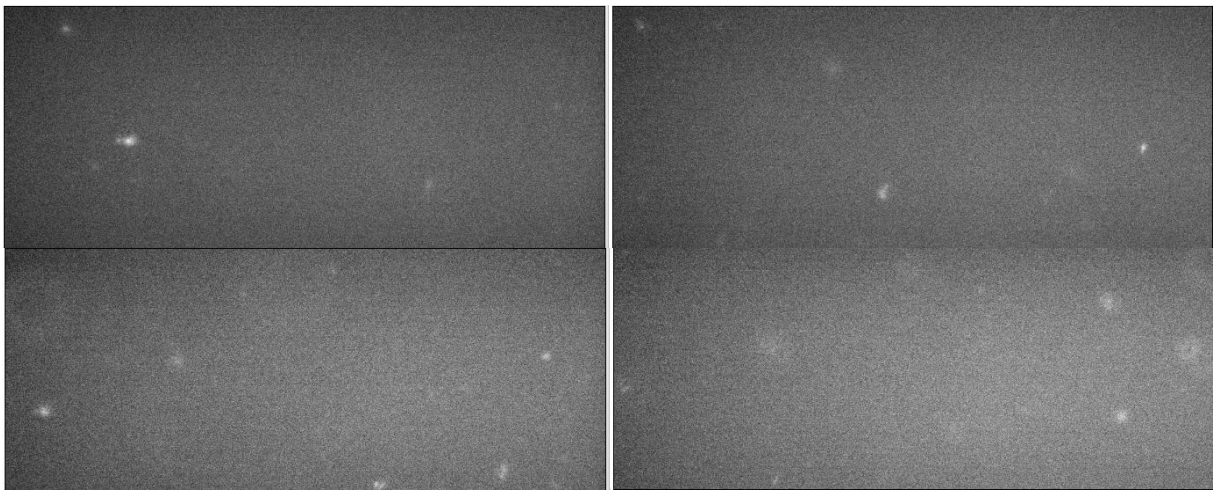

Figure 69. Representative images of αS fibrils stained with Amytracker in a 96 well plate (gain=23 dB). The image size is 130 x 52 µm.

8. Combining SAA and SPC: attempt 1 and 2 (Amytracker)

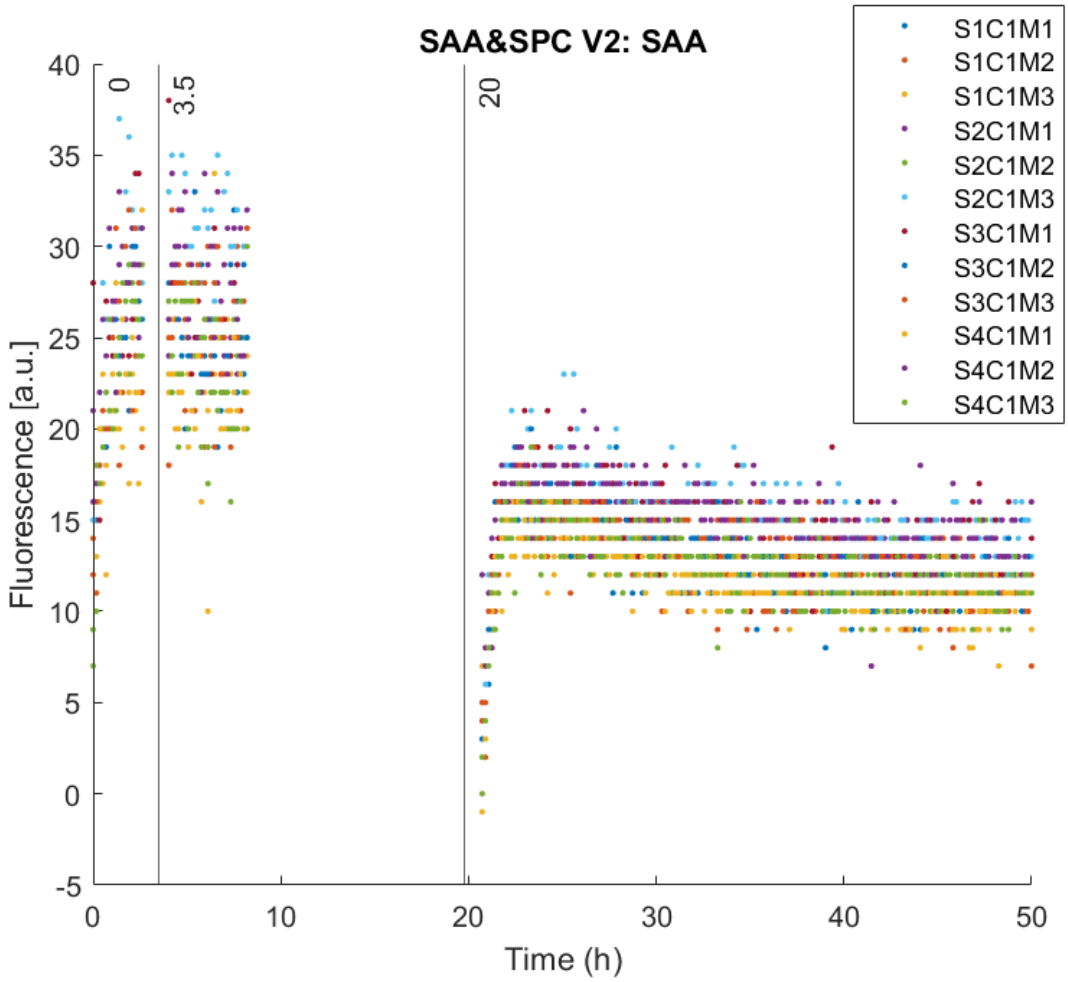

Figure 70. Fluorescent signal of the Amytracker-stained αS fibrils of the second attempt of combining SAA and SPC, limited to the first 50 h. The excitation and emission wavelengths were set correctly to 520 ± 4.5 nm and 630 ± 10 nm respectively. The vertical lines indicate measurement times for the SPC measurements. The gap starting from t = 8 h is the result of the software aborting the measurement for unknown reasons. The samples are described by their coded labels: S indicates αS fibril concentration (in monomer equivalent concentration), C indicates nothing here, and M indicates the samples of a triplo. S1 = 0 M αS fibrils (negative control); S2 = 10^{-6} M; S3 = 10^{-8} M; S4 = 10^{-10} M; M1 = sample 1 of triplo; M2 = sample 2 of triplo; M3 = sample 3 of triplo.

Table 23. Representative images of the first SPC measurement at t = 4.5 h of the first attempt of combining SAA and SPC. Conditions were measured in triplo, one image for each is presented. For image sequences with very few particles, examples of images containing particles are selected. Sample #1 of condition #2 (10^{-6} M αS seed) omitted from the SPC analysis because particles could not be counted. The image size is 173 x 118 µm.

Condition #1: 0 M αS seed (control)

#1 #2 #3

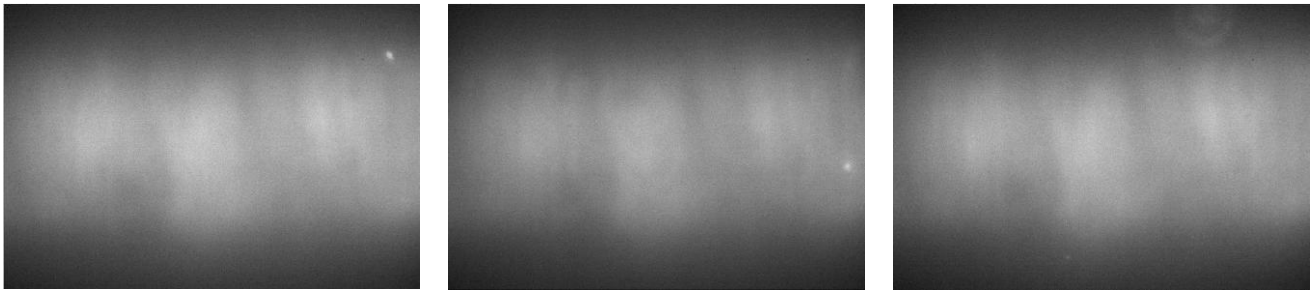

Condition #2: 10^{-6} M αS seed

#1 #2 #3

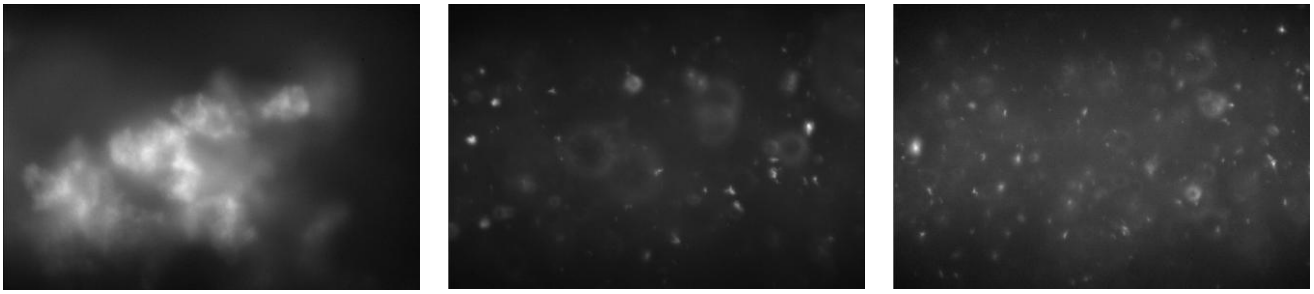

Condition #3: 10^{-8} M αS seed

#1 #2 #3

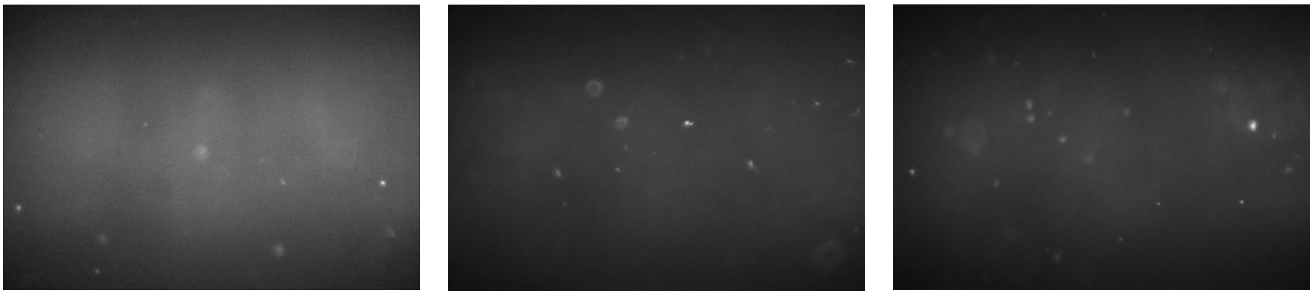

Condition #4: 10^{-10} M αS seed

#1 #2 #3

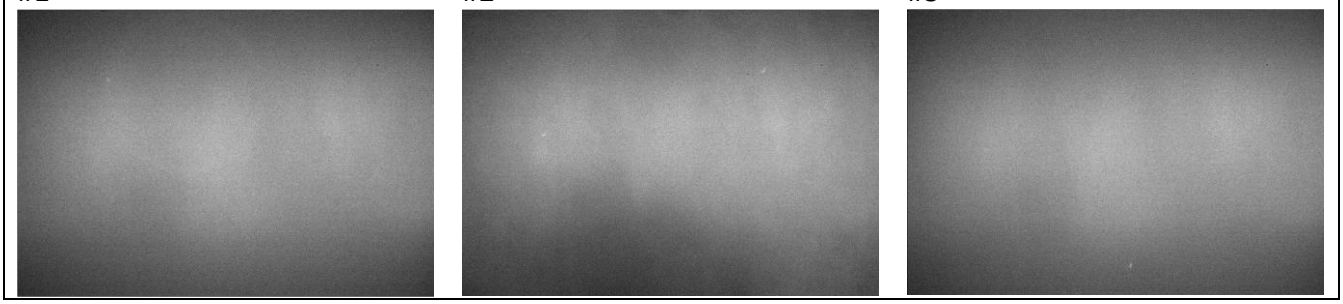

Table 24. Images featuring long fibrils at t = 93 h of the first attempt of combining SAA and SPC. No image indicates there are no images with long fibrils. Sample #1 of condition 2 (10^{-6} M αS seed) had been removed from the dataset because particles could not be counted. Conditions were measured in triplo, one image for each is presented (if applicable). The image size is 130 x 52 µm.

Condition 1: 0 M αS seed (control)		
#1	#2	#3
-	-	-
Condition 2: 10^{-6} M αS seed		
#1	#2	#3
-	-	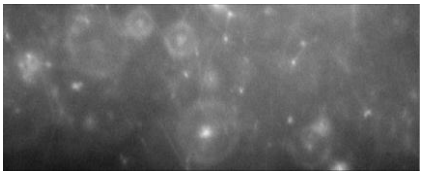
Condition 3: 10^{-8} M αS seed		
#1	#2	#3
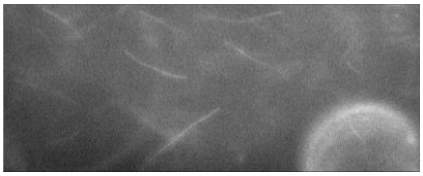	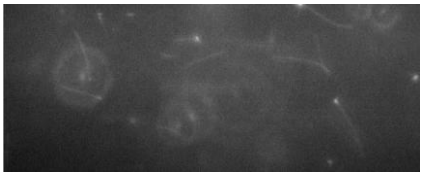	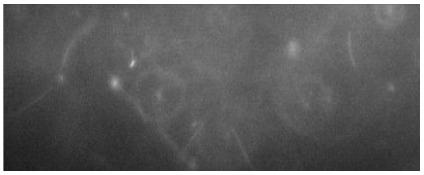
Condition 4: 10^{-10} M αS seed		
#1	#2	#3
	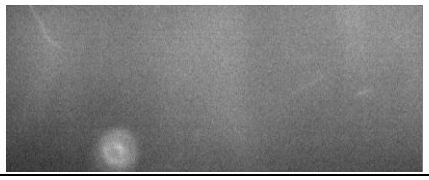	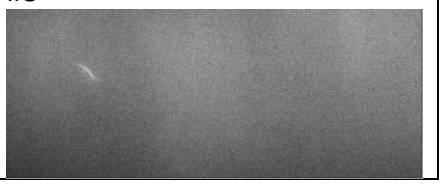

Table 25. Representative images of the first SPC measurement at t = 0 h of the second attempt of combining SAA and SPC. Conditions were measured in triplo, one image for each is presented. Condition 2 (10^{-6} M αS seed) was omitted from the SPC analysis because the particles could not be properly counted. The images of condition 3 at t= 0 h look similar to condition 2, but their countability improves at the subsequent SPC measurements. The image size is 130 x 52 µm.

Condition 1: 0 M αS seed (control)

#1 #2 #3

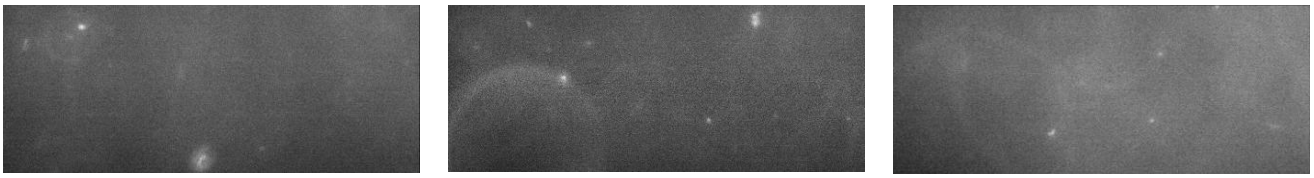

Condition 2: 10^{-6} M αS seed

#1 #2 #3

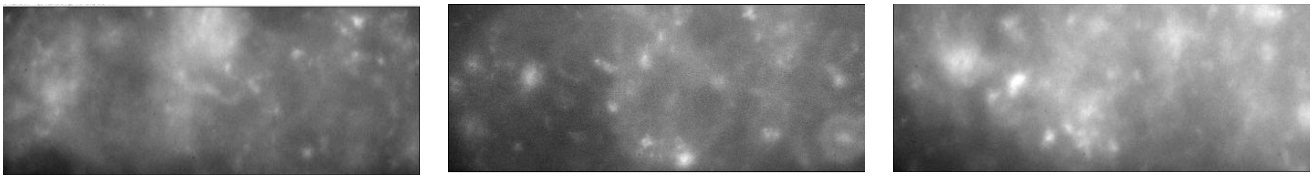

Condition 3: 10^{-8} M αS seed

#1 #2 #3

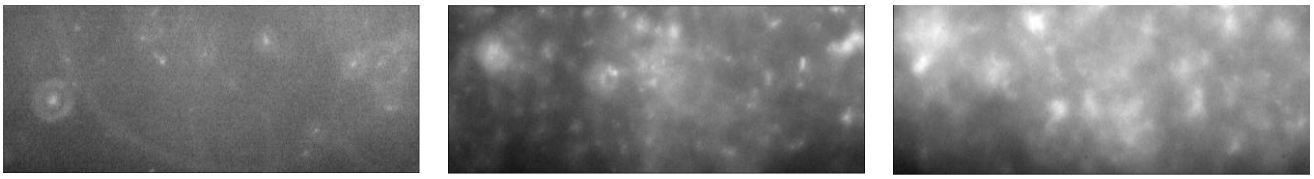

Condition 4: 10^{-10} M αS seed

#1 #2 #3

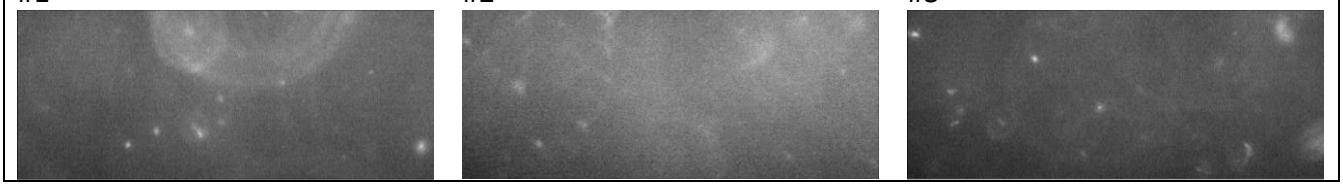

9. SPC can be performed on THT-stained αS fibrils in a 96 well plate

There is no appendix data for this chapter.

10. Combining SAA and SPC: attempt 3 (THT)

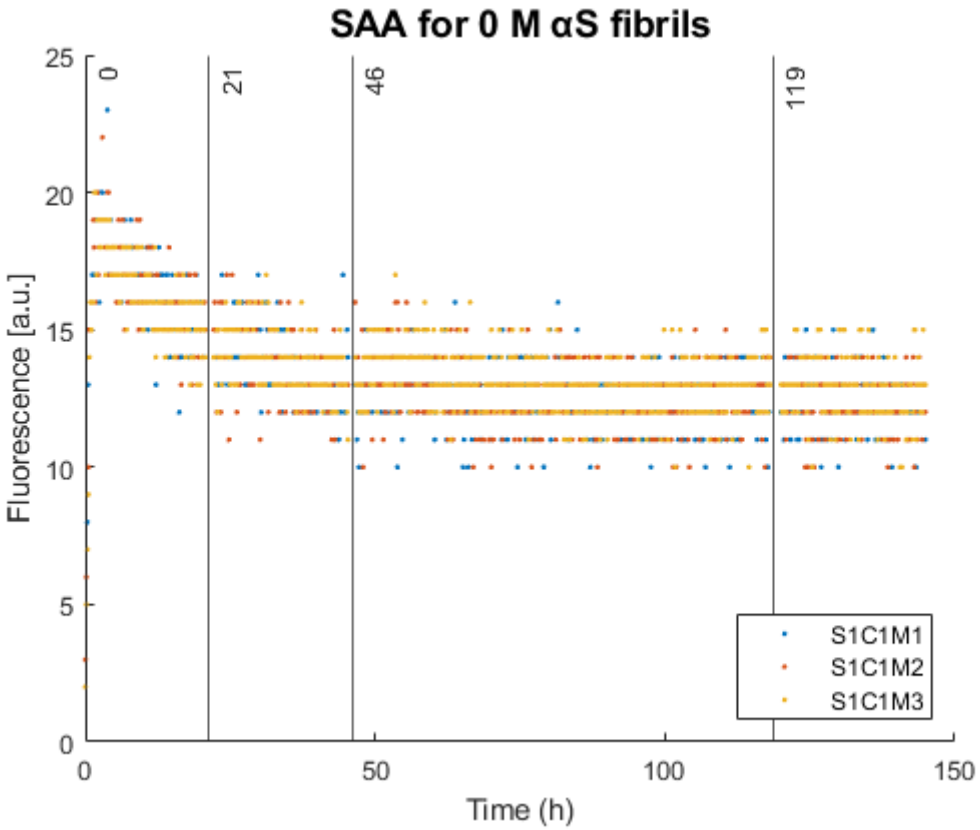

Figure 71. SAA curves for the negative control with 0 M αS fibrils (S1). The vertical lines indicate measurement times for the SPC. M indicates the samples of a triplo.

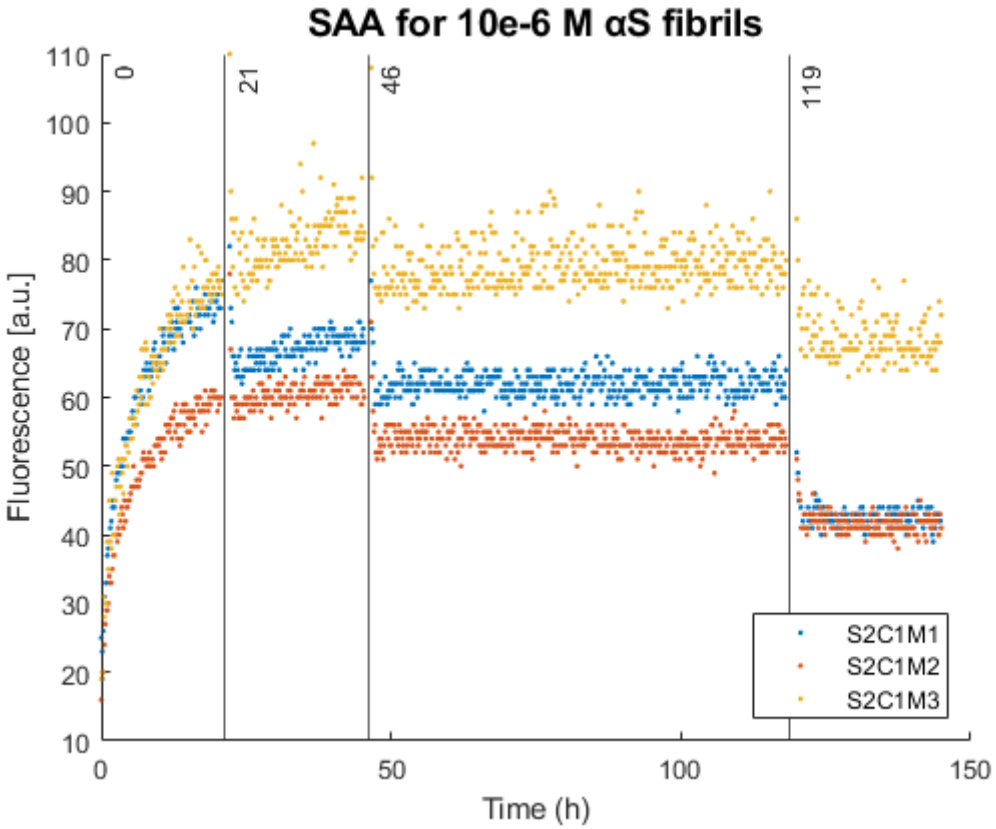

Figure 72. SAA curves for the sample with 10^{-6} M αS fibrils (S2). The vertical lines indicate measurement times for the SPC. M indicates the samples of a triplo.

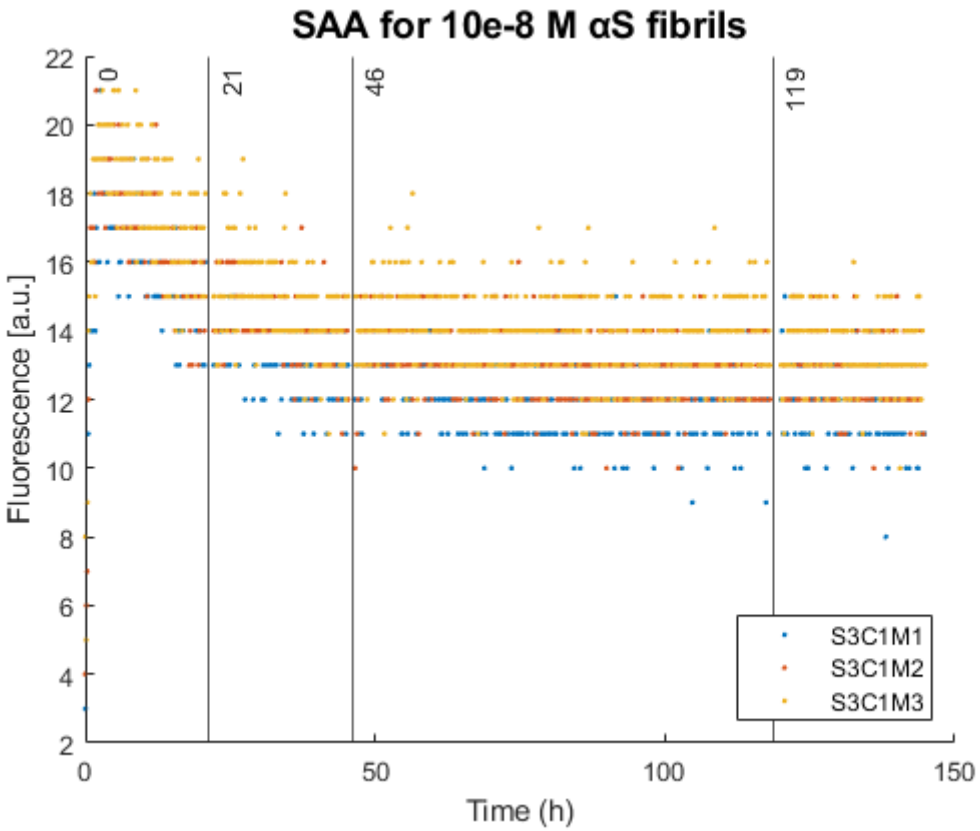

Figure 73. SAA curves for the sample with 10-8 M αS fibrils (S3). The vertical lines indicate measurement times for the SPC. M indicates the samples of a triplo.

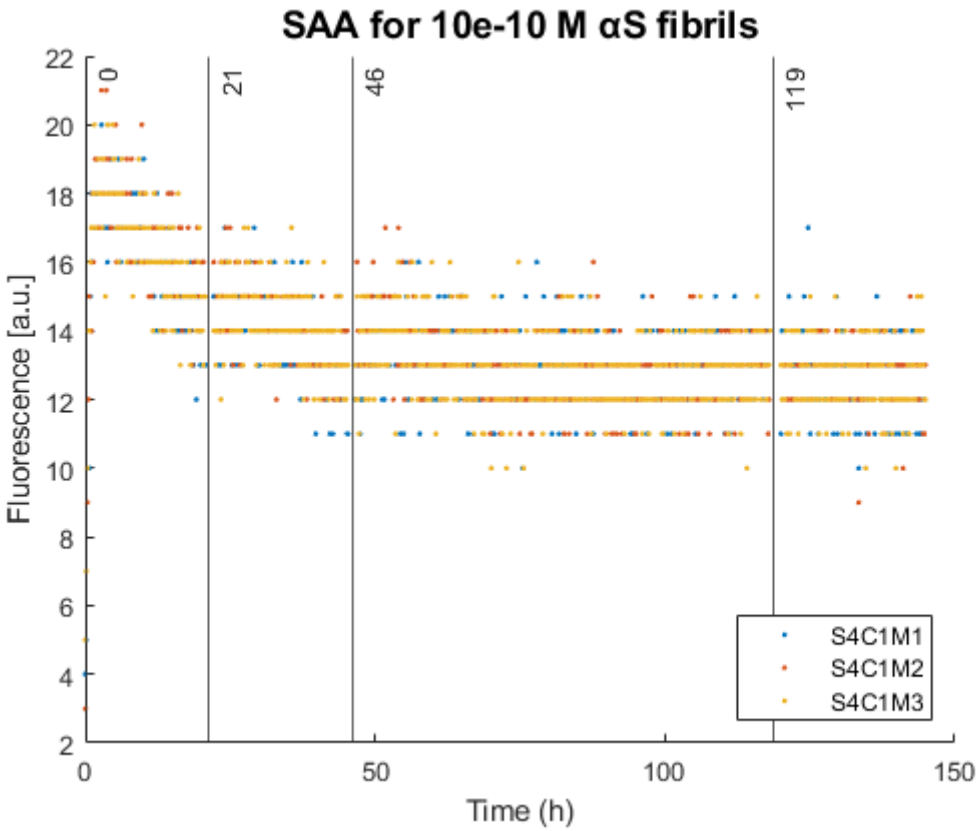

Figure 74. SAA curves for the sample with 10-10 M αS fibrils (S4). The vertical lines indicate measurement times for the SPC. M indicates the samples of a triplo.

Table 26. Representative images of the first SPC measurement on t = 0 h. Conditions were measured in triplo, one image for each is presented. For image sequences with very few particles, examples of images containing particles are selected. The image size is 115 x 58 µm.

Condition 1: 0 M αS seed (control)

#1 #2 #3

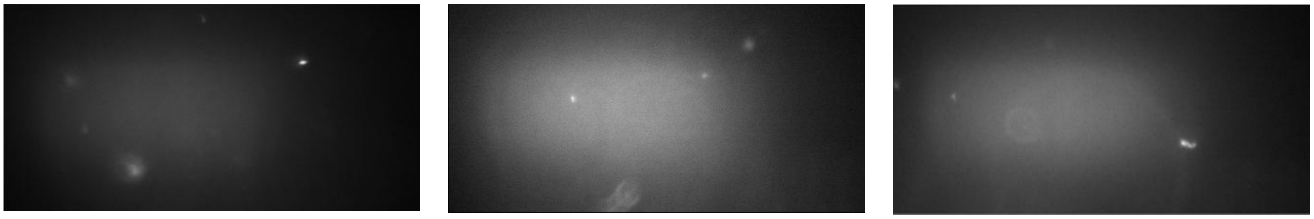

Condition 2: 10^{-6} M αS seed

#1 #2 #3

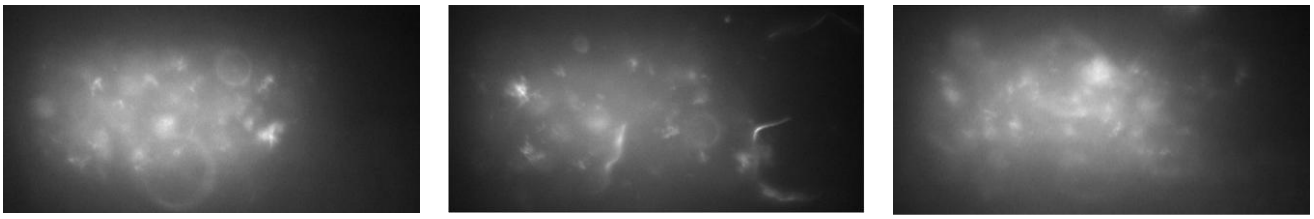

Condition 3: 10^{-8} M αS seed

#1 #2 #3

Condition 4: 10^{-10} M αS seed

#1 #2 #3

Table 27. Images featuring long fibrils of the first SPC measurement on t = 0 h. No image indicates there are no images with long fibrils. The image size is 115 x 58 µm.

Condition 1: 0 M αS seed (control)		
#1	#2	#3
-	-	-
Condition 2: 10^{-6} M αS seed		
#1	#2	#3
-	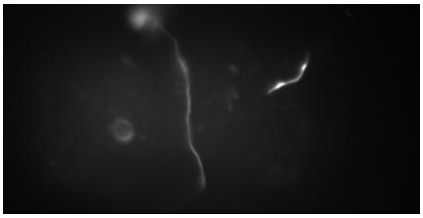	
Condition 3: 10^{-8} M αS seed		
#1	#2	#3
-	-	-
Condition 4: 10^{-10} M αS seed		
#1	#2	#3
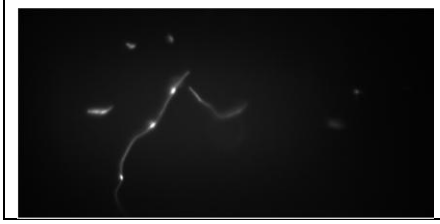	-	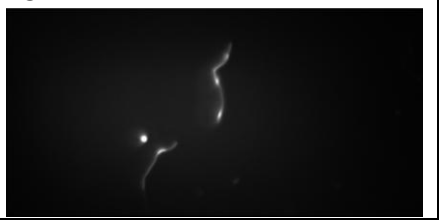

11. Testing the αS aggregation of an alternative batch of αS fibrils and two monomer batches stored at different temperatures

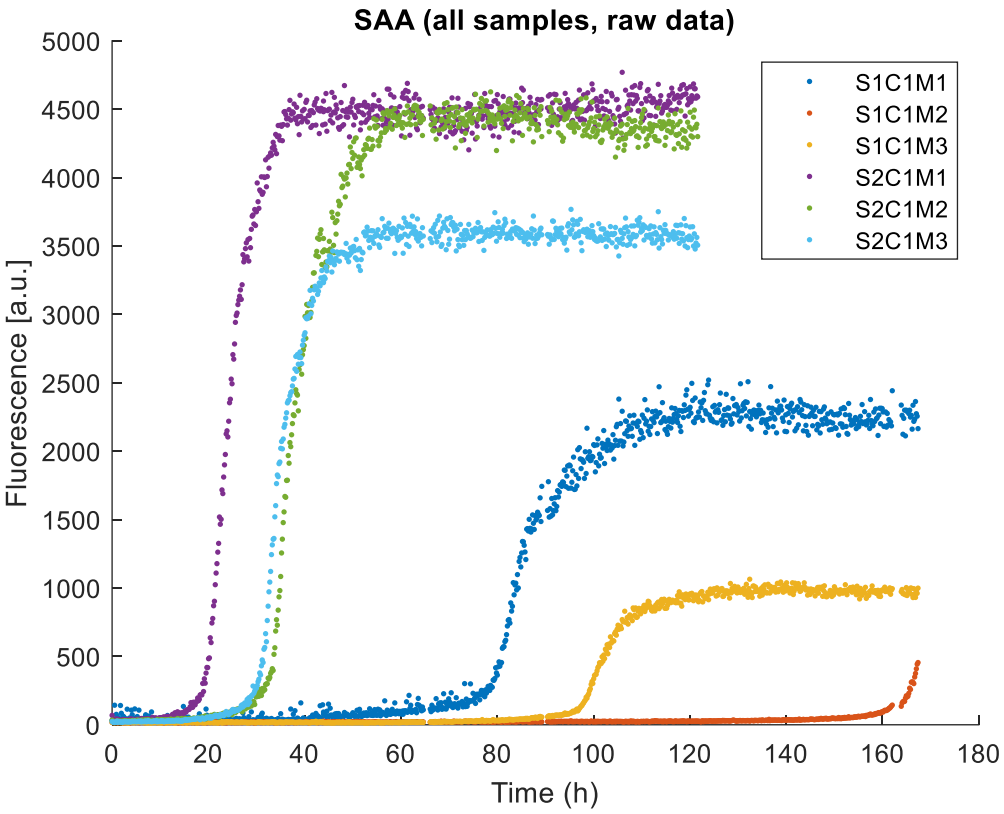

Figure 75. SAA curves of all samples. The samples are described by their coded labels: S indicates storage place of the of reactant αS monomers, C indicates αS fibril concentration (in monomer equivalent concentration) and M the samples of a triplo. S1 = reactant αS monomers stored in the 4°C fridge; S2 = reactant αS monomers stored in the -80°C freezer; C1 = 1 µM; M1 = sample 1 of triplo; M2 = sample 2 of triplo; M3 = sample 3 of triplo.

Table 28. Mean lag time, standard deviation and number of used measurements per condition.

Reactant αS monomer source →	**4°C fridge**	**-80°C freezer**
Mean	105	19
STD	42	3
# measurements	3	3

Table 29. The count and percentage of aggregation categories.

Category	**Count**	**Percentage**
# samples	6	100
# non-aggregated samples	0	0
# aggregated samples	6	100
# ideal cases	3	50
# diff lag time =< 5 h	3	50
# diff lag time > 5 h	0	0

Table 30. Lag times and aggregation label per sample. The samples are described by their coded labels: S indicates αS fibril source, C indicates αS fibril concentration (in monomer equivalent concentration) and M the samples of a triplo. S1 = αS fibrils stored in the 4°C fridge; S2 = αS fibrils stored in the -80°C freezer; C1 = 1 μM; M1 = sample 1 of triplo; M2 = sample 2 of triplo; M3 = sample 3 of triplo.

Sample	Lag time (h)	Aggregation label
S1C1M1	79.13811	ideal
S1C1M2	153.3305	diff lag time =< 5 h
S1C1M3	83.49347	diff lag time =< 5 h
S2C1M1	15.85325	ideal
S2C1M2	22.29917	diff lag time =< 5 h
S2C1M3	19.68581	ideal

12. The effect of αS fibril sonication on αS aggregation of an alternative batch of αS fibrils

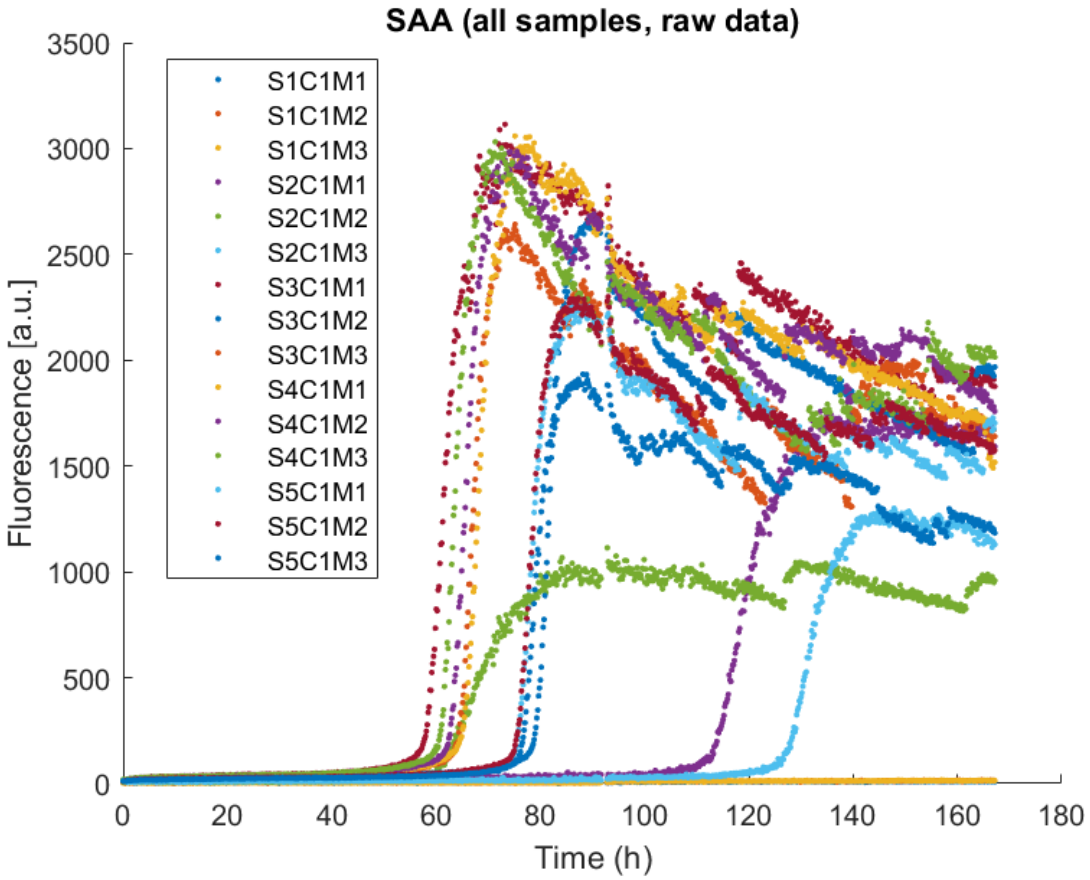

Figure 76. SAA curves of all samples. The samples are described by their coded labels: S indicates sonication time of αS fibrils, C indicates αS fibril concentration (in monomer equivalent concentration) and M the samples of a triplo. S1 = 0 M αS fibrils (negative control); S2 = 0 s sonicated; S3 = 5 s sonicated; S4 = 7 s sonicated; S5 = 10 s sonicated; C1 = 1 µM; M1 = sample 1 of triplo; M2 = sample 2 of triplo; M3 = sample 3 of triplo.

Table 31. Mean lag time, standard deviation and number of used measurements per condition.

Sonication time →	**0 M αS fibrils (negative control)**	**0 s**	**5 s**	**7 s**	**10 s**
Mean	NaN	84	61	57	69
STD	NaN	23	9	1	1
# measurements	0	3	3	3	3

Table 32. The count and percentage of aggregation categories.

Category	Count	Percentage
# samples	15	100
# non-aggregated samples	3	20
# aggregated samples	12	80
# ideal cases	9	60
# diff lag time =< 5 h	1	7
# diff lag time > 5 h	2	13

13. The effect of αS fibril sonication, storage temperature, and vortexing on αS aggregation of an alternative batch of αS fibrils

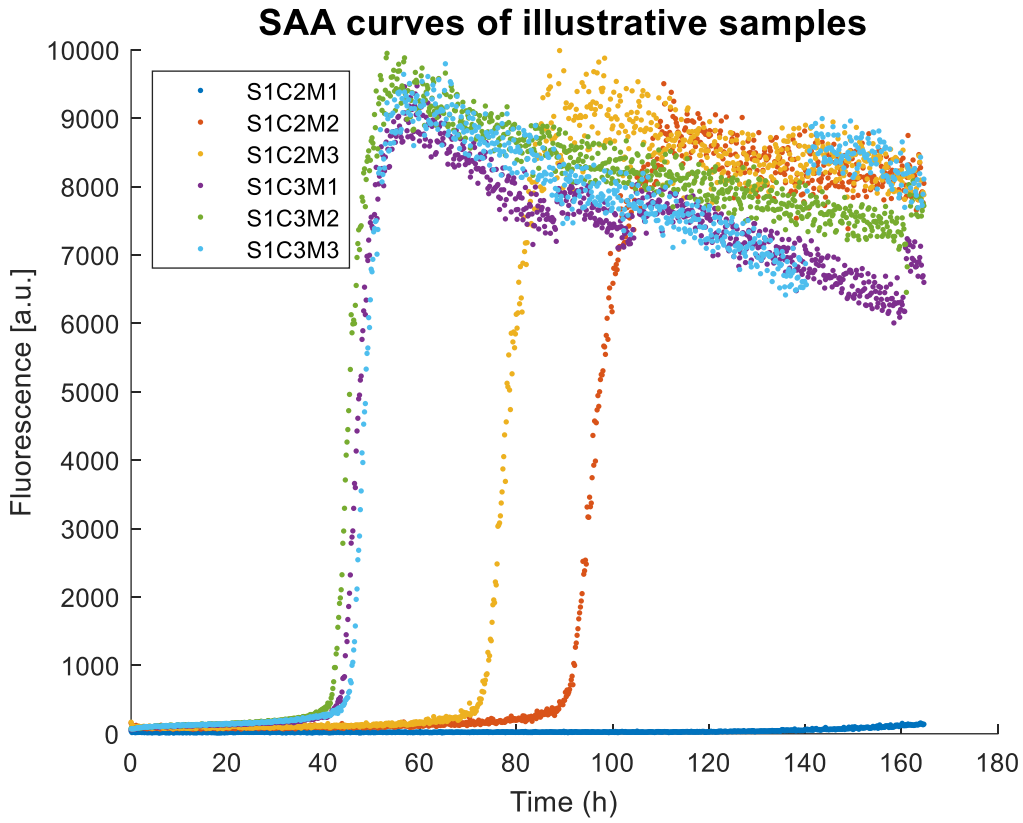

Figure 77. The SAA curves of some illustrative samples. The samples are described by their coded labels: S indicates αS fibril handling (vortexing mode and αS fibril storage temperature), C indicates sonication time of αS fibrils and M the samples of a triplo. S1 = 4°C fridge, no vortexing; S2 = -80°C freezer, no vortexing; S3 = 4°C fridge, vortexing; S4 = -80°C freezer, vortexing. C1 = 0 s sonicated; C2 = 1 s sonicated; C3 = 3 s sonicated; C4 = 5 s sonicated. M1 = sample 1 of triplo; M2 = sample 2 of triplo; M3 = sample 3 of triplo.

Table 33. Mean lag time, standard deviation and number of used measurements per condition.

αS fibril handling →	**4°C fridge, no vortexing**			**-80°C freezer, no vortexing**			**4°C fridge, vortexing**			**-80°C freezer, vortexing**		
Sonication time ↓	Mean	STD	#M	Mean	STD	#M	Mean	STD	#M	Mean	STD	#M
0 s	104	42	3	32	2	3	96	18	3	33	1	3
5 s	41	2	3	50	4	3	52	3	3	58	20	3
7 s	57	15	3	54	10	3	51	3	3	44	1	3
10 s	40	1	3	43	3	3	62	22	3	42	11	3

Table 34. The count and percentage of aggregation categories.

Category	Count	Percentage
# samples	60	100
# non-aggregated samples	11	18
# aggregated samples	49	82
# ideal cases	30	50
# diff lag time =< 5 h	18	30
# diff lag time > 5 h	1	2

14. (Re)testing the effect of various αS fibril parameters on αS aggregation

The SAA curves of each series is displayed in Figure 78, Figure 79, Figure 80, Figure 81, and Figure 82. The samples are described by their coded labels. S indicates αS fibril handling, C indicates sonication time of αS fibrils and M indicates the samples of a triplo. Table 35 and Table 36 list the specifics of the coded labels.

Table 35. Coded labels for the series (αS fibril handling).

Series label	**Series (αS fibril handling)**
S1	Negative control with 0 M αS fibrils
S2	αS stored at bench
S3	αS stored in the 4°C fridge
S4	αS stored in the -80°C freezer
S5	Freshly sonicated αS

Table 36. Coded labels for the conditions (sonication time).

Condition label	**Condition (sonication time)**
C0	Negative control with 0 M αS fibrils
C1	0 s
C2	01 s
C3	03 s
C4	05 s
C5	07 s
C6	10 s
C7	30 s
C8	60 s

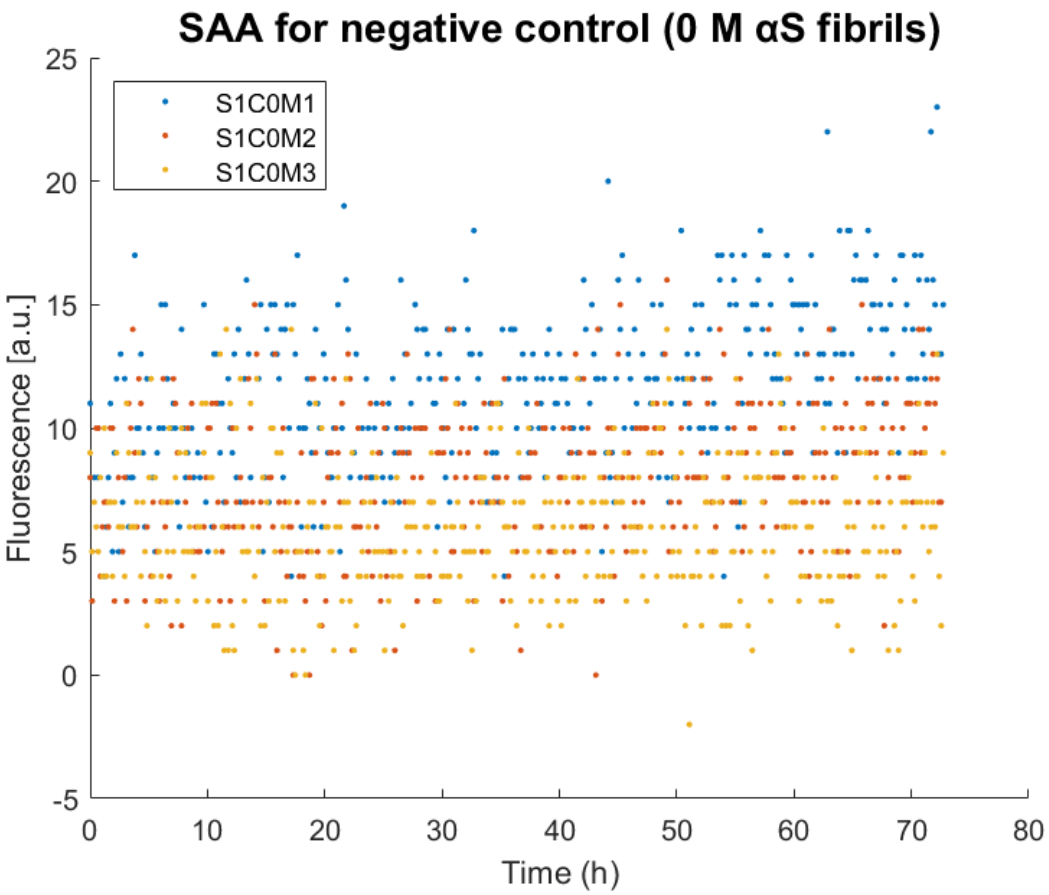

Figure 78. SAA curves for the negative control with 0 M αS fibrils (S1).

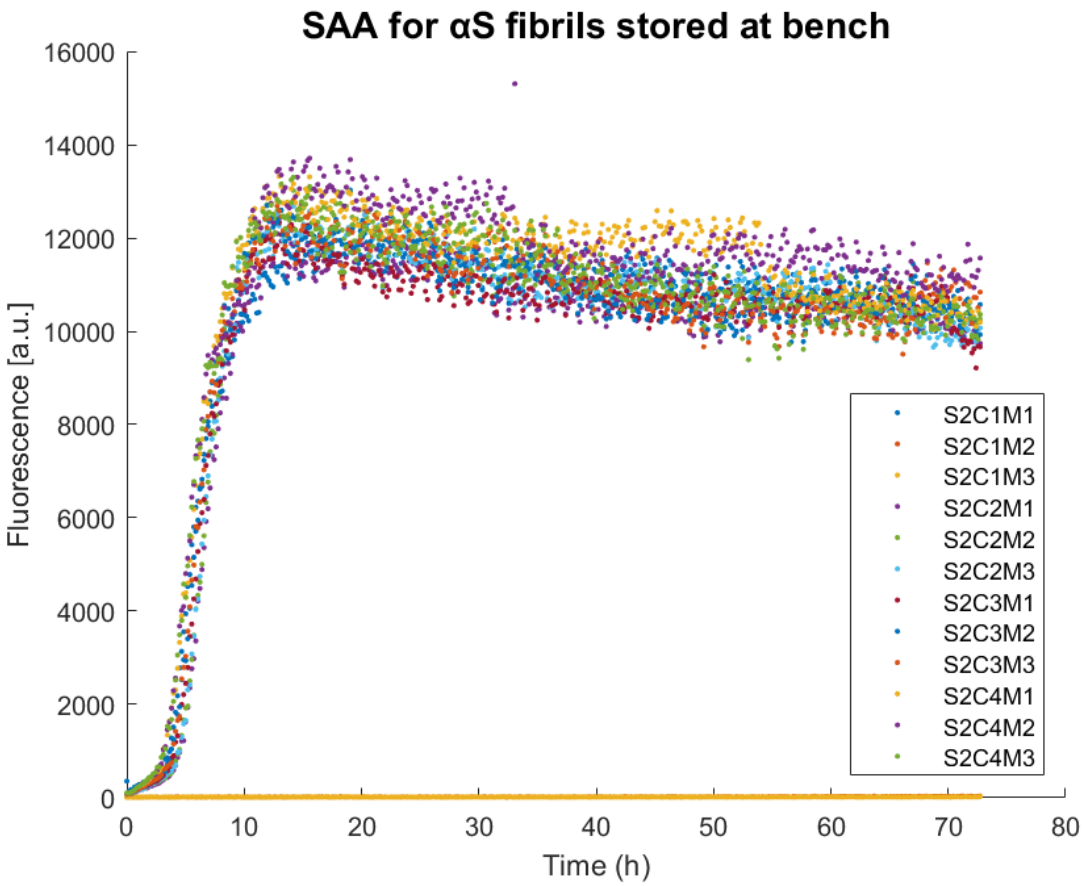

Figure 79. SAA curves for the αS stored at the bench (S2). Only S2C1M2 and S2C1M3 did not aggregate.

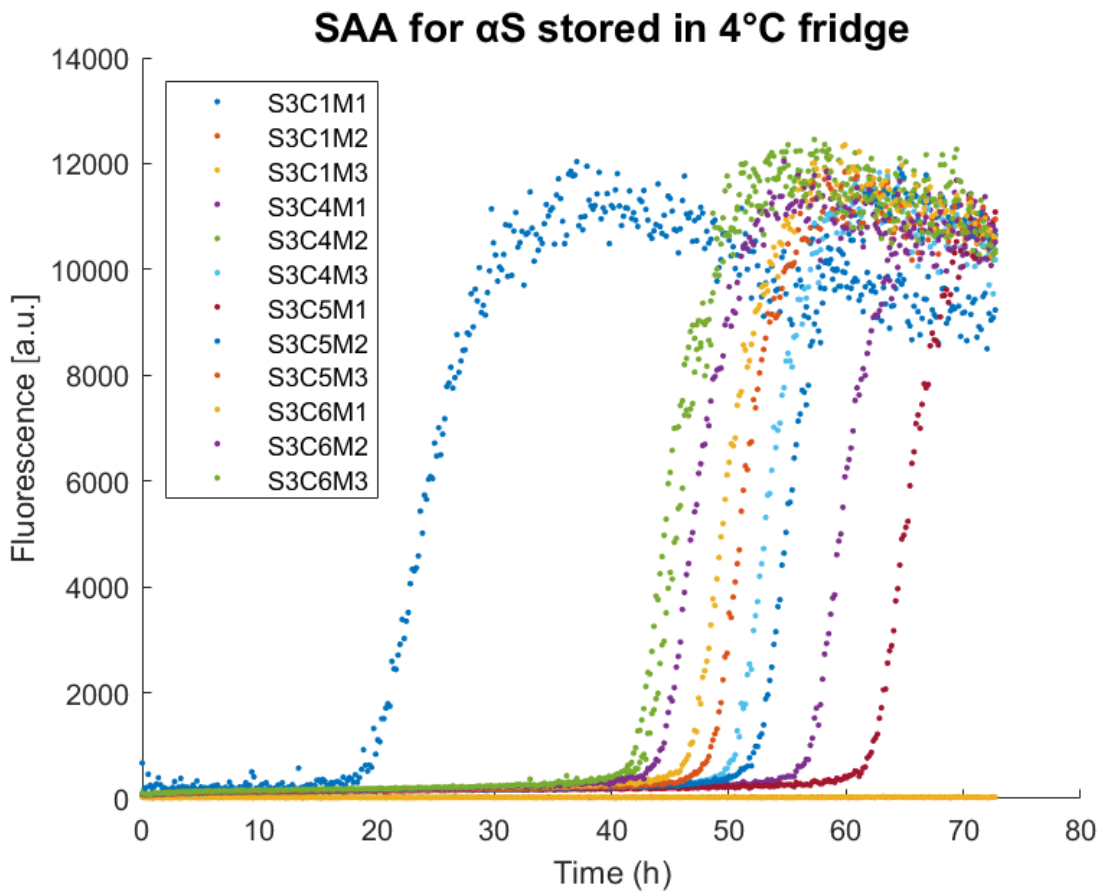

Figure 80. SAA curves for the αS stored in the fridge (S3). Only S3C1M2 and S3C1M3 did not aggregate.

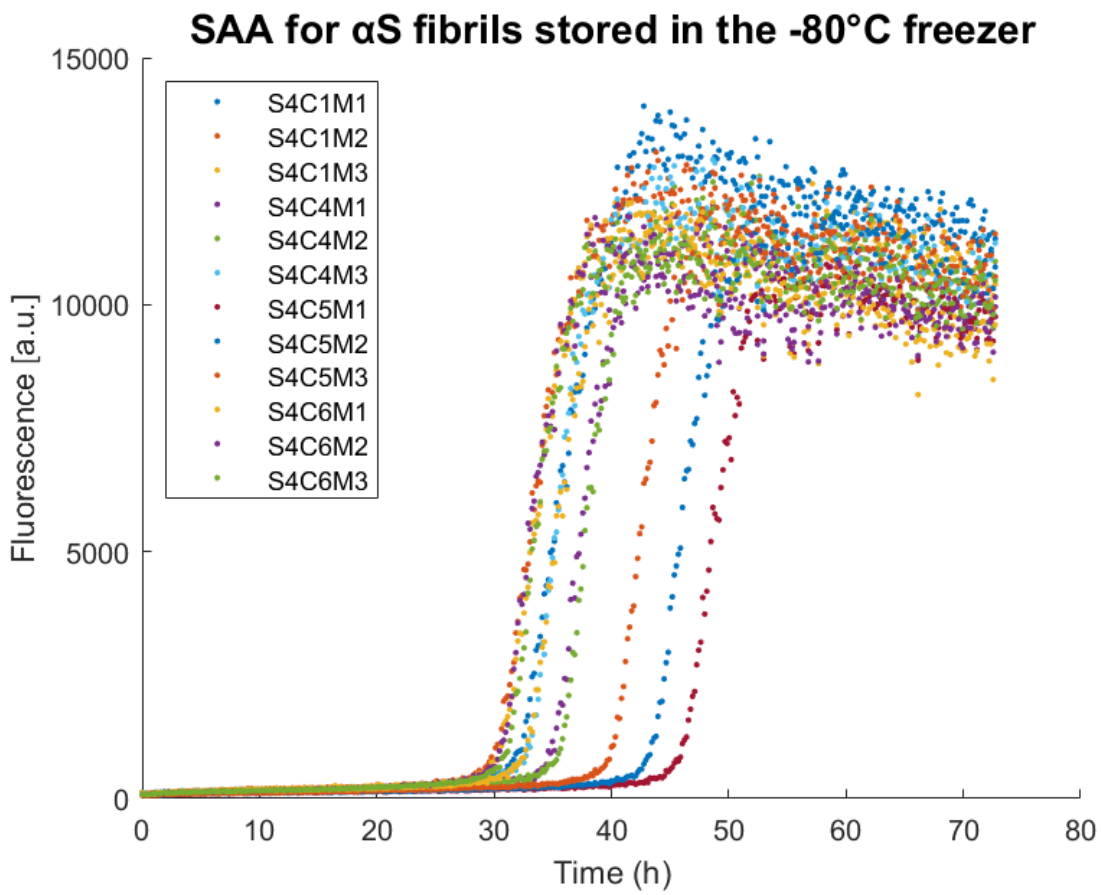

Figure 81. SAA curves for the αS stored in the -80°C freezer (S4).

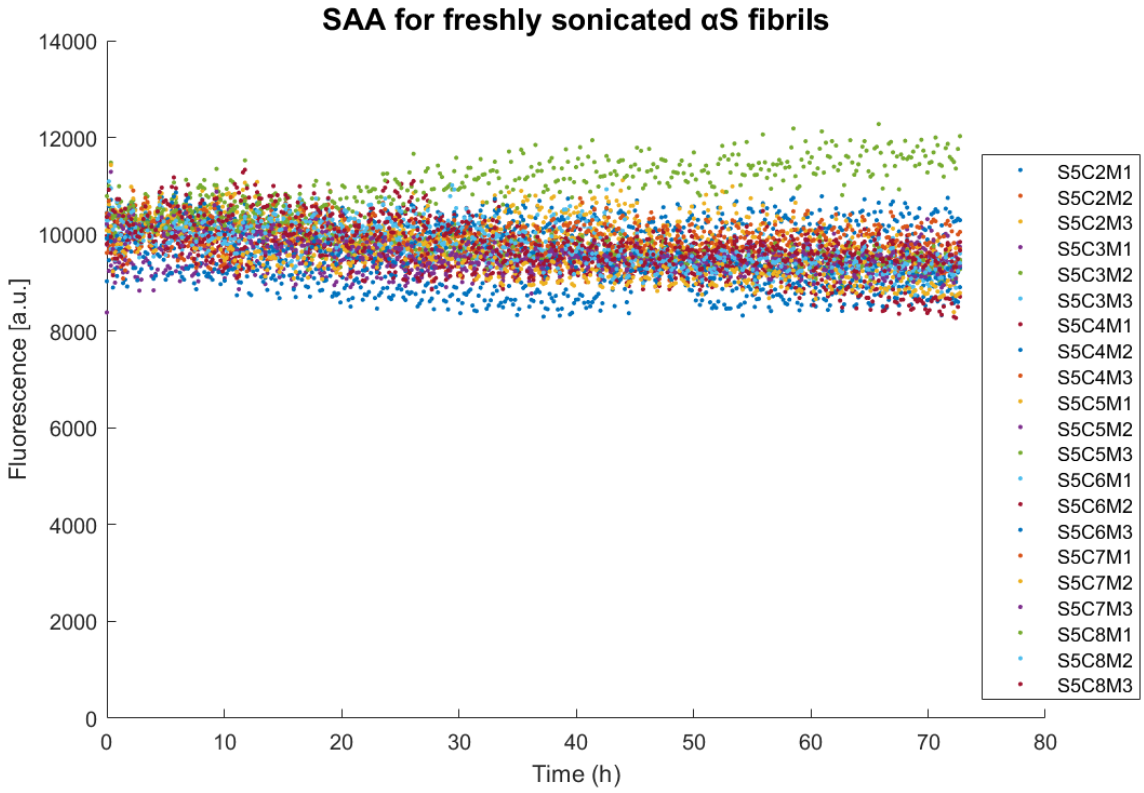

Figure 82. SAA curves for the freshly sonicated αS (S5).

Table 37. The count and percentage of aggregation categories

Category	**Count**	**Percentage**
# samples	60	100
# non-aggregated samples	28	47
# aggregated samples	32	53
# ideal cases	29	48
# diff lag time =< 5 h	3	5
# diff lag time > 5 h	0	0

Table 38. Mean lag time, standard deviation and number of used measurements per condition.

αS fibril handling →	**S1 Negative control with 0 M αS fibrils**			**S2 αS fibrils stored at bench**			**S3 αS fibrils stored in the 4°C fridge**			**S4 αS fibrils stored in the -80°C freezer**			**S5 Freshly sonicated αS fibrils**		
Sonication time ↓	Mean	STD	#M	Mean	STD	#M	Mean	STD	#M	Mean	STD	#M	Mean	STD	#M
Control	NaN	NaN	0	-	-	-	-	-	-	-	-	-	-	-	-
0 s	-	-	-	3.8	0	1	20	0	1	29	1.0	3	-	-	-
1 s	-	-	-	7.3	0.17	3	-	-	-	-	-	-	NaN	NaN	0
3 s	-	-	-	4.3	0.17	3	-	-	-	-	-	-	NaN	NaN	0
5 s	-	-	-	4.0	0	3	47	6.2	3	31	1.8	3	NaN	NaN	0
7 s	-	-	-	-	-	-	51	6.9	3	39	3.2	3	NaN	NaN	0
10 s	-	-	-	-	-	-	42	2.3	3	29	1.1	3	NaN	NaN	0
30 s	-	-	-	-	-	-	-	-	-	-	-	-	NaN	NaN	0
60 s	-	-	-	-	-	-	-	-	-	-	-	-	NaN	NaN	0

Table 39. Comparing the lag times of this experiment's (R14) αS fibrils stored at the bench with the identical conditions of R5.

Sonication time (s)	**R5**			**R14**		
	Mean	STD	#M	Mean	STD	#M
0	33	25	3	3.8	0	1
1	2.8	0.10	3	7.3	0.17	3
3	2.7	0.10	3	4.3	0.17	3
5	2.5	0.10	3	4.0	0	3

Table 40. Comparing the lag times of this experiment's (R14) αS fibrils stored in the 4°C fridge with the identical condition of R12 and R13 (for the latter: no vortexing).

Sonication time (s)	**R12**			**R13**			**R14**		
	Mean	STD	#M	Mean	STD	#M	Mean	STD	#M
0	84	23	3	104	42	3	20	0.0	1
5	61	8.5	3	41	2.4	3	47	6.2	3
7	57	1.3	3	57	15	3	51	6.9	3
10	69	1.1	3	40	1.2	3	42	2.3	3

Table 41. Comparing the lag times of this experiment's (R14) αS fibrils stored in the -80°C freezer with the identical condition of R13 (no vortexing).

Sonication time (s)	**R13**			**R14**		
	Mean	STD	#M	Mean	STD	#M
0	32	1.7	3	29	1.0	3
5	50	4.0	3	31	1.8	3
7	54	9.7	3	39	3.2	3
10	43	3.0	3	29	1.1	3

15. Combining SAA and SPC: attempt 4 (THT)

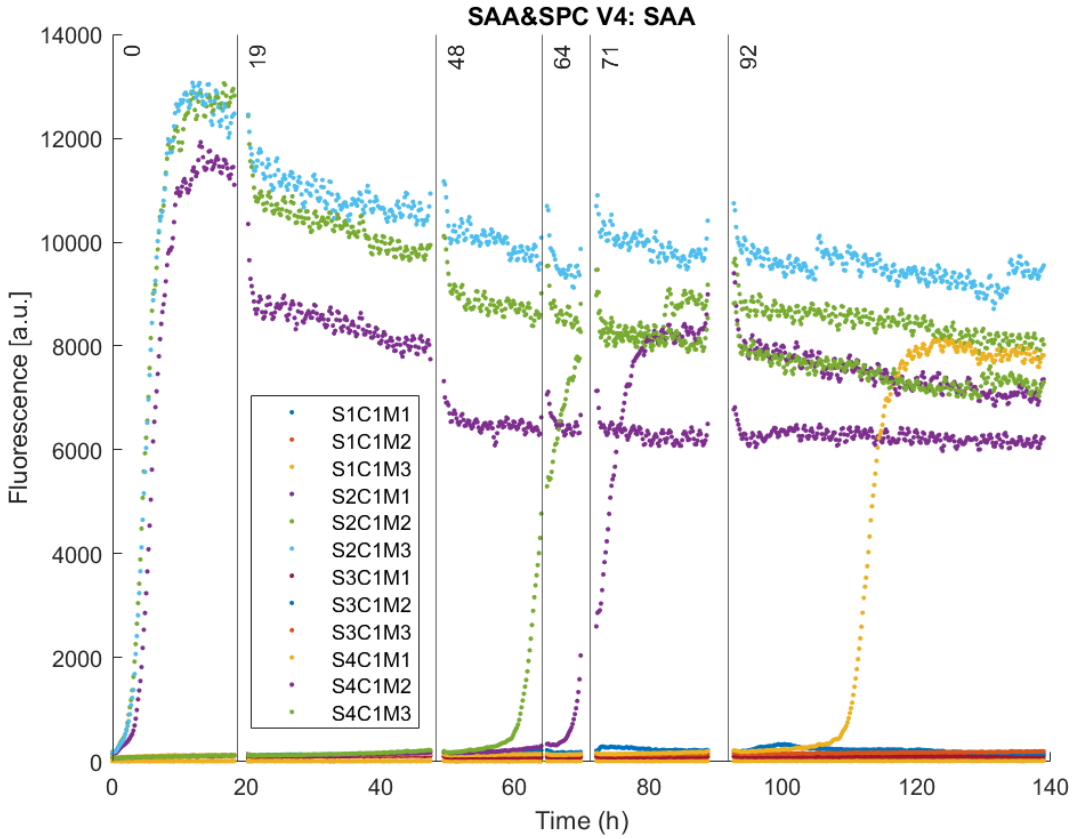

Figure 83. SAA curves for all samples. The vertical lines indicate measurement times for the SPC. The samples are described by their coded labels: S indicates αS fibril series, C indicates nothing here and M the samples of a triplo. S1 = 0 M αS fibrils (negative control); S2 = 5 s sonicated αS fibrils stored at the bench at room temperature; S3 = 5 s sonicated αS fibrils stored in the 4°C fridge; S4 = 10 s sonicated αS fibrils stored in the 4°C fridge; M1 = sample 1 of triplo; M2 = sample 2 of triplo; M3 = sample 3 of triplo.

Table 42. Mean lag time, standard deviation and number of used measurements per condition.

Series →	**0 M αS fibrils (negative control)**	**αS fibrils stored at bench; 5 s sonicated**	**αS fibrils stored in fridge; 5 s sonicated**	**αS fibrils stored in fridge; 10 s sonicated**
Mean	NaN	2.7	73	73
STD	NaN	0.36	0	26
# measurements	0	3	1	3

Table 43. The count and percentage of aggregation categories.

Category	Count	Percentage
# samples	12	100
# non-aggregated samples	5	42
# aggregated samples	7	58
# ideal cases	5	42
# diff lag time =< 5 h	1	8
# diff lag time > 5 h	1	8

Table 44. Comparing the lag times of this experiment's (R15) αS fibrils stored at bench with the identical conditions of R5 and R14.

Sonication time (s)	R5			R14			R15		
	Mean	STD	#M	Mean	STD	#M	Mean	STD	#M
0	33	25	3	3.8	0	1	-	-	-
1	2.8	0.10	3	7.3	0.17	3	-	-	-
3	2.7	0.10	3	4.3	0.17	3	-	-	-
5	2.5	0.10	3	4.0	0	3	2.7	0.36	3

Table 45. Comparing the lag times of this experiment's (R15) αS fibrils stored in the 4°C fridge with the identical condition of R12, R13 (no vortexing), and R14.

Sonication time (s)	R12			R13			R14			R15		
	Mean	STD	#M	Mean	STD	#M	Mean	STD	#M	Mean	STD	#M
0	84	23	3	104	42	3	20	0.0	1	-	-	-
5	61	8.5	3	41	2.4	3	47	6.2	3	73	0	1
7	57	1.3	3	57	15	3	51	6.9	3	-	-	-
10	69	1.1	3	40	1.2	3	42	2.3	3	73	26	3

Table 46. Representative SPC images of the negative control with 0 M αS fibrils (S1). Most images do not contain particles, so images are selected to contain particles.

Measure-ment # Time (h) Image size (µm)	**Representative images**
#1 t = 0 118 x 52	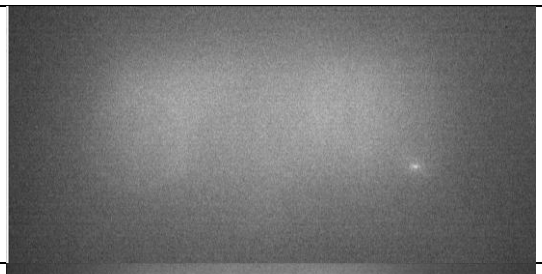
#2 t = 19 140 x 61	
#3 t = 48 140 x 61	
#4 t = 64	No images were taken due to lack of time and because only a black screen was visible.
#5 t = 71 140 x 61	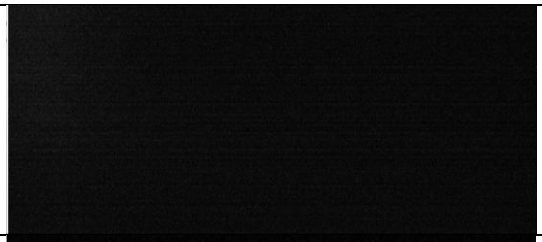
#6 t = 92 140 x 118	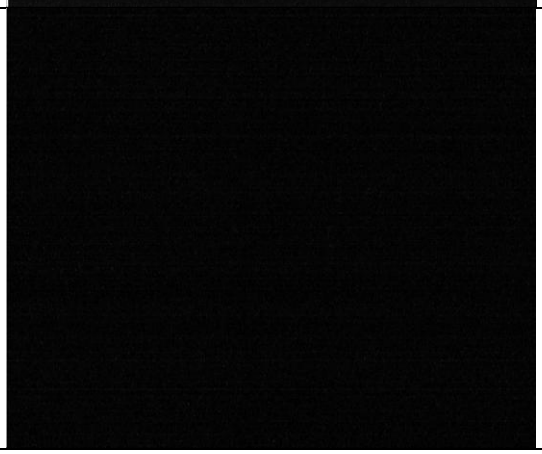

Table 47. Representative SPC images of the 5 s sonicated αS fibrils stored at the bench (S2).

Measure-ment # Time (h) Image size (µm)	**Representative images**
#1 t = 0 118 x 52	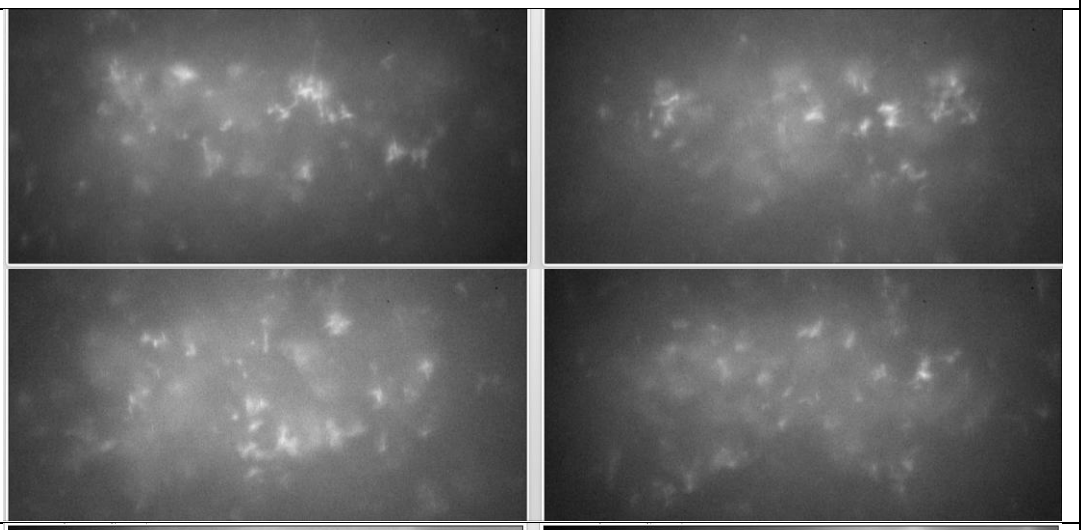
#2 t = 19 140 x 61	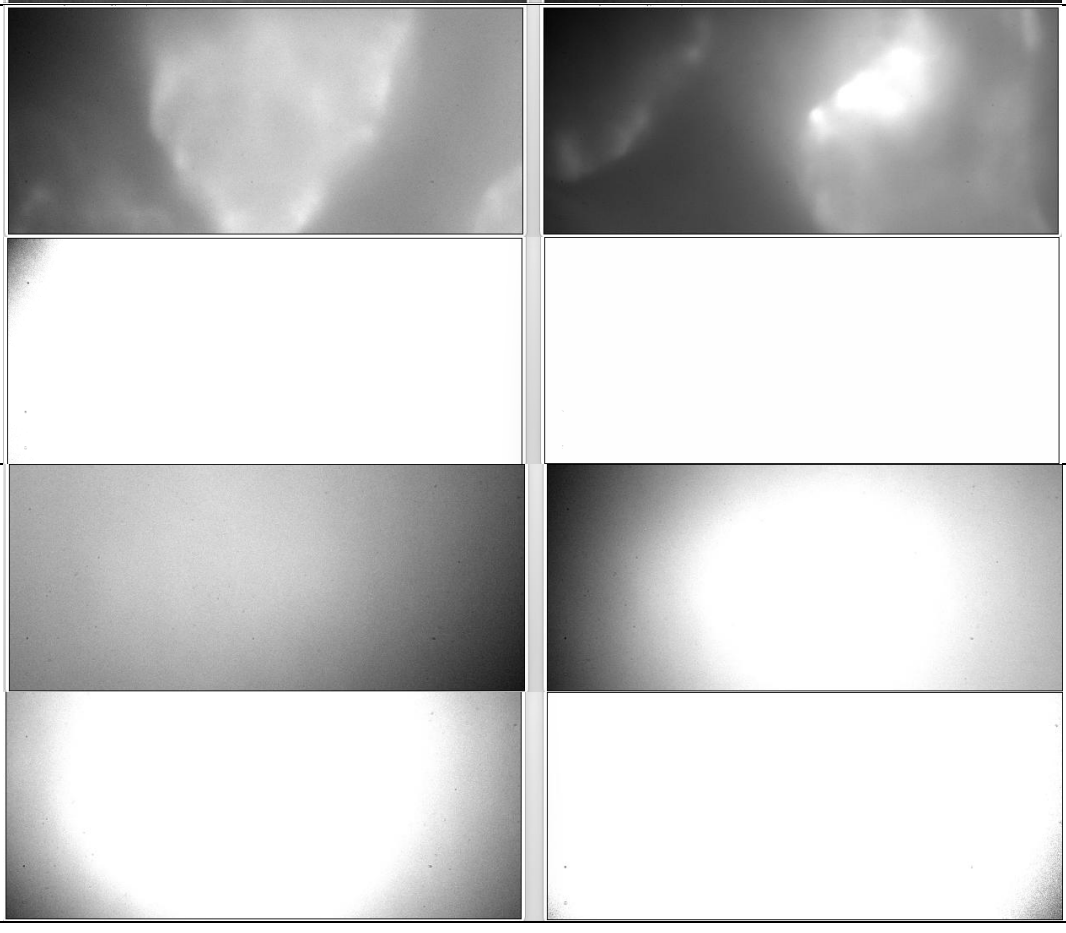
#3 t = 48 140 x 61	

#4 t = 64 140 x 61	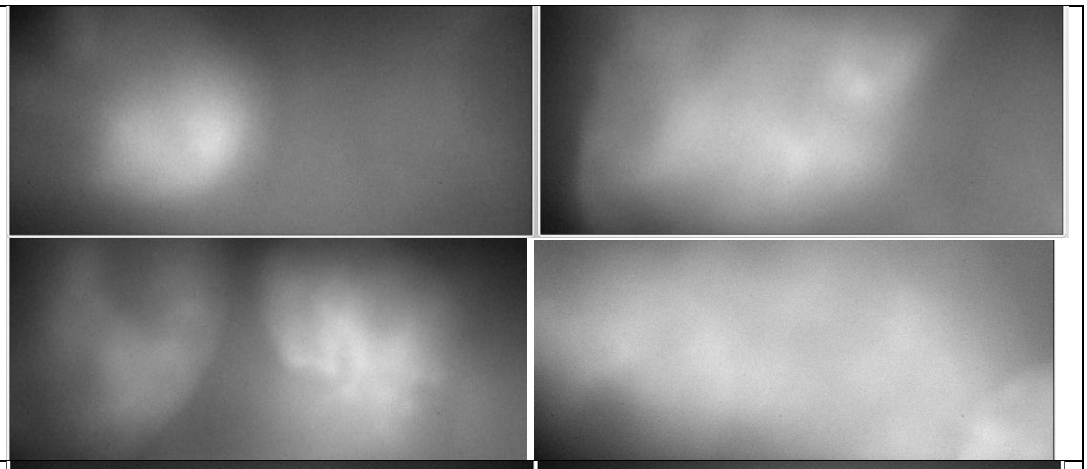
#5 t = 71 140 x 61	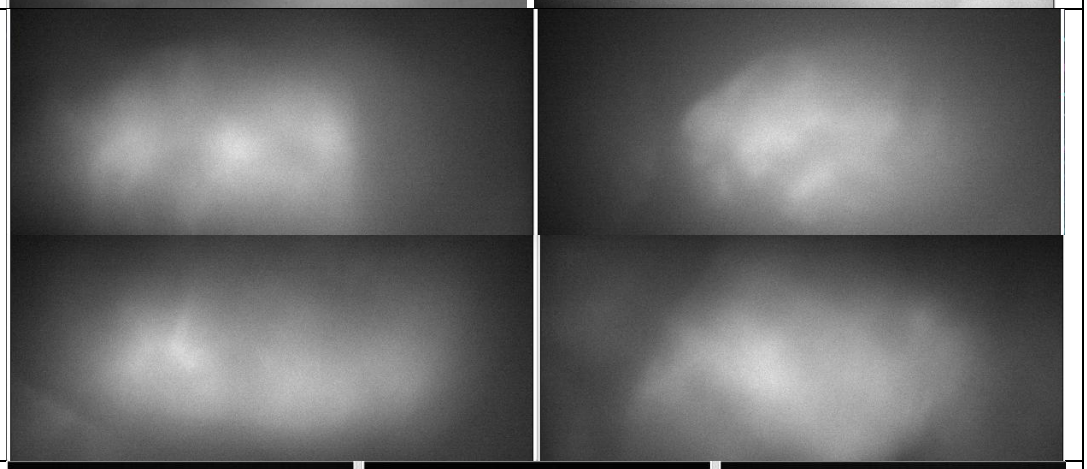
#6 t = 92 140 x 118	

Table 48. Representative SPC images of the 5 s sonicated αS fibrils stored in the fridge (S3).

Measure-ment # Time (h) Image size (µm)	**Representative images**
#1 t = 0 118 x 52	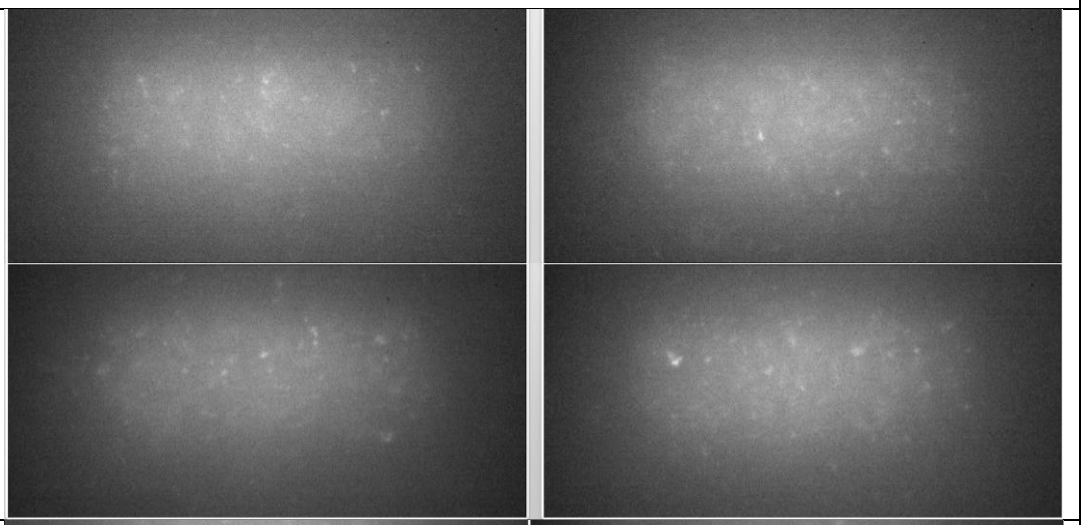
#2 t = 19 140 x 61	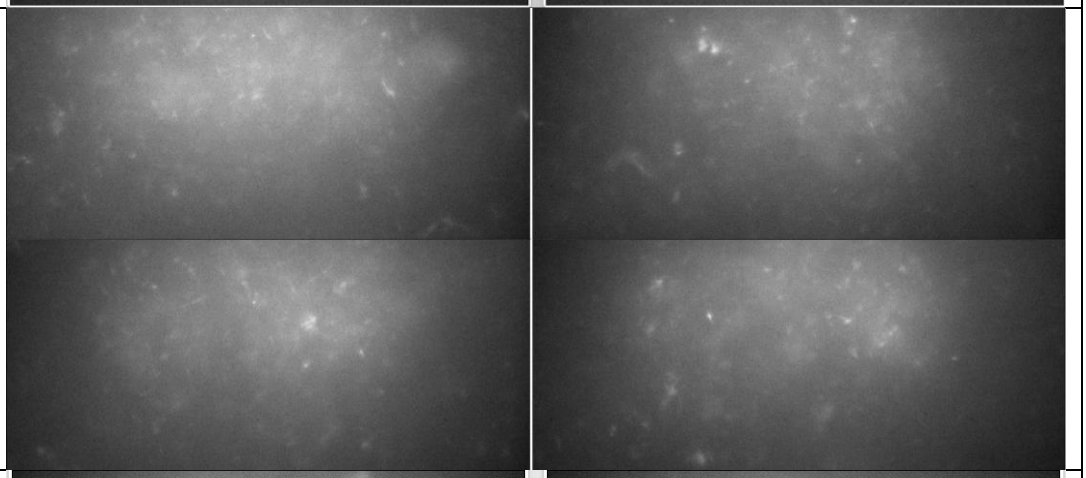
#3 t = 48 140 x 61	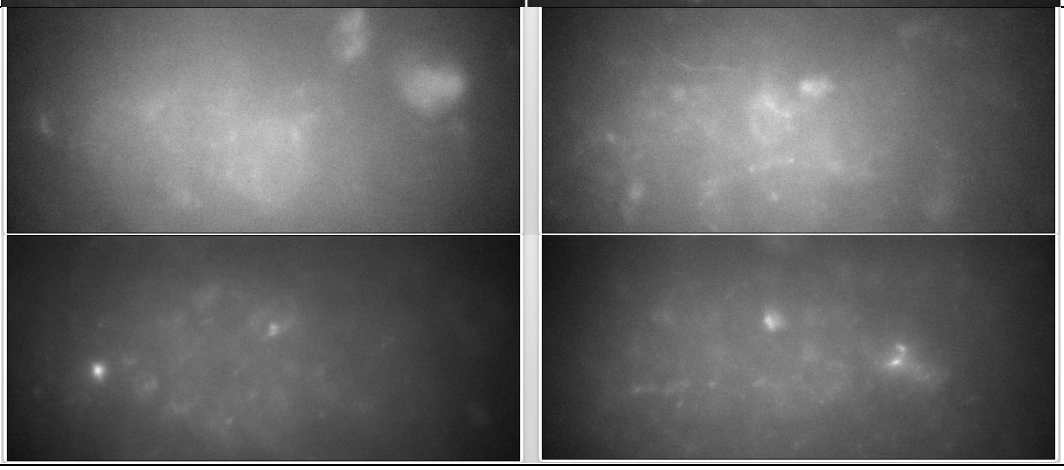

#4 t = 64 140 x 61	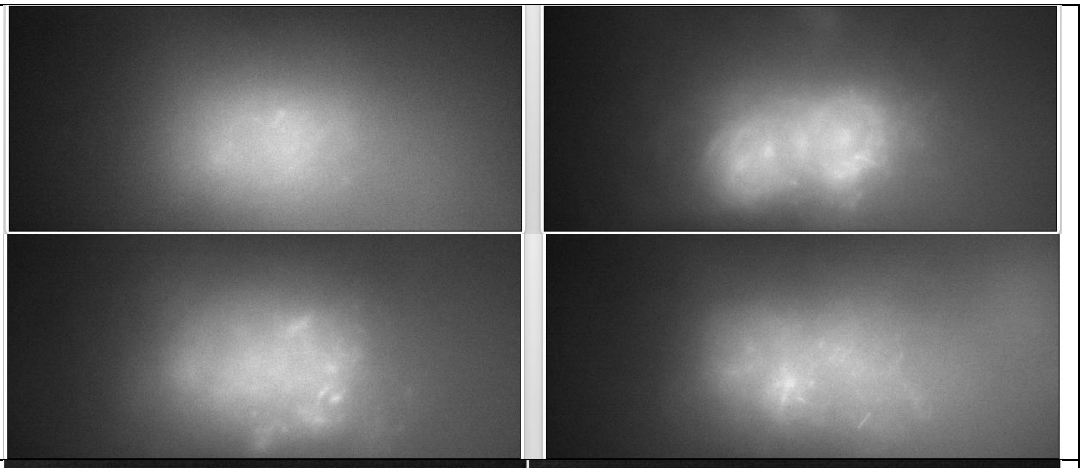
#5 t = 71 140 x 61	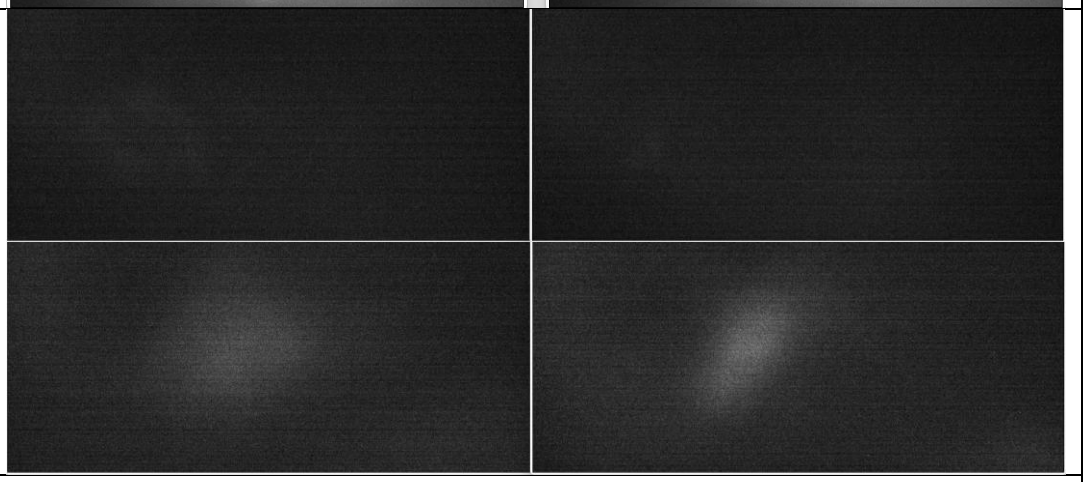
#6 t = 92 140 x 118	Well S3M1 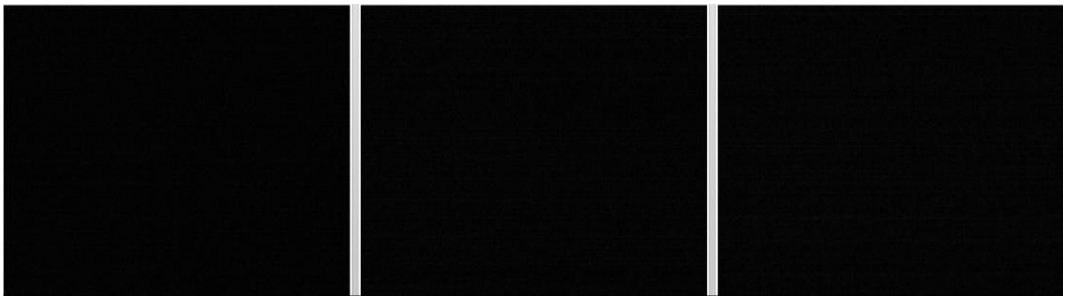 Well S3M2 

Table 49. Representative SPC images of the 10 s sonicated αS fibrils stored in the fridge (S4).

Measure-ment # Time (h) Image size (µm)	**Representative images**
#1 t = 0 118 x 52	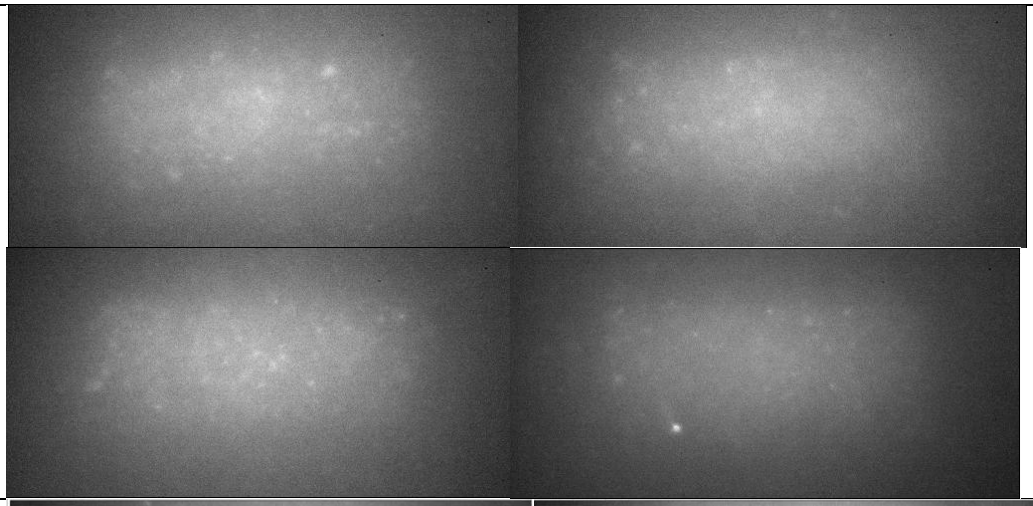
#2 t = 19 140 x 61	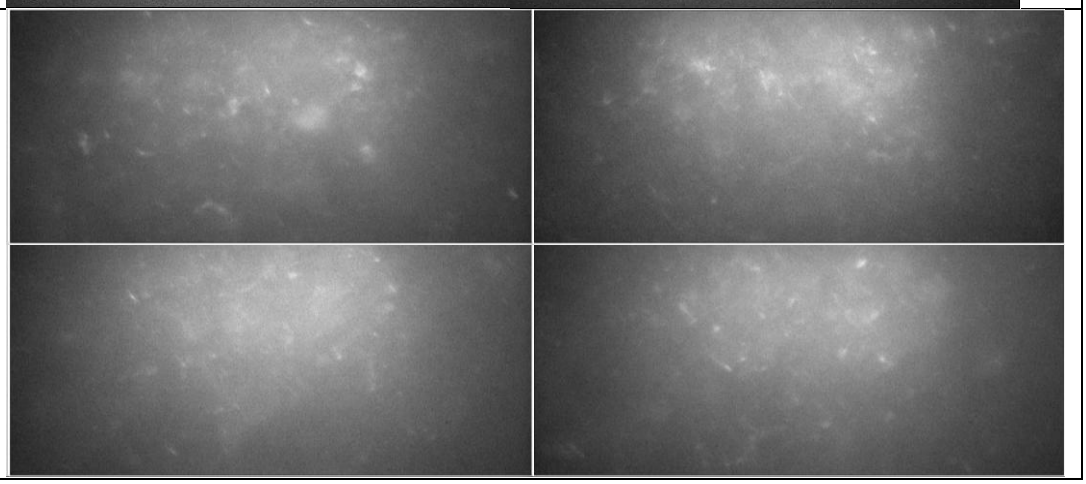

#3 t = 48 140 x 61	Well B5 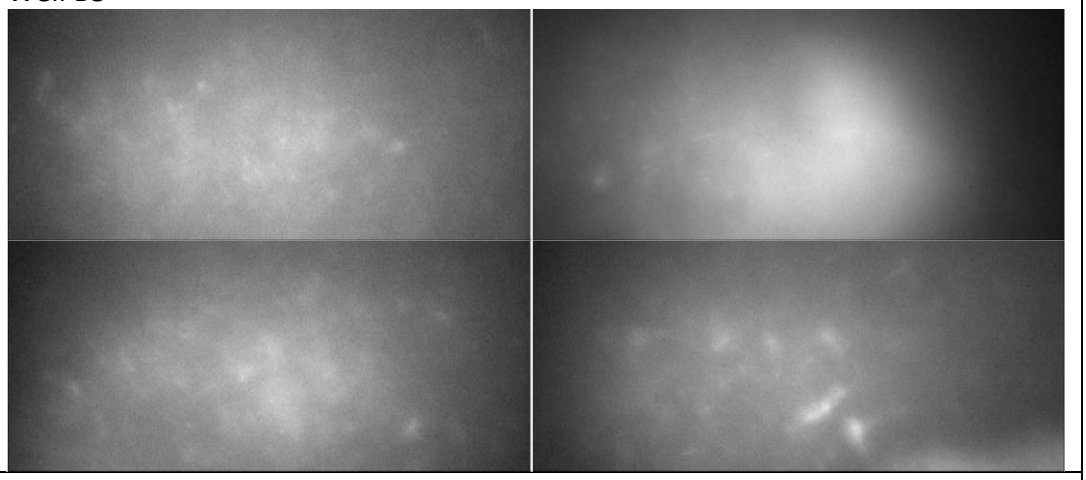
	Well C5 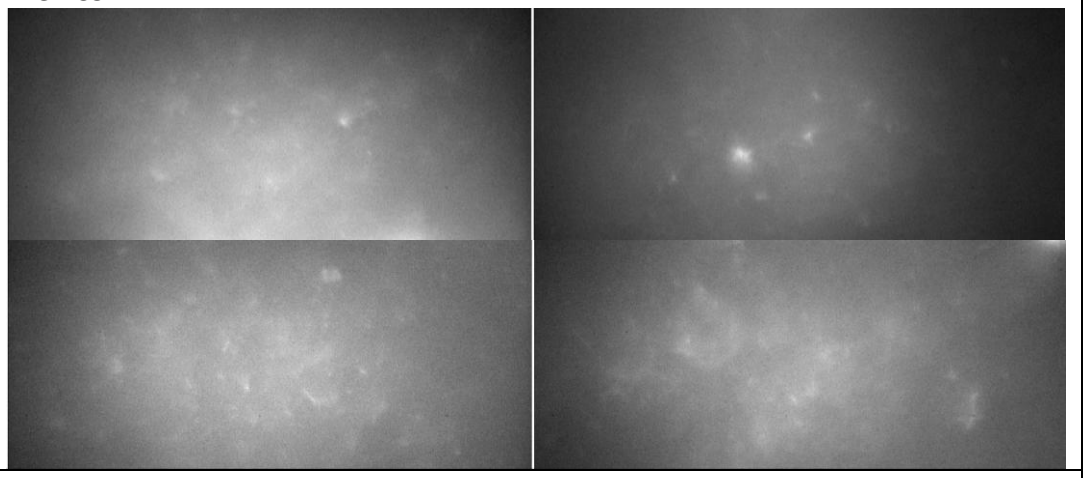
	Well D5 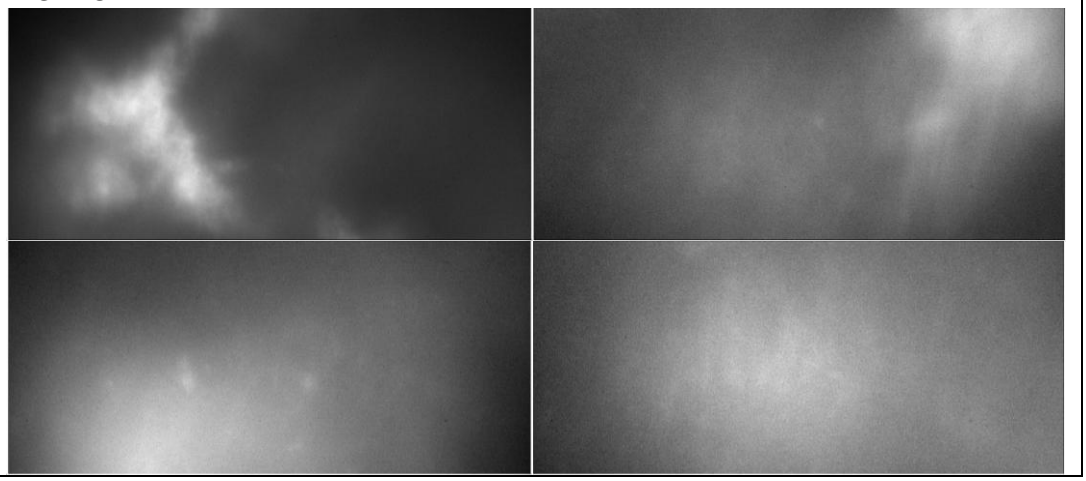

#4 t = 64 140 x 61	Well S4M1 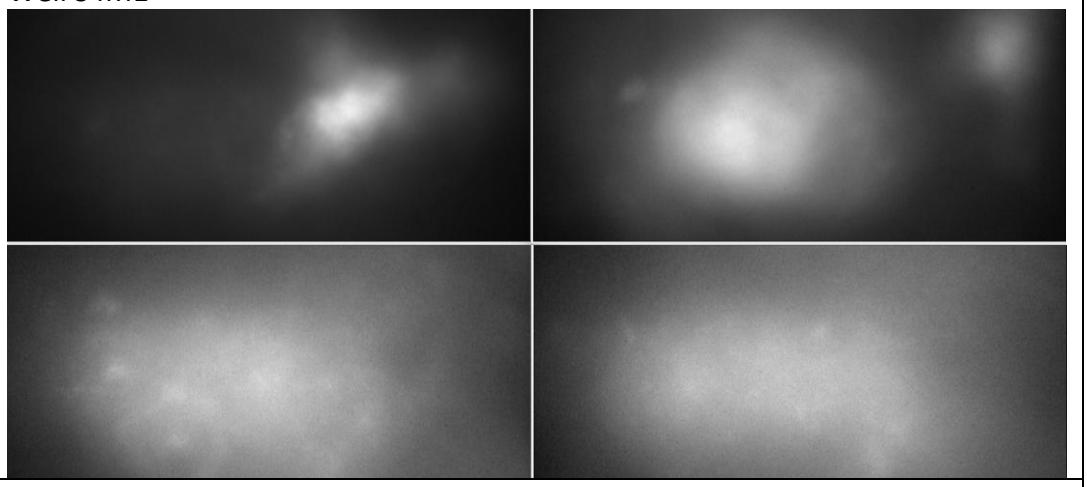
	Well S4M2 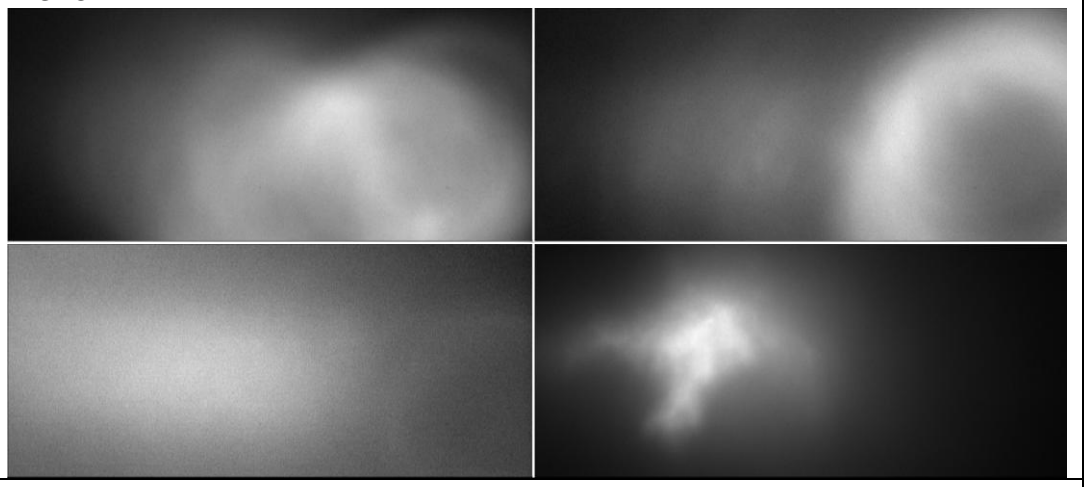
	Well S4M3 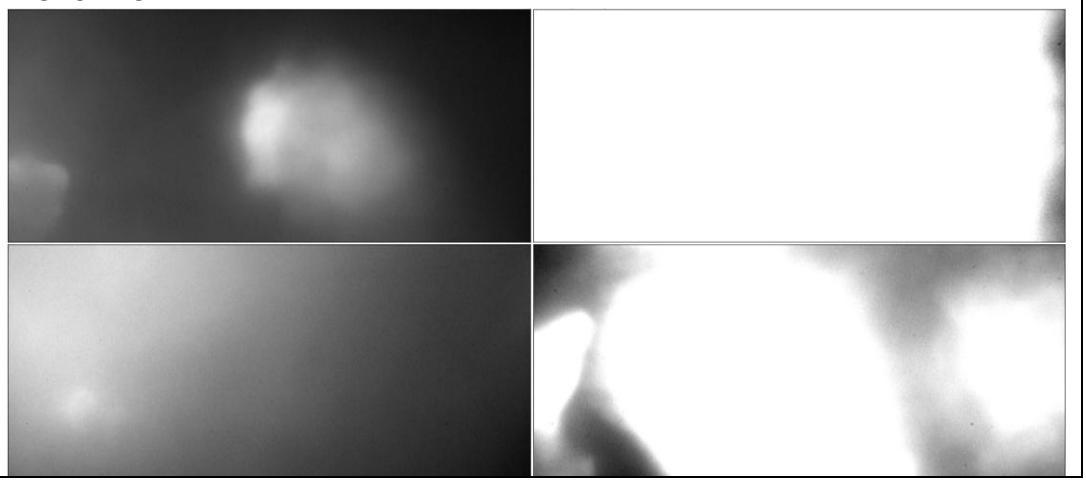

#5 t = 71 140 x 61	Well S4M1 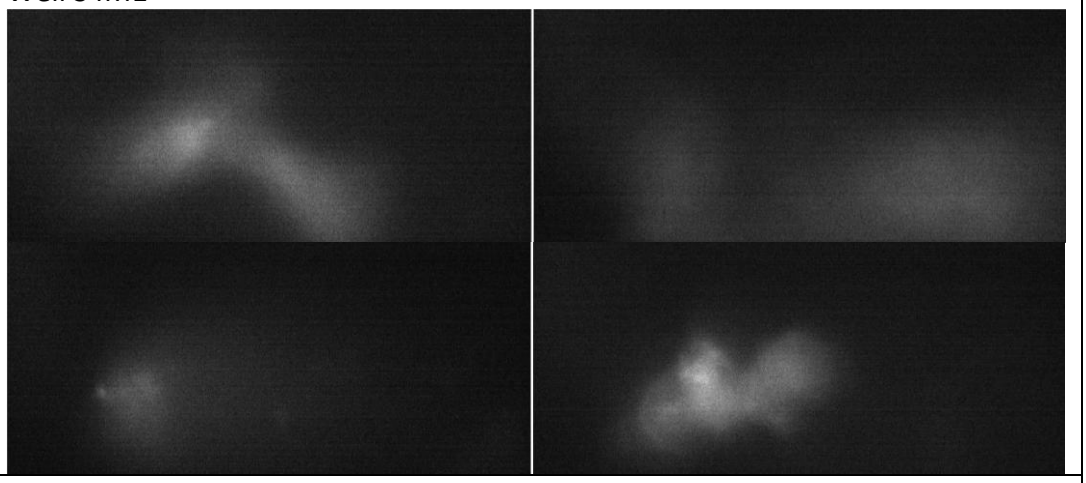
	Well S4M2 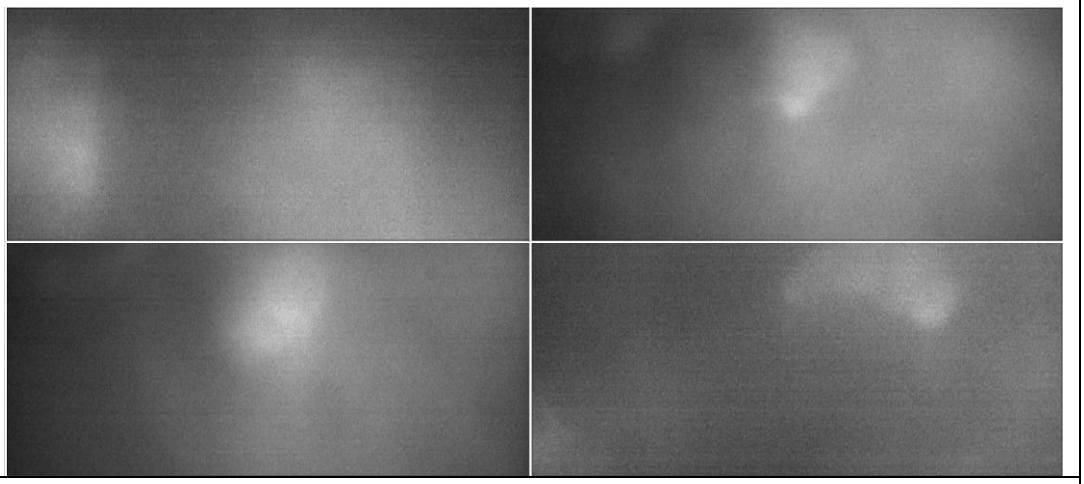
	Well S4M3 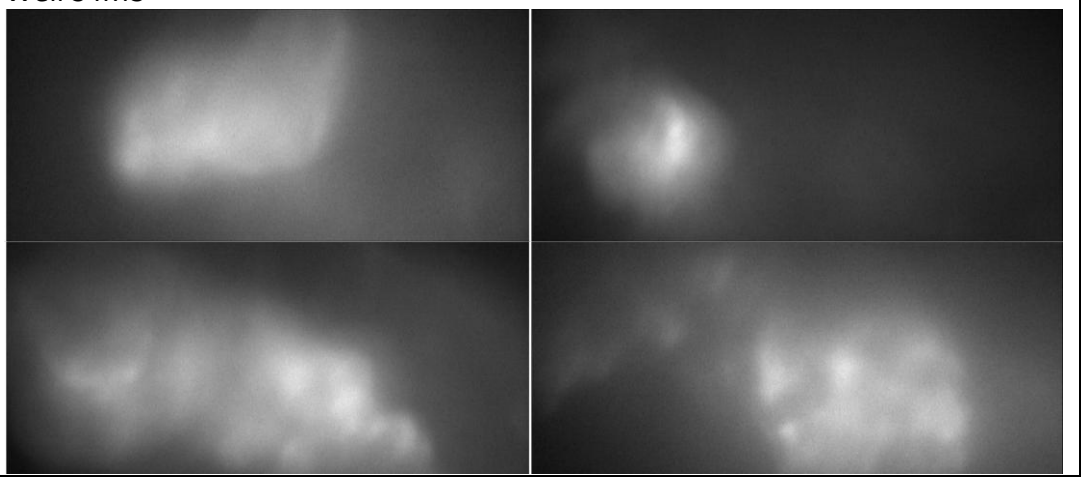

#6 t = 92 140 x 118	Well S4M1 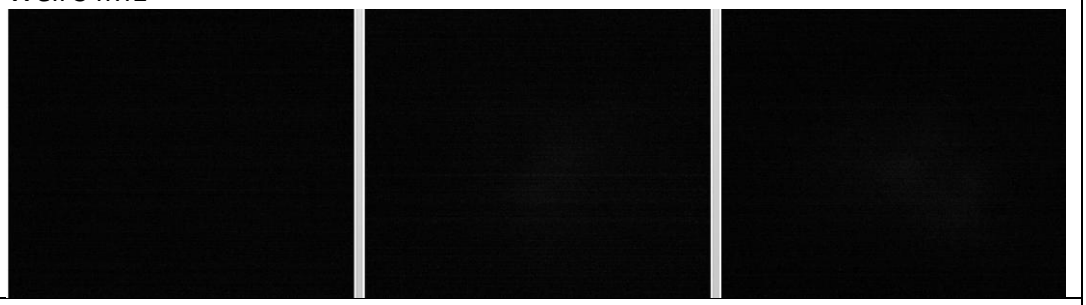
	Well S4M2 
	Well S4M3 

References

1. Armstrong MJ, Okun MS. Diagnosis and Treatment of Parkinson Disease: A Review. *JAMA - J Am Med Assoc*. 2020;323(6):548-560. doi:10.1001/jama.2019.22360
2. Tolosa E, Garrido A, Scholz SW, Poewe W. Challenges in the diagnosis of Parkinson's disease. *Lancet Neurol*. 2021;20(5):385-397. doi:10.1016/S1474-4422(21)00030-2
3. Feigin VL, Krishnamurthi R V., Theadom AM, et al. Global, regional, and national burden of neurological disorders during 1990–2015: a systematic analysis for the Global Burden of Disease Study 2015. *Lancet Neurol*. 2017;16(11):877-897. doi:10.1016/S1474-4422(17)30299-5
4. Dorsey ER, Bloem BR. The Parkinson Pandemic-A Call to Action. *Jama Neurol*. 2018;75(1):9-10. doi:doi:10.1001/jamaneurol.2017.3299
5. Bloem BR, Okun MS, Klein C. Parkinson's disease. *Lancet*. 2021;397(10291):2284-2303. doi:10.1016/S0140-6736(21)00218-X
6. Rizzo G, Copetti M, Arcuti S, Martino D, Fontana A, Logroscino G. Accuracy of clinical diagnosis of Parkinson disease. *Neurology*. 2016;86(6):566-576. doi:10.1212/WNL.0000000000002350
7. Beach TG, Adler CH. Importance of low diagnostic Accuracy for early Parkinson's disease. *Mov Disord*. 2018;33(10):1551-1554. doi:10.1002/mds.27485
8. Andréasson M, Svenningsson P. Update on alpha-synuclein-based biomarker approaches in the skin, submandibular gland, gastrointestinal tract, and biofluids. *Curr Opin Neurol*. 2021;34(4):572-577. doi:10.1097/WCO.0000000000000948
9. Tsukita K, Sakamaki-Tsukita H, Tanaka K, Suenaga T, Takahashi R. Value of in vivo α-synuclein deposits in Parkinson's disease: A systematic review and meta-analysis. *Mov Disord*. 2019;34(10):1452-1463. doi:10.1002/mds.27794
10. Kalia L V., Lang AE. Parkinson's disease. *Lancet*. 2015;386(9996):896-912. doi:10.1016/S0140-6736(14)61393-3
11. Beach TG, Adler CH, Sue LI, et al. Multi-organ distribution of phosphorylated α-synuclein histopathology in subjects with Lewy body disorders. *Acta Neuropathol*. 2010;119(6):689-702. doi:10.1007/s00401-010-0664-3
12. Lee JM, Derkinderen P, Kordower JH, et al. The search for a peripheral biopsy indicator of a-synuclein pathology for Parkinson disease. *J Neuropathol Exp Neurol*. 2017;76(1):2-15. doi:10.1093/jnen/nlw103
13. Goldman JG, Andrews H, Amara A, et al. Cerebrospinal fluid, plasma, and saliva in the BioFIND study: Relationships among biomarkers and Parkinson's disease Features. *Mov Disord*. 2018;33(2):282-288. doi:10.1002/mds.27232
14. Chahine LM, Beach TG, Brumm MC, et al. In vivo distribution of α-synuclein in multiple tissues and biofluids in Parkinson disease. *Neurology*. 2020;95(9):E1267-E1284. doi:10.1212/WNL.0000000000010404
15. Saborio GP, Permanne B, Soto C. Sensitive detection of pathological prion protein by cyclic amplification of protein misfolding. *Nature*. 2001;411:810-813. doi:10.1038/35081095
16. Wilham JM, Orrú CD, Bessen RA, et al. Rapid end-point quantitation of prion seeding activity with sensitivity comparable to bioassays. *PLoS Pathog*. 2010;6(12). doi:10.1371/journal.ppat.1001217
17. Atarashi R, Satoh K, Sano K, et al. Ultrasensitive human prion detection in cerebrospinal fluid by real-timequaking-induced conversion. *Nat Med*.

2011;17(2):175-178. http://hdl.handle.net/10069/25642.
18. Concha-Marambio L, Pritzkow S, Shahnawaz M, Farris CM, Soto C. Seed amplification assay for the detection of pathologic alpha-synuclein aggregates in cerebrospinal fluid. *Nat Protoc*. January 2023:1-18. doi:10.1038/s41596-022-00787-3
19. Kuang Y, Mao H, Huang X, et al. α-Synuclein seeding amplification assays for diagnosing synucleinopathies: an innovative tool in clinical implementation. *Transl Neurodegener*. 2024;13(1):1-17. doi:10.1186/s40035-024-00449-2
20. Mehra S, Sahay S, Maji SK. α-Synuclein misfolding and aggregation: Implications in Parkinson's disease pathogenesis. *Biochim Biophys Acta - Proteins Proteomics*. 2019;1867(10):890-908. doi:10.1016/j.bbapap.2019.03.001
21. Burger VM, Gurry T, Stultz CM. Intrinsically disordered proteins: Where computation meets experiment. *Polymers (Basel)*. 2014;6(10):2684-2719. doi:10.3390/polym6102684
22. Pinotsi D, Buell AK, Galvagnion C, Dobson CM, Kaminski Schierle GS, Kaminski CF. Direct observation of heterogeneous amyloid fibril growth kinetics via two-color super-resolution microscopy. *Nano Lett*. 2014;14(1):339-345. doi:10.1021/nl4041093
23. Joseph T. Jarrett, Jr PTL. Seeding "one-dimensional crystallization" of amyloid: A pathogenic mechanism in Alzheimer's disease and scrapie? *Cell*. 1993;73(6):1055-1058. papers2://publication/uuid/49CF8FDD-786C-494D-AF7B-5174077339CB.
24. Buell AK, Galvagnion C, Gaspar R, et al. Solution conditions determine the relative importance of nucleation and growth processes in α-synuclein aggregation. *Proc Natl Acad Sci U S A*. 2014;111(21):7671-7676. doi:10.1073/pnas.1315346111
25. Shvadchak V V., Claessens MMAE, Subramaniam V. Fibril breaking accelerates α-synuclein fibrillization. *J Phys Chem A*. 2015;119(5):1912-1918. doi:10.1021/jp5111604
26. Wördehoff M, Hoyer W. α-Synuclein Aggregation Monitored by Thioflavin T Fluorescence Assay. *Bio-Protocol*. 2018;8(14):1-11. doi:10.21769/bioprotoc.2941
27. Russo MJ, Orru CD, Concha-Marambio L, et al. High diagnostic performance of independent alpha-synuclein seed amplification assays for detection of early Parkinson's disease. *Acta Neuropathol Commun*. 2021;9(1):1-13. doi:10.1186/s40478-021-01282-8
28. Kang UJ, Boehme AK, Fairfoul G, et al. Comparative study of cerebrospinal fluid α-synuclein seeding aggregation assays for diagnosis of Parkinson's disease. *Mov Disord*. 2019;34(4):536-544. doi:10.1002/mds.27646
29. Saá P, Castilla J, Soto C. Ultra-efficient replication of infectious prions by automated protein misfolding cyclic amplification. *J Biol Chem*. 2006;281(46):35245-35252. doi:10.1074/jbc.M603964200
30. Giehm L, Otzen DE. Strategies to increase the reproducibility of protein fibrillization in plate reader assays. *Anal Biochem*. 2010;400(2):270-281. doi:10.1016/j.ab.2010.02.001
31. Paciotti S, Bellomo G, Gatticchi L, Parnetti L. Are we ready for detecting α-synuclein prone to aggregation in patients? The case of "Protein-Misfolding Cyclic Amplification" and "Real-Time Quaking-Induced Conversion" as diagnostic tools. *Front Neurol*. 2018;9(JUN). doi:10.3389/fneur.2018.00415
32. Oftedal L, Maple-Gørdem J, Tysnes OB, Alves G, Lange J. Seed Amplification Assay as a Diagnostic Tool in Newly-Diagnosed Parkinson's Disease. *J Parkinsons Dis*. 2023;13(5):841-844. doi:10.3233/JPD-230065
33. Fernandes Gomes B, Farris CM, Ma Y, et al. α-Synuclein seed amplification assay as a

diagnostic tool for parkinsonian disorders. *Park Relat Disord*. 2023;117(May). doi:10.1016/j.parkreldis.2023.105807
34. Gilboa T, Swank Z, Thakur R, et al. Toward the quantification of α-synuclein aggregates with digital seed amplification assays. *Proc Natl Acad Sci USA*. 2024;121(3). doi:10.1073/pnas.2312031121
35. Sidhu A, Vaneyck J, Blum C, Segers-Nolten I, Subramaniam V. Polymorph-specific distribution of binding sites determines thioflavin-T fluorescence intensity in α-synuclein fibrils. *Amyloid*. 2018;25(3):189-196. doi:10.1080/13506129.2018.1517736
36. Bellomo G, Bologna S, Cerofolini L, et al. Dissecting the Interactions between Human Serum Albumin and α-Synuclein: New Insights on the Factors Influencing α-Synuclein Aggregation in Biological Fluids. *J Phys Chem B*. 2019;123(20):4380-4386. doi:10.1021/acs.jpcb.9b02381
37. Bellomo G, Paciotti S, Concha-Marambio L, et al. Cerebrospinal fluid lipoproteins inhibit α-synuclein aggregation by interacting with oligomeric species in seed amplification assays. *Mol Neurodegener*. 2023;18(1):1-24. doi:10.1186/s13024-023-00613-8
38. Shaw G. New Assay Detects Abnormal Proteins in Parkinson's Disease and Spinal Muscular Atrophy. *Neurol Today*. 2024. https://journals.lww.com/neurotodayonline/fulltext/2024/03070/new_assay_detects_abnormal_proteins_in_parkinson_s.13.aspx. Accessed February 7, 2025.
39. Chen B, Morales R, Barria MA, Soto C. Estimating prion concentration in fluids and tissues by quantitative PMCA. *Nat Methods*. 2010;7:519-520. doi:10.1038/nmeth
40. Groveman BR, Orrù CD, Hughson AG, et al. Rapid and ultra-sensitive quantitation of disease-associated α-synuclein seeds in brain and cerebrospinal fluid by αSyn RT-QuIC. *Acta Neuropathol Commun*. 2018;6:1-10. doi:10.1186/s40478-018-0508-2
41. Shi S, Mitteregger-Kretzschmar G, Giese A, Kretzschmar HA. Establishing quantitative real-time quaking-induced conversion (qRT-QuIC) for highly sensitive detection and quantification of PrPSc in prion-infected tissues. *Acta Neuropathol Commun*. 2013;2(1):1. doi:10.1186/2051-5960-1-44
42. Henderson DM, Davenport KA, Haley NJ, Denkers ND, Mathiason CK, Hoover EA. Quantitative assessment of prion infectivity in tissues and body fluids by real-time quaking-induced conversion. *J Gen Virol*. 2015;96(1):210-219. doi:10.1099/vir.0.069906-0
43. Pfammatter M, Andreasen M, Meisl G, et al. Absolute Quantification of Amyloid Propagons by Digital Microfluidics. *Anal Chem*. 2017;89(22):12306-12313. doi:10.1021/acs.analchem.7b03279
44. Vaneyck J, Yousif TA, Segers-Nolten I, Blum C, Claessens MMAE. Quantitative Seed Amplification Assay: A Proof-of-Principle Study. *J Phys Chem B*. 2023;127(8):1735-1743. doi:10.1021/acs.jpcb.2c08326
45. Oshina I, Spigulis J. Beer–Lambert law for optical tissue diagnostics: current state of the art and the main limitations. *J Biomed Opt*. 2021;26(10):1-17. doi:10.1117/1.jbo.26.10.100901
46. Thermo Scientific. NanoDrop One User Guide. *Thermo Sci NanoDrop One User Guid*. 2016;Revision B(July):18-19.
47. Guerrero-Ferreira R, Taylor NMI, Mona D, et al. Cryo-EM structure of alpha-synuclein fibrils. *Elife*. 2018;7(i):1-18. doi:10.7554/eLife.36402
48. Allan DB, Caswell T, Keim NC, van der Wel CM, Verweij RW. soft-matter/trackpy:

TrackPy v0.4.2. 2021. https://zenodo.org/doi/10.5281/zenodo.1213240.
49. Usov I, Mezzenga R. FiberApp: An open-source software for tracking and analyzing polymers, filaments, biomacromolecules, and fibrous objects. *Macromolecules*. 2015;48(5):1269-1280. doi:10.1021/ma502264c
50. Koo HJ, Lee HJ, Im H. Sequence determinants regulating fibrillation of human α-synuclein. *Biochem Biophys Res Commun*. 2008;368(3):772-778. doi:10.1016/j.bbrc.2008.01.140
51. Giehm L, Lorenzen N, Otzen DE. Assays for α-synuclein aggregation. *Methods*. 2011;53(3):295-305. doi:10.1016/j.ymeth.2010.12.008
52. Ziaunys M, Sakalauskas A, Mikalauskaite K, Smirnovas V. Polymorphism of alpha-synuclein amyloid fibrils depends on ionic strength and protein concentration. *Int J Mol Sci*. 2021;22(22). doi:10.3390/ijms222212382
53. Murray AN, Palhano FL, Bieschke J, Kelly JW. Surface adsorption considerations when working with amyloid fibrils in multiwell plates and Eppendorf tubes. *Protein Sci*. 2013;22(11):1531-1541. doi:10.1002/pro.2339
54. Amytracker Product Information Sheet. https://www.ebbabiotech.com/collections/amytracker.
55. Jones J. A Biological Breakdown of Autofluorescence: Why Your Samples Naturally Glow. Discovery Blog. https://www.olympus-lifescience.com/en/discovery/a-biological-breakdown-of-autofluorescence-why-your-samples-naturally-glow/. Published 2023. Accessed July 12, 2024.
56. Croce AC, Bottiroli G. Autofluorescence spectroscopy and imaging: A tool for biomedical research and diagnosis. *Eur J Histochem*. 2014;58(4):320-337. doi:10.4081/ejh.2014.2461
57. Product Datasheet Amytracker 680 (DMSO). https://www.biozol.de/en/product/ebb-a680-d-10. Accessed July 11, 2024.
58. Tarutani A, Suzuki G, Shimozawa A, et al. The effect of fragmented pathogenic α-synuclein seeds on prion-like propagation. *J Biol Chem*. 2016;291(36):18675-18688. doi:10.1074/jbc.M116.734707
59. Sidhu A, Segers-Nolten I, Raussens V, Claessens MMAE, Subramaniam V. Distinct Mechanisms Determine α-Synuclein Fibril Morphology during Growth and Maturation. *ACS Chem Neurosci*. 2017;8(3):538-547. doi:10.1021/acschemneuro.6b00287
60. Bousset L, Pieri L, Ruiz-Arlandis G, et al. Structural and functional characterization of two alpha-synuclein strains. *Nat Commun*. 2013;4. doi:10.1038/ncomms3575
61. Polinski NK, Volpicelli-Daley LA, Sortwell CE, et al. Best practices for generating and using alpha-synuclein pre-formed fibrils to model Parkinson's disease in rodents. *J Parkinsons Dis*. 2018;8(2):303-322. doi:10.3233/JPD-171248
62. Ikenoue T, Lee YH, Kardos J, et al. Cold denaturation of α-synuclein amyloid fibrils. *Angew Chemie - Int Ed*. 2014;53(30):7799-7804. doi:10.1002/anie.201403815
63. Bhatnagar BS, Bogner RH, Pikal MJ. Protein stability during freezing: Separation of stresses and mechanisms of protein stabilization. *Pharm Dev Technol*. 2007;12(5):505-523. doi:10.1080/10837450701481157
64. Herva ME, Zibaee S, Fraser G, Barker RA, Goedert M, Spillantini MG. Anti-amyloid Compounds Inhibit α-Synuclein Aggregation Induced by Protein Misfolding Cyclic Amplification (PMCA). *J Biol Chem*. 2014;289(17):11897-11905. doi:10.1074/jbc.M113.542340
65. Narkiewicz J, Giachin G, Legname G. In vitro aggregation assays for the

characterization of α-synuclein prion-like properties. *Prion*. 2014;8(1). doi:10.4161/pri.28125
66. Candelise N, Schmitz M, Thüne K, et al. Effect of the micro-environment on α-synuclein conversion and implication in seeded conversion assays. *Transl Neurodegener*. 2020;9(1):1-16. doi:10.1186/s40035-019-0181-9
67. Ghosh D, Mehra S, Sahay S, Singh PK, Maji SK. A-Synuclein Aggregation and Its Modulation. *Int J Biol Macromol*. 2017;100:37-54. doi:10.1016/j.ijbiomac.2016.10.021
68. Rabe M, Soragni A, Reynolds NP, et al. On-surface aggregation of α-synuclein at nanomolar concentrations results in two distinct growth mechanisms. *ACS Chem Neurosci*. 2013;4(3):408-417. doi:10.1021/cn3001312
69. Meisl G, Kirkegaard JB, Arosio P, et al. Molecular mechanisms of protein aggregation from global fitting of kinetic models. *Nat Protoc*. 2016;11(2):252-272. doi:10.1038/nprot.2016.010